6. ULUSLARARASI LİF VE POLİMER ARAŞTIRMALARI SEMPOZYUMU

INTERNATIONAL FIBER AND POLYMER RESEARCH SYMPOSIUM

24 - 25 Ocak January 2020

Bursa Uludağ Üniversitesi,
Mete Cengiz Kongre Merkezi

www.uludag.edu.tr/ulpas

BİLDİRİ KİTAPÇIĞI

BOOK OF PROCEEDINGS

İTÜ

İSTANBUL TEKNİK ÜNİVERSİTESİ 1773

ULUDAĞ ÜNİVERSİTESİ 1975

BURSA TEKNİK ÜNİVERSİTESİ 2010

F&P FIBER & POLYMER RESEARCH INSTITUTE

Bu kitabın baskı versiyonu bildirilerin tam metinlerini içermektedir. E-kitaba www.uludag.edu.tr/ulpas adresinden ulaşılabilir.

This printed book contains the full texts of the papers presented at the symposium. The pdf version of the Book of Proceedings can be downloaded from the website www.uludag.edu.tr/ulpas.

Ocak 2020

Editörler

Prof. Dr. Yusuf ULCAY

Prof. Dr. Ali DEMİR

Doç. Dr. Ali KILIÇ

Dr. Öğretim Üyesi Şule SELÇUK

Uluslararası Lif ve Polimer Araştırmaları Sempozyumu (1: 2020: Bursa)

6. Uluslararası Lif ve Polimer Araştırmaları Sempozyumu: 24 – 25 Ocak 2020 / editörler

Yusuf Ulcay, Ali Demir … [ve başkaları]

1.Tekstil lifleri-Türkiye-Kongreler 2.Polimerler-Türkiye-Kongreler

Bilim Komitesi / Scientific Committee

Prof. Dr. Yusuf ULCAY, Bursa Uludağ Üniversitesi

Prof. Dr. Ali DEMİR, İTÜ

Prof. Dr. Behnam POURDEYHIMI, NCSU, USA

Prof. Dr. Mohammad JAWAID, UPM, Malaysia

Prof. Dr. Seyed Ali MOUSAVI SHAEGH, MUMS, İRAN

Prof. Dr. Ömer Berk BERKALP, İTÜ

Prof. Dr. Kenan YILDIRIM, BTÜ

Prof. Dr. Hasan Basri KOÇER, BTÜ

Prof. Dr. Mehmet KANIK, Bursa Uludağ Üniversitesi

Prof. Dr. Esra KARACA, Bursa Uludağ Üniversitesi

Prof. Dr. Aslı HOCKENBERGER, Bursa Uludağ Üniversitesi

Prof. Dr. Gökhan GÖKTALAY, Bursa Uludağ Üniversitesi

Prof. Dr. Asım OLGUN, Bursa Uludağ Üniversitesi

Prof. Dr. Mustafa Erdem ÜREYEN, Eskişehir Teknik Üniversitesi

Doç. Dr. Ali KILIÇ, İTÜ

Doç. Dr. Burhan COŞKUN, Bursa Uludağ Üniversitesi

Doç. Dr. Ayşe ÇELİK BEDELOĞLU, BTÜ

Doktora Öğretim Üyesi, Şule SELÇUK, İTÜ

Doç. Dr. Hüseyin AVCI, Eskişehir OGÜ

Assist. Prof. Dr. Tamer HAMOUDA, National Science Foundation, Egypt

Assist. Prof. Dr. Ahmed HASSANIN, Egypt Japan University, Egypt

Assist. Prof. Dr. Abdelrahman ABDELGAWAD, NCSU, USA

Pınar Taşdelen ENGİN, Polyteks-Bursa

Gülşen TARDÜ, Polyteks-Bursa

Organizasyon Komitesi / Organization Committee

Prof. Dr. Yusuf ULCAY, Bursa Uludağ Üniversitesi

Prof. Dr. Ali DEMİR, İTÜ

Prof. Dr. Behnam POURDEYHIMI, NCSU, USA

Prof. Dr. Mohammad JAWAID, UPM, Malaysia

Prof. Dr. Kenan YILDIRIM, BTÜ

Prof. Dr. Mustafa Erdem ÜREYEN, Eskişehir Teknik Üniversitesi

Doç. Dr. Ali KILIÇ, ITÜ

Doç. Dr. Ayşe ÇELİK BEDELOĞLU, BTÜ

Doç. Dr. Hüseyin AVCI, Eskişehir OGÜ

Doktora Öğretim Üyesi Şule SELÇUK, İTÜ

Assist. Prof. Dr. Tamer HAMOUDA, National Science Foundation, Egypt

Assist. Prof. Dr. Ahmed HASSANIN, Egypt Japan University, Egypt

Assist. Prof. Dr. Abdelrahman ABDELGAWAD, NCSU, USA

Dr. İsmail BORAZAN, Bartın Üniversitesi

Araş. Gör. Rumeysa ÇELEN, Bursa Uludağ Üniversitesi

Araş. Gör. Gizem MANASOĞLU, Bursa Uludağ Üniversitesi

Araş. Gör. Nazlı ARMAN, Bursa Uludağ Üniversitesi

Araş. Gör. Yasin ALTIN, BTÜ

Araş. Gör. Ahmet AYDIN, BTÜ

Araş. Gör. Fatma Nur PARIN, BTÜ

Tuğba BAYSAL, İTÜ

Ömer Fırat TURŞUCULAR, Bursa Uludağ Üniversitesi

Merve Nur SAĞIRLI, İTÜ TEMAG Lab

6. Uluslararası Lif ve Polimer Araştırmaları Sempozyumu (6.ULPAS)

3 Mayıs 2019'da İTÜ, Gümüşsuyu Yerleşkesinde 5. ULPAS'ı "Medikal Tekstiller" vurgusuyla gerçekleştirdik. Böyle yapmamızın sebebi, bu sempozyumların ana unsurlarından birisi olan İTÜ'de Tekstil Teknolojileri ve Tasarımı Fakültesinde 30 yıldır faaliyet gösteren "İTÜ TEMAG Laboratuvarı"nın İstanbul Kalkınma Ajansı (İSTKA) destekli yürüttüğü bir proje olan "TR10/18/YMP/0075-MEDİTEKS: Medikal tekstiller Ar-Ge Merkezi"nin kuruluş lansman toplantısıyla birlikte gerçekleştirmekti. İyi de oldu. Sempozyum bu sayede daha farklı bir kitleye daha erişti.

6. ULPAS'da "uluslararası sempozyum" vurgusu ile ve sponsorlarımızın destekleriyle tüm dünyadan konularında öne çıkmış araştırmacıları davet ettik. Yurtdışından gelen bu davetlilerimizi sempoyumda "Ana Konuşmacı" yaptık ve oturumları da aşağıdaki gibi konulara göre düzenlemeye gayret ettik;
- Doku Mühendisliği - Medikal Tekstiller
- Nanoyapılar
- Nanolif Uygulamaları
- Nanolif Üretim Teknikleri – Electrospinning
- Kompozitler ve Doğal Elyaf Takviyetli Kompozitler
- Nonwovenlar
- Lif ve Tekstil Teknolojileri

Bu Bildiriler Kitabı sempozyum esnasında katılımcıların elinde olduğu gibi sempozyum internet sayfası (www.uludag.edu.tr/ulpas) adresinden önceki sempozyumların bildiri kitapları ile birlikte her zaman erişebilecektir.

6. Uluslararası Lif ve Polimer Araştırmaları Sempozyumu'nun da şimdiye kadar olduğu gibi başarılı, katılımcılara için yararlı ve ülkemiz için katkı verici olacağına inancımız tamdır.

Lif ve Polimer Araştırmaları Enstitüsü adına

Prof. Dr. Yusuf ULCAY

Prof. Dr. Ali DEMİR

6th International Fiber and Polymer Research Symposium (6th IF&PRS)

On the 3rd May 2019, we have organised the *5th International Fiber and Polymer Research Symposium (5th IF&PRS)* at İTÜ, Gümüşsuyu Campus-Istanbul with an emphasis on “Medical Textiles”. It was due to the fact that as the main components of these sysmposia, ITU TEMAG Lab had the first announcement meeting for their reserach and developmet Project “TR10/18/YMP/0075-MEDİTEKS: Medical Textiles R&D Center” supported by Istanbul Develeopment Agency (ISTKA). It was a real success and the symposium had a chance to reach a different audience.

As an international reserach and developemtn symposium, we have invited some distiguished researchers in the field of fiber and polymers from all over the world with the the kind financial support of our sponsors. Those internationally pionering names will be our “Keynote Spekers” during the symposium. We have also divided the papers into subject groups as follws;

- Tissue Engineering - Medical Textiles
- Nanostructures
- Nanofiber Applications
- Nanofiber Production Techniques – Electrospinning
- Composites and Natural Fiber reinforced Composites.
- Nonwovens
- Fiber, Polymer and Textile Technologies.

The book of proceedings will be available in printed form during the sysmposium. It can alos be accessed by the link (www.uludag.edu.tr/ulpas) together will all of the previous symposium Book of Proceedings.

As we have experienced so far, we believe that this 6th IF&PRS will also be another success story for all those who have attended as well as our beloved city for Istanbul as well as our country.

On behalf of the Fiber and Polymer Research Institute

Prof. Dr. Yusuf ULCAY

Prof. Dr. Ali DEMİR

İÇİNDEKİLER

Biomimetic Approaches to Tissue Engineering of Organoids

AVCI, Huseyin[1-3]
[1]Metallurgical and Materials Engineering Department, Eskisehir Osmangazi University, Eskisehir, Turkey, [2]Cellular Therapy and Stem Cell Research Center (ESTEM), Eskisehir Osmangazi University, Eskisehir, Turkey, [3]AvciBio Research Group, Eskisehir Osmangazi University, Eskisehir, Turkey www.avcibio.com
havci@ogu.edu.tr

PURPOSE

Recently, in vitro, ex-situ, and etc. methods have gained importance in tissue engineering approaches. Among these methods, the organ on a chip is a recently developed in vitro technique that has the potential to mimic human tissue or organs. On the other hand, textile techniques such as weaving, knitting and braiding using fiber-based scaffolds is a promising platform in tissue engineering. Here, we discuss how engineering efforts by research groups can generate the basis for the assembly on highly complex self-organizing cellular systems.

INTRODUCTION

Today, the treatment of diseases and the development of drugs are closely related to organ physiology and disease etiology with their complex relation. There is a critical need for improved models that can accurately predict the effects of drugs, chemicals and biological agents in the human body. Organ on a chip is a recently developed in vitro technique that has the potential to mimic human tissue or organs in a practical manner. In fact, more than one tissue or 3D organoids in microfluidics are brought together to form human on chip platforms[1-4]. Thanks to these platforms, the mechanical and physiological responses and interactions 3D and micro-dimensional structures in microfluidics can be investigated just like organs in the human body[5-7]. Some of the drugs withdrawn from the pharmaceutical market have been successfully used on these platforms to monitor the side effects as occurs in the human body.

On the other hand, the control of scaffold microarchitecture and mechanical properties to mimic intrinsic morphologies and functions of target living tissue is a crucial to obtain scale of human-sized, clinically effective tissues and organs. Tunable flexibility and structural stability are important parameters for the cells to provide necessary physical, chemical, and biological cues that determine cell growth and function. Depending on the application, the importance of certain mechanical properties of the biomaterials are more pronounced than others. For example, distinct and controlled elastic property is necessary for cardiac muscle and blood vessels, whereas the Young's modulus and strength become more significant for bone, tendons and ligaments.

In the present study, we will discuss a liver on a chip platform which is expected to have a very important milestone in drug development and medical field. In addition, a textile-based polymeric 3D braided structures for tissue-engineered muscle by using core-shell composite fibers (CFs) will be highlighted.

EXPERIMENTAL

Material

Gold-based microelectrode, polydimethylsiloxane (PDMS), chemicals for immobilization such as 11-mercaptoundodecanoicacid, N-Hydroxysuccinimide, streptavidine, biot-Ab, antijens (GST-α), primary human hepatocytes, GelMA and hydrogel were used for liver on a chip and tissue-engineered muscle structures[4,8].

Method

Briefly e-beam evaporation for electrode production, photo and soft lithography for bioreactor and microfluidics, 3D bioprinting for organoids, PrestoBlue® assay, BioTech UV/vis snergy 2 microplate reader, real-time PCR analysis were used[4,8].

EXPERIMENTAL RESULTS AND DISCUSSIONS

Recently, various studies have been conducted to obtain 3D liver micro-devices in different types of chips to investigate the potential side effects of drugs and treatments. In one of these studies, 3D liver organoid has been reported via microfluidic electrochemical (EC) biosensor chip designed for continuous measurement of soluble biomarkers secreted from the cells[4] (Figure 1). In this study, it was determined that hepatotoxicity can be developed by measuring the amount of albumin and GST-α secreted in the medium as a result of successful application of APAP as a model drug with impedance-based biosensors for running approximately one week. The obtained results were confirmed by cell viability and ELISA test results[4]. Here, the effect-response reactions that can be seen in vivo were performed by liver on chip platform without any animal and clinical studies.

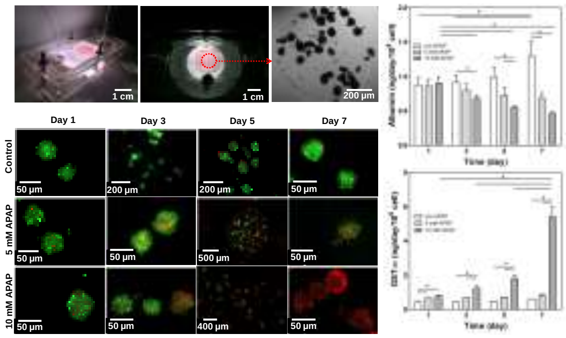

Figure 1. A photo image of liver cells developed in the bioreactor (top), fluorescence image of time-varying administration of APAP at different concentrations (bottom-left); time-varying drug concentration versus albumin and GST- α secreted from the cells (right)[4].

In another study, to obtain different braided structures, four fibers were attached to a single point and they were braided together with a control, all fibers were parallel, pattern. In the second step of the research, these braided patterns were again braided together with 16 (4x4) filaments per pattern (Figure 2) to control better mechanical properties of the patterns. Resulted fibers for engineering of skeletal muscles in which the core was obtained from biocompatible and/or biodegradable polymeric fibrils with a mechanically rigid property and the soft-shell portion from hydrogel containing living cells and other additives[8].

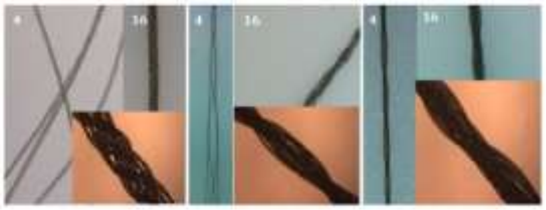

Figure 2. Microscopes images of braid patterns after hydrogel coatings from left to right: 1x1 and 2x2 biaxial; 1x1 triaxial patterns.

CONCLUSIONS

As a result, information obtained from living micro-structures produced with organ on chip platforms is expected to accelerate drug development and treatment of diseases with greatly reduce costs.

Textile braiding technique was demonstrated as a suitable platform to build muscle-like fibrous structures in a facile and highly reproducible with tuning the biomimetic architectures and mechanical properties.

SUGGESTION FOR FURTHER WORK

We are working on personalized organ on chip systems to investigate cancer environments and treatment. In addition, studies are being carried out on the constructions with controlled mechanical, biological and electrochemical properties in engineering tissues using weaving technique via cell-laden 'live' core-shell composite fibers.

ACKNOWLEDGEMENTS/SOURCES OF FUNDING

The author greatly thankful to Prof. Ali Khademhosseini for providing a great research environment. The author also would like to thank Profs. Mehmet R. Dokmeci, Su Ryon Shin, Yu Shrike Zhang and Ali Tamayol for their guidance and help. Dr. Avci would like to thank Scientific and Technological Research Council of Turkey (TUBITAK).

LITERATURE

1. Zhang, Y. S., Zhang, Y. N., & Zhang, W. 2017. "Cancer-on-a-chip systems at the frontier of nanomedicine", Drug Discovery Today, 22(9), 1392-1399.
2. Wainwright, O. Human 'organs-on-chips' could accelerate personalized medicine, eliminate animal testing. Guardian. 29 Haziran 2015.
3. Zhang, Y. S., Aleman, J., Shin, S. R., Kilic, T., Kim, D., Shaegh, S. A. M., Massa, S., Riahi, R., Chae, S., Hu, N., Avci, H....Atala, A., Khademhosseini, A. 2017. "Multisensor-integrated organs-on-chips platform for automated and continual in situ monitoring of organoid behaviors", Proceedings of the National Academy of Sciences, 114(12), E2293-E2302.
4. Shin, S. R., Kilic, T., Zhang, Y. S., Avci, H., Hu, N., Kim, D., ... Kang, J. 2017. "Label-free and regenerative electrochemical microfluidic biosensors for continual monitoring of cell secretomes", Advanced Science, 4(5), 1600522.
5. Esch, M. B., King, T. L., Shuler, M. L. 2011. "The role of body-on-a-chip devices in drug and toxicity studies", Annual Review of Biomedical Engineering, 13, 55-72.
6. Ghaemmaghami, A. M., Hancock, M. J., Harrington, H., Kaji, H., Khademhosseini, A. 2012. "Biomimetic tissues on a chip for drug discovery", Drug Discovery Today, 17(3-4), 173-181.
7. Avci, H., Guzel, F. D., Erol, S., Akpek, A. 2018. "Recent advances in organ-on-a-chip technologies and future challenges: a review", Turkish Journal of Chemistry, 42(3), 587-610.
8. Fallahi, A., Yazdi, I., Serex, L., Lasha, E., Faramarzi, N., Tarlan, F., …, Gomes, M. E. 2019. "Customizable composite fibers for engineering skeletal muscle models", ACS Biomaterials Science & Engineering.

Bioactive Polypropylene Nonwovens via Immobilization of Proteins-embedded Silver Nanoparticles

ABDELGAWAD, Abdelrahman; ROJAS, Orlando
[1]Aachen-Maastricht Institute for Biobased Materials, Maastricht, the Netherlands,
[2] Department of Bioproducts and Biosystems, Aalto University, Finland,
[3] Department of Forest Biomaterials, North Carolina State University, USA
a.abdelgawad@maastrichtuniversity.nl

PURPOSE

Multifunctional wound dressing based on PP nonwoven via immobilization of thrombin protein and silver nanoparticles to acquire hemostatic and antimicrobial properties.

INTRODUCTION

Patients who suffer from kidney failure and need to go for hemodialysis several times a week in order to remove body waste[1]. A flexible tube, catheter, is put into patient neck vein, below the collarbone. There is a high risk of infection due to the movement of the catheter or leakage of body fluids. A wound dressing or bandage is used to cover the catheter and keep the insertion site clean. A functional wound dressing is needed not only to prevent any bacterial growth and promote the granulation and growth of epithelial cells but also to stop any bleeding that might occu[2]. Passive dressings like cotton gauze and polypropylene (PP) nonwovens are being used widely as wound dressing. Soybean protien isolates (SPI) has been used to hydrophilize PP surfaces wth proven efficiency[3]. Silver nanoarticles is considered a very reliable and efficient antimicrobial agent. This might be attributed to their enormous surface to volume ratios and crystallographic surface arrangement for such small structure[4].

EXPERIMENTAL

Material

Soybean protein isolate, silver nitrate, thrombin from bovine, isopropanol, sodium hydroxide**,** and deionized water.

Method

A layer-by-layer technique was employed for the functionalization of PP surface. Firstly, a layer from soybean proteins will be absorbed on PP surface. Secondly, silver nanoparticles will be prepared in-situ during the denaturation of soybean protein and immobilized on PP surface. A third layer from thrombin protein, which is essential in blood clotting cascade, will be absorbed on the top to acquire hemostatic function. Pad-dry technique is being used for this experiment.

EXPERIMENTAL RESULTS AND DISCUSSIONS

Silver nanoparticles were prepared during the denaturation of Soybean Protein Isolates (SPI).

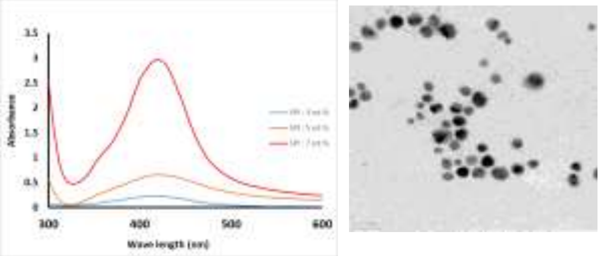

Figure 1. Uv-vis spectra TEM micrograph of silver nanoparticles prepared in soybean protein

Antimicrobial Activity of the SPI/AgNPs treated PP nonwovens were tested against E.coli. SEM images show no bacterial growth on treated samples.

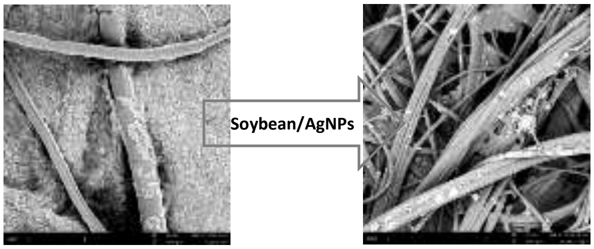

Figure 2. SEM image for E.coli grown on untreated PP nonwoven (left) and PP treated with SPI/Ag-NPs

Thrombin protein successfully immobilized on the surface of PP/SPI nonwovens. Thrombin retained its activity for 30 days after loading on the PP nonwovens and was released to the medium in adequate concentration. Fibrinogen was transformed to fibrin upon the release of thrombin to the medium.

Figure 3. Thrombin release leads to gelation of fibrin (fibrinogen formation)

CONCLUSIONS

Antimicrobial and hemostatic properties were acquired to the surface of polypropylene nonwovens through the immobilization of soybean and thrombin proteins. Silver nanoparticles were prepared in-situ during the denaturation of soybean protein. The functionalized nonwovens remained active for 30 days when stored at room temperature.

SUGGESTION FOR FURTHER WORK

Solvent free (solid state) and large scale synthesis of silver nanoparticles using soybean isolate. In addition, in-vitro blood coagulation assessment should be done on the treated PP nonwovens.

ACKNOWLEDGEMENTS/SOURCES OF FUNDING

The authors are thankful to the United Soybean Board of the United States for providing soybean isolates for the experiments.

LITERATURE

1-Abdelgawad, A. M., et al. (2014). "Antimicrobial wound dressing nanofiber mats from multicomponent (chitosan/silver-NPs/polyvinyl alcohol) systems." Carbohydrate polymers **100**: 166-178.

2-Kamoun, E. A., et al. (2017). "A review on polymeric hydrogel membranes for wound dressing applications: PVA-based hydrogel dressings." Journal of advanced research **8**(3): 217-233.

3-Mermel, L. A. (2000). "Prevention of intravascular catheter–related infections." Annals of internal medicine **132**(5): 391-402.

4-O'grady, N. P., et al. (2011). "Guidelines for the prevention of intravascular catheter-related infections." Clinical infectious diseases **52**(9): e162-e193.

Biofunctionalization of hydrogels for tissue engineering applications

AVCI-ADALI, Meltem[1]
[1]University Hospital Tübingen, Dept. of Thoracic and Cardiovascular Surgery, Tübingen, Germany
meltem.avci-adali@uni-tuebingen.de

PURPOSE

Functionalization of hydrogels for improved tissue regeneration

INTRODUCTION

Hydrogels are one of the most attractive biomaterials for tissue engineering, since they can be used to generate three-dimensional scaffolds to support the cell growth and to improve the healing of tissues [1].

EXPERIMENTAL

Material

For the generation of hydrogels, gelatin methacryloyl (GelMA) or circularized single-stranded DNA were used. VEGF binding aptamers were covalently incorporated into the hydrogels.

Method

Three-dimensional GelMA and DNA hydrogels were generated[2]. These hydrogels were functionalized with VEGF binding aptamers. The functionalization of the hydrogels with the aptamer was analyzed by application of FAM-labelled complementary oligonucleotides. The successful loading of hydrogels with VEGF was determined by using ELISA. The bioactivity of the VEGF in hydrogels was verified by incubation of HUVECs with hydrogels.

EXPERIMENTAL RESULTS AND DISCUSSIONS

The successful loading of the hydrogels with VEGF was demonstrated. Furthermore, improved angiogenesis was shown after the incubation with HUVECs. These results demonstrated the promising application possibilities of aptamers as capturing molecules in three-dimensional hydrogels.

CONCLUSIONS

The generation of aptamer-functionalized hydrogels has a huge potential for regenerative medicine. Aptamers against different targets can be applied to produce hydrogels with altered functions.

SUGGESTIONS FOR FURTHER WORK

In the future, three-dimensional structures will be generated using 3D printing technology. Furthermore, in vivo studies will be performed to verify the obtained in vitro results.

LITERATURE

1 Guan X, Avci-Adali M, Alarçin E, Cheng H, Kashaf SS, Li Y, Chawla A, Jang HL, Khademhosseini A. Development of hydrogels for regenerative engineering. Biotechnology journal. 2017, 12(5):1600394.

2 Stoll H, Steinle H, Stang K, Kunnakattu S, Scheideler L, Neumann B, Kurz J, Degenkolbe I, Perle N, Schlensak C, Wendel HP, Avci-Adali M. Generation of Large-Scale DNA Hydrogels with Excellent Blood and Cell Compatibility. Macromolecular bioscience. 2017, 17(4):1600252.

Biodegradable Polymers for Tissue Engineering

ARMAN, Nazlı [1], ULCAY, Yusuf[1]
Bursa Uludag University, Faculty of Engineering, Department of Textile Engineering
nazliarman@uludag.edu.tr

PURPOSE

Scaffolds are vital for tissue engineering researching. Through manufacturing technologies and studies to improve the properties of polymers biocompatible, scaffolds are made by more compatible with the body. In this article, considering the chemical structure of biodegradable polymers with their relationship with mechanical, biocompatibility, electrical conductivity properties will be examined.

INTRODUCTION

Accidents or various diseases result in tissue or organ losses that significantly affect human's lives. At this point, tissue engineering; provides interdisciplinary studies of health sciences and various engineering to improve or repair existing tissue functions. In therapeutic applications, the mimetic tissue may develop in the patient's body (in vivo), may also develop in the laboratory environment.

2. Polymers Used in Tissue Engineering

The extracellular matrix consists of various proteins and polysaccharides, providing physical support as well as providing organization of cells. The surface of the tissue scaffold to be produced must be considered for the specific chemical and morphological structure (extracellular matrix) for each cell to hold and proliferation. This review article will be discussed commonly used polymers in scaffold applications.

Aliphatic Polyester

Polylactic acid (PLA), polyglycolic acid (PGA), and copolymers of these polymers are poly (lactide-co-glycolide) (PLGA). They are degraded by hydrolysis of ester groups in their main chains. PGA is highly crystalline and rapidly soluble in water. The disadvantage is that it loses its mechanical strength considerably within 2-4 weeks of implantation. Degredation rate; molecular weight, the design of the tissue scaffold and the structure of the environment in which it is placed. PLA, the second most widely used biodegradable polymer, is more hydrophobic than PGA due to the extra methyl group in the structure, and thus loses its mechanical strength significantly, although it takes several years to degrade in the body completely. Poly (ε-caprolactone) (PCL) is a semi-crystalline material and has a rubbery behavior throughout the body since its glass transition temperature is about -60 ° C [3].

Polyurethanes

Due to the easy modification of the chemical structure of the polyurethane, which consists of two different segments (diisocyanate and polyol), materials with very different physical and biocompatibility properties, can be produced. The products formed as a result of degradation do not show toxic effects. In recent studies, it has been observed that by using amino acid-derived diisocyanate, more cells are attached and produced on the surface of the material than polyurethane produced by toluene diisocyanate. Today, artificial capillaries, cartilage and hard bone tissue, nerve tissue, and is used in areas such as drug transport [1,4].

Poly (glycerol sebacic acid)

The Langer research group synthesized it in 2002, during the search for new materials with better mechanical and chemical properties for soft tissue production. It is synthesized by condensation of glycerol and sebacic acid. It shows cross-linked elastomer behavior due to the hydrogen bond formed between hydroxyl groups. In order to adjust the rate of degradation by considering the characteristics of the target tissue to be imitated, curing time and temperature, monomer concentration, the ratio of acrylate group in the structure by changing the different properties of polyglycerol sebacic acid derivatives can be produced. It has various applications such as hard bone tissue, drug delivery [3].

CONCLUSİON

The studies in the field of tissue engineering are increasing day by day. It is predicted that the success rate will increase with the developments in the materials and production technologies whose properties are developed. Following the production of tissues such as vascular and nerve tissues, which are very difficult to imitate, the next stage is the production of artificial organs.

RESOURCES

1-Bergmeister H., 2014. "Biodegradable, thermoplastic polyurethane grafts for small diameter vascular replacements", Acta Biomaterialia, 2.
2-Christiaan L. E. Nijst, 2007. "Synthesis and Characterization of Photocurable Elastomers

from Poly(glycerol-co-sebacate)", Biomacromolecules, 3067-3073.

3-GUO BaoLin, 2014. "Synthetic biodegradable functional polymers for tissue engineering: a brief review", Science China Chemistry, 2.

4-Skarjia G. A., 2001. "In vitro degradation and erosion of degradable, segmented polyurethanes containing an amino acid-based chain extender", J. Biomater. Sci. Polymer Edn, Vol. 12, No. 8, pp. 851–873.

DESIGN AND DEVELOPMENT OF A PERSONALIZED MEDICINE ORIENTED MICROFLUIDIC ORGAN ON A CHIP PLATFORM

KIZILKURTLU, Ahmet Akif[1], AKPEK, Ali[1]
[1]Gebze Technical University
aliakpek@gtu.edu.tr

PURPOSE

The main purpose of the experiment was fabricating a novel skin-on-a-chip system via using PMMA plate that was consisting of ten layers with eight bolt and loafs insertion holes. Furthermore, two different GelMA-Sodium Alginate solution was prepared to be used as bio-ink for skin scaffold.

INTRODUCTION

Bringing a drug in health sector costs about 2 billion dollars and the process takes from 12 to 15 years. One of the most important step of these studies is preclinical testing, the other names is animal testing, which is also so crucial in cosmetic toxicity testing and disease modelling. Preclinical testing consists of two different implementations as in vitro analyses by using proper cell line models and in vivo studies via using animal models. All of these processes are conducted to determine not only validity and toxicity, but also pharmacokinetic and pharmacological characteristics testing to analyze the absorption, distribution, metabolism and excretion rate of the substance, which is crucial for detecting the he basic safety and potential usefulness of the drug (candidate). Eventually, the compounds that are passed the previous procedures are subjected to clinical trials (human trials) in order to specify the ultimate validity, effectivity, and usefulness of the drug. Although the investigation and researches on new drug candidates for acute, chronic and genetic diseases are being performed accelerando, the rate of finding successful and effective drug reagents is dramatically low [3, 5, 6]. That is because either lack of clinical efficacy or intolerable toxicity of the drug candidates during investigation process [2, 4]. Since the mentioned processes are expensive and time consuming [1], it is very important to detect the compounds that are potentially ineffective or have an unacceptable toxicity and dismiss in early stages of drug development. Therefore, development of in vitro cell-based testing methods are crucial and necessary to provide possibility to predict precisely for efficacy and safety of drug candidates. Cell cultures for both drug development and disease modelling can be categorized as 2D cell culture, 3D cell culture (involves 3D bio-printing technology), and microfluidic systems. Microfluidic systems that are most advanced discovery and the whole of the applications of engineering disciplines such as bioengineering, chemical engineering, and material engineering. These systems have demonstrated that they can be suitable candidates and platforms for drug development, cosmetic toxicity testing, and disease modelling implementation instead of animal models by the studies of organ-on-a-chip systems.

EXPERIMENTAL Material

The materials that were used in this study can be specified as: PMMA plate, 8 bolts, 8 loafs, injection pipe (silicon), Mouse fibroblast cells, micropipettes, confocal microscopy, glass-plastic petri dishes (120 x 15, 90 x 15), injectors (50 ml, 20 ml), syringe pump

Method

Fabrication of skin chip via using PMMA plate by utilizng laset etching machine. Production of skin scaffold by using GelMA- Sodium Alginate solution as bioink. Mouste fibroblast cell culture on skin scaffold that placed on skin chip. Utilizng Confocal microscopy for analyzing cell viability.

EXPERIMENTAL RESULTS AND DISCUSSION

The results of the experiments has shown that the skin chip system has demonstrated that it was more successful compared to petri dihes. The general composition of the scaffold was more stable in the chip, because the scaffold in petri dishes were torn apart in second day. Furhermore, detected amount of fibroblast cells were higher in the chip system. Besides, dead-alive cell ratio was better in the chip system. The chip system has proven that it was better and more effective against petri dish. Therefore it can be used as disease modelling, durg validity, effectivity, and cosmetic toxicicty testing. Figure 1 shows an example of cells in chip and Figure 2 shows an example of cells in petri. Figure 3 shows the detected amount of cells in the systems and Figure 4 shows the detected amount of dead-alive cell ratio.

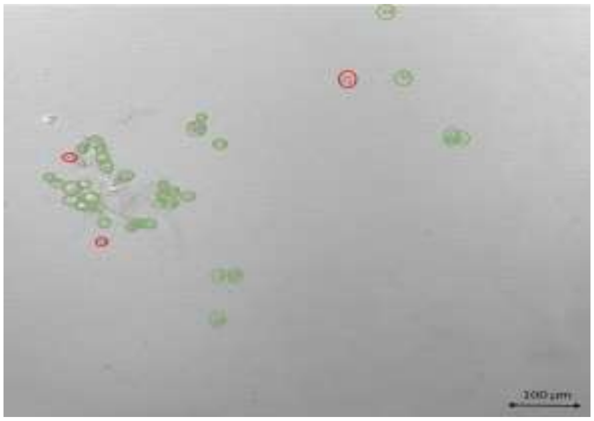

Figure 1, and image of second day image of cells in the microfluidic system

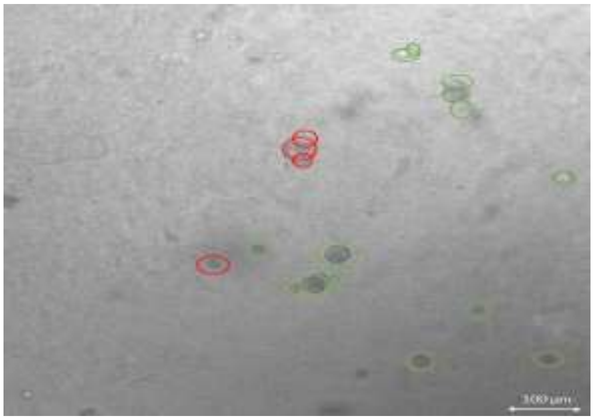

Figure 2, an image of second day image of cells in the petri,

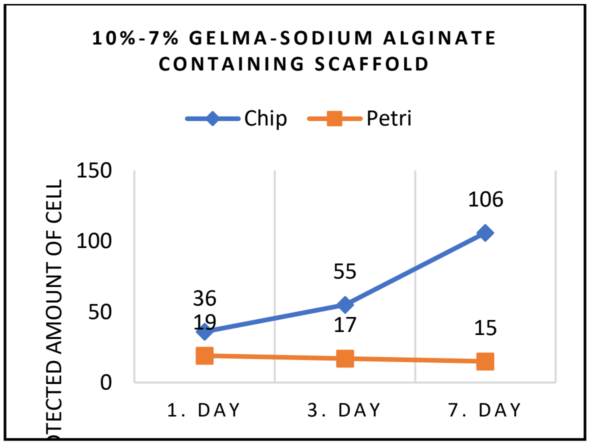

Figure 3, detected amount of the cells in the chip and in the petri

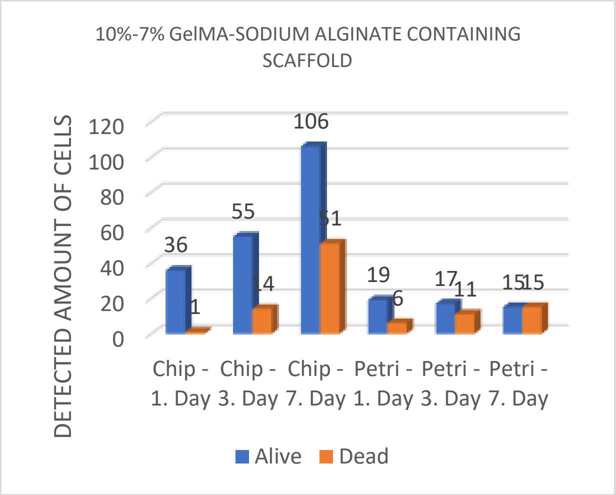

Figure 4, detected amount of dead-alive cell in 10%-7% GelMA-Sodium Alginate containing scaffold

CONCLUSION

In this study, PMMA was utilized as main material of the skin-on-a-chip. It was fabricated ten-layered structure. Eight hole in the same size were inserted in the system during the design in order to provide easy integration and disintegration for reproducibility. The bolts were used to integrate the layers of the chip. Besides, two different scaffolds were printed. The former one was comparing the chip system with glass petri with 7%-5% GelMA-Sodium Alginate mixture and the latter one was comparing the chip system with plastic petri with 10%-7%. Mouse fibroblast cells were used for cell culturing.

SUGGESTION FOR FURTHER WORK

The further and more detailed optimizations such as optimizing the cell chamber dimeter, width of the inlet and outlet channels, tighter integration of the layers and the flow rate of the medium from injection pump are the following objectives of this study. If the mentioned enhancements can be executed, the chip will have shown a great promise to use as a platform for drug delivery, toxicity, and effectivity testing instead of animal models , cosmetics toxicity testing, disease modelling and most importantly personal-oriented disease modelling.

LITERATURE

1. DiMasi, J.A., R.W. Hansen, and H.G. Grabowski, *The price of innovation: new estimates of drug development costs.* Journal of health economics, 2003. **22**(2): p. 151-185.
2. Hopkins, A.L., *Network pharmacology: the next paradigm in drug discovery.* Nature chemical biology, 2008. **4**(11): p. 682.
3. Hutchinson, L. and R. Kirk, *High drug attrition rates—where are we going wrong?* 2011, Nature Publishing Group.
4. Kola, I., *The state of innovation in drug development.* Clinical Pharmacology & Therapeutics, 2008. **83**(2): p. 227-230.
5. Kola, I. and J. Landis, *Can the pharmaceutical industry reduce attrition rates?* Nature reviews Drug discovery, 2004. **3**(8): p. 711.
6. Pangalos, M.N., L.E. Schechter, and O. Hurko, *Drug development for CNS disorders: strategies for balancing risk and reducing attrition.* Nature Reviews Drug Discovery, 2007. **6**(7): p. 521.

Enhancement of Mechanical Properties of Poly(lactic acid) by Blending with Epoxidized Natural Rubber

GUMUS, Omer Yunus[1], OZBAY, Ceren[2]
[1]Bursa Technical University, Department of Fiber and Polymer Engineering, Bursa, Turkey.
[2]Brisa Bridgestone Sabanci Tyre Manufacturing and Trading Inc., Material Development Department, Kocaeli, Turkey.
omer.gumus@btu.edu.tr

PURPOSE

In this study, imporovement in mechanical properties of poly(lactic acid) (PLA) is aimed by blending with natural rubber (NR). NR was epoxidized in order to ensure compatibility with PLA. Mechanical properties and optical microscope images of PLA blends with NR and epoxidized natural rubber (ENR) were comperativly investigated.

INTRODUCTION

Demand on polymeric materials have been increasing for decades due to their supreme properties over other class of materials such as lightness, corrosion resistance, easy processing, elasticity etc. The annual global production of polymers elevated from about 100 million tonnes in 1990 to 200 million tonnes and reached 350 million tonnes in 2017 (Nova Institute report). As a consequence of the unconscious consumption, polymeric wastes have become one of the main environmental problem for the planet. In recent years some measures and solutions have been seeking to overcome this issue. Usage of biodegradable polymers has been evaluated as one of the promising solution for the pollutions.

Beside the negative effect on the environment, petroleum based polymers have also some economical risks. Finite reservoir of crude oil and its fluctuating prices imposed by political inconsistencies may be shown as major reasons for the economic concerns. Bio based polymers can be considered as substantial alternative in terms of resource diversity. Hence decreasing of dependence on petroleum in polymer industry may sustain stability of the prices.

PLA is one promising polymer as it is both bio based and biodegradable. However, it is usage in many application is limited because of high brittleness. Many efforts have been done to remove this drawback of PLA. Preparation of blends and composites is the main strategy to enhance mechanical properties of PLA (Hedayati et al.) (Eselini et al.). However, in order to conserve bio material classification, all the materials used in blend or composite besides PLA should be also bio-based. In this sense, natural rubber (NR) with its high toughness is a good candidate for PLA blends. At that point, the weak compatibility of NR with PLA appears as a problem to achieve a homogenous structure in the blend.

To improve the miscibility between PLA and NR many study have been carried out in the literature. Cao et al. (Cao et al.) used cellulose nanocrystals as a compatibilizer for PLA/NR blends. In another work, Huang and coworkers prepared NR-PMMA copolymers to achieve homogeneity in PLA/ NR-PMMA/NR ternary blend (Huang et al.). Maleic anhydride (Klinkajorn and Tanrattanakul), multiwalled carbon nanotube (Desa et al.), PMMA-grafted-cellulose (Rosli et al.) were also used as a compatibilizer.

In this study, epoxidized natural rubber (ENR) was used as a toughening material for PLA. Firstly, ENR was obtained from NR. Then PLA/ENR blends were prepared. Morphological and mechanical properties of PLA/NR and PLA/ENR blends were investigated and the results were comparatively evaluated.

EXPERIMENTAL

Material

In this study NR (SVR3L grade) and PLA (NatureWorks Ingeo 4043D Natural) were used. H_2O_2 (50%) and glacial acetic acid were purchased from Sigma-Aldrich. Toluen, chloroform, acetone and methanol were purchased from Merck.

Method

ENR was obtained from reaction of NR with peracetic acid at room temperature.

Solution casting method was used to prepare the blend films.

Morphologies of the blend films were investigated by optical microscope. Mechanical tests were carried out by using SHİMADZU - AGS-X universal test instruments.

EXPERIMENTAL RESULTS AND DISCUSSIONS

In order to investigate miscibility of PLA with NR and ENR, optical microscope images of the blend films were recorded. As seen from Figure 1a, a phase separation occurred in %50PLA/NR blend film. This result clearly shows that there is not adequate compatibility between PLA and NR which results in a heterogeneous structure formation. A phase separation is not desired to achieve good mechanical properties. In contrast, formation of an entirely homogeneous structure was observed for %50PLA/ENR blend films. This result is attributed to the introduction of polar epoxy rings to the NR structure which enables a demanded interaction with ester moieties in the PLA structure.

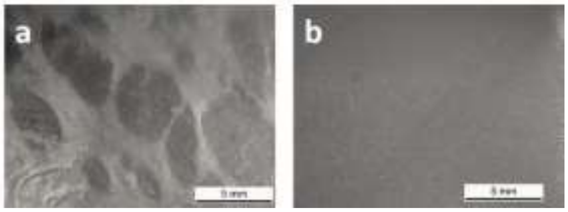

Figure 1. Optical microscope images of (a)%50PLA/NR, (b) %50PLA/ENR blend films

Stress and strain curves of the samples were given in Figure 2. It is clearly seen that stress and strain values of PLA/ENR blend at break is four and three times higher, respectively, than those of PLA/NR blend owing to the better miscibility and homogeneous structure.

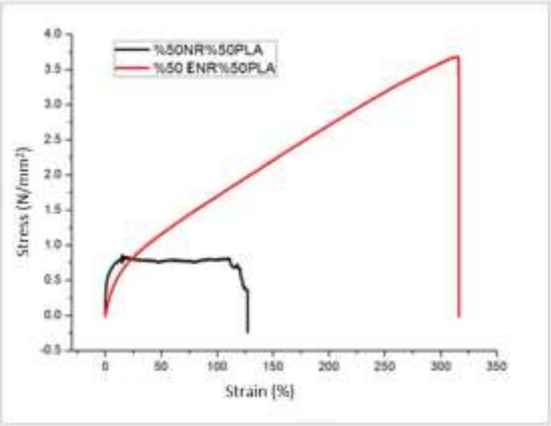

Figure 2. Stress and strain curves of %50PLA/NR and %50PLA/ENR blend films

CONCLUSIONS

PLA has better miscibility with ENR than NR, since interaction between polar moieties. Therefore, a homogeneous structure was achieved with PLA/ENR blend. PLA/ENR blend film exhibits better mechanical propertied than PLA/NR blend due to its homogenous structure.

SUGGESTION FOR FURTHER WORK

Blend films can be prepared with various PLA content. Thermal properties and crystallinities of the blends may also be investigated in order to further discuss mechanical properties.

ACKNOWLEDGEMENTS/SOURCES OF FUNDING

We are grateful to Scientific Research Projects Units of Bursa Technical University for the financial support (Project No: 172L21)

LITERATURE

Cao, L. M., C. Liu, D. J. Zou, S. D. Zhang, and Y. K. Chen. 2020. 'Using cellulose nanocrystals as sustainable additive to enhance mechanical and shape memory properties of PLA/ENR thermoplastic vulcanizates', Carbohydrate Polymers, 230: 8.

Desa, Mszm, A. Hassan, A. Arsad, and R. Arjmandi. 2019. 'Effect of core-shell rubber toughening on mechanical, thermal, and morphological properties of poly(lactic acid)/multiwalled carbon nanotubes nanocomposites', Journal of Applied Polymer Science, 136: 7.

Eselini, N., S. Tirkes, A. O. Akar, and U. Tayfun. 'Production and characterization of poly (lactic acid)-based biocomposites filled with basalt fiber and flax fiber hybrid', Journal of Elastomers and Plastics: 16.

Hedayati, F., N. Moshiri-Gomchi, M. Assaran-Ghomi, S. Sabahi, N. Bahri-Laleh, S. Mehdipour-Ataei, J. Mokhtari-Aliabad, and S. A. Mirmohammadi. 'Preparation and properties of enhanced nanocomposites based on PLA/PC blends reinforced with silica nanoparticles', Polymers for Advanced Technologies: 8.

Huang, J. M., W. J. Mou, W. T. Wang, F. Lv, and Y. K. Chen. 'Influence of DCP content on the toughness and morphology of fully biobased ternary PLA/NR-PMMA/NR TPVs with co-continuous phase structure', Polymer-Plastics Technology and Materials: 11.

Klinkajorn, J., and V. Tanrattanakul. 2020. 'Compatibilization of poly(lactic acid)/epoxidized natural rubber blend with maleic anhydride', Journal of Applied Polymer Science, 137: 9.

Rosli, N. A., I. Ahmad, F. H. Anuar, and I. Abdullah. 2019. 'Application of polymethylmethacrylate-grafted cellulose as reinforcement for compatibilised polylactic acid/natural rubber blends', Carbohydrate Polymers, 213: 50-58.

Tıbbi Plaster Kumaşı Üretimi İçin İplik Haşıl Kriterlerinin Araştırılması ve Performans Testleri

KOPTAGEL, Hüner[1], GÜRLER, Hale[1], TURGUT, Halil İbrahim[1]
[1]Harput Tekstil San. ve Tic. A.Ş., Ar-Ge Merkezi
huner.koptagel@harputtekstil.com.tr

AMAÇLAR

Çalışmada Türkiye'de üretimi yapılmayan ve ülkemize ithal olarak giren, yara üzerine yapıştırılarak mikroplardan koruyan tıbbi ipek görünümlü plaster kumaşının üretilebilmesi için ipek görünümlü selüloz asetat (CA) ipliğinin haşıllanma süreçleri çalışılmıştır.

GİRİŞ

Tekstilin tıp alanında kullanımı tıbbi tekstiller olarak bilinen yeni bir şubeye yol açmıştır[1]. Tıbbi tekstil malzemeleri, farklı elyaf ve tekstil yapılarına sahip çok çeşitli elyaf bazlı ürünleri içerir. Tıbbi tekstiller, tıbbi bir ortamda ya bir yaralanmanın tedavisi için ya da bir yaranın ya da bir hastalığın klinik tedavisinde uygun bir koşulun sağlanması için kullanılmaktadır[2].

Uygulamalara bağlı olarak, tıbbi tekstiller için ana gereklilikler emicilik, dayanıklılık, esneklik, yumuşaklık, biyouyumluluk ve zaman zaman biyolojik kararlılık veya biyobozunurluktur. Bu gereksinimler, çeşitli son kullanıcıların ihtiyaçlarını karşılamak için doğru yapılara sahip liflere ve tekstillere işlenmiş uygun polimerler kullanılarak karşılanır. Biyouyumlu, biyobozunur ve toksik olmayan doğal polimerlerin kullanımına yönelik genel bir hareket vardır [2].

Selüloz asetat (CA) lifleri yenilenebilirlik, non-toksik ve bozunabilirlik gibi avantajlara sahiptir. Ek olarak, CA elyafları mükemmel nem adsorpsiyonu ve nem serbest bırakma özelliklerine sahiptir. Bu nedenle, CA elyafları kullanım rahatlıkları ve ipek benzeri hisleriyle tanınmaktadır[3]. Selüloz asetatın çeşitli uygulamaları arasında tıbbi gazlı bez, kurdela, tabut astarı, ev eşyaları, dokuma kadife, dokuma satenler ve diğerleri sayılabilir. Ek olarak, ürün iyi tokluk, derin parlaklık ve yüksek şeffaflık sunar. Nem tutma ve bakteriyel türlere (Staphylococcus aureus, Escherichia Coli ve Candida albicans mayası) karşı antibakteriyel özellikleri nedeniyle yara pansumanlarında, kişisel hijyen ürünlerinde ve emici çamaşır ve mendillerde kullanılır. Uygulama segmentinde sigara filtreleri, fotoğraf filmleri, bantlar ve etiketler, gözlük çerçeveleri de yer almaktadır[4].

Bu çalışmada,biyobozunur özelliğe sahip çevre dostu, yenilenebilir ve sağlık açısından herhangi bir tehdit oluşturmayan selüloz asetat liflerine sentetik haşıl maddesinin aplikasyonu çalışılmıştır.

DENEYSEL

Malzeme

Çalışmada 50 denye ham parlak selüloz asetat lifleri ile çalışılmıştır. Dokuma yapısı oluşturabilmek için çözgü ipliklerine fiziksel ve yapısal olarak mukavemet kazandırılması için polyester reçine esaslı haşıl maddesi kullanılmıştır. Ayrıca SSM bobin aktarma makinesi kullanılmıştır.

Yöntem

Çalışmada 2 yöntem ile çalışılmıştır. Bunlar tek tel soğuk haşıl ve soğuk haşıldan sonra ısıtıcı yardımıyla kurutulması şeklindedir. Her iki yöntemde de farklı hız denemeleri yapılmıştır.
İplik numarası ISO 2060, iplik kopma mukavemeti ve uzama değerleri ISO 2062 standartlarına göre belirlenmiştir.

DENEYSEL SONUÇLAR/TARTIŞMA

Çalışma kapsamında asetat ipliğine işletme şartlarında haşıl teknesinde işlem yapılması öngörülmüştür. Haşıl teknesinde iş akışında temel adımlar çözgü hazırlama, haşıllama işlemi, haşıllı ipliğin kurutulması, haşıllanan ipliğin dokuma levendine sarımı şeklindedir. Ancak hem ipliğin 50 denye ve filamenti yapıda olması hemde otomasyon tabanlı tansiyonel sebeplerle çözgü hazırlıktan haşıl prosesine geçiş prosesinde başarılı olunamamıştır.
Bu sebeple selüloz asetat ipliğini tek tel halinde haşıllamak üzere arge çalışmaları başlatılmıştır. Öncelikle çalışmalar haşıl dairesinden iplik aktarma dairesine taşınmıştır. Bobin aktarma ünitelerinde, ipliğin sakal yapmasını,elektriklenmesini ve kopmasını engellemek amacıyla, içinin endüstriyel yağ ile dolu olduğu bir hazne mevcuttur.
Bu hazne içerisine polyester reçine esaslı haşıl maddesi konularak haşıl kimyasalının ipliğe aplike edilmesi sağlanmıştır.

Analizi yapılan numune (bobin dönüş hızı/yağ rulo dönüş hızı) (dev/dk)	Dtex	Uzama (%)	Mukavemet (cN/dtex)
Ham İplik	57,5	16,32	1,14
250/4	62	16,97	1,34
250/6	64,5	17,14	1,30
450/4	59,5	17,89	1,41
450/6	63	17,10	1,32

Tablo 1. Polyester reçine uygulanmış selüloz asetat ipliği test sonuçları

Analizi yapılan numune (bobin dönüş hızı/yağ rulo dönüş hızı) (dev/dk)	Dtex	Uzama (%)	Mukavemet (cN/dtex)
Ham İplik	57,5	16,32	1,14
250/4 infrared kurutmalı	64	18,10	1,32
250/6 infrared kurutmalı	63,5	14,58	1,24
450/4 infrared kurutmalı	62,5	16,78	1,26
450/6 infrared kurutmalı	64	18,22	1,32

Tablo 2. İnfrared kurutma sistemli polyester reçine uygulanmış selüloz asetat ipliği test sonuçları

Tablo 1 ve 2 de yapısına aynı haşıl malzemesi aplike edilmiş selüloz asetat ipliklerinin test sonuçları verilmiştir. Bobin sarım hızı ve yağ rulo hızlarında değişkilikler yapılarak yapıya alınan haşıl madde miktarının iplik mukavemetine etkisi gözlemlenmiştir.

Tablolar incelendiğinde 250/4 ve 450/4 denemelerinde mukavemet değerlerinin daha fazla iyileştiği görülmektedir. İnfrared kurutuculu sistemin ise iplik mukavemetine olumsuz yönde etki ettiği görülmüştür.

GENEL SONUÇLAR

Kateter, sargı bezi ve yara örtüsü gibi tıbbi malzemeleri cilt üzerine sabitlemek için üretilmesi amaçlanan selüloz asetat esaslı plasterin ilk ve en önemli adımı olan haşıl süreci verimli geçmiştir.

Bobin aktarma makinasında yapılan küçük değişikliklerin iplik mukavemeti ve uzama değerlerinde önemli ölçüde değişiklikler meydana getirdiği görülmüştür.

KAYNAKLAR

1 Vaishya, R. Agarwal, A. K. Tiwari, M. Vaish, A. Vijay, V. Nigam, Y. 2018. “Medical textiles in orthopedics: An overview”, Journal of Clinical Orthopaedics and Trauma, 9, 26-33.

2 Qin, Y. 2016. Medical Textile Materials. Woodhead Publishing.

3 Yuan W. Wu K. Liu N. Zhang Y. Wang H. 2018. “Cellulose acetate fibers with improved mechanical strength prepared with aqueous NMMO as solvent”, Cellulose, 25, 6395–6404.

4 “Cellulose Acetate Market 2019: by Type, by Type, by Application, by Region- Global Market Size, Share, Development, Growth, and Demand Forecast-2023”. https://www.marketwatch.com/press-release/cellulose-acetate-market-2019-by-type-by-type-by-application-by-region--global-market-size-share-development-growth-and-demand-forecast---2023-2019-03-27,

SONRAKİ DÖNEM ÇALIŞMALARI

Verimli geçen ipik haşıllama sürecinden sonra kontrüksüyonu tasarlanan plaster kumaşı dokuma prosesi gerçekleştirilmesi ve performans testlerinin bünyede bulunan test ekipmanları ile yapılması amaçlanmaktadır.

TEŞEKKÜR/BILGILENDİRME/FON KAYNAĞI

Çalışmada emeği geçen iplik büküm departmanına, iplik performans testlerinin yapılmasında destek veren Harput Tekstil çatısı altındaki Miranlı İplik firmamıza ve finansman sağlayıcısı olan Harput Tekstil San. Ve Tic A.Ş. ye teşekkürü borç biliriz.

Characterization Study of Drug Loaded PLA Electrospun Nanofibers

BARBAK, Zarife[1], KARAKAŞ Hale[1], SARAÇ, A.SEZAİ[2]
[1]Istanbul Technical University, Faculty of Textile Technologies and Design, ISTANBUL
[2]Istanbul Technical University, Faculty of Science and Letters, ISTANBUL
zadogan@itu.edu.tr

PURPOSE OF THE STUDY

This study was aimed to fabrication and characterization of silversulfadiazine (SSD) loaded poly(lactic acid) (PLA)/Polyetyleneoxide (PEO) composite nanofiber patches for drug delivery systems. The SSD loaded nanofibers were investigated by SEM and XRD.

INTRODUCTION

Nanofibers have unique properties such as high porosity, high surface area, imitating the Extra Cellular Matrix (ECM), formation of suitable conditions for cell proliferation and enabling drug delivery. Because of these desirable characteristics, nanofibers are widely used in biomedical applications such as wound dressings, drug delivery systems, scaffolds and artificial blood vessels **[1]**.

Drug-delivery systems consist of a formulation or a device that facilitates introduction of a drug in the body and enhances the treatment efficiency, supplies sufficient drug content in the blood during the release action and carries drug to target point safely and reduces side effects of release within the body **[2]**.

Silver sulfadiazine (SSD) is a non-ionised, water insoluble complex silver salt. SSD is used extensively in topical treatment of infected burns. However, the solubility problem of SSD lacks treatment efficiency. Thence, some authors focused on to increase the solubility of SSD with using different dosage forms **[3]**.

Hydrophilic / hydrophobic polymer blends have been electrospun into nanofibers to control of drug delivery. The hydrophobic polymer degrades slowly that makes release at a steady state whereas the hydrophilic polymer degrades rapidly that accelerates the drug release **[4]**. In this context, hydrophilic PEO and hydrophobic PLA were blended and utilized for controlled drug release.

PEO is a widely used polymer in drug delivery because of water solubility, low toxicity, biocompatibility and biodegradability. PEO interacts with the body fluid due to hydrophilicity quickly that results in degradation. PEO was utilized in the polymer matrix to enhance solubility and bioavailability of SSD due to its high water solubility. Furthermore, PEO provides homogenuous drug distribution **[5]**. While PEO is a hydrophilic polymer, PLA is a hydrophobic aliphatic polyester and has a renewable source, making it favorable for biomedical applications. Hydrophobicity of PLA provides long term degradation rate thus sustained and controlled drug release could be achieved **[6]**.

In this study, firstly process and solution parameters were optimized for the nanofiber production, SSD was used as a drug and added into the PEO solution. SSD was loaded into PEO. Then PEO+SSD and

PLA solutions were blended thus composite electrospun nanofibers were fabricated.

XRD analysis was performed with SSD loaded and pure nanofibers. Also surface morphology of nanofibers were carried out by SEM.

EXPERIMENTAL

Materials

Poly (lactic acid) (PLA), Polyetileneoxide (PEO) Silversulfadiazine were purchased from Sigma Aldrich.

3,5% PEO solution was prepared in Acetonitrile/acetic acid. SSD was loaded into 3.5% PEO solution at a concentration of 12%, respect to the PEO polymer. 6% PLA solution was prepared in Acetonitrile/Chloroform. Finally, to obtain a homogenous blend solution, PLA and SSD loaded PEO solutions were mixed 7:3 (w/w).

Method

Electrospinning method was used to produce nanofibers. Electrospun nanofibers were fabricated with 14 kV high voltage and 1 mL/h feeding rate. The grounded electrode plate was utilized as a collector with a fixed distance from the tip to the collector (12–14 cm).

EXPERIMENTAL RESULTS AND DISCUSSION

SEM images show that (Figure 1), SSD loaded smooth and bead free nanofibers were obtained. PEO fiber diameter decreases from 330 to 290 nm with the addition of SSD. This is related to the conductive nature of SSD. When SSD was added into the polymer solution, the electrical conductivity of the polymer jet increases that resulting in smaller fiber diameters. Otherwise, there are bead defects in native PLA however smooth, uniform, bead free fibers were obtained in PLA/PEO+SSD composite nanofiber morphology (Figure 2). This indicates that blend of PLA, PEO and SSD molecules have good interaction in the fiber structure. Moreover, SSD was dissolved and distributed in PLA/PEO matrix perfectly.

XRD analysis was carried out to determine the crystallinity of the SSD loaded into the nanofibers. XRD pattern of silver sulfadiazine loaded PEO nanofibers and pure PEO nanofibers shown in Figure 3. The diffraction pattern of SSD loaded nanofibers showed the microcrystalline nature of SSD, as indicated by the distinctive peaks at 9.7-10,4° and 19,3°**[7,8]** .

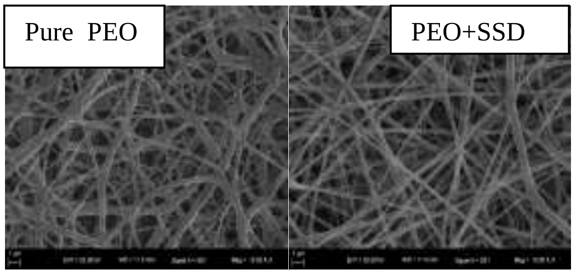

Figure 1. SEM Images of Pure and SSD loaded PEO nanofibers

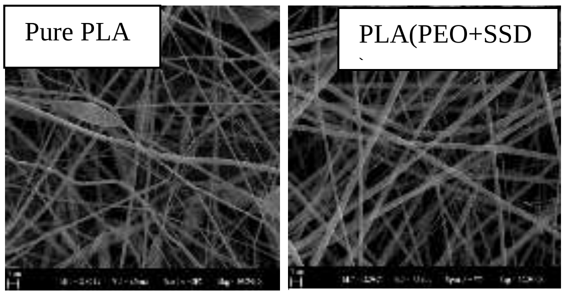

Figure 2. SEM Images of a) Pure PLA b) SSD loaded PLA/PEO (7:3) Composite Nanofiber

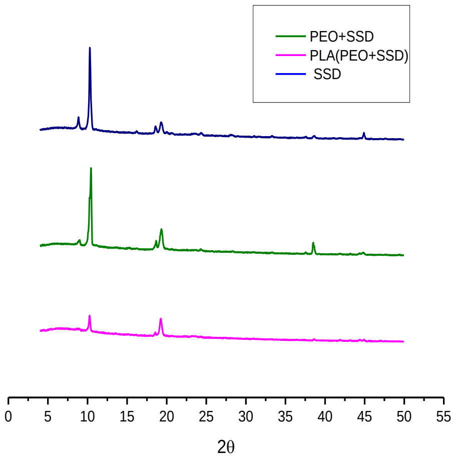

Figure 3. XRD Pattern of Pure SSD, (PEO+SSD) and PLA (PEO +SSD) nanofibers

CONCLUSIONS

Insoluble SSD was loaded into the electrospun nanofibers successfully. SEM images showed that; smooth, uniform and bead free composite PLA(PEO+SSD) nanofibers were fabricated. Decreasing fiber diameter is related to the increased in electrical conductivity because of the SSD charged particles. The XRD patterns confirmed the microcrystalline structure of SSD in the PEO nanofibers. Thereby first steps were taken to a new formulation for topical drug delivery.

FUTURE WORK

Experimental studies showed that composite PLA/PEO nanofibers can be good candidates for topical drug delivery systems. In future studies, in vitro drug release studies will be carried on.

ACKNOWLEDGMENT

This study was supported by Istanbul Technical University Scientific Research Project (ITU-BAP).

REFERENCES

[1] Dash K. T., Konkimalla B. V.(2012). ‘’Poly-ϵ-caprolactone based formulations for drug delivery and tissue engineering:A review’’, Journal of Controlled Release 158, 15–33

[2] Zamani, M., Prabhakaran, P. M., Ramakrishna, **S.** (2013). Advances in drug delivery via electrospun and electrosprayed nanomaterials, *International Journal of Nanomedicine*, 8, 2997–3017

[3] White R. J., Cooper R.,(t.y.). ‘’Silver sulphadiazine: A review of the evidence’’, Wounds UK 51-61

[4] Nagam Hanumantharao, S., & Rao, S. (2019). Multi-functional electrospun nanofibers from polymer blends for scaffold tissue engineering. *Fibers*, *7*(7), 66. blend

[5] Dubey P. and Gopinath P. (2016). ‘’Fabrication of electrospun poly(ethylene oxide)– poly(capro lactone) composite nanofibers for co-delivery of niclosamide and silver nanoparticles exhibits enhanced anti-cancer effects in vitro’’, Journal of Materials Chemistry B,4, 726-742

[6] Tyler, B., Gullotti, D., Mangraviti, A., Utsuki, T., & Brem, H. (2016). Polylactic acid (PLA) controlled delivery carriers for biomedical applications. *Advanced Drug Delivery Reviews*, *107*, 163-175**.**

[7] Aguzzia C., Sandri G., Bonferoni C., Cerezo P., Rossi S., Ferrari F., Caramella C., Viserasa C. (2014). ‘’Solid state characterisation of silver sulfadiazine loaded onmontmorillonite/chitosan nanocomposite for wound healing’’, Colloids and Surfaces B: Biointerfaces 113 152– 157

[8] Ghodekar S. V., Chaudhari S.P., Ratnaparakhi M.P.(2012). ‘’Development And Characterization Of Silver Sulfadiazine Emulgel For Topical Drug Delivery’’, Int J Pharm Pharm Sci, 4, 4, 305-316

Photocatalytic Activities of ALD (Atomic Layer Deposition) TiO_2 and ZnO films on Glass Fabrics

Islam, Shafiqul [1], Akyıldız, Halil I[1]
[1]Bursa Uludag University, Department of Textile Engineering
shafiqislam94@gmail.com

PURPOSE

The photocatalytic activities of TiO_2 and ZnO thin films fabricated on glass fabrics by atomic layer deposition were investigated for possible environemental applications.

INTRODUCTION

Important environmental elements such as water, air and soil are contaminated, which is damaging the ecological balance on earth. Among them water is the most essential element for life cycle of all living species. Fresh water sources has been contaminated by industries and agricultural activities leaving hazardous waste such as pharmaceuticals waste, pesticide, herbicides, textile dyes, resins, and phenolic compounds[1,2]. Various methods have been proposed to treat waste waters but cheaper and less time consuming is the prime interest in this matter. Among the porposed techniques are adsorption on activated carbon, ultrafiltration via reverse osmosis, coagulation by chemical agents, ion exchange on synthetic adsorbent, etc. These methods can remove the pollutant from the water without changing the toxicity of them. The photocatalytic method offers a way to eliminate the organic pollutants out of waste water, ideally using sunlight as a stimulant and reducing toxicity of the componuds by reducing or oxidizing them. Semioconductor metal oxides like TiO_2 and ZnO have the ability to create radical species upon absorption of the light[3,4]. Performance of a catalytic material increases with increasing surface area. Therefore many photocatalysis studies being conducted on nanoparticle materials requiring removal of the particles from water. As a solution to the problem thin film materials of photocatalytic materials can be coated on high surface area substrates such as textiles.

Thin film materials can be formed via chemical vapor deposition (CVD) and physical vapor deposition techniques. Atomic layer deposition (ALD) is a CVD technique in which highly conformal films can be created even on high surface area substrates due to self liiting nature of the reactions. ALD also provides precise thickness and composition control during film formation making the technique advantegous over other thin film methods[5]. In this study, phocatalytic activities of TiO_2 and ZnO films deposited on glass fiber fabrics via ALD. Especially effect of annealing on photocatalytic activity as well as structure of the films was investigated.

EXPERIMENTAL

Material

Glass fabric, fused quatrz, silicon wafer and glass slide was used as substates. Tetrakis (Dimethylamido) Titanium (TDMAT) and Diethyl Zinc (DEZ) were used as ALD precursors for TiO_2 and ZnO respectively. Water was used for all thin films as oxygen source.Methylene blue (MB) was used as the organic pollutant for photocatalytic activity tests.

Method

A 300W solar simulator (UVA) and a 100W UV were used to as light sources of photocatalytic test. ALD thin film deposited glass fabrics were placed into 50 ml of MB (5×10^{-5} M) solution placed 10 cm below the light source. UV-Vis spectrophotometer (Shimadzu 3600) was used to measure the relative concentration (c/c_0) change of MB. Absorption spectra of the materials were obtained using same spectrophotometer.

RESULTS AND DISCUSSIONS

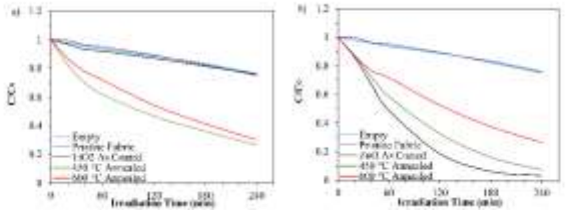

Fig 1: Photocatalytic activity of a) TiO_2 ALD thin film b) ZnO ALD thin films under solar simulator.

Photocatalytic activity of approximately 10 nm of TiO2 and ZnO films before and annealing is given in Figure 1. As coated TiO2 film shows no photocatalytic activity attributed to the amorphous nature of the ALD TiO2 films.After annealing TiO2 films photocatalytic activity first increases then decreases slightly suggesting the annealing as annealing temperatures increases either larger crsytals are forming or phase is changing[6]. As coated ZnO show highiest photocatalytic activity since films are crystalline. Upon annealing photocatalytic activity decreases which is attributed to the growth of the crystal grains therefore reducing the defect sites such as grain boundaires.[7,8]

CONCLUSIONS

ALD coated fabrics substrates showed promising photocatalytic activity. Annealing of the films crsytallize the films in some cases increasing the photocatalytic activity. However annealing at very high temperatures can have adverse effect on the photocatalytic activity. Changes in photocatalytic activity can be explained by the changes in the optical properties of the films.

ACKNOWLEDGEMENTS/SOURCES OF FUNDING

Authors acknowledge and would like to thank for partial funding from Bursa Uludag University (Bilimsel Araştırma Projeleri, OUAP-2018/7) and TUBİTAK (Project Numbers; 118M617 and 218M275).

LITERATURE

1. Chong, M. N., Jin, B., Chow, C. W., & Saint, C. (2010). Recent developments in photocatalytic water treatment technology: a review. *Water research*, *44*(10), 2997-3027.
2. Gupta, V. K., Ali, I., Saleh, T. A., Nayak, A., & Agarwal, S. (2012). Chemical treatment technologies for waste-water recycling—an overview. *Rsc Advances*, *2*(16), 6380-6388.
3. Lee, C. S., Kim, J., Son, J. Y., Choi, W., & Kim, H. (2009). Photocatalytic functional coatings of TiO2 thin films on polymer substrate by plasma enhanced atomic layer deposition. *Applied Catalysis B: Environmental*, *91*(3-4), 628-633.
4. Di Mauro, A., Fragalà, M. E., Privitera, V., & Impellizzeri, G. (2017). ZnO for application in photocatalysis: from thin films to nanostructures. *Materials Science in Semiconductor Processing*, *69*, 44-51.
5. Johnson, R. W., Hultqvist, A., & Bent, S. F. (2014). A brief review of atomic layer deposition: from fundamentals to applications. *Materials today*, *17*(5), 236-246.
6. Sugapriya, S., Sriram, R., & Lakshmi, S. (2013). Effect of annealing on TiO2 nanoparticles. *Optik-International Journal for Light and Electron Optics*, *124*(21), 4971-4975.
7. Raoufi, D., & Raoufi, T. (2009). The effect of heat treatment on the physical properties of sol–gel derived ZnO thin films. *Applied Surface Science*, *255*(11), 5812-5817.
8. Umar, A., Kumar, R., Kumar, G., Algarni, H., & Kim, S. H. (2015). Effect of annealing temperature on the properties and photocatalytic efficiencies of ZnO nanoparticles. *Journal of Alloys and Compounds*, *648*, 46-52.

IMMOBILIZATION OF CU-BTC ON THE COTTON FIBERS FOR SENSOR APPLICATIONS

SAYGI, Gizem[1], ÇAKICIOĞLU ÖZKAN, Fehime[1], GÜNER, Cemal[1]
[1]Izmir Institute of Technology, Department of Chemical Engineering, İzmir, Turkey
gizemsaygi@iyte.edu.tr

PURPOSE

The aim of this study is to synthesize Cu-BTC and immobilize onto the cotton fabric using for sensor activity. The chemical sensing property of Cu-BTC deposited cotton aganist NH_3 gas was studied.

INTRODUCTION

Metal-organic frameworks (MOFs) which are prepared in the form of one, two or three-dimensional networks using inorganic salts and multidentate organic linkers have recently gained considerable attention due to their large surface areas, large internal pore volume and ability to bear various functionalities. Due to these reasons, MOFs have a wide range of application areas such as gas storage, sensor, adsorption/separation, and catalysis. They could be prepared in some various forms such as beads, pellets and thus, a low-pressure drop and high performance could be obtained in the industrial applications [1,5].

The detection of toxic chemicals is a significant issue to protect people to prevent the inhalation of toxic chemicals. If the toxic chemicals were not detected, then many people could be affected from the toxic chemicals. MOFs have chemical sensing properties and they could be used to detect several hazardous gases such as ammonia, chlorine, cyanogen chloride, hydrogen sulfide, nitrogen dioxide, nitrogen oxide, sulfur dioxide, phosphine, arsine, radon [6].

Cu-BTC has ability to interact with chemicals so that it has chemical sensing property. Cu-BTC is used to detect the hydride gases which are ammonia, arsine, and hydrogen sulfide [3]. Hazardous gases which are sulfur dioxide, chlorine, radon, cyclohexane, tetrahydrothiophene, benzene, toluene, dichloromethane, and ethylene oxide are also detected by Cu-BTC [6].

The deposition of Cu-BTC on different substrates provides an easy way to use for sensor activity in various fields. The deposition of Cu-BTC on different substrates could be obtained by solvothermal and non-solvothermal processes [7]. Before the deposition process, sometimes the surface of the support material should be charged with required ions to increase the effectiveness of the deposition process. For deposition of the Cu-BTC, carboxymethylation is used to obtain a suitable charge on the surface of cellulose substrates [2].

Pinto et al.[4] deposited Cu-BTC on cotton, a cellulosic fibrous, substrate and then tested for gas selectivity and toxic chemicals removal. In order to investigate the importance of carboxylate groups onto the surface of anionic cellulose. According to the results, the attachment of Cu-BTC on the cotton surface was obtained successfully and the order of addition of $Cu(OAc)_2$-copper acetate, BTH3 [4].

In this study, Cu-BTC was deposited onto the cotton fabric to investigate the sensing properties. Cotton fabric consists of cellulose which is an abundant material in nature. A characterization study was performed to comprehend whether the deposition of Cu-BTC was achieved successfully or not. Cu-BTC deposited cotton fabric was characterized by XRD, SEM, and ATR-IR analysis to investigate the crystalline structure, surface morphology and framework vibration of all samples, respectively.

EXPERIMENTAL

Material

Cotton fabric were purchased from Viking Kağıt ve Selüloz A.Ş. Copper (II) nitrate trihydrate, trimesic acid, ethanol, N-dimethylformamide (DMF), sodium hydroxide and sodium chloroacetate were obtained from Emsure, Sigma Aldrich and Merck.

Method

In order to deposite Cu-BTC on cotton fabric, firstly, the cotton fabric was carboxymethylated to obtain anchoring points. Then, Cu-BTC was immobilized onto the cotton fabric using layer by layer method.

EXPERIMENTAL RESULTS AND DISCUSSIONS

The Cu-BTC was deposited onto the cotton fibers successfully. SEM analysis shows that Cu-BTC crystals were orderly distributed along the cotton fabrics (Figure 1). Additionally, the surface of the cotton fabric was intensely covered with Cu-BTC crystals.

The effect of deposition cycle number for layer by layer method on the amount of deposited Cu-BTC on cotton fabrics was investigated and the optimum cycle number was chosen as 10.

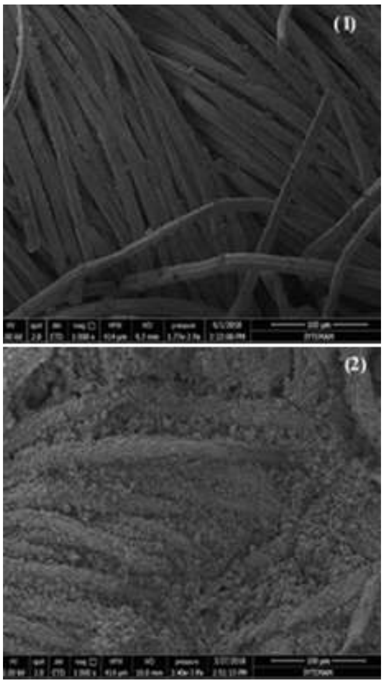

Figure 1. SEM micrographs of the cotton fabric (1) and Cu-BTC deposited cotton fabric (2).

Cu-BTC deposited cotton fabrics have initially light blue color. After NH_3 exposure, the color of the Cu-BTC deposited cotton fabrics changed and their color turned to dark blue (Figure 2). Therefore, they have NH_3 sensing property.

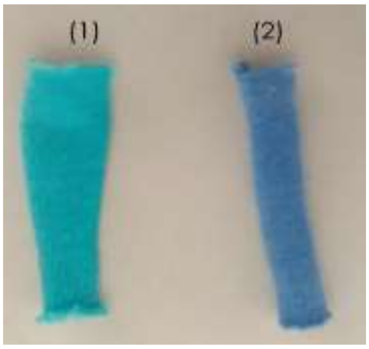

Figure 2. Cu-BTC deposited cotton fabric (1), NH_3 exposed Cu-BTC deposited cotton fabric (2).

CONCLUSIONS

Cu-BTC was synthesized and immobilized onto the cotton fabric. Consequently, the results of the characterization study revealed that the Cu-BTC was deposited on the cotton fibers successfully. The optimum cycle number of layer by layer method was found as 10. Besides, their sensing properties against the NH_3 gas was investigated. The Cu-BTC deposited substrates showed sensing activity against NH_3 gas.

REFERENCES

1. Abdelhameed, R. M.; Emam, H. E. ; Rocha, J. ; Silva, A. M. S. 2017. "Cu-BTC Metal-Organic Framework Natural Fabric Composites for Fuel Purification", Fuel Processing Technology, 159, 306-312.
2. Küsgens, P., et al. 2009. "Characterization of metal-organic frameworks by water adsorption", Microporous and Mesoporous Materials 120(3), 325-330.
3. Peterson, G. W. ; Britt, D. K. ; Sun, D. T. ; Mahle, J. J. ; Browe, M. ; Demasky, T, ; Smith, S. ; Jenkins, A. ; Rossin, A. 2015. "Multifunctional Purification and Sensing of Toxic Hydride Gases by CuBTC Metal-Organic Framework", Industrial & Engineering Chemistry Research, 54, 3626-3633.
4. Pinto, S. ; Augusto, C. ; Hinestroza, J. P. 2012. "In Situ Synthesis of a Cu-BTC Metal–Organic Framework (MOF 199) onto Cellulosic Fibrous Substrates: Cotton", Cellulose, 19, 1771-1779.
5. Siegle, S.; Kaskel, S. 2009. "Crystal Growth of the Metal-Organic Framework $Cu_3(BTC)_2$ on the Surface of Pulp Fibers", Advanced Engineering Materials, 3, 93–95.
6. Woellner, M. ; Hausdorf, S. ; Klein, N. ; Mueller, P. ; Smith, M. W. ; Kaskel, S. 2018. "Adsorption and Detecdion of Hazardous Trace Gases by Metal-Organic Frameworks", Advanced Materials, 30, 1346-1370.
7. Zhuang, J.; Kind, M. ; Grytz, C. M. ; Farr, F. ; Diefenbach, M. ; Tussupbayev, S. ; Holthausen, M. C. ; Terfort, A. 2105. "Insight into the Oriented Growth of Surface-Attached Metal−Organic Frameworks: Surface Functionality, Deposition Temperature, and First Layer Order", Journal of the American Chemical Society, 137, 8237-8243.

One-step preparation and characterization of a nanostructured hybrid electrode material through a microwave energy-based approach

POYRAZ, Selçuk[1]
[1]Department of Textile Engineering, Faculty of Engineering, Adıyaman University, 02040 Adıyaman/TURKEY
spoyraz@adiyaman.edu.tr

PURPOSE

To prepare a hybrid electrode material (HEM) composed of carbonized conducting polymer (CP), e.g. polypyrrole (PPy), nanofibers (CNFs) decorated with nanostructured zinc oxide (nano-ZnO) and carbon nanotubes (CNTs) through a one-step, hassle-free, rapid and highly efficient microwave (MW) energy-based approach.

INTRODUCTION

The growing global demand for clean and renewable energy,[1] the gradual exhaustion of natural fossil fuel sources,[2] and common concerns about the air pollution and global warming issues[3] have stimulated the academic and industrial societies to spend intense research efforts on both the development/improvement of efficient energy storage devices and on sophisticated energy conversion systems from available natural sources.[4] In this context, the electrochemical energy storage systems, i.e. supercapacitors (SCs),[2,3,5-9] have attracted a great deal of attention, and in recent years, they have gained a great technological significance[10] upon emerging as an ideal frontline technology[11] to answer these needs and concerns. An ideal hybrid SC[13,14] is mainly composed of both the electric double-layer carbon (EDLC)-based electrode materials with high surface area, conductivity and chemical stability,[2,13] and also the pseudo-capacitor (PC) ones with much higher specific capacitance,[10-12] but with much lower stability and conductivity.[8,12-14] The logic behind the nanostructured synthesis of all these materials lies beneath the great enhancement opportunity of their final performance in SCs as the active electrode materials. For instance, PPy and ZnO-based electrodes have been observed to exhibit many-fold increases in their capacitive properties if they possess nanostructured morphologies. However, most of the synthetic approaches to obtain these materials in nano-size, have the potential drawbacks of being; (i) wet-chemistry dependent (involving volatile organic solvents, harsh acids/bases, hazardous reducing agents and potential impurity carry-overs), (ii) time consuming, and (iii) having multiple steps with high temperature and pressure requirements.[12,20,21] As an attempt to tackle such drawbacks in synthetic approaches and to lower the electrode material fabrication costs,[13] in recent years, people have come up with the idea of using MW energy,[10,19] which have emerged as an affordable, facile, versatile and promising one-step alternative, based on heating the MW energy absorbing polar reactants up to elevated temperatures within very short time frames. In order to fully benefit from all different components in one hybrid nano-architecture,[22] in this study, a HEM with accrued advantages,[11] i.e. the EDLC property of CNTs and PC properties of both nano-ZnO and PPy NFs, was prepared through a well-established and universal one-step MW energy-based approach called Pop tube.[23] It was reasonably envisaged[18] and speculated that the as-prepared nanostructured HEM would exhibit enhanced; (i) energy density (via the synergistic contribution of its each component's electro-active features),[1,6,11-13,15] and (ii) power density values (by providing an efficient solution for the common electrolyte ion diffusion problem). Last but not the least, other significant advantages of the one-step MW energy-based approach can be summarized as being; (i) sustainable,[15,21] (ii) commercially viable,[11] (iii) wet-chemistry free,[12] (iv) affordable, (v) easily tunable/scalable for industrial level,[2,12] and (vi) being able to fabricate intimately connected HEMs for the next-generation SCs. Thus, the nanostructured HEM obtained from this approach is aimed to be the material of preference for relevant applications.

EXPERIMENTAL

Material

The materials used in this study include; pyrrole (98%), ammonium peroxydisulfate (APS, 98%, $(NH_4)_2S_2O_8$), and ferrocene (99%, $Fe(C_5H_5)_2$) from Alfa Aesar, zinc acetate dihydrate (ZAD, $Zn(CH_3COO)_2.2H_2O$) from EMD Chem. Inc., HCl, acetone, and potassium hydroxide (KOH) from J. T. Baker, colloidal graphite paste (isopropanol base) from Electron Microscopy Sciences. V_2O_5 sol-gel NF seeds were prepared based on a previously reported method[24] by using ammonium metavanadate (NH_4VO_3, 99.5%) from Acros Organics and Dowex Marathon (H) ion exchange resin from Sigma Aldrich in DI water.

Method

In a standard process, firstly, 70 mg of the as-synthesized HCl-doped PPy NF powder and 70 mg ferrocene were placed in a capped 10 mL plastic cup and blended in a speed mixer at 3500 rpm for 2 min. Next, this mixture was flatly laid at the bottom of a glass vial and then its surface was homogenously powdered with a 100 mg of fine ZAD in the form of a secondary white layer. After that, the glass vial was loosely capped and placed into the MW chamber for a short-time heat treatment that lasted for 30, 60 or 120 s (Figure 1). Within 10 s of the heating process the mixture was started smoking and arcing, respectively, and then it continuously glowed red hot inside the glass vial for the rest of the process time.[22-26] Eventually, the darkened glass vial was taken out of the MW and left to cool down to room temperature. Finally, the dark residue with a grayish tint was gently collected from the glass vial bottom, and then mixed for 5 min in a speed mixer to achieve homogeneity. The as-obtained product was then stored for further structural and electrochemical characterization steps.

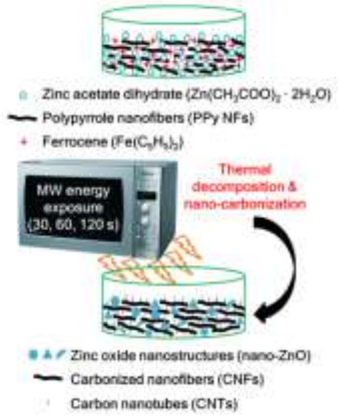

Figure 1. Schematic illustration of one-step HEM preparation via MW energy-based approach

RESULTS AND DISCUSSION

The as-prepared HEMs' both morphological and electrochemical characterization test results are shown in Figure 2. Here, increased process times allow the Fe catalyst core in ferrocene to remain its activity for a longer period, and to direct more graphene layers' growth from the C shell surrounding it.[27-29] In good agreement with this situation, thicker (up to ~2 μm) and much longer (>10 μm) earth worm-like CNTs were grown on the 120 s MW processed HEM sample's surface, as can be seen in Figure 2(top/left).[22,30,31] The as-prepared HEMs' in-depth microstructural characteristics were identified by the TEM image shown in Figure 2(top/middle). Here, the nano-ZnO filled CNFs are observed along with hexa/heptagonal nano-ZnO crystal flakes' and carbonized PPy nanogranule (NG)s' surface decoration on them. Additionally, the nano-ZnO mounds covering the HEM sample's surface dominantly exhibit crystal flake shapes as they were exposed to MW energy for a longer period, i.e. 120 s, as shown in Figure 2(top/right).

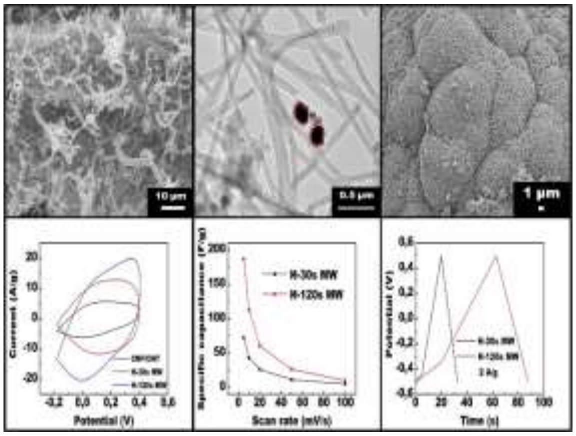

Figure 2. (Top) SEM images of; 120 s MW HEM sample (left), the as-formed nano-ZnO mounds that are majorly composed of both crystal nanoflakes and NG clusters (right), TEM image of 120 s MW HEM sample's CNFs filled with nano-ZnO, and decorated both with hexa/heptagonal shaped nano-ZnO crystal flakes and carbonized PPy NG clusters (middle). (Bottom) voltammograms of the selected samples at 100 mV/s scan rate (left), changes in 30 s and 120 s MW HEM samples' specific capacitance values at different scan rates, e.g. 5-100 mV/s (middle), changes in 30 s and 120 s MW processed HEM samples' C-D curves in 6 M aq. KOH electrolyte at 2 A/g current density (right).

Enhanced electrochemical performance is expected from the as-prepared HEM due to its components' coordinative interactions that would lead to a unique synergistic effect on their functions. In terms of shape and symmetry, CNT/CNF and the HEM-based electrodes' voltammograms exhibit a big similarity, but when it comes to their sizes, i.e. current density, approximately two and four folds of difference can be observed in such samples' voltammograms as shown in Figure 2(bottom/left).[31] This is a clear proof of a similar electrochemical process mechanism with much higher capacitive performance difference between these electrodes. The main reason behind this phenomenon is the presence of nano-ZnO compound and its significant PC property contribution to the HEM sample. Moreover, the MW process time difference and its previously mentioned outcomes on HEMs' morphological structures can be given as another major reason behind the difference between these samples' electrode performances. Under these circumstances, 120 s MW HEM-based electrode exhibited ~190 F/g capacitance value, whereas the 30 s MW HEM-based one could only reach ~75 F/g, as shown in Figure 2(bottom/middle). To gain a better understanding about the HEM-based electrodes' electrochemical energy storage performance, further galvanostatic dis-/charge (C-D) tests were conducted at different current densities and their results are shown in Figure 2(bottom/right). Here, these electrodes' C-D curves are observed to exhibit symmetrical and quasi-triangular shapes due to their good reversibility and ideal capacitive nature.

CONCLUSION

In conclusion, nano-sized HEMs that are composed of CNT and nano-ZnO decorated CNFs with controllable morphological features were successfully prepared via one-step, facile and efficient MW energy-based approach, in an affordable manner. On one hand, the as-prepared HEMs have been granted an ideal electrochemical capacitive nature with respect to the presence of both highly capacitive amorphous C from CNFs and the highly conducting graphitic C from CNTs in their structure. On the other hand, the simultaneous growth of PC-based nano-ZnO crystals along with such active C species has been proven to synergistically contribute on HEM's electrochemical reaction kinetics, cycling stability, and as well as its overall capacitive nature. Thus, in terms of electrochemically active material performance, promising results were obtained for the as-prepared HEMs from the relevant tests. As it was aimed at the beginning, the universal MW energy-based carbonization method's success is once more confirmed, as a substantial approach to prepare multi-component and multi-functional materials that can be used for various advanced applications, through this study.

REFERENCES

1. Li, S. Z., Wen, J., Mo, X. M., Long, H., Wang, H. N., Wang, J. B., Fang, G. J. 2014. "Three-dimensional MnO2 nanowire/ZnO nanorod arrays hybrid nanostructure for high-performance and flexible supercapacitor electrode", Journal of Power Sources, 256, 206-211.
2. Zhao, Y., Jiang, P. 2014. "MnO2 nanosheets grown on the ZnO-nanorod-modified carbon fibers for supercapacitor electrode materials", Colloids and Surfaces a-Physicochemical and Engineering Aspects, 444, 232-239.
3. Kim, C. H., Kim, B. H. 2014. "Electrochemical behavior of zinc oxide-based porous carbon composite nanofibers as an electrode for electrochemical capacitors", Journal of Electroanalytical Chemistry, 730, 1-9.
4. Guo, X. M., Qian, C., Shi, R. H., Zhang, W., Xu, F., Qian, S. L., Zhang, J. H., Yang, H. X., Yuan, A. H., Fan, T. X. 2019. "Biomorphic Co symbol of the klingon empire N symbol of the klingon empire C/CoOx composite derived from natural chloroplasts as efficient electrocatalyst for oxygen reduction reaction", Small, 15(8), 1804855-1804864.
5. Wang, Z. L., Guo, R., Ding, L. X., Tong, Y. X., Li, G. R. 2013. "Controllable template-assisted electrodeposition of single- and multi-walled nanotube arrays for electrochemical energy storage", Scientific Reports, 3, 1204-1211.
6. Kalpana, D., Omkumar, K. S., Kumar, S. S., Renganathan, N. G. 2006. "A novel high power symmetric ZnO/carbon aerogel composite electrode for electrochemical supercapacitor", Electrochimica Acta, 52(3), 1309-1315.
7. Zhang, Y. P., Sun, X. W., Pan, L. K., Li, H. B., Sun, Z., Sun, C. P., Tay, B. K. 2009. "Carbon nanotube-ZnO nanocomposite electrodes for supercapacitors", Solid State Ionics, 180(32-35), 1525-1528.
8. Zhang, Y. P., Sun, X. W., Pan, L. K., Li, H. B., Sun, Z., Sun, C. Q., Tay, B. K. 2009. "Carbon nanotube-zinc oxide electrode and gel polymer electrolyte for electrochemical supercapacitors", Journal of Alloys and Compounds, 480(2), L17-L19.
9. Zhang, Y. P., Li, H. B., Pan, L. K., Lu, T., Sun, Z. 2009. "Capacitive behavior of graphene-ZnO composite film for supercapacitors", Journal of Electroanalytical Chemistry, 634(1), 68-71.
10. Selvakumar, M., Bhat, D. K., Aggarwal, A. M., Iyer, S. P., Sravani, G. 2010. "Nano ZnO-activated carbon composite electrodes for supercapacitors", Physica B-Condensed Matter, 405(9), 2286-2289.
11. Sidhu, N. K., Rastogi, A. C. 2014. "Vertically aligned ZnO nanorod core-polypyrrole conducting polymer sheath and nanotube arrays for electrochemical supercapacitor energy storage", Nanoscale Research Letters, 9, 453-468.
12. Aravinda, L. S., Nagaraja, K. K., Nagaraja, H. S., Bhat, K. U., Bhat, B. R. 2013. "ZnO/carbon nanotube nanocomposite for high energy density supercapacitors", Electrochimica Acta, 95, 119-124.
13. Pandiselvi, K., Thambidurai, S. 2014. "Chitosan-ZnO/polyaniline ternary nanocomposite for high-performance supercapacitor", Ionics, 20(4), 551-561.
14. Su, D. Q., Tang, Z. H., Xie, J. F., Bian, Z. X., Zhang, J. H., Yang, D. D., Zhang, D., Wang, J. C., Liu, Y., Yuan, A. H., Kong, Q. H. 2019. "Co, Mn-LDH nanoneedle arrays grown on Ni foam for high performance supercapacitors", Applied Surface Science, 469, 487-494.
15. Li, Y. M., Liu, X. 2014. "Activated carbon/ZnO composites prepared using hydrochars as intermediate and their electrochemical performance in supercapacitor", Materials Chemistry and Physics, 148(1-2), 380-386.
16. Bayrakceken, H., Naktiyok, J., Ozer, A. K., Yurtcan, A. B. 2017. "Investigation of the thermal behavior of polypyrrole/carbon nanotube composites

and utilization as capacitive material or support for catalysts", Chemical Engineering Communications, 204(8), 916-925.

17. Hou, Y., Cheng, Y. W., Hobson, T., Liu, J. 2010. "Design and synthesis of hierarchical MnO2 nanospheres/carbon nanotubes/conducting polymer ternary composite for high performance electrochemical electrodes, Nano Letters, 10(7), 2727-2733.

18. Lu, T., Zhang, Y. P., Li, H. B., Pan, L. K., Li, Y. L., Sun, Z. 2010. "Electrochemical behaviors of graphene-ZnO and graphene-SnO2 composite films for supercapacitors", Electrochimica Acta, 55(13), 4170-4173.

19. Ramadoss, A., Kim, S. J. 2013. "Facile preparation and electrochemical characterization of graphene/ZnO nanocomposite for supercapacitor applications", Materials Chemistry and Physics, 140(1), 405-411.

20. Lu, T., Pan, L. K., Li, H. B., Zhu, G. A., Lv, T. A., Liu, X. J., Sun, Z., Chen, T., Chua, D. H. C. 2011. "Microwave-assisted synthesis of graphene-ZnO nanocomposite for electrochemical supercapacitors", Journal of Alloys and Compounds, 509(18), 5488-5492.

21. Haldorai, Y., Voit, W., Shim, J. J. 2014. "Nano ZnO@reduced graphene oxide composite for high performance supercapacitor: Green synthesis in supercritical fluid", Electrochimica Acta, 120, 65-72.

22. Liu, Z., Zhang, L., Poyraz, S., Smith, J., Kushvaha, V., Tippur, H., Zhang, X. Y. 2014. "An ultrafast microwave approach towards multicomponent and multi-dimensional nanomaterials", Rsc Advances, 4(18), 9308-9313.

23. Liu, Z., Wang, J. L., Kushvaha, V., Poyraz, S., Tippur, H., Park, S., Kim, M., Liu, Y., Bar, J., Chen, H., Zhang, X. Y. 2011. "Poptube approach for ultrafast carbon nanotube growth", Chemical Communications 47(35), 9912-9914.

24. Bailey, J. K., Pozarnsky, G. A., Mecartney, M. L. 1992. "The direct observation of structural development during vanadium pentoxide gelation", Journal of Materials Research, 7(9), 2530-2537.

25. Liu, Z., Chen, L., Zhang, L., Poyraz, S., Guo, Z. H., Zhang, X. Y., Zhu, J. H. 2014. "Ultrafast Cr(VI) removal from polluted water by microwave synthesized iron oxide submicron wires", Chemical Communications, 50(59), 8036-8039.

26. Zhang, X. Y., Manohar, S. K. 2006. "Microwave synthesis of nanocarbons from conducting polymers", Chemical Communications, (23), 2477-2479.

27. Amelinckx, S., Zhang, X. B., Bernaerts, D., Zhang, X. F., Ivanov, V., Nagy, J. B. 1994. "A formation mechanism for catalytically grown helix-shaped graphite nanotubes", Science, 265(5172), 635-639.

28. Hofmann, S., Blume, R., Wirth, C. T., Cantoro, M., Sharma, R., Ducati, C., Havecker, M., Zafeiratos, S., Schnoerch, P., Oestereich, A., Teschner, D., Albrecht, M., Knop-Gericke, A., Schlogl, R., Robertson, J. 2009. "State of transition metal catalysts during carbon nanotube growth", Journal of Physical Chemistry C, 113(5), 1648-1656.

29. Sinnott, S. B., Andrews, R., Qian, D., Rao, A. M., Mao, Z., Dickey, E. C., Derbyshire, F. 1999. "Model of carbon nanotube growth through chemical vapor deposition", Chemical Physics Letters, 315(1-2) 25-30.

30. Poyraz, S., Liu, Z., Liu, Y., Zhang, X. Y. 2013. "Devulcanization of scrap ground tire rubber and successive carbon nanotube growth by microwave irradiation", Current Organic Chemistry, 17(20), 2243-2248.

31. Liu, Y., Zhang, X. Y., Poyraz, S., Zhang, C., Xin, J. H. 2018. "One-step synthesis of multifunctional zinc-iron-oxide hybrid carbon nanowires by chemical fusion for supercapacitors and interfacial water marbles", ChemNanoMat, 4(6), 546-556.

Production of Fibrous Gelatin Mat as Antibacterial Wound Dressing Material via Centrifugal Spinning Method

GUNGOR, Melike[1, 4], SAGIRLI, Merve Nur[1, 3], CALISIR, D. Mehmet[1, 2], KILIC, Ali[1, 3, 4*]
[1]TEMAG Labs, Textile Tech. and Design Faculty, Istanbul Tech. Uni., Istanbul, Turkey
[2]Faculty of Engineering, Recep Tayyip Erdogan University, Rize, Turkey
[3]Areka Group Advanced Technologies LLC, Istanbul, Turkey
[4]Research and Development Center for Medical Textiles, Istanbul, Turkey
alikilic@itu.edu.tr

PURPOSE

In this study, it is aimed to produce stable gelatin-based fibrous mats with antibacterial activity and high biocompatibility for wound dressing applications.

INTRODUCTION

Gelatin which is a water-soluble, natural material comprising of glycine, proline, and hydroxyproline amino acids, has been widely used as a scaffold in tissue engineering because of its biodegradable, biocompatible, and non-immunogenic features[1]. Additionally, being abundant, easily processable and applicable, and having high cell attachment capability are the other important features of the gelatin.

The gelatin has the ability to absorb large amounts of water/wound fluid, which makes it attractive as a wound dressing material, but shows very poor stability to water/moisture. The stability of the gelatin can be improved by crosslinking and, among chemical and physical crosslinking methods, chemical crosslinking gives the highest degree of crosslinking for the gelatin. However, chemical crosslinking methods are not suitable for gelatin to be used in wound dressings because of the toxic effects of chemicals[2]. Among the physical crosslinking methods, thermal crosslinking has many advantages such as improving the mechanical properties of the mats and being sterile[3].

Among different forms of wound dressing materials, fibrous scaffolds that provide high surface area and high porosity, play an important role in wound healing by allowing a high oxygenation rate[4]. Additionally, the high mechanical strength of the fibers can also provide and flexible support to the wound area[1].

The electrospinning is known as the conventional method for the production of fibrous materials, has some drawbacks like low production rate, safety problems, and solution dependency. The centrifugal spinning which is a safer, cost-effective and highly productive method than the electrospinning, is used to produce fibers from viscous polymer solutions by the effect of centrifugal forces[5].

In the present study, fibrous gelatin mats were prepared by centrifugal spinning from the gelatin-acetic acid solution. Additionally, the optimal fibrous gelatin mats were thermally cross-linked to stabilize the structure against water. In order to give the antibacterial property of the produced fibrous mat, a certain amount of silver nitrate was added into the polymer solution and colloidal silver – gelatin solution was prepared with a UV-induced reduction reaction. The silver is known for its antibacterial activity and used for centuries in the treatment of wounds[6]

Morphology of the fibrous mats and distribution of Ag NPs into the fibers were examined via SEM –EDX analysis. The efficiency of the reduction reaction of the $AgNO_3$ to Ag NPs was screened via UV-Vis photospectroscopy. Change in the chemical structure of the fibers was analyzed before and after thermal crosslinking via FTIR. The antibacterial activity of neat gelatin and Silver NPs incorporated gelatin mats were also investigated against Escherichia coli and Staphylococcus aureus bacteria.

EXPERIMENTAL

Material

Type B bovine skin gelatin (G) powder (Bloom 200-220) was purchased from Halavet Gıda LLC (Istanbul, Turkey). Glacial acetic acid (AA) (Anhydrous, 100 % purity) and silver nitrate ($AgNO_3$, Extra pure) were purchased from Merck. The chemicals were used without any special treatments.

Method

20wt.% G/AA solution (G20) was prepared for the production of only gelatin fibrous mat while silver nitrate was added into 20wt.% G/AA was added to the G20 solution with the $AgNO_3$/gelatin weight ratio of 0.015 (1.5 Ag-G20). In order to reduce the $AgNO_3$ to Ag NPs, the Ag included solution was stirred under UVC light until the solution gets a blurry-yellowish appearance. Both solutions were centrifugally spun at 7000 rpm. After spinning, they were introduced to heat treatment at 170°C for 24h to perform the thermal cross-linking.

RESULTS AND DISCUSSIONS

As shown in Figure 1, in the cases of both dark conditions and under UVC light, the absorbance peaks were seen around 350-450 nm region, which shows the reduction of $AgNO_3$ into Ag NPs. This means that $AgNO_3$ also reduced with acidic conditions without the existence of UVC. However, the existence of UVC light produced finer NPs with narrower size distribution which was understood from the shape and position of the surface plasmon resonance (SPR) peak of the silver. The widen and peak at higher wavelength means bigger NPs with large size distribution and vice versa.

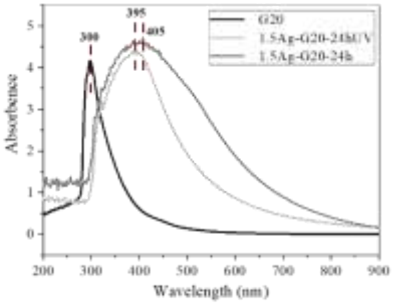

Figure 1. UV-Vis absorption spectra of G20 and 1.5 Ag-G20 solutions after stirring for 24 h under dark and UVC light, respectively.

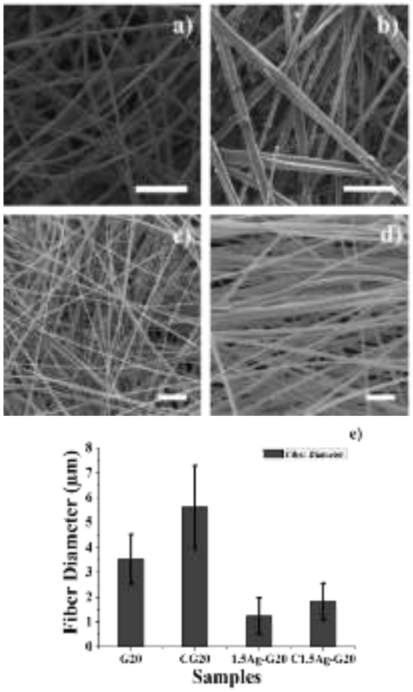

Figure 2. SEM images of the samples after thermal crosslinking and adding silver a) G20, b) cross-linked G20 (CG20), c) 1.5Ag-G20, d) 1.5Ag-CG20 and e) their fiber diameter distribution

The SEM images of produced fibers are shown in Figure 2. When cross-linked and non-cross-linked samples were compared, it is seen that after cross-linking, the fibers have got thicker in both cases. This can be attributed to the melting and fusion of the fibers[7]. In addition, it is a well-known fact that fiber diameters produced from homogeneous spinning solutions are known to be directly proportional to the solution's viscosity in the centrifugal spinning method[8]. Thus, finer fibers from the Ag-G20 solution can also be attributed to its lower viscosity.

According to the results of the stability test against water, the thermally cross-linked showed the highest structural stability and undissolved in the water. Additionally, 1.5Ag-G20 fibrous mat exhibited high antimicrobial activity against E.coli and S.aerus bacteria while there is no antibacterial activity seen on the only G20 mat.

CONCLUSIONS

Production of gelatin-based fibrous mats has been conducted via the centrifugal spinning method. The mats showed antibacterial activity with the addition of silver NPs. Stabilization of fibrous mats is provided via thermal cross-linking. Antibacterial and nontoxic fibrous wound dressing mats were obtained successfully.

SUGGESTIONS FOR FURTHER WORK

The effect on wound healing and cell proliferation tests will be carried out. Also, the mats will be applied to mechanical analyses.

ACKNOWLEDGEMENTS

The work was supported by the Istanbul Development Agency under the name of the "Medical Textile R&D Center: MEDITEKS" project. The authors also acknowledge to Areka Group LLC for making freely available the lab-scale centrifugal spinning system.

LITERATURE

[1] M. Mohiti-Asli and E. G. Loboa, *Wound Healing Biomaterials*, Elsevier, 2016, pp. 483–499.

[2] T. Takigawa and Y. Endo, *Jrnl of Occup Health*, vol. 48, no. 2, pp. 75–87, Mar. 2006, doi: 10.1539/joh.48.75.

[3] M. G. Haugh, M. J. Jaasma, and F. J. O'Brien, Journal of Biomedical Materials Research Part A, vol. 89A, no. 2, pp. 363–369, May 2009, doi: 10.1002/jbm.a.31955.

[4] M. Naghibzadeh, Trends in Biomaterials & Artificial Organs, vol. 26, no. 2, pp. 86–102, Apr. 2012.

[5] X. Zhang and Y. Lu, Polymer Reviews, vol. 54, no. 4, pp. 677–701, Oct. 2014, doi: 10.1080/15583724.2014.935858.

[6] M. Rai, A. Yadav, and A. Gade, Biotechnology Advances, vol. 27, no. 1, pp. 76–83, Jan. 2009, doi: 10.1016/j.biotechadv.2008.09.002.

[7] Zhang, Y. Z., Venugopal, J., Huang, Z.-M., Lim, C. T. & Ramakrishna, S. Polymer 47, 2911–2917 (2006).

[8] Melike, G. et al. Journal of Industrial Textiles 1528083719865041 (2019) doi:10.1177/1528083719865041.

Manufacture of Nanofibers: Current Status and Promising Developments

BORAZAN, İsmail* [1], KAPLAN, Müslüm [1] and ÜZÜMCÜ, Memik Bünyamin [2]
[1]*Department of Textile Engineering, Bartin University, 74100 Bartın, Turkey*
[2]*Fashion and Textile Design Department, Gaziantep University, 27310 Gaziantep, Turkey*
* iborazan@itu.edu.tr

OBJECTIVES

There are many ways to fabricate nanofibers, such as self-assembly, electrospinning, conjugate spinning and phase separation. This work explores the current status and promising development of nanofiber technology, with an emphasis on its manufacturing processes. First, we introduce the various established nanofiber synthesis techniques. After that we focus on the emerging nanofiber manufacture technics, such as electrohydrodynamic direct, Plasma-induced synthesis, and centrifugal jet spinning. Herewith we aimed to inform about current and promising production processes and form a guide to textile engineers for their futures studies.

INTRODUCTION

Nanofibers are being studied and developed because they embrace significant promise for variety of applications and achieve some advantages of their nanostructure. The reduction in dimension of fibrous materials from µm to nm has been recognized in significant increase in surface area[1], biological reactivity[2,3], electronic properties[4] and mechanical properties[5]. Considering the potential opportunities provided by nanofibers, there is an increasing interest in nanofiber manufacturing technology incorporated in different applications area such as energy generation and storage, water treatment and environmental remediation and healthcare and biomedical engineering which they are three major themes of last several years.

This work explores the current status and promising development of nanofiber technology, with an emphasis on its manufacturing processes. First, we introduce the various established nanofiber synthesis techniques, especially the electrospinning, self-assembly, and phase separation. After that we focus on the emerging nanofiber manufacture technics, such as electrohydrodynamic direct, Plasma-induced synthesis, and centrifugal jet spinning. Herewith we aimed to provide a broad overview about current and promising production processes and form a guide to textile engineers for their futures studies.

CURRENT METHODS FOR FABRICATION OF NANOFIBERS

There are many techniques to fabricate nanofibers. The three most important current methods to produce nanofibers are self-assembly, electrospinning, and phase separation.

Electrospinning

Of all the current methods available for polymer nanofibers, electrospinning is most conventional and widely approved techniques due to unique properties such as simplicity, affordability, high porosity, and yields continuous fibers.

Self-assembly

In this method atoms, molecules and molecular aggregates assemble themselves through weak and non-covalent forces such as hydrogen bonding, electrostatic interactions, and hydrophobic forces into stable construction at the meso- and nanoscale dimensions[6].

Phase separation

The phase separation (also called as sol-gel) process is a wet-chemical technique. In this process, a polymer is initially blended with a solvent before suffering gelation. The process consists of in five basic steps such as dissolution, gelation, solvent extraction, freezing, and freeze-drying[7].

EMERGING METHODS FOR FABRICATION OF NANOFIBERS

Until now, electrospinning is the most studied nanofiber production method. However, the wide-spread commercial use of electrospinning is limited mainly due to its low production rate. Other nanofibrous material production methods, such as phase separation and self-assembly, are complex and can only be used to make nanofibers from limited types of polymers. For example, the phase separation method involves 5 multi-steps and so far only a few polymers, such as polylactide (PLA) and polyglycolide, have been made into nanofibers using the phase separationmethod[7].

Centrifugal jet spinning

Centrifugal jet spinning (CTS), also called rotary spinning, rotational jet spinning or patented technology “Forcespinning®”, gained attention due to its low production cost and high production rate, which is 500 times faster than conventional electrospinning[10,11]. In fact, this method is not new to the industry. Centrifugal spinning has been widely used in the fiberglass industry for making micrometer-scale glass fibers (which called fiberglass or glass wool) for thermal insulation and filtration requests for decades[11].

The apparatus of the CTS contains a spinneret containing material which is in solution form such as polymer solutions, then the motor drives the spinneret to spin about its axis of symmetry. During fiber creation, the spinning fluid is in a rotating spinning head, which is perforated with multiple nozzles around the sidewall. Just after the rotating speed reaches a critical value, the centrifugal force overcomes the surface tension of the spinning fluid to eject a liquid jet from the nozzle tip of the spinning head[11].

Theoretically, the morphology of nanofibers using CTS is dependent on several processing parameters such as centrifugal force, viscoelasticity, surface tension, molecular structure, molecular weight and mass transfer characteristics of the spinning solutions. The elasticity and evaporation rate of spinning solution and solvent deeply affect the final diameter of the as-prepared nanofiber[10].

Electrohydrodynamic direct writing

Electrohydrodynamic (EHD) direct writing technique is a popular method of nanofiber synthesis due to its versatility for producing ultra-thin fibers, by nearly one hundred different materials, with diameters ranging from several micrometers down to a few nanometers[12]. It is rooted in conventional electrospinning and can be used to print solid/liquid straight/serpentine nanofibers onto large-area substrate, in a direct, continuous, and controllable manner. It is pioneer to direct-write fibers below 100 nm on rigid/flexible substrate by using organic materials[13].

Plasma-induced synthesis

Using the plasma-induced synthesis method can be developed of metal oxide (such as CuO) nanofibers from themselves metal wire electrode in water without any chemical additions and template. Plasma is generated using a power supply between a metal (for example Cu) electrode pair. The process based on several steps such as, rapid energetic radicals' bombardment to electrodes' surface, atom vapor diffusion, plasma expansion, solution medium condensation, and in situ oxygen reaction and further growth. By using plasma-induced process is possible to synthesis of CuO nanofibers with diameters between 15 and 25 nm in water[14].

CO_2 laser supersonic drawing

CO_2 laser supersonic drawing (CLSD) is a novel technique is that uses laser irradiation to easily prepare different endless nanofibers in a supersonic jet without combining processes or chemical solvents[15].

CLDS technique is applicable wide range of thermoplastic polymers such as polylacticacid (PLLA), polyethylene terephthalate (PET), Polyamide (PA, Nylon) and polyglycolic acid (PGA). By using CLSD technique original fibers with thinnest Nylon 66 fiber diameter of 0.337 μm are produced with a melting point of 274 °C, which is 15°C higher than that of the original fiber[16].

Solution blow spinning

Solution blow spinning (SBS has emerged as a rapid and scalable technique to produce polymeric and ceramic materials into micro-/nanofibers. By using SBS is possible to produce nanofibers at a significantly higher rate (about ×100 times faster) compared to conventional electrospinning[17]. By using pressurized gas as the driving force SBS technique overcomes some of the drawbacks of electrospinning which are the use of electric fields and thick fibrous networks with low porosities; furthermore, fibers can be deposited in situ on virtually any surface[17].

PERSPECTIVES AND OUTLOOK

Current status and remarkable potential of nanofibers has been represented in this review. With their significant physical, electronic, biological and mechanical properties specifically high surface, porous structure nanofibrous materials researched for numerous fields of industry. However, nanofiber synthesis techniques and applications are still limited within academic and research activities. There is an important gap between academia and industry in utilizing and researching of nanofiber technology. The textile industry needs extensive studies to implement large commercial applications of nanofibers. Scientific publications on nanofibers are progressing incredibly rapidly. The novel synthesis methods are noticed at an ever-increasing rate. Nevertheless, some challenges need to be addressed in order to go implementation of nanofibers in commercial and industrial level. The produce high quality nanofibers with an industrial scale productivity is the most important challenge. Electrospinning, most conventional technique, suffers from this challenge. Novel nanofiber synthesis strategies such as centrifugal jet spinning developed to overcome this drawback.

As a result, we foresee that nanofibers will be able to overcome the all drawbacks and continue to be applied at the commercial and industrial level.

References

(1) Forward, K. M.; Flores, A.; Rutledge, G. C. Production of Core/Shell Fibers by Electrospinning from a Free Surface. *Chem. Eng. Sci.* **2013**, *104*, 250–259. https://doi.org/10.1016/j.ces.2013.09.002.

(2) Eatemadi, A.; Daraee, H.; Zarghami, N.; Yar, H. M.; Akbarzadeh, A. Nanofiber: Synthesis and Biomedical Applications. *Artif. Cells, Nanomedicine Biotechnol.* **2016**, *44* (1), 111–121. https://doi.org/10.3109/21691401.2014.922568.

(3) Lee, A.-R.; Tsai, W.-B.; Lin, W.-H.; Wu, Y.-K.; Lin, C.-W.; Yu, J. Electrospun PLGA Fibers Incorporated with Functionalized Biomolecules for Cardiac Tissue Engineering. *Tissue Eng. Part A* **2014**, *20* (13–14), 1896–1907. https://doi.org/10.1089/ten.tea.2013.0008.

(4) Norris, I. D.; Shaker, M. M.; Ko, F. K.; MacDiarmid, A. G. Electrostatic Fabrication of Ultrafine Conducting Fibers: Polyaniline/Polyethylene Oxide Blends. *Synth. Met.* **2000**, *114* (2), 109–114. https://doi.org/10.1016/S0379-6779(00)00217-4.

(5) Almetwally, A. A.; El-Sakhawy, M.; Elshakankery, M. H.; Kasem, M. H. Technology of Nano-Fibers: Production Techniques and Properties - Critical Review. *J. Text. Assoc.* **2017**, *78* (1), 5–14.

(6) Hartgerink, J. D.; Hartgerink, J. D.; Beniash, E.; Stupp, S. I. Self-Assembly and Mineralization of Peptide-Amphiphile Nanofibers. **2011**, *1684* (2001), 1684–1689. https://doi.org/10.1126/science.1063187.

(7) Ma, P. X.; Zhang, R. Synthetic Nano-Scale Fibrous Extracellular Matrix. *J. Biomed. Mater. Res.* **1999**, *46* (1), 60–72. https://doi.org/10.1002/(SICI)1097-4636(199907)46:1<60::AID-JBM7>3.0.CO;2-H.

(8) Zhang, Y.; Gu, H.; Yang, Z.; Xu, B. Supramolecular Hydrogels Respond to Ligand-Receptor Interaction. *J. Am. Chem. Soc.* **2003**, *125* (45), 13680–13681. https://doi.org/10.1021/ja036817k.

(9) Yang, Z.; Xu, B. Supramolecular Hydrogels Based on Biofunctional Nanofibers of Self-Assembled Small Molecules. *J. Mater. Chem.* **2007**, *17* (23), 2385–2393. https://doi.org/10.1039/b702493b.

(10) Ren, L.; Ozisik, R.; Kotha, S. P.; Underhill, P. T. Highly Efficient Fabrication of Polymer Nanofiber Assembly by Centrifugal Jet Spinning: Process and Characterization. *Macromolecules* **2015**, *48* (8), 2593–2602. https://doi.org/10.1021/acs.macromol.5b00292.

(11) Zhang, X.; Lu, Y. Centrifugal Spinning: An Alternative Approach to Fabricate Nanofibers at High Speed and Low Cost. *Polym. Rev.* **2014**, *54* (4), 677–701. https://doi.org/10.1080/15583724.2014.935858.

(12) Kenry; Lim, C. T. Nanofiber Technology: Current Status and Emerging Developments. *Prog. Polym. Sci.* **2017**, *70*, 1–17. https://doi.org/10.1016/j.progpolymsci.2017.03.002.

(13) Bu, N.; Xiong, Y.; Yin, Z.; Liu, H.; Pan, Y.; Huang, Y.; Duan, Y. Electrohydrodynamic Direct-Writing. *Nanoscale* **2013**, *5* (24), 12007. https://doi.org/10.1039/c3nr04329k.

(14) Hu, X.; Zhang, X.; Shen, X.; Li, H.; Takai, O.; Saito, N. Plasma-Induced Synthesis of CuO Nanofibers and ZnO Nanoflowers in Water. *Plasma Chem. Plasma Process.* **2014**, *34* (5), 1129–1139. https://doi.org/10.1007/s11090-014-9546-0.

(15) Suzuki, A.; Imajo, K. Poly(l-Lactic Acid) Nanofiber Multifilament Prepared by Carbon Dioxide Laser Supersonic Multi-Drawing. *Polymer (Guildf).* **2016**, *91*, 24–32. https://doi.org/10.1016/j.polymer.2016.03.053.

(16) Suzuki, A.; Mikuni, T.; Hasegawa, T. Nylon 66 Nanofibers Prepared by CO2laser Supersonic Drawing. *J. Appl. Polym. Sci.* **2014**, *131* (6), 1–11. https://doi.org/10.1002/app.40015.

(17) Magaz, A.; Roberts, A. D.; Faraji, S.; Nascimento, T. R. L.; Medeiros, E. S.; Zhang, W.; Greenhalgh, R. D.; Mautner, A.; Li, X.; Blaker, J. J. Porous, Aligned, and Biomimetic Fibers of Regenerated Silk Fibroin Produced by Solution Blow Spinning. *Biomacromolecules* **2018**, *19* (12), 4542–4553. https://doi.org/10.1021/acs.biomac.8b01233.

Poliamid 6,6’nın Isıl İletkenliğinin Geliştirilmesinde Karbon Elyafın Etkisi

BEYAZ, Rumeysa[1], ÖKSÜZ, Mustafa[2]
[1] Yalova Üniversitesi, Fen Bilimleri Enstitüsü, 77200, Yalova, Türkiye
[2] Yalova Üniversitesi, Polimer Mühendisliği Bölümü, 77200, Yalova, Türkiye
rmysbeyaz@gmail.com

AMAÇLAR

Bu çalışmada PA 6,6’nın ısıl özellikleri ve morfolojik özellikleri üzerinde karbon elyafının kullanılmasıyla oluşan etkinin incelenmesi amaçlanmıştır. Bu amaca uygun olarak farklı oranlarda hazırlanan karışımlara ısıl iletkenlik ölçümü uygulanmış, mikroyapı incelemeleri gerçekleştirilmiştir. En uygun karışım oranları belirlenerek parametrelerin optimizasyonuna ve endüstriyel olarak kullanımının yaygınlaştırılmasına katkı sağlanmasına çalışılmıştır.

GİRİŞ

Endüstride kullanım amacına uygun olarak, farklı malzemelerin belirli bir düzende bir arayagetirilmesi ile istenilen amaca uygun kompozit malzemeler üretilmektedir. Kompozit malzemelerde ki temel amaç, malzeme özelliklerinin iyileştirilmesi yada farklı malzemelerin iyi özelliklerinin tek bir malzemede toplanmasıdır[1]. Günümüzde gelişen teknoloji ile birlikte havacılık ve askeri araçlar, uzay uygulamaları, otomobil sanayii, deniz araçları, spor ve eğlence ekipmanlarına yönelik olarak ısıl ve elektirik özellikleri geliştirilmiş, darbe dayanımı artırılmış kompozit malzemeleri üretmek için farklı polimer türleri, farklı dolgu ve katkı maddeleri kullanılarak polimer kompozitleri hazırlanmaktadır[2].Elektrik elektronik uygulamalarda kullanılan malzemelerde ısı birikmesi bazı problemlemlere sebep olmaktadır[3,5,6]. Bu problemler yüksek ısıl iletkenlik özelliklerine sahip malzemeler kullanarak biriken ısının hızlı bir şekilde dağıtılması ile giderilmektedir[4,7]. Polimer malzemelerin ısıl iletkenliği genellikle 0,1–0,5 W/mK arasındadır[6,7]. Polimer malzemelerin, ısıl iletkenliközellikleri karbon, seramik ve metalik dolgu malzemeleri kullanılarak geliştirilmektedir[3,8,9].

Poliamid 6,6 (PA 6,6) ısıl iletkenliği yaklaşık 0.29 W/Mk olan yarı kristalin bir polimerdir[10].Poliamid çeşitleri arasında Poliamid 6,6 (PA 6,6) en dayanıklı poliamid olarak bilinmektedir[10]. Poliamid 6,6 yüksek dayanım, iyi elektiriksel ve kimyasal özellikleri sayesinde endüstride birçok uygulama alanında tercih edilmektedir[10]. Poliamd 6,6 kullanılarak üretilen ürünler ısıya maruz kaldığında ürünün şeklini ve mekanik özelliklerini olumsuz etkilemektedir[11]. Bu olumsuzluklar yüksek iletkenlik katsayılı takviye malzemeleri kullanılarak giderilmektedir. Düşük ısıl iletkenlik özelliğine sahip PA 6,6’nın ısıl iletkenlik özellikleri, bağlayıcı ajanlar, elyaf ve iletken dolgu malzemeleri ilavesi ile geliştirilmektedir[12].İletkenlik özelliği genellikle karbon nanotüp, karbon elyaf, metal partiküller ve bor esaslı bileşikler eklenerek geliştirilmektedir[13,14].

Isıl iletkenliğin önemli olduğu uygulamalarda yüksek performans ve daha uzun yorulma dayanımı beklentisi nedeniyle farklı katkı ve dolgu maddelerinin kullanımına ve bunların karakterizasyonuna büyük önem verilmektedir. Literatürde ki çalışmalar incelendiğinde PA 6,6’nın ısıl özelliklerinin geliştirilmesi üzerine çok fazla bir çalışmanın olmadığı görülmektedir. Genellikle yapılan çalışmalarda matris malzemesi olarak yüksek yoğunluklu polietilen (HDPE)[15], polipropilen (PP)[16], Poliamid 6 (PA 6)[17]gibi polimer malzemelerin ve ısıl iletken dolgu malzemesi olarak hegzagonal bor nitrür (hBN)[15,16], karbon nanotüp (KNT)[17] gibi dolgular kullanılmıştır.

Bu çalışmada matris olarak PA 6,6, dolgu malzemesi olarak farklı oranlarda karbon elyafı kullanılarak polimer kompozit malzemeleri üretilmiştir. Farklı oranlarda hazırlanan karbon elyaf/PA6,6 kompozitlerinden elde edilen sonuçlar birbirleriyle karşılaştırılarak en uygun dolgu oranı tespit edilmiştir.

DENEYSEL

Malzeme

Çalışmada matris malzemesi olarak yoğunluğu 1,14 g/cm^3, iletkenliği 0,3 W/mK olan poliamid 6,6 kullanılmıştır. Dolgu malzemesi olarak karbon elyaf kullanılmıştır. Antioksidan olarak Irgafos kullanılmıştır.

Yöntem

Malzemeler önce ekstrüzyon yöntemi ile harmanlanarak karışım hazırlanmıştır. Poliamid 6,6 matrisine Tablo 1’de verilen oranlarda karbon elyaf ilave edilerek kompozitler hazırlanmıştır. Poliamid 6,6 kompoztileri çift vidalı ekstrüder de 270-290 ºC sıcaklıklarında homojen olarak karıştırılarak granül haline getirilmiştir. Granül haline getirilen örnekler enjeksiyonla kalıplanmıştır. Üretilen test numunelerine ısıl test uygullanmış ve mikroyapı incelemeleri gerçekleştirilmiştir.

Tablo 1. Karışım parametreleri

Deney Kodu	PA 6,6 (%)	Karbon Elyaf(%)
PA 66	100	-
PA 66 CF 10	90	10
PA 66 CF 20	80	20
PA 66 CF 30	70	30

DENEYSEL SONUÇLAR/TARTIŞMA

Çalışmada kullanılan karbon elyafının poliamid 6,6'nın ısıl iletkenliğine etki ettiği görülmüştür. Şekil 1 incelendiğinde, karbon elyaf miktarıartıkça poliamid 6,6'nın ısıl iletkenliğinin de arttığı görülmektedir. Referans numuneden daha yüksek ısıl İletkenlik elde edilmiştir. Karbon elyaf ilavesi ile ısıl iletkenliğin 0.3 W/mK'dan 0,65 W/mK'ya yükseldiği gözlemlenmiştir.

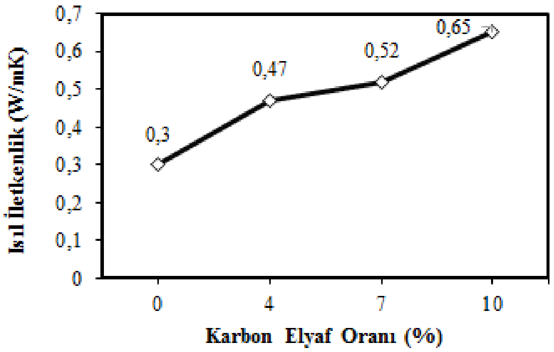

Şekil 1. PA6,6 nın ısıl iletkenliğinin karbon elyaf ilavesi ile değişimi

CF / PA 6,6 kompozitlerinin SEM görüntüleri sırasıyla Şek. 2, 3 ve 4 de verilmektedir. SEM görüntülerine bakıldığında karbon elyafın matriste homojen olarak dağıldığı ve gömülü olduğu görülmektedir. Bu durum karbon fiberin yüzeylerde iyi bir fiber-matris bağının olduğunu desteklemektedir.

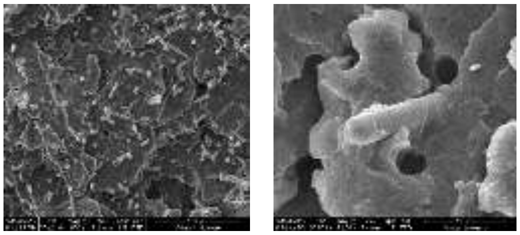

Şekil 2. % 10 karbon elyaf ilavesi ile hazırlanan PA 6,6 (PA66CF10) numunesine ait SEM görüntüleri

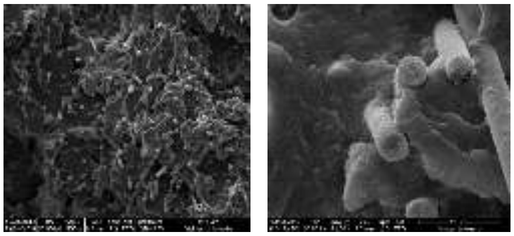

Şekil 3 %20 karbon elyaf ilavesi ile hazırlanan PA6,6 (PA66CF20) numunesine ait SEM görüntüleri

Şekil 4 'de karbon elyaf ve PA 6,6 matrisinin etkileşiminin güçlü olduğu görülmektedir. Bu durumun kompozitin mekanik özelliklerini olumlu etkileyeceği tahmin edilmektedir. Kompozitlerin iletkenliğini geliştirmek için kullanılan iletken dolguların iletim yolu oluşturması gerekmektedir[18]. Şekil 1'de verilen ısıl iletkenlik sonuçlarında da görüldüğü gibi karbon elyaf ilavesi ile ısıl iletkenlik artmıştır. Karbon elyafları polimer matris içerisinde homojen dağılarak iletim yolu oluşturarak iletkenliği artırdığı düşünülmektedir.

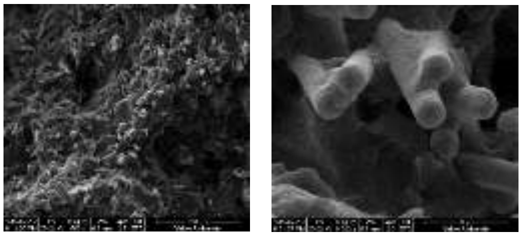

Şekil 4 %30 karbon elyaf ilavesi ile hazırlanan PA6,6 (PA66CF20) numunesine ait SEM görüntüleri

GENEL SONUÇLAR

Karbon elyaf ilavesi ile iyi mekanik özellikleri sahip ve ısıl iletkenliği geliştirilmiş poliamid 6,6 kompoziti üretilmiştir. Farklı oranlarda ilave edilen karbon elyafın poliamid 6,6'nın iletkenliğini artırdığı sonucuna varılmıştır. SEM fotoğrafları incelendiğinde, karbon elyafın matris ile iyi etkileşim sağladığı görülmektedir. Bu durum üretilen kompozitlerin iyi mekanik özellikleri sahip olduğunu göstermektedir. Üretilen ısıl iletken poliamid 6,6 kompozitleri, elektronik montaj ve otomotive ait bazı yeni uygulama alanlarında kullanılabilir.

TEŞEKKÜR/BILGILENDIRME/FON KAYNAĞI

Bu çalışma Yalova ÜniversitesiBilimsel Araştırma Projeleri Komisyonu tarafındandesteklenmiştir. Proje Numarası: 2018/YL/0017

KAYNAKLAR

1. Saçak, M., 2005, Polimer Teknolojisi, Gazi Kitap Evi, Ankara, Türkiye.
2. Smith W. F., 2006, Mazleme Bilimi ve Mühendisliği, 3.baskı, Çeviri Kınıkoğlu N., Literatür Yayıncılık, İstanbul, Türkiye.
3. Ha S.M, Kwon O.H, Oh Y.G, Kim Y.S., Lee S.G, Won J.C, Cho K.S, Kim BB.G andYoo Y,2015.Thermally conductive polyamide 6/carbon filler composites based on a hybrid filler system, Science and Technology of Advanced Materials, 16, 065001.
4. Zhou W.,Qi S., An S., Zhao H., Liu N.,2007. Thermal conductivity of boron nitride reinforce polyethylene composites, Materials Research Bulletin, Department of Applied Chemistry, School of Science, Northwestern Polytechnical University, 42, 1863-1873.
5. Morishita T, Matsushita M, Katagiri Y and Fukumori K, 2011. A novel morphological model for carbon nanotube/polymer composites having high thermal conductivity and electrical insulation, Journal of Material Chemistry , 2, 5610.
6. Zhou W.,Yu D., Min C., Fu Y. andGuo X.,2009. Thermal, Dielectric, and Mechanical Properties of SiC Particles Filled LinearLow-Density Polyethylene Composites, Journal of Applied Polymer Science, 112, 1695.
7. Chen H.,Ginzburgb V..V,Yang J., Yang Y., Liu W., Huang Y., Du L., Chen B., 2016. Thermal Conductivity of Polymer-based Composites:Fundamentals and Applications, Progress in Polymer Science, 59, 41–85.
8. Choi S. W.,Yoon K. H. And Jeong S.S., 2013, Morphology and thermal conductivity of polyacrylate composites containing aluminum/multi-walled carbon nanotubes, Composites A, 45.
9. Yu A.,Ramesh P., Sun X., Bekyarova E., Itkis M. E.and Haddon R. C., 2008. Enhanced Thermal Conductivity in a Hybrid Graphite Nanoplatelet – Carbon Nanotube Filler for Epoxy Composites, Advanced Material, 20, 4740.
10. Gür, Poliamid 66 / Sepiyolit Kompozitlerin Üretim Ve Özelliklerinin Karakterize Edilmesi, 2011, Yüksek Lisans Tezi, Sakarya Üniversitesi, Metalurji Mühendisliği Anabilim.
11. Semiz S., 2017, Yüksek Isıl İletimli, Düşük Sürtünme Katsayılı Yeni Nesil Termoplastik Poliüretan, İzmir Katip Çelebi Üniversitesi, Fen Bilimleri Enstitüsü, Yüksek Lisans Tezi, İzmir.
12. Öz E. K., Karagöz İ., Öksüz M., 2015, Poliamid 6/ Polipropilen (PA 6/PP) Karışımlarının Yapı ve Özellikleri, I. Ulusal Plastik Teknolojileri Sempozyumu, İstanbul, Türkiye.
13. Yuan D., Yan-FangGao, Zhao-XiaGuo, JianYu, 2017. Improved thermal conductivity of ceramic filler-filled polyamide composites by using PA6/PA66 1:1 blend as matrix, Journal of Applied Polymer Science, 134, 45371.
14. Liu T.,Li J., Wang X., Deng Z., Yu X., Lu A., Yu F. and He J., 2015. Preparationandproperties of thermal conductive polyamide 6,6 composites, Journal of Termoplastic Composite, 28, 32-45.
15. Muratov D.S., Stepashkin A.A., Anshin S.M., Kuznetsov D. V., 2018. Controlling thermal conductivity of high density polyethylene filled with modified hexagonal boron nitride (hBN), Journal of Alloys and Compounds, 735, 1200-1205.
16. Muratov D.S., Kuznetsov D.V., Il'inykh I.A., Mazov I.N., Stepashkin A.A., Tcherdyntsev V.V., 2013. Thermal conductivity of polypropylene filled with inorganic particles, Journal of Alloys and Compounds, 586, 451-454.
17. Ha S.M, Kwon O.H, Oh Y.G, Kim Y.S., Lee S.G, Won J.C, Cho K.S, Kim BB.G and Yoo Y, 2015. Thermally conductive polyamide 6/carbon filler composites based on a hybrid filler system, Science and Technology of Advanced Materials. 16, 065001.
18. Molefi J. A., Luyt A. S., Krupa I., 2009. Comparison of the influence of Cu micro- and nano-particles on the thermal properties of polyethylene/Cu composites, eXPRESS Polymer Letters.

A Comparative Study of Silica Fibers Prepared by Solution Blowing (SB) and Electro-Solution Blowing (ESB) Methods

CALISIR Mehmet D[1,2]., GUNGOR Melike[1], KILIC Ali[1]
[1]TEMAG Lab, Istanbul Technical University, Istanbul, Turkey
[2]Recep Tayyip Erdogan University, Faculty of Engineering, Rize, Turkey
[3]Areka Group Advanced Technologies LLC, Istanbul, Turkey
alikilic@itu.edu.tr

PURPOSE

Production of SiO_2 fibers via SB and ESB methods and subsequent calcination was performed. Also, the effects of applied electrical voltage on fiber morphology were investigated.

INTRODUCTION

Metal oxides are ionic compounds formed as a result of electrostatic interactions between the positive metallic and negative oxygen ions. Most of the metal oxides exhibited good thermal and chemical stability as a result of completely filled s-shells orbitals[1].

In the last few decades, one-dimensional (1D) materials especially nano- and submicron fibers, have gained much more interest because of their large surface area, scalable porosity, and versatility[2]. Among organic and inorganic materials in the fibrous structures, the metal oxide fibers have been researched because of their stable structure, ability to bind functional groups and modifiable properties.

The most common inorganic nanofibers are ZnO[3], TiO2[4], SiO_2[2], ZrO2[5], and Al2O3[6,7]. Among these, silica fibers have attracted considerable attention as they can meet the need for wide range applications from sensing[8] and biomedical[9] to environmental applications[10,11] due to their unique properties such as low thermal conductivity, chemically inertness and non-toxicity[12].

Electrospinning is by far the most widely investigated method for fabrication ultrafine nanofibers. However, the different spinning behavior of the solutions, low production yield and the output requirements of electrospinning led to new spinning methods such as solution blowing. In this method, the polymer solution is fed through a concentric nozzle around which pressured air passing. The solution comes into contact with high speed flowing air at the nozzle tip and is stretched out with the shear effect created by the air. The solvent in the stretched solution is evaporated during the way to the collector and gains a fibrous structure on the collector. However, the production of a homogeneous and impeccable (droplet and bead-free) fibrous network is relatively difficult due to the presence of high speed flowing air which causes the solvent in the precursor solution to evaporate rapidly at the nozzle tip especially for the viscous solutions or solutions prepared with solvents that have low-boiling point. This leads to the accumulation of the concentrate precursor solution at the tip of the nozzle, and when the accumulated amount exceeds the tolerable limits, it goes to the collector as a whole and results in droplets. The use of external forces like electro-propulsion forces to complement the stretching forces of the pressurized air can overcome the mentioned problems.[7,]. This is a new spinning method called as electro-solution blowing method.

In this study, we investigate the effect of the electrical field on the formation and morphology of solution blown SiO_2 fibers. In the production of SiO_2 fibers, PVP was used as a sacrificial polymer template. According to SEM images, SB and ESB is a facile method for the production of SiO_2 fibers and XRD and FTIR results showed that fibers were amorphous SiO_2 structure and did not include any organic residue after calcination. Additionally, while the fiber diameters increased with increasing voltage as opposite to literature[7], the defects like droplets, beads on the fibrous mat have vanished.

EXPERIMENTAL

Material

Polyvinylpyrrolidone (PVP, Mw=1,300,000g/mol, Aldrich), tetraethyl orthosilicate (TEOS, Merck) were used carrier matrix and silica precursor, respectively. TEOS dissolved in ethanol-PVP (10 wt. %) solution and 1 M HCl and distilled water with a ratio of 0.015 HCl to TEOS and 2.65 and H2O to TEOS were used as catalyst and hydrolysis substance, respectively.

Method

PVP-TEOS composite fibers were produced with a solution feeding rate of 7.5 ml/h through a nozzle with a diameter of 0.4 µm and air pressure of 0.5 bar. The produced fibers were calcinated in a muffle surface at 600°C for 1 hour with a heating rate of 5°C/ min. and then allowed to cool down to room temperature without any special treatment.

RESULTS AND DISCUSSIONS

In Figure 1, SEM images of PVP-TEOS and SiO_2 NFs and their fiber diameter distributions were given. According to graphs, the green and calcinated samples produced with the only SB included a high number amount of beads/droplets while the density of the beads getting lower with the applying DC voltage.

However, the fiber diameters were getting larger with increasing voltage. The finest and thickest SiO_2 fibers were obtained from SB (400 nm) and ESB-30 kV (500 nm) samples, respectively.

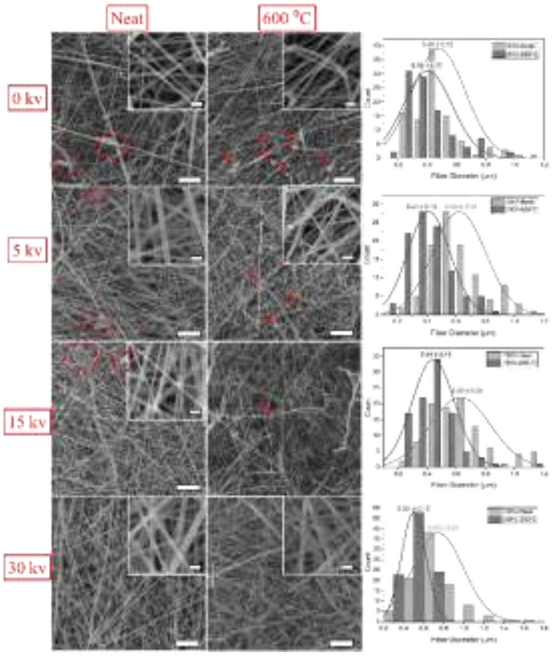

Figure 1: SEM images of PVP-TEOS and SiO_2 NFs and their fiber diameter distribution graphs

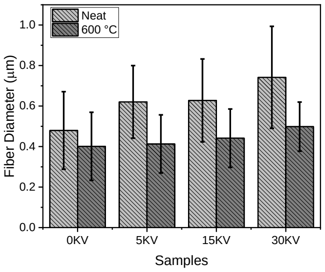

Figure 2: Comparison of fiber diameters of PVP-TEOS and SiO_2 samples.

Table 1: Table of the shrinkage ratio of the fibers with the calcination process and expansion of fibers with the presence of the electrical field.

Sample	***% Expansion of green fibers according to SB***		***% Shrinkage with calcination***
0 kV	*Neat*	*600 °C*	*16.36*
5 kV	*29.39*	*2.93*	*33.46*
15 kV	*30.90*	*10.02*	*29.70*
30 kV	*54.65*	*24.21*	*32.82*

Additionally, the presence of the electrical field also has an influence on the shrinkage ratio of the fibers with the calcination process. While only SB samples showed 16 % shrinkage after calcination, the fibers produced via ESB showed nearly 30 %. Additionally, higher electrical voltage resulted in larger diameter fiber and this effect is given as expansion of the fibers in Table 1. This can be explained the reduced number of droplets.

CONCLUSIONS

As conclusions, SiO_2 nanofibers can be successfully produced via SB and ESB methods and followed calcination. According to XRD and FTIR results, obtained fibers were amorphous SiO_2 and the polymer template was completely removed via calcination process. While the S-blown fibrous mat has lots of droplets, the density of the droplets was decreased with increasing voltage in ESB. However, an increase in the electrical field resulted in thicker fibers, and this is attributed to the removal of the droplets in the structure. In addition, both SB and ESB fibrous mats have a fragile nature.

SUGGESTIONs FOR FURTHER WORK

The fragile nature of the fibrous mat can be sourced it's dense structure. Because during the thermal treatment, fibers got shrunk and the compact nature of the fibrous mat caused more stress on the calcined fibers. The authors recommend using a collector system that is in parallel with the airflow direction or has a higher nozzle- collector distance.

ACKNOWLEDGEMENTS

The authors acknowledge the Areka Advanced Llc. for the lab-scale electro-solution blowing devices.

LITERATURE

1. Lee, J. et al. Nature Materials 7, 222–228 (2008).
2. Chang, M.-J., Cui, W.-N. & Liu, J. Journal of Nanomaterials (2017) doi:10.1155/2017/9621515.
3. Mahmood, K., Khalid, A., Ahmad, S. W. & Mehran, M. T. Surface and Coatings Technology 352, 231–237 (2018).
4. Soo, J. Z., Lee, K. M., Ang, B. C. & Ong, B. H. Physica status solidi (a) 216, 1900066 (2019).
5. Wang, H. et al. Small 14, e1800258 (2018).
6. Liao, Y., Fukuda, T. & Wang, S. Nanofiber Research - Reaching New Heights (2016) doi:10.5772/63414.
7. Li, L. et al. Materials Letters 160, 533–536 (2015).
8. Batool, S. S. et al. Vacuum 87, 1–6 (2013).
9. Liu, Y. et al. J Nanosci Nanotechnol 8, 1528–1536 (2008).
10. Mao, X. et al. RSC Adv. 2, 12216–12223 (2012).
11. Tepekiran, B. N., Calisir, M. D., Polat, Y., Akgul, Y. & Kilic, A. Aerosol Science and Technology 0, 1–13 (2019).
12. Shahhosseininia, M., Bazgir, S. & Joupari, M. D. Materials Science and Engineering: C 91, 502–511 (2018).

Antibakteriyel HEPA Filtrelerin Elektro Üfleme Yöntemi ile Üretimi

TOPTAŞ, Ali[1,3], AKGÜL, Yasin[2,3], GÜNGÖR, Melike[3], KILIÇ, Ali[3], DEMİR, Ali[3].
[1]Karabük Üniversitesi Safranbolu Meslek Yüksekokulu,
[2]Karabük Üniversitesi Mühendislik Fakültesi,
[3]İstanbul Teknik Üniversitesi Tekstil Teknolojileri ve Tasarım Fakültesi Temag Laboratuvarı
alitoptas@karabuk.edu.tr

AMAÇLAR

Bu çalışmanın amacı, nanolif yapılı yüksek performans parçacık filtrelerinin elektro üfleme yöntemiyle üretilmesi; üretilen yüksek performanslı filtrelere antibakteriyel ajanlarla katkılandırma yapılarak performansının iyileştirilmesidir.

GİRİŞ

PA-6 polimeri membran, hava filtresi, süperkapasitör, batarya ve özel tekstil ürünlerini üretmek için üstün fiziksel, kimyasal, mekanik ve termal özelliklere sahiptir[1]. Literatür araştırmalarında da görülmüştür ki[2], PA-6 ile ilgili nanolifli ağlar üretmek üzere yapılmış ve başarı ile sonuçlanmış birçok çalışma mevcuttur. Fakat bu çalışmaların büyük bir kısmında[3] PA-6 polimeri ile nanolif elde etmek için elektro üretim yöntemi kullanılmaktadır. Elektro üretim yöntemi uzun yıllardır kullanılan ve nanolif üretimi için iyi bilinen bir yöntemdir[4]. Ancak elektro üretim yönteminin santrifüjle lif üretimi ve çözeltiden üfleme sistemlerine göre düşük üretim verimliliğine sahip olması bu yöntemi laboratuvar ölçekten endüstriye taşımakta zorluk çekmiştir[5]. Santrifüjle lif üretimi ve çözeltiden üfleme sistemleri yüksek hızları nedeniyle öne çıkmaktadır[6,7]. Ancak bu sistemlerde de elektro üretim yönteminde üretilen lifler kadar düşük lif çapı pek mümkün olmamaktadır. Bu çalışmada elektro üfleme geliştirilerek çözelti üfleme sisteminin yüksek üretim hızı ile elektro üretim yönteminin daha ince lif elde edilmesi avantajlarının bir araya getirilmesi amaçlanmıştır. Bunun yanı sıra, antibakteriyel etkinliği bilinen[8] insan vücudu için hiçbir yan etkisi olmayan[9] Ag nanopartiküllerin ilavesi ile antibakteriyel filtreler elde edilmesi amaçlanmıştır.

DENEYSEL

Malzeme

PA-6 granülleri BASF Türk Kimya San. ve Tic. Ltd. Şti.'nden temin edilmiştir. %85 saflıkta formik asit TEKKİM'den temin edilmiş ve daha fazla saflaştırılmadan kullanılmıştır. İkinci çözücü olan %100 saflıkta asetik asit ise ISOLAB'dan temin edilmiştir. $AgNO_3$ tozu da Labor Teknik AŞ'den satın alınmıştır.

Yöntem

Ağırlıkça %11 PA-6 içeren çözelti için çözücü olarak %67 asetik asit ve %33 formik asit kullanılmıştır. Çözeltiyi hazırlamak için çözücü karışımına PA-6 eklendikten sonra 50 °C sıcaklıkta 24 saat boyunca manyetik karıştırıcıda çözünmesi beklenmiştir. Ardından çözünen solüsyona katı polimer ağırlığının %0,5, %2 ve %5 oranlarında $AgNO_3$ ilave edilmiş ve 24 saat boyunca 50 °C sıcaklıkta karıştırıcı üzerinde bekletilmiştir. Çizelge 1'de verilen parametrelere göre elektro üfleme yöntemiyle üretim gerçekleştirilmiştir.

Çizelge 1: $AgNO_3$ katkılı antibakteriyel filtrelerin üretim parametreleri.

Parametre	Miktar	Birim
Konsantrasyon	11	% (ağırlıkça)
Basınç	3	Bar
Elektrik voltajı	30	kV
Besleme hızı	5	ml/saat
Toplama mesafesi	50	cm

DENEYSEL SONUÇLAR/TARTIŞMA

Çözelti Viskoziteleri ve Lif Morfolojisi

Çözeltilere ait viskozite değerleri Çizelge 2'de gösterilmiştir. Yapıdaki $AgNO_3$ miktarı arttıkça çözelti viskozitesinin arttığı görülmüştür.

Çizelge 2: Çözeltilerin viskozite değerleri.

Numune	**Çap**	**Viskozite (mPa.s)**	**rpm**
%0,5 $AgNO_3$	R3	145,2	100
%2 $AgNO_3$	R3	187,1	100
%5 $AgNO_3$	R3	285,6	100

Üretilen numunelerin yüzey morfolojilerini incelemek için 1.000 ve 10.000 büyütmelerle TESCAN-Vega 3 modeli taramalı elektron mikroskobu (SEM) kullanılmıştır. SEM görüntüleri Şekil 1- 3'de gösterilmiştir.

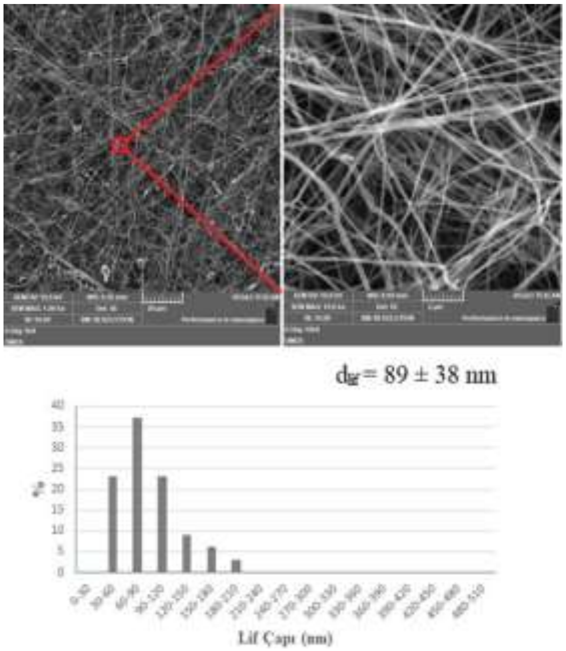

Şekil 1: %0,5 $AgNO_3$ içeren numunenin SEM görüntüsü ve lif çapı dağılımı.

Çözeltideki PA-6 polimer miktarının %0,5 katı kadar $AgNO_3$ içeren numunenin ortalama lif çapı 89 ± 38 nm iken %2 $AgNO_3$ içeren numunenin ortalama lif çapı 94 ± 47 nm'dir. $AgNO_3$ miktarı, %5' e çıkarıldığında ise ortalama lif çapı 113 ± 55 nm'ye çıkmıştır.

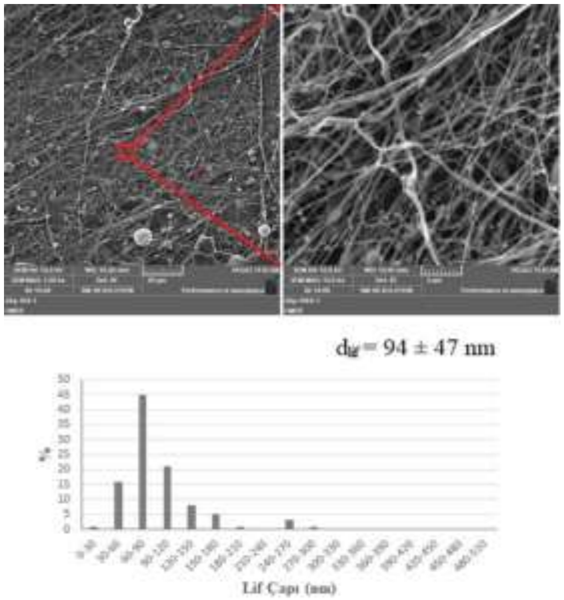

Şekil 2: %2 AgNO3 içeren numunenin SEM görüntüsü ve lif çapı dağılımı.

$AgNO_3$, miktarının artmasıyla lif çapının artması viskozitenin artması ile açıklanabilmektedir. Çünkü viskozitedeki artış lif çapında artışa sebep olan önemli bir etmendir.

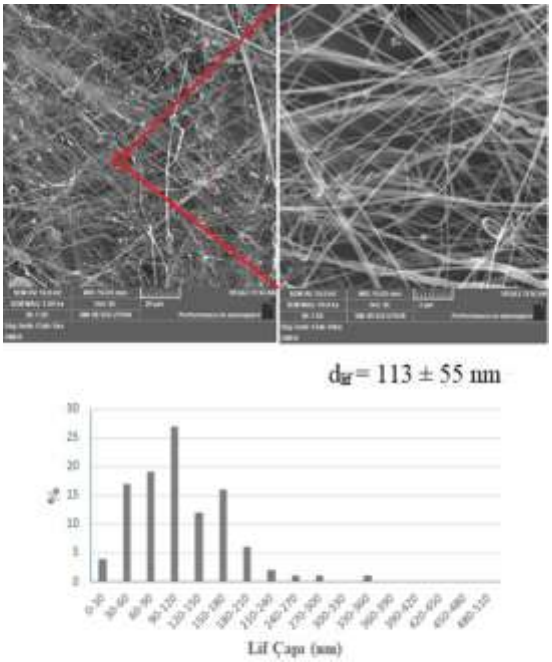

Şekil 3: %5 $AgNO_3$ içeren numunenin SEM görüntüsü ve lif çapı dağılımı

Gümüş (Ag) nanopartiküllerin numunelerde varlığını göstermek üzere gerçekleştirilen SEM-EDX analizinde Ag pikleri görülmüştür.

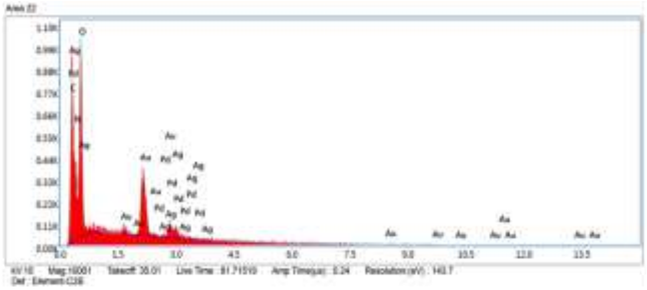

Şekil 4: %5 $AgNO_3$ içeren numunenin EDX analizi sonuçları.

Hava geçirgenlik testi

ASTM D 737 standardı kullanarak hava geçirgenliği testi uygulanan numunelerin değerleri Çizelge 3'de verilmiştir. Her numune için 5 ölçüm yapılarak ortalama değeri verilmiştir. Ortalama lif çapı arttıkça artan gözenek büyüklüklerine bağlı olarak numunelerin hava geçirgeliği de artmıştır.

Çizelge 3: $AgNO_3$ katkılı numunelerin hava geçirgenlikleri.

Numuneler	Hava Geçirgenliği (mm/s)
%0,5 $AgNO_3$	27,2
%2 $AgNO_3$	33
%5 $AgNO_3$	44,2

Hava filtrasyonu performansı testi

Üretilen numunelere (TSI Model 8130A) model filtre test santralinde hava filtrasyonu testleri yapıldı. Elde edilen filtre test sonuçları Çizelge 4'de verilmiştir.

Çizelge 4: %0,5, %2 ve %5 $AgNO_3$ katkılı numunelerin filtre verimlilikleri.

Numuneler	Basınç mmH$_2$O	Verim %	Kalite Faktör 1/Pa
%0,5 $AgNO_3$	9,5	99,21	0,51
%2 $AgNO_3$	8,4	99,14	0,57
%5 $AgNO_3$	6,5	98,61	0,66

Filtre performansı değerlendirilirken, penetrasyon oranının yüksek, basınç düşüşünün az olması beklenir. Bu minvalde, yani kalite faktörü açısından değerlendirildiğinde en iyi filtrasyon performanslarını %5 $AgNO_3$ katkılı numune sahip olduğu 0.66 değerle göstermiştir. Ortalama lif çapı artıkça kalite faktörü artmaktadır. Çünkü filtreler daha kalındır, daha fazla nanolif içerirler. Filtre malzemesindeki lif yoğunluğu ve tutulan partiküllerin artması nedeniyle havanın sıkışmasına ve çıkışta daha düşük bir basınca sahip olmasına neden olmaktadır. Böylece basınç düşüşü miktarı artmaktadır. Ancak ortalama lif çapı daha fazla olduğu için liflerin oluşturduğu gözenek boyutları da daha fazladır. Böylece daha küçük partiküllerin penetrasyonu zorlaşmaktadır. Daha küçük lif çaplarında penetrasyon oranı daha fazla olmaktadır.

Antibakteriyellik test sonuçları

PA-6 polimerine Ag nanopartiküllerinin eklenmesiyle elde edilen numunelerin ve antibakteriyel özelliği bilinen ancak yan etkiler nedeniyle tercih edilmeyen triklosan damlatılmış referans numunenin E. coli ve S. aureus bakterilerine karşı inhibisyon bölgelerinin değerlendirilmesi yoluyla antibakteriyel etkisi Şekil 5-7' de gösterilmiştir.

S. Aureus bakterisine karşı etkinlik görülmemiştir. Şekil 6'da görüldüğü üzere yalnızca %5 Ag katkılı numune E. Coli bakterisi üzerinde diğer numunelere göre daha az etkinlik göstermiştir. Bu sebeple %2 ve %5 Ag katkılı numuneler için nonwoven üzerine toplanan lif miktarı arttırılarak test tekrarlandı. Numuneler elektro üfleme yöntemi ile 40 dk boyunca üretildiler. Fakat miktarın artması S. Aureus bakterisi için yine yeterli olmadı. Şekil 7'de görüldüğü üzere yalnızca %5 Ag katkılı numune E. Coli bakterisi üzerinde etkinlik gösterdi. Daha kalın numune eldesi E. Coli'ye karşı inhibisyon alanını yaklaşık 2 cm genişliğinde bir alana çıkardı. Daha yüksek inhibisyon alanı için Ag nanopartiküllerinin oranının arttırılması gerekmektedir.

Gram-negatif bakteriler (E. Coli), muhtemelen, membran yükünden ve bakteri türlerinin ince veya kompleks hücre duvarından kaynaklanan Gram-pozitif (S. Aureus) bakterilerine kıyasla nanokompozit filmler tarafından oldukça baskılanmıştır. Genel olarak, Gram-pozitif bakteri türleri, Gram-negatif bakterilerden üç boyutlu daha kalın bir peptidoglikan (PG 20-80 nm) tabakasından oluşur. PG katmanı, daha kısa peptitler ile çapraz bağlanmış lineer polisakkarit zincirlerine sahiptir ve bu nedenle Ag nanopartiküllerin Gram-pozitif bakterilere nüfuz etmesini zorlaştıran karmaşık bir yapı oluşturur. Ancak, Gram-negatif bakteriler, negatif yüklü bir dış zar ve Ag nanopartiküllerin penetrasyonunu kolaylaştıran ince PG katmanı (7-8 nm) ile kaplanır[10].

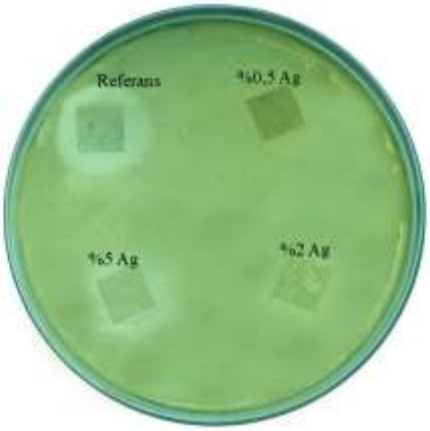

Şekil 5: Farklı oranlarda Ag nanopartikülleri içeren numunelerin S. aureus bakterisine karşı inhibisyon bölgesi.

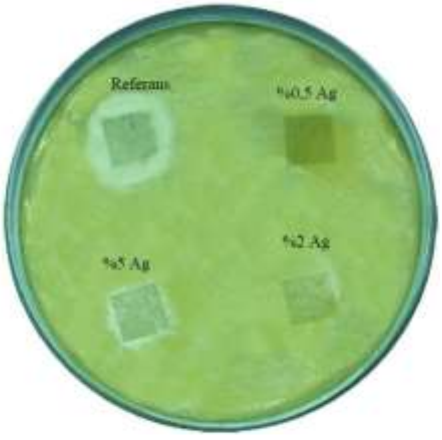

Şekil 6: Farklı oranlarda Ag nanopartikülleri içeren numunelerin E. Coli bakterisine karşı inhibisyon bölgesi.

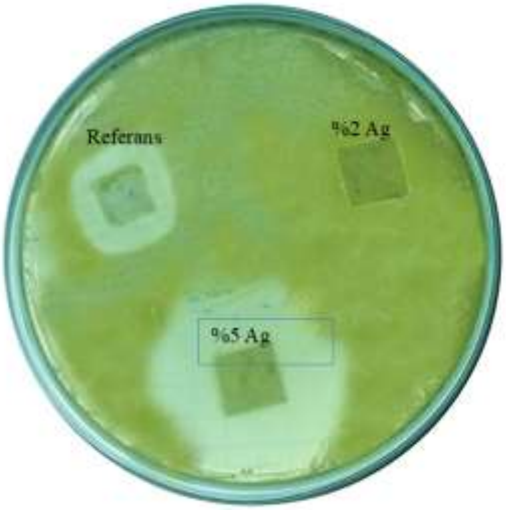

Şekil 7: Farklı oranlarda Ag nanopartikülleri içeren numunelerin E. coli bakterisine karşı inhibisyon bölgesi.

GENEL SONUÇLAR

Bu çalışmada, farklı oranlarda $AgNO_3$ içeren PA-6 nanolifleri elektro üfleme yöntemiyle üretilmiştir. %5 $AgNO_3$ içeren numunenin E. Coli bakterisine karşı antibakteriyel etkinlik gösterdiği görülmüştür. Aynı zamanda bu numune 0,66 ile en yüksek kalite faktörüne sahip numunedir. Ag nanopartikülleri eklenerek S. aureus ve E. coli bakterilerine karşı antibakteriyel etkinlik değerlendirmeleri yapılmış ve %5 Ag içeren numunelerin E. coli bakterisine karşı etkinlik alanı gösterdiği görülmüştür. Numunelerdeki artan Ag nanopartikül oranının antibakteriyel etkinliğin artmasında olumlu rol oynadığı görülmüştür. Dolayısıyla üretilen bu malzemenin antibakteriyel özellikleri iyileştirilerek filtrasyon uygulamaları için umut verici bir malzeme olduğu düşünülmektedir.

SONRAKİ DÖNEM ÇALIŞMALARI

Elektro üfleme ile nanolif üretim yöntemi, elektro üretim ve çözeltiden üfleme yönteminin üretim avantajlarını kullanarak endüstriyel alanda kullanılabilecek bir yöntem olduğu görülmüştür. Dolayısıyla, hava filtrasyonun yanı sıra, su filtrasyonu, koruyucu giysiler, yara örtüleri gibi birçok alanda daha çalışmalar yapılacaktır.

TEŞEKKÜR

Yazarlar, çalışmaya verdikleri maddi destekten dolayı Areka Filtrasyon Teknolojileri Ltd. Şti.’ ye teşekkür etmektedirler.

KAYNAKLAR

1. Shi, L., Zhuang, X., Tao, X., Cheng, B. & Kang, W. Solution blowing nylon 6 nanofiber mats for air filtration. *Fibers Polym* **14**, 1485–1490 (2013).
2. Marsano, E., Francis, L. & Giunco, F. Polyamide 6 nanofibrous nonwovens via electrospinning. *J. Appl. Polym. Sci.* 1754–1765 (2010) doi:10.1002/app.32118.
3. Subbiah, T., Bhat, G. S., Tock, R. W., Parameswaran, S. & Ramkumar, S. S. Electrospinning of nanofibers. *J. Appl. Polym. Sci.* **96**, 557–569 (2005).
4. Sahay, R. *et al.* Electrospun composite nanofibers and their multifaceted applications. *J. Mater. Chem.* **22**, 12953 (2012).
5. Zhang, X. & Lu, Y. Centrifugal Spinning: An Alternative Approach to Fabricate Nanofibers at High Speed and Low Cost. *Polymer Reviews* **54**, 677–701 (2014).
6. Gundogdu, N. A. S., Akgul, Y. & Kilic, A. Optimization of centrifugally spun thermoplastic polyurethane nanofibers for air filtration applications. *Aerosol Science and Technology* **52**, 515–523 (2018).
7. Polat, Y. *et al.* Solution blowing of thermoplastic polyurethane nanofibers: A facile method to produce flexible porous materials. *J. Appl. Polym. Sci.* **133**, (2016).
8. Berger, T. J., Spadaro, J. A., Chapin, S. E. & Becker, R. O. Electrically Generated Silver Ions: Quantitative Effects on Bacterial and Mammalian Cells. *Antimicrobial Agents and Chemotherapy* **9**, 357–358 (1976).
9. Altuner, E. E. Production of Nano Creams. *KSEJ* **4**, 52–57 (2014).
10. Duncan, T. V. Applications of nanotechnology in food packaging and food safety: Barrier materials, antimicrobials and sensors. *Journal of Colloid and Interface Science* **363**, 1–24 (2011).

Grafen Katkılı Karbon Nanoliflerin Süperkapasitörlerde Kullanımı

ALTIN, Yasin*[1], BEDELOĞLU, Ayşe**[1]
[1]Bursa Teknik Üniversitesi, Lif ve Polimer Mühendisliği Bölümü
* yasin.altin@btu.edu.tr ; ** ayse.bedeloglu@btu.edu.tr

AMAÇLAR

Esnek süperkapasitörler giyilebilir elektronik uygulamalarının enerji ihtiyacının sağlanmasında kullanılabilecek önemli enerji depolama teknolojilerindendir. Karbon nanolifler esneklik, hafiflik, geniş yüzey alanı gibi üstün özellikleri ile süperkapasitörlerde elektrot olarak kullanılabilmektedir. Bu elektrotların performansları karbon bazlı nanomalzemeler (grafen, karbon nanotüp vb), iletken polimerler ve metal oksit nanopartiküller ile artırılabilmektedir. Bu çalışmada karbon nanolif içerisine farklı oranlarda grafen ilave edilerek elde edilen nanoliflerin morfolojik ve elektrokimyasal özellikleri incelenmiştir.

GİRİŞ

Çevresel ve insan sağlığı gibi kaygılar nedeni ile enerji üretiminde fosil yakıt kullanımı yerini güneş ve rüzgar gibi yenilenebilir enerji kaynaklarına bırakmaktadır. Fakat bu yenilenebilir enerji kaynakları çevresel değişimlerden doğrudan etkilenen ve istendiği zaman enerji üretiminin gerçekleştirilemediği sitemlerdir. Bu yenilenebilir enerji kaynaklarının sürdürülebilir bir şekilde kullanımı bu sitemlerin enerji depolama sistemleri ile entegre edilmesi ile mümkün olmaktadır.

Diğer taraftan güneş pili, piezoelektrik ve triboelektrik nanojeneratörler gibi enerji üretim sistemleri son yıllarda tekstil yüzeylerine entegre edilmektedir. Bu sistemlerden üretilen enerjinin verimli kullanımı ancak üretilen enerjinin yine tekstil yüzeylerine uygulanabilen sistemlerde depolanabilmesi ile mümkün olmaktadır.

Süperkapasitörler enerji depolama teknolojileri arasında yüksek güç yoğunluğu, uzun döngü ömrü, hızlı şarj/deşarj edilebilme gibi özellikleri ile ön plana çıkmaktadır[1-3]. Süperkapasitörler elektrot, elektrolit, ayırıcı ve akım toplayıcı tabakalardan oluşmaktadır. Süperkapasitörler için en önemli komponenti elektrotlar oluşturmaktadır. Aktif karbon, grafen, karbon nanotüp gibi karbon bazlı malzemeler, iletken polimerler ve metal oksitler süperkapasitörlerde elektrot olarak kullanılmaktadır.

Karbon nanaolifler geniş yüzey alanı, mükemmel elektriksel iletkenliği ve mekanik stabilitesi nedeni ile çift tabakalı süperkapasitörlerde elektrot olarak kullanılmaktadır. Uzun yıllardır bilinen bir malzeme olan karbon nanoliflerin kapasitans özellikleri grafen, karbon nanotüp gibi karbon bazlı nanomalzemeler veya pseudokapasitif özellik gösteren metal oksit ve iletken polimerlerin ilavesi ile geliştirilmektedir. Bu sayede daha fazla enerji depolayabilen süperkapasitörler üretilebilmektedir.

Bu çalışmada karbon nanolifler üretimi için çıkış malzemesi olarak poliakrilonitril (PAN) polimeri kullanılmıştır. Öncelikle PAN nanolif dokusuz yüzeyleri elektroüretim yöntemi ile üretilmiş ve sonrasında sırasıyla oksidasyon ve karbonizasyon işlemlerine tabi tutularak karbon nanolifler elde edilmiştir. Diğer taraftan PAN nanolif üretimi öncesinde çözelti içerisine %1-20 arasında değişen oranlarda grafen oksit (GO) ilave edilmiş ve elektroüretim gerçekleştirilmiştir. Elde edilen GO katkılı PAN nanolifler sırasıyla oksidasyon ve karbonizasyon işlemlerine tabi tutulmuştur. Bu işlemler sırasında PAN nanolifler karbon nanoliflere dönüşürken aynı zamanda içerisine katkılanan grafen oksit plakaları da inert atmosferde yüksek sıcaklıkta indirgenerek grafene dönüşmektedir. Bu sayede başarılı bir şekilde grafen katkılı karbon nanolif yüzeyler elde edilmiştir.

DENEYSEL

Malzeme

Grafen oksit sentezi için grafit tozu Fisher Scentific'ten, HCl (%33-35), H_2SO_4 (95–98%), H_3PO_4 (85%) ve H_2O_2 (%30) Sigma Aldrich (USA)'den temin edilmiştir. Nanolif üretimi için dimetil formamid (DMF) ve dimetilsülfoksit (DMSO) Sigma Aldrich (USA)'den, poliakrilonitril (PAN) (MA: 150000 gr/mol) J&K Scientific'ten temin edilmiştir. Tüm kimyasallar ilave bir saflaştırma işlemi yapılmadan kullanılmıştır.

Yöntem

Grafen Oksit Sentezi: Grafen oksitin üretiminde geliştirilmiş Hummer's metodu kullanılmıştır[4]. 1 gr grafit tozu, H_2SO_4/H_3PO_4 (120 ml/13,33 ml) karışımı içerisine eklenerek manyetik karıştırıcı ile karıştırılmış ve üzerine 6 gr $KMnO_4$ ilave edilerek yağ banyosu içerisinde 50 °C'de 12-24 saat boyunca reaksiyona bırakılmıştır. Reaksiyon sonunda karışım 150 ml buz banyosu üzerine dökülerek üzerine 1 ml %30'luk H_2O_2 ilave edilmiştir. Sonrasında karışım içerisindeki katı malzeme santrifüj ile ayrılıp sırası ile 2 defa saf su, metanol, etanol, %37'lik HCl ile yıkanmış sonrasında ise pH 7'ye gelene kadar saf su ile yıkanmaya devam edilmiştir[4].

__Grafen Oksit Katkılı PAN Nanoliflerin Üretimi:__ Çalışma kapsamında grafen oksit farklı konsantrasyonlarda (kütlece %1-20 arasında) PAN çözeltisi içerisine katılarak GO oksit katkılı nanoliflerin üretimi optimum elektroüretim şartlarında gerçekleştirilmiştir.

__Grafen/Karbon Nanoliflerin Üretimi:__ Üretilen grafen katkılı nanolifler öncelikle 300 °C'de hava ortamında okside edilmiş, sonrasında ise argon ortamında tüp fırın içerisinde 1000 °C'de karbonize edilmiştir. PAN nanoliflerin karbonizasyonu sırasında inert atmosferde grafen oksit plakaları indirgenerek grafen plakalarına dönüşmüştür.

DENEYSEL SONUÇLAR/TARTIŞMA

Grafen oksit geliştirilmiş Hummers' metodu ile sentezlenmiş ve sonrasında FT-IR ile karakterize edilmiştir. Şekil 1'de çıkış malzemesi olarak kullanılan grafit ve grafen oksidin FT-IR spektrumları görülmektedir. Şekil 1'de görüldüğü üzere grafit spektrumunda herhangi bir pik görülmezken oksidasyon sonrasında GO'in oksidasyonunu gösteren karakteristik pikler gözükmektedir.

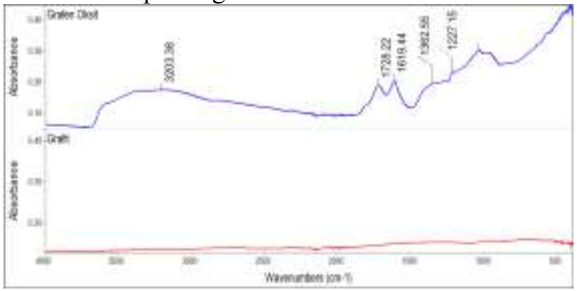

Şekil 1. Grafit ve grafen oksidin FT-IR spektrumları

Şekil 2'de elde edilen GO katkılı PAN nanoliflerin görüntüleri görülmektedir. %100 PAN nanolif beyaz iken GO miktarı arttıkça rengi koyulaşmaktadır.

Şekil 2. Üretilen GO katkılı PAN nanoliflerin görüntüsü.

Şekil 3'te ise oksidasyon ve karbonizasyon işlemi sonrası numunelerin görüntüsü görülmektedir. Renk değişimlerinden işlemlerin başarılı bir şekilde gerçekleştirildi gözlemlenmekle birlikte FT-IR analizi ile oksidasyon ve karbonizasyon işlemlerinin başarılı bir şekilde gerçekleştirildiği teyit edilmiştir.

Şekil 3. GO katkılı PAN nanoliflerin oksidasyon ve karbonizasyon sonrası görüntüleri.

Elde edilen grafen katkılı karbon nanoliflerin elektrokimyasal özellikleri 3 elektrot sisteminde CHI608E model cihaz ile gerçekleştirilmiştir. Referans elektrot olarak Ag/AgCl, karşıt elektrot olarak Pt elektrot kullanılmıştır. Elektrolit olarak ta 1 M'lık H_2SO_4 çözeltisi seçilmiştir.

Üretilen elektrotların elektrokimyasal özellikleri ölçülmüş ve birbiri ile kıyaslanmıştır.

GENEL SONUÇLAR

Grafen oksit başarılı bir şekilde sentezlenerek PAN nanoliflerin içerisine farklı oranlarda entegre edilmiştir. Elde edilen nanokompozit nanolifler başarılı bir şekilde karbonize edilerek grafen katkılı karbon nanolifler üretilmiştir. Üretilen nanokompozit elektrotların morfolojik ve elektrokimyasal özellikleri incelenmiştir.

TEŞEKKÜR/BILGILENDIRME/FON KAYNAĞI

Bu çalışma Bursa Teknik Üniversitei Bilimsel Araştırma Projesi (BAP) No:172D32 tarafından desteklenmiştir.

KAYNAKLAR

1. Wang, G.P., L. Zhang, and J.J. Zhang, 2012, "A review of electrode materials for electrochemical supercapacitors". Chemical Society Reviews. 41(2): p. 797-828.
2. Chee, W.K., et al., 2016, "Flexible Graphene-Based Supercapacitors: A Review". Journal of Physical Chemistry C. 120(8): p. 4153-4172.
3. Zang, X.B., et al., 2015, "Graphene/polyaniline woven fabric composite films as flexible supercapacitor electrodes". Nanoscale. 7(16): p. 7318-7322.
4. Marcano, D.C., et al., 2010, "Improved Synthesis of Graphene Oxide". Acs Nano. 4(8): p. 4806-4814.

Usage of Polyacrylonitrile Nanofibers Containing MgO Nanoparticles on Particulate Filtration and Toluene Adsorption

DEMIR, Ali[1], BAYSAL, Tugba[2,3]
[1] Department of Textile Engineering, Istanbul Technical University
[2] Department of Nanoscience and Nanoengineering, Istanbul Technical University
[3] Department of Nanoscience and Nanoengineering, Gebze Technical University
ademir@itu.edu.tr

PURPOSE

The aim of this study is to investigate the use of MgO / PAN nanofibers in air filtration and to investigate the effect of MgO nanoparticles and their different concentrations on both particle holding efficiency and toluene adsorption ability.

INTRODUCTION

Due to the increasing population, increasing industrialization and millions of vehicles of transportation, very fine dust particles and gases are emitted into the environment. As a result, air quality has been decreasing day by day. In addition, there are volatile organic compounds (VOCs), many of which can be evaporated even at room temperature, in many materials such as adhesives, air fresheners, glues, paints, liquid cleaners, floor polishes, solvents, which we frequently use in our daily lives. Although most of these affects mainly the respiratory system, they can cause hematological problems and even cancer. Toluene, benzene, formaldehyde, xylene and styrene are among the major VOCs [1].

The holding of these gaseous substances is achieved by adsorption. For this purpose, an adsorbent with a high surface area, a suitable pore size (micro-meso pores) and distribution and which will able to interact with VOCs chemically or physically is required [2]. Considering all these properties, functionalized nanofibers are a good filter material that can be used in both VOCs adsorption and particulate filtration studies with their superior properties such as high surface areas, porosity and being easily combined with many materials [3].

Metal oxides such as MgO, Al_2O_3, SnO_2, MnO, TiO_2, ZnO and their nanoparticle (NP) forms can chemically react with toxic gases in the air and convert them to harmless or less harmful by-products due to their catalytic properties [4]. Metal oxides especially in the form of nanoparticles, exhibit more catalytic properties due to their high surface area, higher number of reactive oxide / hydroxide ions on the surface, and structural surface defects [5]. Furthermore, the added nanoparticles increase the surface area by causing protrusions on the nanofiber surface and, also cause to reduce the pore size. This increases both filtration performance and adsorption capability [6].

In this study, we added MgO NPs at various concentrations to PAN polymer solution to produce functional nanofibers and demonstrated the effect of MgO NPs and their concentration on both particle holding efficiency and toluene adsorption ability.

EXPERIMENTAL STUDIES

Materials

Industrial PAN powder (AKKIM), dimethylformamide (DMF) as a solvent and MgO NPs (Sigma Aldrich) was used during our study.

Fabrication of PAN Nanofiber Containing MgO Nanoparticles

First, the MgO NPs in the various contents (7 wt%, 17 wt%) was added into DMF, then the solution is stirred for 1 hour with the ultrasonic stirrer. Then, 13%wt of PAN powder (it keeps constant for all solutions) was dissolved in the mixture solution of the DMF-MgO NPs by using magnetic stirrer for 6 hours.

The MgO/PAN filter media was fabricated onto a non-woven PP support (25 csm) by electrospinning device with 2 needles. The distance from the needle tip to the collector, the voltage, flow rate, homogeneity and drum speed were set at 23 cm, 26 kV, 2.2 ml/h, 20 mm/s – 90 mm, and 200 rpm respectively.

Particulate Filtration Test/Toluene Adsorption Test

An automated filter tester (model 8130A) was used to evaluate the filtration performance of the MgO/PAN filter samples. Charge-neutralized monodisperse solid sodium chloride (NaCl) aerosol particles with diameter size of 300−500 nm was used as an ultra-fine particle agent.

Toluene gas adsorption studies were carried out using the test setup established in ITU environmental laboratory (Figure 1). Toluene gas was sent into filter media at constant speed, the existing toluene gases were collected and analysed by GC-MS. The Scanning Electrone Microscopy (SEM) was used for morphological characterisation.

Figure 1 Toluene gas adsorption test setup

EXPERIMENTAL RESULTS AND DISCUSSION

The surface morphology of MgO NP free PAN NF, %20 MgO/PAN NF (%13 PAN and %7 MgO NP), and %30 MgO/PAN NF (%13 PAN and %17 MgO NP) at certain coating times of 20,40 and 60 mins, is depicted in Figure 2.

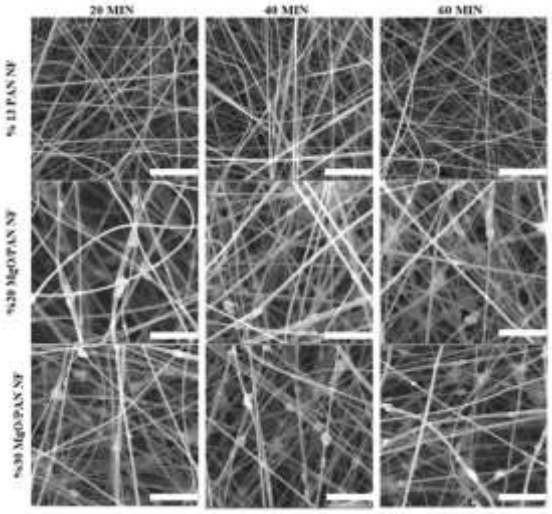

Figure 2 SEM images of produced samples (scale bar is 5 μm and magnification:5 kx for all images)

According to SEM results, 13% PAN NFs are smooth, flat, and they have uniform fiber morphology with no bead formation. Although MgO NPs were generally homogeneous spread on the nanofiber surface, agglomeration of MgO NPs occurs in some regions. Increase in MgO NPs content in filter media cause to increase roughness of nanofibrous surface. These nanoprotrusions cause to decrease in pore size between the nanofibers.

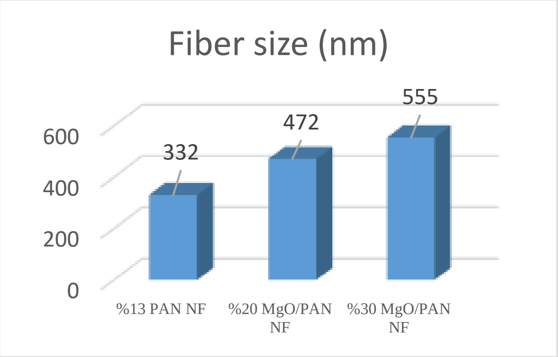

Figure 3 Average fiber size of produced samples

As seen in Figure 3, size of nanofibers increases with increasing MgO NPs content into polymer solution related to increased viscosity of solution.

In Figure 4, Filtration efficiency and pressure drop results of produced samples is shown. It is known that, as the fibre diameter of nanofiber decreases, its pore size and porosity decreases. When pore size reduces, filtration efficiency and pressure drop increases [7]. In our study, as the MgO NPs content into polymer solution increased, the fiber diameter decreased. However, pore diameters decreased as the added nanoparticles caused protrusions on the surface. So, filtration efficiency and pressure drop increases related to increased filter thickness and increased nanoparticle concentration (Figure 4).

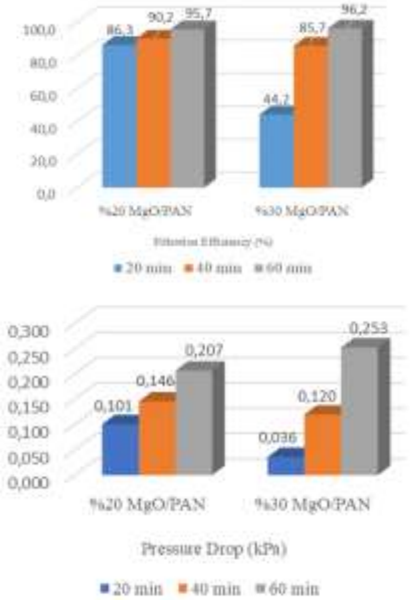

Figure 4 Thickness and nanoparticle concentration effect on filtration Efficiency (above) and pressure drop (below)

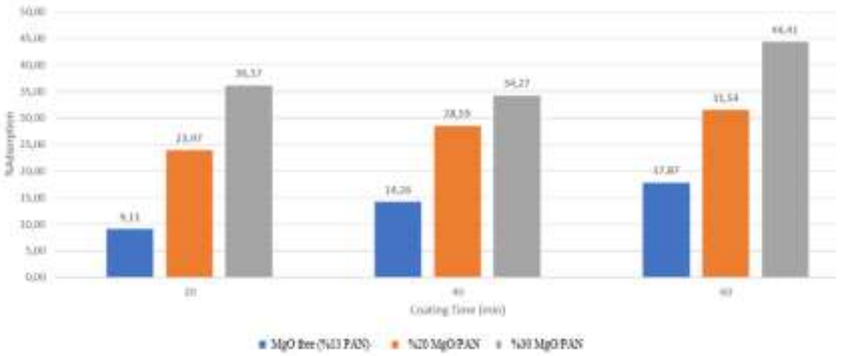

Figure 5. Nanoparticle Concentration Effect on Toluene Adsorption

Toluene adsorption test results of produced samples are shown in Figure 5. According to results, As the concentration of MgO NPs increases, the amount of adsorbed toluene onto samples increases. This is related to the pore size. As mentioned above, after addition of MgO NPs into solution, the pore size among nanofibers decreased and, thus adsorption ability increases. In our study, we hoped to see the catalytic effect of MgO NPs. Unfortunately, we were only able to achieve toluene adsorption, no harmless by-product formation was observed. Moreover, we can say that as the coating time increases, the amount of adsorbed toluene onto samples increases. As the coating time increases, the thickness of the filter media produced increases and micro-meso channels form in the structure, and the nanoparticles may find more space for adsorption.

CONCLUSIONS

In our study, we added MgO NPs to the polymer solution, thus we obtained a rough surface. As the formed protrusions reduced pore sizes, the filtration efficiency and pressure drop of the filters produced increased, but also caused a large increase in the amount of toluene adsorption. Due to the catalytic properties of MgO NPs we expected to break down toluene and convert it to harmless by-products. Unfortunately, we could not obtain catalytic degradation products at the MgO NP concentration studied. However, we were able to capture ultra-fine particles with a high yield of 96.2%, a pressure drop of 253 Pa. In addition, we have demonstrated that nanofibers are a promising material for gas filtration. We were able to adsorb 44.4% of toluene, a harmful gas.

FUTURE STUDIES

We aim to produce MgO / PAN NF with higher MgO content, so that we can see the catalytic effect of MgO NPs.

REFERENCES

[1] M. Kampa and E. Castanas, ‘Human health effects of air pollution’, *Environ. Pollut.*, vol. 151, no. 2, pp. 362–367, Jan. 2008, doi: 10.1016/j.envpol.2007.06.012.

[2] X. Zhang, B. Gao, A. E. Creamer, C. Cao, and Y. Li, ‘Adsorption of VOCs onto engineered carbon materials: A review’, *J. Hazard. Mater.*, vol. 338, pp. 102–123, Sep. 2017, doi: 10.1016/j.jhazmat.2017.05.013.

[3] M. Zhu *et al.*, ‘Electrospun Nanofibers Membranes for Effective Air Filtration’, *Macromol. Mater. Eng.*, vol. 302, no. 1, p. 1600353, Jan. 2017, doi: 10.1002/mame.201600353.

[4] A. Vanangamudi, S. Hamzah, and G. Singh, ‘Synthesis of hybrid hydrophobic composite air filtration membranes for antibacterial activity and chemical detoxification with high particulate filtration efficiency (PFE)’, *Chem. Eng. J.*, vol. 260, pp. 801–808, Jan. 2015, doi: 10.1016/j.cej.2014.08.062.

[5] S. Dadvar, H. Tavanai, M. Morshed, and M. Ghiaci, ‘The Removal of 2-Chloroethyl Ethyl Sulfide Using Activated Carbon Nanofibers Embedded with MgO and Al_2O_3 Nanoparticles’, *J. Chem. Eng. Data*, vol. 57, no. 5, pp. 1456–1462, May 2012, doi: 10.1021/je201328s.

[6] J. Su, G. Yang, C. Cheng, C. Huang, H. Xu, and Q. Ke, ‘Hierarchically structured TiO2/PAN nanofibrous membranes for high-efficiency air filtration and toluene degradation’, *J. Colloid Interface Sci.*, vol. 507, pp. 386–396, 2017.

[7] H.-J. Choi *et al.*, ‘Filtration Properties of Nanofiber/Microfiber Mixed Filter and Prediction of its Performance’, *Aerosol Air Qual. Res.*, vol. 17, no. 4, pp. 1052–1062, 2017, doi: 10.4209/aaqr.2016.06.0256.

Interaction of Phosphate-Buffered Saline on the Surface of Carbon Nanofiber Electrodes

SAHTANİ Karima[1], ALADAĞ TANİK Nilay[1], AYKUT Yakup[1,2]
[1]Bursa Uludag University, Graduate School of Natural and Applied Sciences, Textile Engineering, 16059, Nilufer, Bursa, Turkey
[2]Bursa Uludag University, Engineering Faculty, Department of Textile Engineering, 16059, Nilufer, Bursa, Turkey
aykut@uludag.edu.tr

OBJECTIVES

Investigation of the interaction of PBS solution with carbon nanofibers surface since PBS will be used for dissolving miRNA molecules to immobilize them on carbon nanofiber surface or the solution will be used as electrochemical measurement medium.

INTRODUCTION

Nanofibers are great materials because of their high specific surface area and very applicable for variety of applications such as energy[1,2], environment[3], biomedical[4] and biosensors[5]. Electrospinning is a feasible technology to produced nanofibrous mat structure by using very broad spectrum of the materials including polymers[6], ceramic[7], carbon[8] and composites [2].

Carbon nanofibers are produced from an electrospun polymer precursor such as polyacrylonitrile[9], polyvinyl alcohol[10],[11], lignin[12], etc. The precursor nanofibers are properly thermally treated to convert them into carbon nanofiber structures[13]. Most of the electrospun carbon nanofibers have been produced by using PAN as a precursor polymer in the literature for very diverce applications such as energy storage[8], oil-water separation[14], biosensors[15], etc.

Carbon based electrodes are used as the working electrodes for electrochemical biosensor analysis of genetic molecules[16,17]. Since carbon nanofibers have very high specific surface are, more molecules can be interact on the surface and biosensor device performance could be enhanced.

In order to immobilize genetic molecules on the surfaces of the electrodes for electrochemical characterization, in some studies, first the genetic molecules were dissolved in PBS and then the prepared dissolution were applied on the surface of the electrode, or the solution is used as electrochemical measurement medium[18–20].

Carbon nanofibers are potential candidate as working electrode for electrochemical miRNA biosensor applications. So, the interaction of PBS and the electrode surface should be taken into consideration. Based on this motivation, in this study, carbon nanofibers were produced with the addition of hemoglobin and lawsone in the PAN/DMF electrospinning solutions. As-spun precursor nanofibers were heat treated for a proper carbonization. Finally, SEM and contact angle measurements with PBS were carried out.

EXPERIMENTAL

Materials

Polyacrylonitrile (average Mw 150000, Sigma Aldrich), N,N-Dimethylformamide, hemoglobin, lawsone, phosphate-buffered saline.

Method

8 wt. % of PAN dissolved in N,N-Dimethylformamide by magnetic stirring. A defined amount of hemoglobin and lawsone were added into the prepared solution separately and stirred for 24 hours. “L” refers to Lawsone and “H” refers to Hemoglobin, and the number with the letter “L” and “H” refers to weight percentage of lawsone respect to PAN in the electrospinning solution (ex: L15 means 15 wt.% PAN in 8 wt. % PAN/DMF). Then, the prepared solutions were electrospun into the precursor nanofibrous mat. Electrospinning conditions were adjusted as 12 kV applied voltage, 0.5 ml/hours feeding rate, and 15 cm from the tip of needle to collector. The precursor nanofibers stabilized in air atmosphere at 280ºC for 1 hour and then carbonized in nitrogen atmosphere at 800 ºC for 2 hours[21,22]. After morphological analyzes with a scanning electron microscope, contact angle measurements were conducted by dropping PBS on the carbon nanofibrous mat surfaces.

EXPERIMENTAL RESULTS/DISCUSSION

Precursor electrospun PAN nanofibers were stabilized and carbonized sequentially as it was explained in the experimental section. Carbonized nanofiber morphologies were inspected by observing SEM images. As seen from Figure 1, carbonized nanofibers were very well randomly distributed in the mat structure and fibers uniformity hasn’t been lost. Even though some beaded structures are presented on the carbonized fibers, these defects are not seen all around the web.

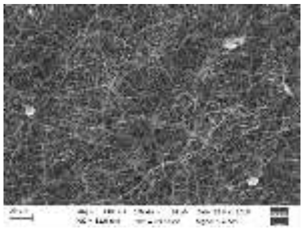

Figure 1. SEM image of neat carbon nanofiber surface.

Different amount of lawsone was added into electrospun PAN/DMF solution, and PAN/lawsone precursor nanofibers were obtained after a proper electrospinning process. As-spun precursor PAN/lawsone nanofibers were also stabilized and carbonized sequentially bu following the same procedure. The morphologies of lawsone added carbonized PAN nanofibers were observed with SEM microscopy and the results are given in Figure 2.

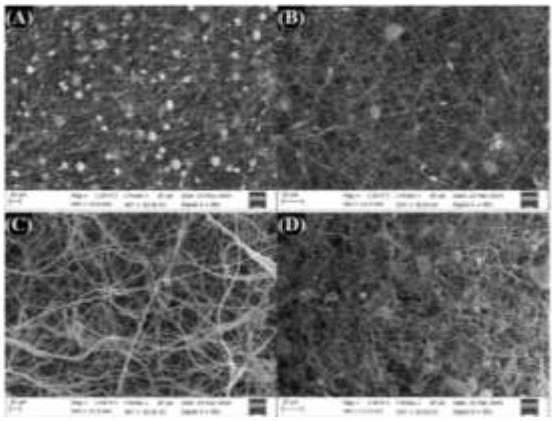

Figure 2. SEM image of lawsone added (in precursor PAN NFs) carbon nanofiber surface: (A) L15, (B) L30, (C) L70 ve (D) L100.

As seen from Figure 2, when a small amount of lawsone was presented in the precursor solution, very much bead structures (called bead-on-a-string[23]) are presented on and among the fibers. When the amount of lawsone was increased in the precursor solution, beaded morphology turned the uniform nanofibers structures.

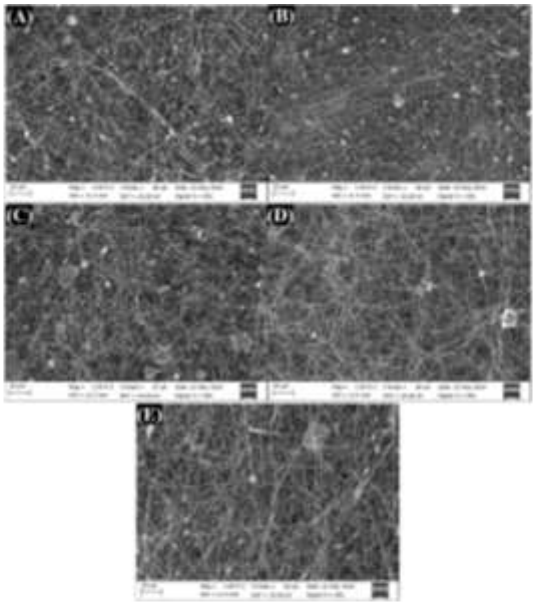

Figure 3. SEM image of hemoglobin added (in precursor PAN NFs) carbon nanofiber surface: (A)H0.5, (B) H1, (C) H3, (D) H15 ve (E) H30.

As seen in Figure 3, when hemoglobin powder was added into the precursor electrospinning solution, beaded defect structure was also seen in the mat structures. The amount of beaded structure is not stable with the hemoglobin concentration that could be related the solution preparation time and condition since 24 hours were not enough to obtain a proper solution after adding hemoglobin in the solution. Some hemoglobin particles were not dissolved and precipitated in the syringe during the electrospinning process.

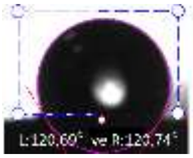

Figure 4. PBS çözeltisi kullanılarak saf karbon nanolif yüzeydeki temas açısı ölçüm sonucu.

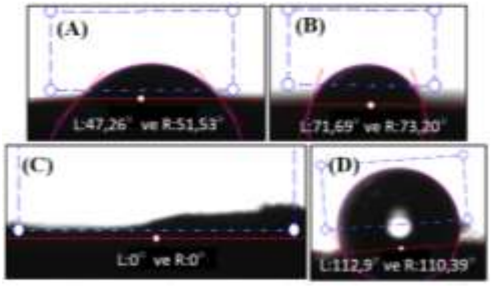

Figure 5. PBS çözeltisi kullanılarak lawsone katkılı karbon nanoliflerde temas açısı ölçüm sonuçları: (A)

L15, (B) L30, (C) L70 ve (D) L100. 49,39; 72,44; 111,64

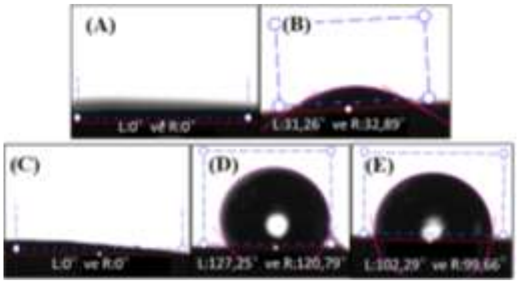

Figure 6. PBS çözeltisi kullanılarak hemoglobin katkılı karbon nanoliflerde temas açısı ölçüm sonuçları: (A) H0.5, (B) H1, (C) H3, (D) H15 ve (E) H30.

Physical interaction of phosphate-buffered saline with the surface of carbon nanofiber mats were investigated via contact angle measurements. When the droplet of PBS was touched the surface, the angle was about 120° at pure carbon nanofibers as seen in Figure 4. When lawsone was presented in the precursor nanofibers then carbonized, the contact angle angle were 49.39 °, 72.44 °, and 111.64 ° for L15, L30 and L100 samples as seen in Figure 5. The PBS droplet was directly sucked by the L70 sample. At hemoglobin added samples in Figure 6, the droplet was directly sucked by H0.5 and H3 samples, and the contact angles were 32.07°, 124.02 °, and 100.97 ° for H1, H15 and H30 samples. As it is seen the contact angles at the carbonized nanofiber mat surfaces were decreased at the initial addition of lawsone and hemoglobin into their precursor nanofibers, and the angle increased again with increasing lawsone and hemoglobin ratio in the fibers. The results are revealed that the affinity of the PBS at the lawsone and hemoglobin added carbonized fiber samples were fluctuated due to surface properties and the added materials in the precursor fibers.

GENERAL CONCLUSIONS

Contact angle measurements of electrospun PAN derived neat carbon nanofibers and PAN/lawsone and PAN/hemoglobin derived carbon nanofibers with PBS were carried out. Highest contact angle was measured with neat carbon nanofiber mat surfaces. Even though initial addition of lawsone and hemoglobin reduced the contact angle and increasing lawsone and hemoglobin content also increased the contact angle at carbonized nanofibers mat surfaces, since PBS droplet was directly sucked by some samples (L70, H0.5 and H3) it is concluded that the contact angle is not only depend on the lawsone and hemoglobin content, it is also depend on the surface properties of the carbonized nanofiber mat.

NEXT TERM STUDIES

miRNA molecules will be immobilized on the surface of the produced carbon nanofibers and electrochemical measurement will be carried out to investigate the applicability of the produced carbon nanofibers as a working electrode in the electrochemical miRNA measurement system.

ACKNOWLEDGEMENT/FUNDING

The present study was part of a research project funded by The Scientific & Technological Research Council of Turkey (TUBITAK, Project no. 118M231). The study is a part of Karima Sahtani’s PhD thesis work in the Graduate School of Natural and Applied Sciences at Bursa Uludag University.

REFERENCES

1. Kim, I-D., Hong, J-M., Lee, B.H., kim, D.Y. 2007. "Dye-sensitized solar cells using network structure of electrospun ZnO nanofiber mats", Applied Physics Letter, 91, 163109.
2. Zhong, Z., Cao, Q., Jing, B., Li, S., Wang, X. 2012. "Novel electrospun PAN-PVC composite fibrous membranes as polymer electrolytes for polymer lithium-ion batteries", Ionics, 18, 853–859.
3. Beck, R.J., Zhao, Y., Fong, H., Menkhaus, T.J. 2017. "Electrospun lignin carbon nanofiber membranes with large pores for highly efficient adsorptive water treatment applications", Journal of Water Processing Engineering, 16, 240-248.
4. Góra, A., Sahay, R., Thavasi, V., Ramakrishna, S. 2011. "Melt-electrospun fibers for advances in biomedical engineering, clean energy, filtration, and separation", *Polymer Reviews*, 51, 267-287.
5. Gokce, Z.G., Akalın, P., Kok, F.N., Sarac, A.S. 2018. "Impedimetric DNA biosensor based on polyurethane/poly(m-anthranilic acid) nanofibers" Sensors and Actuators B: Chemical, 254, 719–726.
6. Huang, Z.M., Zhang, Y.Z., Kotaki, M., Ramakrishna, S. 2003. "A review on polymer nanofibers by electrospinning and their applications in nanocomposites", Composites Science and Technology, 63, 2223-2253.
7. Aykut, Y., Parsons, G.N., Pourdeyhimi, B., Khan, S.A. 2013. "Synthesis of mixed ceramic MgxZn1-xO nanofibers via Mg2+ doping using Sol-Gel electrospinning", Langmuir, 29, 4159-4166.
8. Ji, L., Medford, A.J., Zhang, X. 2009. "Porous carbon nanofibers loaded with manganese oxide particles: Formation mechanism and electrochemical performance as energy-storage materials". Journal of Materials Chemistry, 19, 5593-5601.
9. Zhang, L., Aboagye, A., Kelkar, A., Lai, C., Fong,

H. 2014. "A review: Carbon nanofibers from electrospun polyacrylonitrile and their applications", Journal of Materials Science, 49, 463–480.

10. Gupta, A., Dhakate, S.R. 2017. "Development of structurally stable electrospun carbon nanofibers from polyvinyl alcohol", *Materials Research Express*, 4, 045021.
11. Xuyen, N.T., Ra, E.J., Geng, H.Z., Kim, K.K., An, K.H., Lee, Y.H. 2007, "Enhancement of conductivity by diameter control of polyimide-based electrospun carbon nanofibers", The Journal of Physical Chemistry B, 111, 11350-11353.
12. Ma, X., Kolla, P., Zhao, Y., Smirnova, A.L., Fong, H. 2016. "Electrospun lignin-derived carbon nanofiber mats surface-decorated with MnO2 nanowhiskers as binder-free supercapacitor electrodes with high performance", Journal of Power Sources, 325, 541-548.
13. Aykut, Y., Pourdeyhimi, B., Khan, S.A. 2013. "Effects of surfactants on the microstructures of electrospun polyacrylonitrile nanofibers and their carbonized analogs", Journal of Applied Polymer Science, 130, 3726-3735.
14. Tai, M.H., Gao, P., Tan, B.Y.L., Sun, D.D., Leckie, J.O. 2014. "Highly efficient and flexible electrospun carbon-silica nanofibrous membrane for ultrafast gravity-driven oil-water separation", ACS Applied Materials and Interfaces, 6, 9393-9401.
15. Liu, D., Zhang, X., You, T. 2014. "Electrochemical performance of electrospun free-standing nitrogen-doped carbon nanofibers and their application for glucose biosensing", ACS Applied Materials and Interfaces, 6, 6275-6280.
16. Congur, G., Eksin, E., Erdem, A. 2015. "Impedimetric Detection of microRNA at Graphene Oxide Modified Sensors", Electrochimica Acta, 172, 20-27.
17. Karimi-Maleh, H., Tahernejad-Javazmi, F., Atar, N., Yola, M.L., Gupta, V.K., Ensafi, A.A. 2015. "A Novel DNA biosensor based on a pencil graphite electrode modified with polypyrrole/functionalized multiwalled carbon nanotubes for determination of 6-mercaptopurine anticancer drug", Industrial Engineering Chemistry Research, 2015, 54, 3634–3639.
18. Kara, P., Kerman, K., Ozkan, D., Meric, B., Erdem, A., Ozkan, Z., Ozsoy, M. 2002. "Electrochemical genosensor for the detection of interaction between methylene blue and DNA", Electrochemistry Communications, 4, 705-709.
19. Shen, H.Y., Zheng, H.M., Zhu, N., Liu, Y.Q., Gao, J., Li, J. 2010. "Electrochemical investigation of DNA interaction with melamine and its related compounds", International Journal of Electrochemical Science, 5, 1587-1596.
20. Tanik, N.A., Demirkan, E., Aykut, Y. 2018. "Guanine oxidation signal enhancement in DNA via a polyacrylonitrile nanofiber-coated and cyclic voltammetry-treated pencil graphite electrode", Journal of Physics and Chemisty of Solids, 118, 73-79.
21. Pirzada, T., Arvidson, S.A., Saquing, C.D., Shah, S.S., Khan, S.A. 2014. "Hybrid carbon silica nanofibers through sol-gel electrospinning", Langmuir, 51, 15504-15513.
22. Aykut, Y. 2013. "Electrospun MgO-loaded carbon nanofibers: Enhanced field electron emission from the fibers in vacuum", Journal of Physics and Chemistyr of Solids, 74, 328-337.
23. Lin, T., Wang, H., Wang, H., Wang, X. 2004. "The charge effect of cationic surfactants on the elimination of fibre beads in the electrospinning of polystyrene", Nanotechnology, 15, 1375.

Understanding the Electrospinnability of Polyvinyl Alcohol (PVA) and Controlled Release of Curcumin Through the Electrospun Mat

MAHMUD, Md Musavvir [1], PARVEEN, Asma [2], ZAMAN, Sumaiya [3], JAHAN, Rumana A[4], ARAFAT, M Tarik[*] [1]
[1]Department of Biomedical Engineering, Bangladesh University of Engineering and Technology (BUET), Dhaka, Bangladesh,
[2]Department of Mechanical Engineering, Nazarbayev University, Astana, Kazakhstan,
[3]Department of Microbiology, University of Dhaka, Dhaka, Bangladesh,
[4]Centre for Advanced Research in Sciences (CARS), University of Dhaka, Dhaka 1000, Bangladesh.
[*]tarikarafat@bme.buet.ac.bd

INTRODUCTION

Electrospinning offers to fabricate fibers of various sizes and shape from both natural and synthetic polymers. The electrospinning process can be applied to a wide range of applications of various fields because of the high surface-to-volume ratio and easily tunable morphology of electrospun fibers. Polyvinyl alcohol (PVA) is a biocompatible and highly hydrophilic polymer which has also numerous applications. Curcumin is a natural antibacterial chemical extracted from the spice turmeric. In this study, at first PVA solutions were prepared using different binary solvent mixtures to study the spinnability of PVA in non-water solvent as curcumin is not soluble in water. Tea's graph was introduced to map the solubility and spinnability of the prepared solutions. After optimizing the solvent, PVA/curcumin solution was prepared in an appropriate solvent and electrospun. To stabilize the PVA/curcumin electrospun mats, physical crosslinking was carried out by heat treatment at different temperatures and UV-exposure for a different period. The crosslinking also ensured the controlled release of curcumin from the electrospun fiber mats. All the electrospun fiber mats were evaluated with a scanning electron microscope (SEM), X-ray diffraction (XRD), Fourier transform infrared spectroscopy (FTIR) and differential scanning calorimetry (DSC). Finally, the antibacterial efficacy of the electrospun PVA/curcumin was evaluated by antibacterial test.

EXPERIMENTAL

Method

7%, 10% and 15% (w/v) PVA solutions were prepared in water, 20% acetic acid, 50% acetic acid, 20% ethanol and 50% ethanol and the corresponding solutions were electrospun. Solubility and spinnability of the solutions were mapped with Tea's graph. Furthermore, 10% PVA solutions with 1%, 2% and 5% curcumin (w/w with respect to PVA) were prepared to investigate the drug release. To stabilize in aqueous medium and control the release of curcumin the PVA/curcumin fiber mats were crosslinked by heat treatment and UV-exposure. Heat treatment was carried out at 80 ˚C, 120˚C and 160˚C for 2 hours. On the other hand, UV-exposure was carried out at 40W for 30 minutes, 1 hr and 2 hr. Drug release study was carried out in phosphate buffer saline (PBS) for 24 hours. The antibacterial test was carried out against *E. coli* and *S. aureus* to evaluate the antibacterial properties of curcumin.

EXPERIMENTAL RESULTS AND DISCUSSIONS

The study reveals that the morphology of electrospun PVA fibers from different binary solvent mixtures differs significantly from each other. While solutions prepared with acetic acid-water binary solvent mixture (AW) and water produce cylinder-shaped fibers, solutions prepared with ethanol-water binary solvent mixture (EW) produce flat-shaped fibers. Diameters of fibers spun from AW solutions exhibit the smallest diameter in the range of 70-238 nm. On the other hand, the diameter of fibers spun from EW solutions was much higher in the range of 270-955 nm. However, adding curcumin with PVA decreases the average fiber diameter. The more curcumin was added, the more decrease in diameter was observed. Crosslinking by heat treatment caused a marginal increase in fiber diameter whereas no significant change was observed in the case of UV-exposure. The controlled release of curcumin was achieved by both types of crosslinking. The release of curcumin was slowed down up to 20% by heat treatment and 9% by UV-exposure at 24 hr. The antibacterial study showed all bacteria killed within 6 hours.

CONCLUSIONS

Electrospinning of PVA from binary solvent mixtures was evaluated and utilized in drug delivery application where curcumin was used as an antibacterial drug. Fibers of different sizes and shapes were fabricated by using different solvents. While incorporating curcumin, it was successfully electrospun with PVA and crosslinked by heat treatment and UV-exposure. The controlled release of curcumin was achieved by both types of crosslinking.

Excellent antibacterial properties were also observed. It is expected that the stable antibacterial nanofibrous mat with controlled curcumin release capability could be a potential candidate for wound dressing application.

Nanolif Esaslı Piezoelektrik Nanojeneratörlerde Elektrosprey Yoluyla Elektrot Uygulamaları

ÜNSAL, Ömer Faruk[1], ÇELİK BEDELOĞLU, Ayşe[2]
[1]Bursa Teknik Üniversitesi, İleri Teknolojiler A.B.D, Yıldırım/Bursa,Türkiye
[2]Bursa Teknik Üniversitesi, Lif ve Polimer Mühendisliği Bölümü, Yıldırım/Bursa,Türkiye
unsal.omerf@gmail.com, ayse.bedeloglu@btu.edu.tr

AMAÇLAR

Bu çalışmanın amacı, elektrosprey metodu ile iletken partikül kaplanması ve kaplamaların mekanik-elektriksel enerji dönüşümündeki performansının incelenmesidir. Üretilen nanojeneratör sistemlerden alınan çıkış voltajları ele alınarak elektrotların kalınlıkları ile performansları arasındaki ilişki belirlenmiştir.

GİRİŞ

Nanojeneratörler, verimsiz kullanılan, yani atık durumdaki mekanik veya ısıl enerjinin geri kazanımını sağlayan sistemlerdir[1]. Mekanik enerjinin elektrik enerjisine dönüşüm mekanizmasında itici güç olarak yer değiştirme akımı kullanılmaktadır[2]. Nanojeneratörler isimlerini üretilen çok küçük enerji miktarlarından almaktadırlar; üretildikleri materyallerin nano-malzeme olma şartı yoktur.

Nanojeneratörler piezoelektrik, triboelektrik veya piroelektrik prensiple çalışırlar. Piezoelektrik ve triboelektrik nanojeneratörler mekanik enerjinin dönüşümünü sağlarken piroelektrik nanojeneratörler ısıl enerjinin elektrik enerjisine dönüşmesini sağlar[3].

Piezoelektrik etki, moleküler simetri eksikliğinden kaynaklanan ve mekanik stres altında gerçekleşen polarizasyondan kaynaklanmaktadır[4]. Bu bağlamda en çok kullanılan piezoelektrik malzemeler würtzite kristaller, perovskit kristaller ve polimerlerdirler. Piezoelektrik etki kullanılarak üretilen nanojeneratörlerdeki gelişim ilk zamanlarda metal oksitler üzerinden ilerlese de bu malzemelerin kırılganlıklarından dolayı yerini piezoelektrik polimerlere bırakmışlardır[5].

Poliviniliden florit (PVDF), $(CH_2\text{-}CF_2)_n$ kapalı formülüne sahip bir floropolimerdir. PVDF'in α, β, γ, δ ve ε olmak üzere beş farklı kristalin fazı vardır. Bunlardan β ve γ kristalin fazlarda H ve F atomlarının polarizasyonu en yüksek oranına ulaşmaktadır. Bu sebeple bu kristal yapılarda PVDF piezoelektrik etki gösterir[6].

Grafen, karbon nanotüm, grafen oksit, metal nanoteller gibi nano malzemeler, nanojeneratörlerde katkı malzemesi olarak sıkça kullanılmaktadır. İletken katkı, piezoelektrik malzemedeki yer değiştirme akımının malzemenin yüzeyine taşınmasını sağlamaktadır[7,8]. Bunun yanı sıra bu malzemeler, ince kaplama olarak kullanıldıklarında esnekliğe müsaade ettiklerinden nanojeneratör elektrodu olarak da kullanımları oldukça yaygındır [9-12].

DENEYSEL

Malzeme

Çalışma kapsamında üretilecek nanolifler için çözücü olarak aseton (Sigma-Aldrich) ve dimetil formamid (DMF) (Merck); polimer olarak ise poliviniliden florür (PVDF) (Alfa Aesar) (d: 1,76 g/cm3) kullanılmıştır. Elektrosprey işlemi için ise deiyonize su ve 2-propanol (Sigma) kullanılmıştır.

Grafen oksit üretimi için grafit (Merck), sülfürik asit (%98, Merck), fosforik asit (%85, Sigma-Aldrich), potasyum permanganat (Sigma), hidrojen peroksit (%35, Sigma-Aldrich), hidroklorik asit (%37, Fischer Chemicals) ve etil alkol (ISOLAB) kullanılmıştır. İndirgeme işlemi için ise hidrazin hidrat (%55, Sigma) kullanılmıştır.

Yöntem

Grafen oksit üretimi için önceki çalışmalarımızda[13] da kullandığımız Geliştirilmiş Hummers Metodu kullanılmıştır.

Nanojeneratörlerde piezoelektrik bileşen olarak PVDF nanolifler kullanılmıştır. Nanolif üretimi için polimer solüsyonu ağırlıkça %10 PVDF içermektedir. Çözücü olarak ise ağırlıkça 2:1 oranda aseton ve DMF karışımı kullanılmıştır. Elektro-üretim işlemindeki parametreler ise 4 mL/sa çözelti besleme hızı ile 23 kV voltaj ve 15 cm mesafeden gerçekleştirilmiştir.

Üretilen nanolifler, PET elektrot şablonlarının arasına konularak elektro-püskürtme işlemi gerçekleştirilmiştir. Püskürtme çözeltisi, 0,5 mg/mL grafen oksit (GO) içeren hacimce 2:1 deiyonize su 2-propanol karışımından ibarettir. Elektro-püskürtme işlemi ise 30 mL/sa çözelti besleme hızı ile 8 cm mesafeden 33-37 kV voltaj aralığında gerçekleştirilmiştir. Tüm nanolifin bir yüzeyine 2,5 mg, 5,0 mg, 7,5 mg ve 12,5 mg GO tekabül edecek sürelerde püskürtme işlemi gerçekleştirilmiştir.

Kaplanan nanolifli yapılar 1 gece boyunca çeker ocakta kurumaya bırakılmıştır. Elektro-püskürtme ile GO kaplanmış nanolifli yapılar, 80 mL 0,1 M hidrazin hidrat çözeltisi içinde 95 °C'de 3 saat indirgeme işlemine tabi tutulmuştur. İndirgeme işlemi ile GO kaplı yüzeylerin kahverenginden siyah renge döndüğü gözlenmiştir. Bu aşamada GO kaplama, indirgenmiş grafen oksit (rGO)'a dönmüştür.

Nanolifli yapıların nanojeneratöre dönüştürülmeleri için her biri iki alüminyum bant arasına alınmış ve bu sandviç yapı PDMS ile kaplanmıştır.

Nanojeneratörlerden alınan elektriksel kontaklar, bir osiloskopa bağlanmış ve nanojeneratörler önceki çalışmalarda[13] tasarlanmış test düzeneğinde periyodik olarak bükülmeye maruz kalmıştır. Osiloskop yardımı ile büküme bağlı voltaj değişimleri gözlenmiş ve kaydedilmiştir.

Ayrıca nanolifli yapıların kristalin faz analizleri için FT-IR ve XRD analizleri gerçekleştirilmiştir. Kaplanmış nanoliflerin indirgeme işleminden önce ve sonra alınan SEM görüntüleri ile kaplamanın iki farklı formu da gözlenmiştir.

DENEYSEL SONUÇLAR/TARTIŞMA

Toz PVDF'e, PVDF nanolifli yapıya ve kaplamalı numunelere indirgeme işleminden sonra yapılan FT-IR analizlerinde β kristalin faz pikleri gözlenmiştir. Toz polimerde α kristalin faz fikleri yoğun bir şekilde gözlenmektedir. Elektro-üretim esnasında polimer omurgasına bağlı atomların elektrik alan ve solüsyondaki yüksek mobiliteleri, β faza geçişi bir oranda sağlamaktadır. Fakat bunun da ötesinde, kaplamalı nanolifli yapıların hidrazin hidrat ile indirgeme işleminin ardından α kristalin faz pikleri şiddetlerini oldukça düşürmüş ve β kristalin faz pik şiddetleri yükselmiştir (Şekil 1).

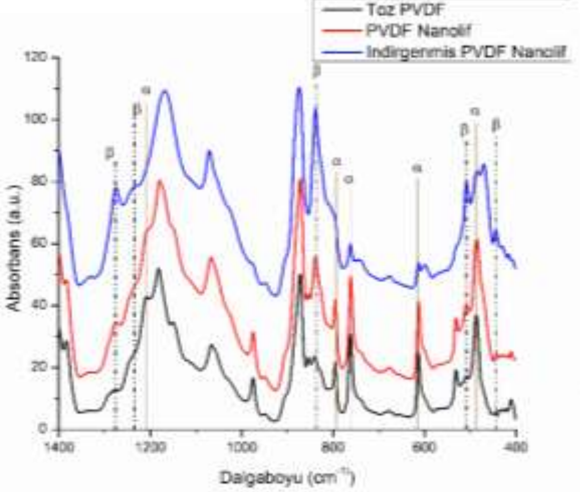

Şekil 1. Nanolifli yapılara ve toz polimere uygulanan FT-IR analizinin spektrumları

PVDF için kristalin yapı analizleri, XRD testlerinde de doğrulanmıştır. Toz PVDF'de gözlenmeyen β faz pikleri nanolifli yapı halinde gözlenebilmiştir. (Şekil 2).

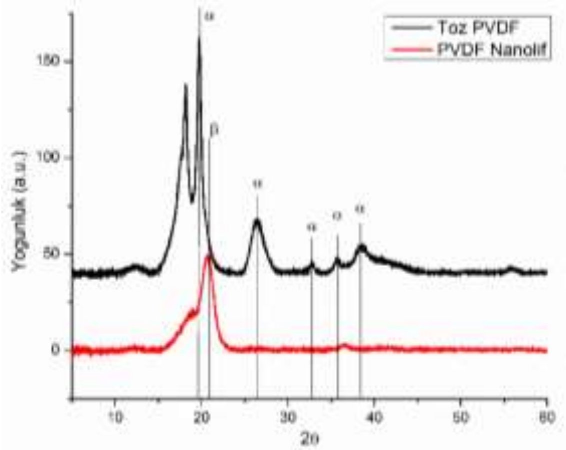

Şekil 2. Toz ve nanolif PVDF'e yapılan XRD analizinin sonuçları

Numunelere yapılan piezoelektrik testler sonucu elektrosprey metodu ile uygulanan elektrotların enerji dönüşümüne etkisi gözlenmiştir. Kaplama işleminin maksimum voltajı yükselttiği görülmüştür. Kaplama kalınlığının artırılması ile ise maksimum voltajın bir noktaya kadar yükseldiği ve kalınlık artışının maksimum voltajı düşürdüğü görülmüştür (Şekil 3). Nanojeneratörlerin ürettikleri maksimum voltaj değerleri ise şekil 4'te verilmiştir.

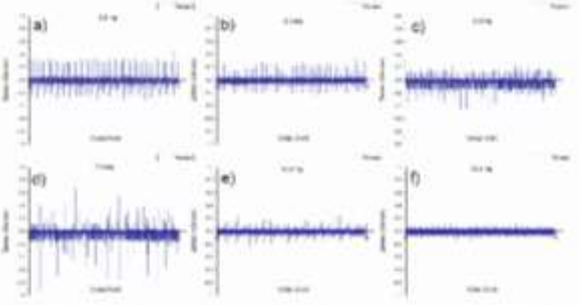

Şekil 3. Kaplamasız ve kaplamalı numunelerin zamana karşı ürettikleri gerilim sinyalleri

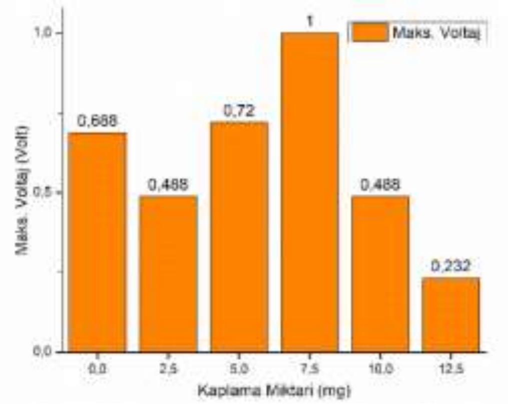

Şekil 4. Nanojeneratörlere ait maksimum voltaj değerleri

Kaplamalı numunelere indirgeme işleminden önce ve sonra yapılan SEM görüntüleme işlemleri sonucu indirgeme işlemi doğrulanmaktadır. İndirgeme işleminden önce GO, daha yumuşak bir yüzey görüntüsü verirken indirgeme işleminin ardından levhasal rGO katmanlar gözlenmiştir (Şekil 5).

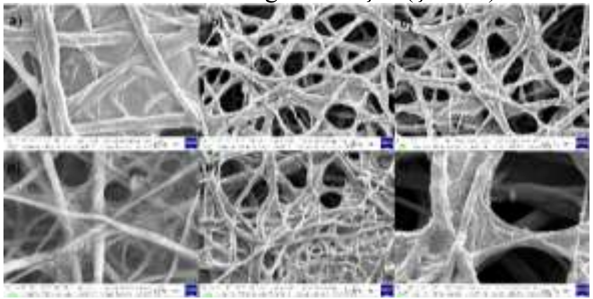

Şekil 5. a),b) ve c) İndirgeme işleminden önceki ve d), e) ve f) indirgeme işleminden sonra alınmış SEM görüntüleri

GENEL SONUÇLAR

PVDF üzerinde yapılan FT-IR analizlerinde β faz pikleri gözlenmiştir. Elektroüretim aşamasında polimerin solüsyon formunda olması, bu sayede yan grupların yüksek hareket kabiliyeti mevcuttur. Bu esnada uygulanan yüksek elektrik alan, H ve F atomlarının yeterince polarize olmasını sağlamaktadır. β faz piklerinin indirgeme işlemi ile daha da şiddetlenmesi ise indirgeme işleminde kullanılan hidrazin molekülünün sıcaklığın da etkisi ile zincirlerin arasına girmesi ve polarizasyonu desteklemesi ile açıklanabilir.

Nanolifli yapılarak yapılan piezoelektrik testlerde ise en ince kaplamalarda maksimum voltajın kaplamasız numuneye kıyasla düşüşe uğradığı, 7,5 mg GO kaplanmasına kadar ise düzenli olarak arttığı gözlenmiştir. Daha kalın kaplamalarda ise üretilen elektrik enerjisinin rGO elektrotların direncinde elimine olduğu söylenebilmektedir.

SONRAKİ DÖNEM ÇALIŞMALARI

İlerideki çalışmalarda, üretilecek nanojeneratörlerin kaplama homojeniteleri ve bunun enerji üretimindeki etkisi araştırılacaktır. Bunun yanı sıra nanojeneratörlerden elde edilecek gücün net bir şekilde tespit edilebilmesi amacı ile eş zamanlı voltaj ve akım ölçümleri gerçekleştirilecektir.

KAYNAKLAR

1. Wang, X., *et al.*, *Science* (2007) **316** (5821), 102
2. Wang, Z. L., *Nano Energy* (2019), 104272
3. Ünsal, Ö. F., and Bedeloğlu, A. Ç., *Afyon Kocatepe Üniversitesi Fen Ve Mühendislik Bilimleri Dergisi* (2018) **18** (2), 640
4. Erhart, J., *Physics Education* (2013) **48** (4), 438
5. Abolhasani, M. M., *et al.*, *Composites Science and Technology* (2017) **138**, 49
6. Fukada, E., and Furukawa, T., *Ultrasonics* (1981) **19** (1), 31
7. Saravanakumar, B., *et al.*, *Carbon* (2015) **84**, 56
8. Roy, K., and Mandal, D., CdS decorated rGO containing PVDF electrospun fiber based piezoelectric nanogenerator for mechanical energy harvesting application. In *AIP Conference Proceedings*, AIP Publishing(2018), Vol. 1942, p 050125
9. Shin, D.-M., *et al.*, *Nano Energy* (2015) **12**, 268
10. Son, M., *et al.*, *Advanced Materials Technologies* (2018) **3** (4), 1700355
11. Fuh, Y. K., *et al.*, *Small* (2016) **12** (14), 1875
12. Garain, S., *et al.*, *ACS applied materials & interfaces* (2016) **8** (7), 4532
13. Ünsal, Ö. F., *et al.*, *Journal of Applied Polymer Science* (2019)

An Innovative Development Towards The Industrialization of Electrospinning Process - Hybrid Electrospinning Technology

Demir, Ali[1], Saat, Gülbahar [1,2], Keskin, Yusuf[1,2], Bülbül, Ertuğrul[2]
[1]İstanbul Teknik Üniversitesi,
[2] Inovenso Teknoloji Ltd.
info@inovenso.com

PURPOSE

Early discoveries about the electrospinning process date back to the 1930s. Since then, thousands of scientific papers and patents have been published on electrospinning processes, nanofibers and their application areas. The advantages offered by nanofibers for different applications have been scientifically proven and accepted by all concerned. In spite of the enormous application potential, electrospun nanofibers have not been widely used in practice. The main reason is that the fiber production rate of conventional systems is far lower than the requirement for commercial usage. In this context, it is possible to find investigations on many different system designs for high speed application of the process in the literature. In this context, many studies have been made to increase the production speed and different system configurations have been tried. In this paper we will focus on a new approach, which is defined as hybrid electrospinning technology.

INTRODUCTION

Although it is possible to encounter different definitions in the literature, nanofibers are generally defined as fibers under 1-micron diameter. With their unique properties like surface area and volume ratios, porosity, mechanical characteristics, usability of a wide range of materials, ease of the production methods, nanofibers are considered as an advantageous material by the actors of science and technology areas.

The simplicity of the fabrication scheme, the diversity of materials suitable for use with electrospinning, as well as the unique and interesting features associated with electrospun nanofibers, make them attractive for many different applications like; tissue engineering scaffolds, wound dressing and healing materials, advanced air filters, water and wastewater filtration membranes, sensors, battery separators, supports for catalysis, regenerative medicine materials etc.

There are several methods to produce nanofibers from different polymers, such as drawing, phase separation, template synthesis, self-assembly, island-in-the-sea, centrifugal spinning and electrospinning. Among those methods, electrospinning has been accepted as the most effective and versatile technology for producing nanofibers from various polymeric materials [1].

Figure 1. Application areas of nanofibers (Inovenso, 2019)

The electrospinning process is an excellent method for the formation of nano-sized polymeric or composite fibrous structures, allowing the control of fiber orientations. Easily changing the effective parameters on the electrospinning process makes it possible to control the fiber properties[2]. These parameters can be summarized as solution parameters, operation parameters and environmental conditions.

The history of the electrospining process is based on the practice of the British physicist William Gilbert in the 1600s by applying a controlled electric field to a drop of liquid. The first patents were granted by Anton Formhals between 1934 and 1944 in the process of developing electrospining as a commercial value generating method. In the same period, the work of producing fiber from melt C.L. Norton and patented in 1936[3].

The theoretical background of the process was built by Sir Geoffrey Ingram Taylor between 1964 and 19694. In his studies, Taylor examined the shape behavior of the cone formed by liquid droplet under the influence of an electric field with mathematical model studies. This characteristic droplet shape is now known as Taylor cone.

A simple electrospining assembly consists of three different components (Figure-2). These are the pump used to feed the solution into the medium and the nozzle at the end of the feed line (usually a syringe needle, although different feeding systems may be used), a grounded (or opposite charged load) conductor collector, a high voltage power source for generating an electric field between the collector and the nozzle.

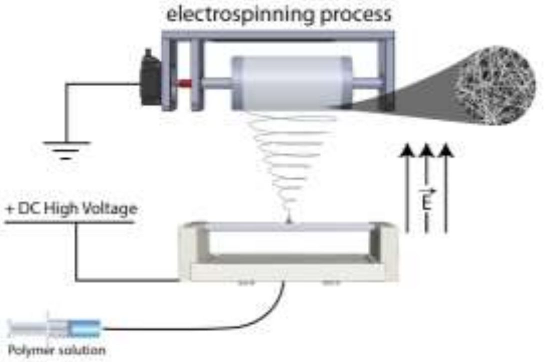

Figure 2: A basic scheme of electrospinning process (Inovenso, 2019).

Electrospinning is an electro-hydrodynamic process by working systematic. In electro-hydrodynamics (EHD), electrical charges enable any fluid to move within an electric field. During the process, the transport and distribution of these charges generate stresses that result in the movement of the fluid. The driving force in the electrospinning process is the potential difference of the static electric field. With this force, the electrically charged polymer solution or melt is pushed into a grounded collector assembly, where a dry membrane structure is formed[5].

The solution droplet at the top of the electrospinning needle is held by the surface tension forces that it has when electrospinning forces in the electrospinning area is not enough. As the voltage increased (by decreasing collector and spinneret distance of increasing the applying high voltage to the system). As the voltage is increased, the solution droplet at the tip elongates and a conical shape is formed. When the applied voltage reaches a critical value V_c, the electrostatic forces overcomes the surface tension and consequently a thin electrically charged jet is stretched from the apex of the cone (Figure-3)[6].

As mentioned before, there are several parameters affecting the characteristics of nanofiber medium. Solution properties are the most important. The solution parameters are the most effective in determining fiber properties. These are viscosity of polymer solution, solvent selection, surface tension and conductivity of solution. The most critical factor in controlling the structural morphology of the nanofibrous structure is polymer solution viscosity. For obtaining nanofibers, the viscosity must be in a range. That means there is a minimum and maximum value for viscosity to produce nanofibers. Below that minimum value, beaded fibers or just particles can be obtained. Increasing viscosity of solution increases polymer chain entanglements in the solution. After increasing viscosity more than maximum value, the surface tension becomes so high and it becomes impossible to jet formation from tip to collector. It is understood that a specific level of solution viscosity depending on the types of polymer-solvent system is necessary to counteract the electrostatic forces and produce a uniform electrospun jet during electrospinning. Hence this would lead eventually to the collection of defect-free nanofibres[6].

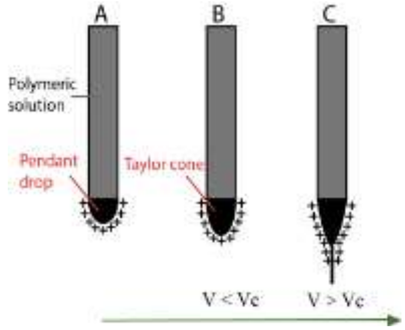

Figure 3: Schematic illustration of the Taylor cone and jet formation: (A) the applied electric field creates surface charges in the polymeric solution; (B) increasing the voltage causes change in the shape of droplet (C) The VC is critical voltage where the electrostatic force becomes equal to surface tension force. when the current voltage is higher than VC, the polymeric jet is formed and travels towards the collector due to the charge repulsion[6].

Another important solution parameter is the conductivity. The solution stretches and forms nanofibers by the repulsion of the electrical charges at the surface of the electrospinning jet. The electrospinning jet carries more charges when the solution has higher conductivity, as a result A significant reduction in the diameter of the electrospun nanofibers can be observed. When the conductivity of the polymer solution is high, the enormous tensile force will be created with respect to the voltage applied. This, in turn, helps in the formation of nanofibers with a reduced diameter[7].

Applied voltage, electrospinning process distance and flow rate are the most important operation parameters. Increasing the applied voltage reduces the drawing stress and hence decreases the diameter of the resultant fibers. However, maintenance of the control over the electrospun fibers is highly challenging at high voltage. Because increased drawing stress can result in the breakage of fibers. So for obtaining defectless fibers, applying optimal voltage during the spinning process becomes important[8].

To increase the productivity increasing flow rate is a solution in electrospinning. Higher flow rates will increase the production rate of the electrospinning process but can have adverse effects on the morphology of the fibers if not properly controlled[9]. The electrospinning system has to be designed for this purpose to obtain good fibers.

Similar to the high voltage that is applied to the system, the flow rate of the polymer solution, spinneret type; the electrospinning process distance (the distance between collector and spinneret). Nanofiber morphology is affected by the distance, because the distance is directly related with the deposition time, evaporation rate, and whipping or instability interval[10]. In their study Matabola et. al[10] observed that, with an increase in the distance, the fiber diameter decreased from 397 to 314 nm with improved uniformity. This change is attributed to the complete solvent evaporation of the solvent, more stretching and thinning which favors the formation of thinner fiber[10].

A schematic diagram of a typical electrospinning apparatus is given with Figure 2. That type of one-nozzle system is a good solution for researchers. Although many researchers have used single-needle schemes for electrospinning, the low fluid throughput in spinning has limited the industrial use of single-needle systems[7].

Besides the conventional electrospinning technique, different variations of the well-known mechanism of process have been developed. These include the multi-needle and needleless or open surface electrospinning. Both multi-needle and needleless electrospinning techniques comes with multi-jet formation to enhance the productivity of the conventional electrospinning[11].

Application of electrospinning process via multijet ejection is the technique for improving the productivity of nanofibers. But the most important question that comes to mind here is the possibility of the electrical interferences between charged jets, the instabilities are enhanced further, which can become problematic for the mass production of uniform nanofibrous membrane. So, high efficiency production of uniform nanofibers through multiple jets is of great importance to the industrial applications of electrospinning technique[12].

To meet the high liquid throughput requirements, several multi-jet systems have recently been tested. Several methods have been developed to enhance the electrospinning production rate. They can be classified as multi-needle and needleless methods.

Several researchers have tried to mass-produce nanofibers by using a free surface of polymer solution, including electrospinning based on a two-layer system, bubble electrospinning, spider spinning, ball electrospinning, disc electrospinning, cleft electrospinning, porous tube electrospinning, porous electrospinning with drilled hole, ring electrospinning, stepped pyramid stage, wire electrode, and etc[13].

Multi-nozzle electrospinning has been under ongoing investigation, since not only is it an easy method for enhancing productivity but it is also a simple technique for producing composite fibers from polymers which cannot provide a solution in a common solvent. The disadvantage of the multi-nozzle system is repulsion by adjacent jets and the non-uniform electrical field at each nozzle tip of the spinneret[14].

Conventional multi-needle electrospinning systems has a good process control, but they have a very limited production rate. Needleless systems can overcome that problem with their modified spinnerets, but needleless systems have open surface solution feeding system and that can cause a big problem to maintain consistent solution concentration and viscosity. Those changes can cause big differences on the fiber morphology during the production. On the other hand, it is almost impossible to work with rapid evaporating solvents with the needleless systems. Fiber morphology and quality are not precisely controlled, the raw materials that can be utilized are limited, which in turn limits versatile fiber production and process parameters such as flow rate, cannot be controlled.

In recent years, Inovenso made a lot of innovations for pilot and industrial systems. One of the most important innovations is a hybrid electrospinning nozzle which can increase production rate 3-4 times than conventional needles. Advantages of Inovenso's industrial system starts with a homogeneous distribution of solution to the spinnerets. That gives a uniform solution feeding capability, on the other hand the homogeny distribution of electric field in the process area is not affected. Higher production rates can be obtained by making a little increase on high voltage value. Almost same flow rates values can be seen with open surface needleless systems, while the high voltage is quite lower than them. The production rate can be increased by increasing high voltage a little. In that stronger electrical power, almost five jets can be obtained from modified nozzles. In Table-1 there is a comparison of different systems.

Table-1: Comparison of different Industrial electrospinning systems.

Conventional Needle Based Systems	Hybrid Electrospinning Technology	Needleless Electrospinning Systems

Easy to Set-up	Easy to set-up	Complex set-up procedure
Fast evaporating solvents can be a problem with needle clogging.	Possible to work with each kind of solutions like conventional needles	Not available for working with fast evaporating solvents
Normal electrical power like laboratory scale electrospinning systems. (e.g. 15-20 kV)	Relatively higher electrical power than conventional needle base systems, but lower than the open surface needleless systems. (e.g. 35-45 kV)	Very high electrical power required to start electrospinning process. (e.g. 70-90 kV)
Uniform jet distribution	Uniform and stable jet distribution	Non-controllable jet during operation
Low production rates	Higher production rate	Higher production rate
Uniform fiber morphology	Uniform fiber morphology	Non-uniform fiber morphology
Fully control of electrospinning	Precise and full control of the process	Not a complete control on all of the process parameters.
Defectless nanofibers	Defectless nanofibers	Generally beaded and defected nanofibers
Control of solution concentration	Full control of solution concentration and viscosity	Difficult to maintain consistent solution concentration and viscosity

EXPERIMENTAL

Materials and Methods

PVDF (Arkema, Kynar-761) was used as polymeric material. The solvents for the experiment were DMF and Acetone of Merck. LiCl was used for increasing the conductivity of solution. Ingredients and the properties of the solution is given in Table-2.

Table-2: Solution properties

PVDF (%w/w)	DMF(%w/w)	Acetone(%w/w)
14	60	26
LiCl (gr)	Viscosity (mPa.s)	Conductivity (μS)
0,05	1910	445

In order to improve the production capacity, different spinneret designs were made and the effect of each on the capacity was examined by applying different solutions. In this paper only the data related to the design with the highest efficiency is presented.

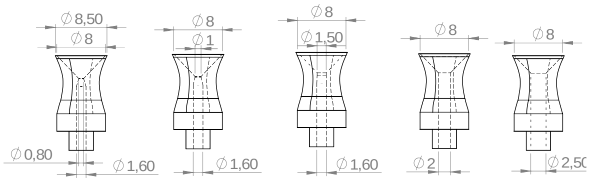

Figure 4: Used hybrid nozzles during operation. From left to right outer diameter for each nozzles are same and inner diameters are 0,8mm, 1mm, 1,5mm, 2mm and 2,5mm)

For this experiment, PE 550 model pilot scale electrospinning system of Inovenso was used. That system has 55 nozzles on it and it can coat surfaces of 550 mm width and continuous substrate by roll-roll collector. The high voltage during process was 40 kV. System was operated under same ambient conditions. For each type of nozzles maximum achievable flow rate was checked. The distance between nozzle and collector was 140 cm.

For defect control on coated nanofiber layer, SEM images were taken by Semoscope (by Inovenso) Scanning Electron Microscope.

EXPERIMENTAL RESULTS AND DISCUSSIONS

In order to improve the production capacity of electrospining, some of the design-performance studies carried out in the inovenso laboratory were evaluated here. In Table 2, maximum achievable flow rates can be seen for each nozzle type and as control nozzle 18G blunt syringe nozzle was used.

Table-2: Maximum achievable flow rates for each nozzles.

Outer Diameter		**2.8 mm**	**4.0 mm**	**6.0 mm**	**8.0 mm**	**18G**
Inner Diameter	**1.0 mm**	16 ml/h	16,5 ml/h	16,5 ml/h	21 ml/h	4 ml/h

	1.5 mm	16,5 ml/h	16,5 ml/h	17 ml/h	21,5 ml/h	
	2.0 mm	16,5 ml/h	17 ml/h	17 ml/h	24 ml/h	
	2.5 mm		17 ml/h	17,5 ml/h	28,5 ml/h	

The most efficient design can be seen at Fig-5. Achieved flow rate value for this nozzle is 28,5 ml/h.

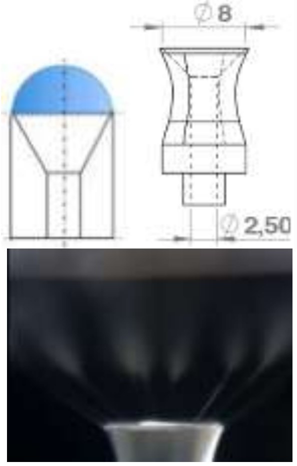

Figure 5: Hybrid electrospinning spinneret.

SEM images for all of the nozzles on this experiment were taken. But here only for the nozzle which gave the highest performance is given. SEM images are given with Fig-6

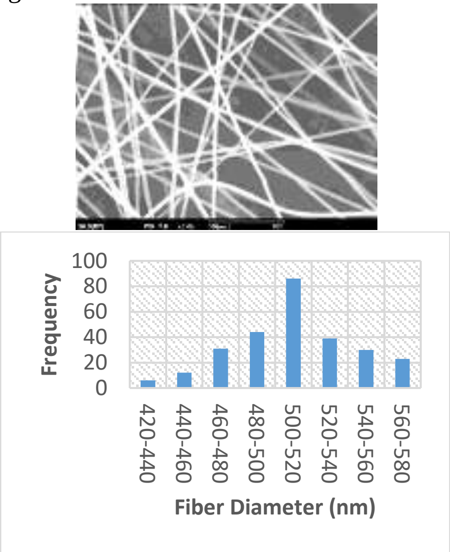

Figure 6: SEM image and fiber diameter distribution for the nozzle which has OD:8mm and ID:2,5mm

For making comparison SEM image for standard syringe needle is given at Figure-7. In this image it can be clearly seen that nanofiber layer has defects.

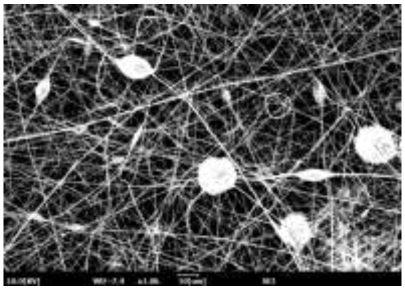

Figure 7: SEM image for 18G blunt standard syringe needle

CONCLUSIONS

In this study, the effect of various nozzle designs, which were developed to increase nanofiber production speed, on the effect of feed flow was investigated. When the inner and outer diameters of the hybrid nozzles were examined, the highest yield was obtained with nozzle which has an ID of 2.5mm and an OD of 8mm.

The morphology of the nanofiber coating produced was examined by SEM and no serious defect affecting the coating quality was observed.

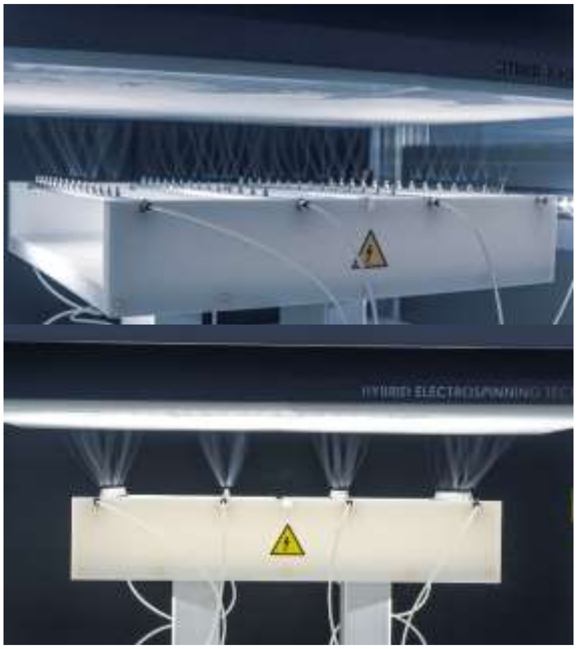

Figure: Electrospinning process area of PE300.

ACKNOWLEDGEMENTS/SOURCES OF FUNDING

This project is funded by Inovenso Teknoloji Ltd. All the production and analysis were done at Inovenso’s facility.

LITERATURE

1. Akpınar, H. S. N. Production Of Electrospun Polyacrylonitrile Nanofiber Yarn. (Technical University Of Istanbul, 2018).

2. Merritt, S. R., Exner, A. A., Lee, Z. & von Recum, H. A. Electrospinning and Imaging. Adv. Eng. Mater. 14, B266–B278 (2012).

3. Norton, C. L. Method Of And Apparatus For Producing Fibrous Or Filamentary Material. 1–4 (1933).

4. Taylor, G. Electrically Driven Jets. Proc. R. Soc. London 313, 453–475 (2014).

5. Collins, G., Federici, J., Imura, Y. & Catalani, L. H. Charge generation, charge transport, and residual charge in the electrospinning of polymers: A review of issues and complications. J. Appl. Phys. 111, (2012).

6. Casasola, R. Electrospinning of poly (lactic) acid for biomedical applications: analysis of solution properties and process parameters, drug encapsulation and release. (2016).

7. Angammana, C. J. & Jayaram, S. H. Fundamentals of electrospinning and processing technologies. Part. Sci. Technol. 34, 72–82 (2016).

8. Mishra, R. K. et al. Electrospinning production of nanofibrous membranes. Environmental Chemistry Letters (Springer International Publishing, 2018). doi:10.1007/s10311-018-00838-w

9. SalehHudin, H. S., Mohamad, E. N., Mahadi, W. N. L. & Muhammad Afifi, A. Multiple-jet electrospinning methods for nanofiber processing: A review. Mater. Manuf. Process. 33, 479–498 (2018).

10. Matabola, K. P. & Moutloali, R. M. The influence of electrospinning parameters on the morphology and diameter of poly(vinyledene fluoride) nanofibers- Effect of sodium chloride. J. Mater. Sci. 48, 5475–5482 (2013).

11. Kenry & Lim, C. T. Nanofiber technology: current status and emerging developments. Prog. Polym. Sci. 70, 1–17 (2017).

12. Zheng, G. et al. Multinozzle high efficiency electrospinning with the constraint of sheath gas. J. Appl. Polym. Sci. 136, 1–12 (2019).

13. Valipouri, A. Production Scale Up of Nanofibers : A Review. J. Text. Polym. 5, 8–16 (2017).

14. Park, C. H., Pant, H. R. & Kim, C. S. Novel robot-assisted angled multi-nozzle electrospinning set-up: Computer simulation with experimental observation of electric field and fiber morphology. Text. Res. J. 84, 1044–1058 (2014

Development of Self-healing EVA Films

SEZER HİÇYILMAZ, Ayşe[1], ÇELİK BEDELOĞLU, Ayşe [1]
[1]Bursa Technical University, Fiber and Polymer Engineering, Bursa, TURKEY

aysesezerh@gmail.com, ayse.bedeloglu@btu.edu.tr

PURPOSE

In recent years, self-healing materials have attracted attention due to rapid recovery and wide application area. The aim of this study was to provide self-healing properties of ethylene vinyl acetate (EVA) films and to characterize the properties of newly developed films.

INTRODUCTION

Self-healing materials heal themselves autonomically or non-autonomicaly by help of external interventions such as heat, light, oxygen or healing agents [1]. Self-healing materials are environmentally friendly, sustainable, cost-effective due to their long service life and the fact that they do not require replacement. More importantly, self-healing materials give users more secure handling because they can be repaired autonomously, easily and quickly compared to traditional materials [2]. Therefore, in this study, EVA polymer, which is used in a wide range of applications from flexible packages to electrical cables, has been chosen as the main material. [3]. Nanoparticles are special materials that have superior properties such as electrical conductivity, thermal conductivity, antibacterial, super hydrophobicity etc. [4]. Moreover, it is possible to obtain self-healing materials with nanoparticles. Silver nanowires have high thermal conductivity and photothermal property so they are suitable to produce self-healing materials with polymers that have low melting temperature. Healing mechanism of this nanocomposites based on re-entanglement of linear chains by softening or melting with heating of the damaged region. In the literature, Li et al. produced the near-infrared light induced healable, electrically conductive, flexible silver nanowires (AgNWs) deposited thermoplastic polycaprolactone (PCL)/poly(vinyl alcohol) (PVA) composite film. Recyclable healing is obtained by irradiating mild NIR light the damaged region. AgNWs act as electricity conductor and NIR light-induced heater. AgNW absorbs NIR light and converts into heat then transfer to the matrix. When the heated $(PCL/PVA)_6$ film reached to above of the melting temperature (65 °C), polymer flows to heal the cutted region and recover the electrical conductivity property (Figure 12) [5]. Kim et al fabricated photoinduced self-healing, stretchable and transparent TPU electrode with incorporating of AgNW. Damaged surface was irradiated by intense-pulsed-light (IPL) to induce plasmonic heating. Rapid and repeatedly healing of the microcracks was achieved by the help of thermally conductive AgNW [6]. In this study, silver nano wire (AgNw) reinforced ethylene vinil acetate (EVA) nanocomposites were produced to obtain thermally self-healing property. Generally in the literature silver nanowires were coated onto polymer surface, in this study, rapid, repeatable and high effective self-healing films were produced by dispersing AgNw in the polymer matrix. Developed self-healing nanocomposite transparent films could be used in applications such as flexible packaging, tempered glass laminates, electric cables, footwear etc.

EXPERIMENTAL

Material

Greenflex ® Ethylene vinyl acetate copolymer (EVA) was purchased from Resinex, ClearOhm® Ink- Silver nanowire (AgNw) solution was purchased from Cambrios and used as is. Dichlorobenzene was purchased from Sigma Aldrich Chemical Company.

Method

EVA -DCB solution (10% wt/wt) was prepared at 130 °C. To prepare EVA-AgNw solution (5 % wt/wt), Ag Nw was dispersed in DCB for 3 hours, then ultrasonicated for 5 seconds. AgNw-DCB dispersion was added into EVA-DCB solution at 130 °C. The films were produced with solution casting method. Hot polymer solutions poured onto glass petri dishes that stands on 130 °C hot plates. The solvent evaporated and the films cooled down gradually. The films were named as EVA and AgNw-EVA. The thicknesses of films were between 0.15-0.25 mm.

Self-healing property evaluated with scratch test method [7]. Films were scratched with a razor blade to an approximately 50% thickness of the films and heated in the 130 °C oven (Figure 1). Heating temperature and time effect on the self-healing property were investigated.

Figure 1. Scratched EVA films in petri dish.

Self-healing effect was observed with a light optical microscope (Leica DM2500) and also mechanical strength of the films tested according to ASTM D882 standard with A Shimadzu AGS X–Static Mechanical Tester.

EXPERIMENTAL RESULTS AND DISCUSSIONS

Self-healing tests were done at 90, 100, 110, 120 ve 130 °C for 1, 2.5, 5, 7.5 10, 15 minutes. Self-healing behavior of the films were observed with optical microscope. According to the results, AgNw-EVA films at 90, 100 and 110 °C recovered for long periods of time such as 1 hour, 35 minutes, 20 minutes, respectively. Therefore these temperatures indicate that it is not sufficient for rapid recovery. AgNw–EVA films recovered at 120 °C after 10 minutes, while the non-reinforced EVA film recovered after 15 minutes. The fastest self-healing took place at 130 °C, the AgNw-EVA film recovered after 5 minutes, while the EVA film did not recover after 5 minutes (Figure 2). These results indicated that %5 AgNw reinforcement increase the self-healing effect of EVA film obviously and also self-healing time decreased at least 66,66%. Silver nanowires increase the healing time by increasing thermal conductivity of the films.

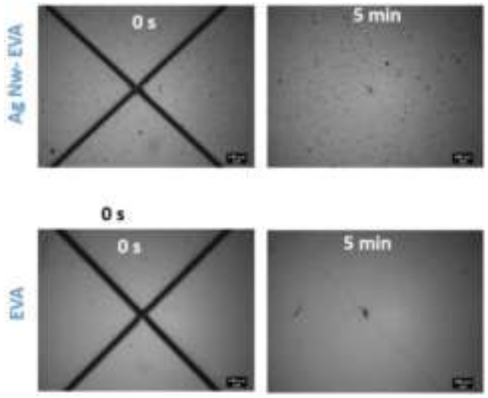

Figure 2. Optical microscope images of EVA and AgNw films before and after self-healing test at 130 °C

Mechanical strengths of the films were investigated and test results were shown in Table 1. Mechanical test results confirm optical microscope results. Silver nanowire reinforcement decreased the mechanical strength of the EVA films slightly. But after the self-healing test (5 minutes), the AGNw-Eva film is completely healed and achieves higher tensile stress compared to pristine AgNw-EVA film due to re-entanglement of the EVA chains with heat.

Table 1. Tensile test results of pristine and healed (at 130 °C) EVA and AgNw-EVA films.

Sample	**Tensile Stress (N/mm^2)**
EVA	17,34
EVA-5 min	16,52
EVA-10 min	17,36
AgNw-EVA	16,73
AgNw-EVA-5 min	17,41
AgNw-EVA-10 min	17,14

CONCLUSIONS

Rapid self-healable EVA films were developed with low amount of AgNw reinforcement (5%). Developed films protect transparent structure and also mechanical strength. These films could be used in wide range of applications such as electric cables, packages, coatings etc. Also it can be used as tampered glass laminates due to high transparency

SUGGESTION FOR FURTHER WORK

Scratch formation process need to be optimized via scratch maker devices. Silver nanowire dispersion could be increased by using surfactant materials. On the other hand, different reinforcement amounts and also film thickness effects will be investigated in the future works. Local self-healing tests will be conducted in the next works.

REFERENCES

1 Thakur VK, Kessler MR, 2015."Self-healing polymer nanocomposite materials: A review". Polymer, (69),369-83.

2 Bekas D, Tsirka K, Baltzis D, Paipetis A, 2016."Self-healing materials: a review of advances in materials, evaluation, characterization and monitoring techniques". Composites Part B: Engineering, (87),92-119.

3 Chen Z, Fang P, Wang H, Zhang S, Wang S, 2006."Property of ethylene vinyl acetate copolymer in melting processing". Journal of applied polymer science, (101),3,2022-6.

4 Ajayan PM, Schadler LS, Braun PV. 2006 Nanocomposite science and technology John Wiley & Sons.

5 Li Y, Chen S, Wu M, Sun J, 2014."Rapid and efficient multiple healing of flexible conductive films by near-infrared light irradiation". ACS applied materials & interfaces, (6),18,16409-15.

6 Kim K-S, Choi SB, Kim DU, Lee C-R, Kim J-W, 2018."Photo-induced healing of stretchable transparent electrode based on thermoplastic polyurethane with embedded metallic nanowires". Journal of Materials Chemistry A.

7 Xu Y, Chen D, 2016."A novel self-healing polyurethane based on disulfide bonds". Macromolecular Chemistry and Physics, (217),10,1191-6.

Potential of Ethiopian Enset Fiber for Textile Application

TEMESGEN, Alhayat G. [1*], TURŞUCULAR, Ömer F.[1*], EREN, Recep [1], AYKUT, Yakup [1]

[1]Department of Textile Engineering, Engineering Faculty, Bursa Uludag University, Bursa, Turkey

Corresponding author:[*] mottaget@gmail.com, omerfirattursucular@gmail.com

PURPOSE OF THE STUDY

Growing of environmental issue, increasing demand of new materials, the evolution of new technology and economic concerns as well as the finite petrochemical resources have pushed researcher to find out alternative materials to substitute synthetic fibers. Enset plant was one of the most known drought tolerance than most cereal crops, grows in every season and multipurpose plant in Africa especially, in Ethiopia, which is used as source of food in southwestern part of the country. Enset fiber was obtained from the agricultural waste of Enset plant after extraction of edible part the so called “Kocho”. The fundamental problem of farmers were disposal of agro-waste material like enset fiber. Utilization of agro-waste materials were generate additional income for the low income farmer and poverty alleviation program. The fibers, sometimes called false banana under Ensete Ventricosum family, were new and un-utilized agro waste obtained from the pseudo stem (bast) and mid ribs of the plant. Enset fiber had relatively low density, low moisture content and good specific strength than from most common bast and leaf fibers. Its abundantly available, low cost, reduced energy consumption, carbon dioxide sequesterization, and biodegradability were the merits of the fiber from other most natural fiber used in reinforced green composite and technical textiles like Geo textile and Agro textile areas.

Key words: Enset Fibers, Extraction, Composite, Physical properties, Textile Potential.

1. INTRODUCTION

Textile production has been developing to increase efficiency to serve consumer’s needs. As the convenience increases, villagers tend to neglect traditional fiber harvesting process and turn to synthetic fibers and chemicals to achieve production capability, including expensive imported fibers and yarns purchased from foreign traders, whereas the local cheap material available in their hometown is ignored [1, 2 and 3]. Interest in using natural fibers has increased significantly in the last few years, especially because of their use as an agent of reinforcement and more recently as heavy metals bio-adsorbent [1,4]

Enset plant is in Musa family like banana. The plant is a large perennial herb with leaf sheaths that form pseudo stem. Its height can be 3.0-12.2 meters surrounding with 8-12 large leaves. The leaves are up to 9 feet long and 2 feet wide (2.7 meters and 0.61 meter). Its fruits are approximately 4-12 inches (10.2-30.5 centimeters) [3, 5, 6, 7, 8]. Different parts of banana trees serve different needs, including fruits as food sources called ”KOCHA”, leaves as wrapping, and stems for fiber and robe. The fiber is obtained from outer layers from the stalks of the plant. It is light, strong and durable. After extraction and dry, it provides a white lustrous color fiber (figure 1). One particular characteristic of the fiber over all other fibers of its class is the great strength and resistance to the action of water, therefore its will be particular adaptability for marine ropes [9]. It is available in some part of Africa (Figure 2).

According to environmental concerns in European countries, recently, natural fibers play an important role as reinforcing fillers in polymer composites. The advantages of natural fibers over synthetic fibers are their low cost, less tool wear during the process, low density, environmental friendliness and biodegradability [1,3,10]. For that reason, enset fibers will be another option to be investigated for its fiber source potential.

Figure 1: Enset fiber

Generally there are the six major kinds of Ensete in the Musa family[5,11].

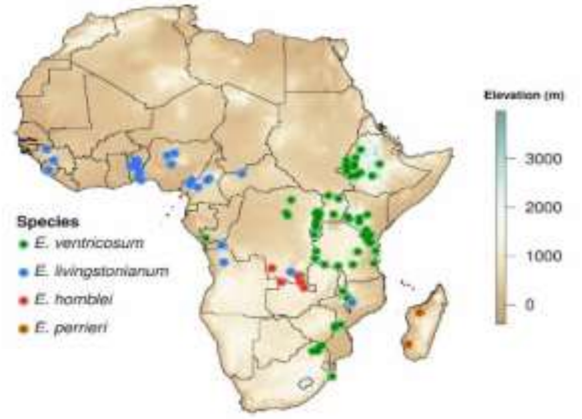

Figure 2. Ensete in Africa (source: Alun Salt, 2019)

Fibers have an average equivalent diameter of 194-206 µm and a length of 0.5 to 4.5 m. These long technical fibers are generally characterized by hard, stiff and coarse in texture. Different type of enset fibers are collected from different region of Ethiopia and mechanical and physical properties of the fibers will be characterizations done [1, 2, 3, 12-15]. In addition to this, we are try to compare and contrast with the overall properties if the fiber with banana fiber. Finally we will try to find out the possible enset fiber extraction techniques to optimize the fiber strengths [1, 2, 3, 12.13].

The significances of this study was using left-over banana trunk as raw material in environmental-friendly manner to optimize natural fiber processes and decrease chemical and toxic agents in the process. As the material is available locally, villagers are not necessary to purchase or grow new plant and using extra chemicals, fertilizers, or pesticides. Utilizing enset fibers will promote sustainable development in the community, since villagers will be able to produce this fiber in their household. This research focused on the amount of fiber extraction, the comparison of fiber extraction methods, characterization of the fiber and investigation of the potential application in technical textile. The findings from this research presented that the yield test of is acceptable for light weight composite production. The result expresses the possibility for more exploration in industrial area, which should include the whole process of fully utilizing enset plant after harvesting the food “Kocho”, enset fiber and enset pulp.

2. MATERIALS AND METHODS

Fibers were collected and extracted from different part of Ethiopia from mid ribs and pseudo stem of the enset plants and studied. Fibers were continuously scratched by hand followed by washing, cleaning and manual fiber separation. Microscopic view of the fiber was seen by using SEM with 150x magnification power. FTIR test was analyzed with measuring range: 4000 - 650cm^{-1}, number of scans: 32 and resolution: 4cm$^{-1.}$ Tests have been conducted under standard conditions: ISO 139 20°C ± 2°C and 65% ± 4% R.H in BUTAL and Bursa Uludag University laboratory, Bursa Turkey.

3. RESULTS AND DISCUSSIONS

3.1. Enset Fibers Extraction

Enset fibers are extracted from the pseudo stem and mid ribs of the plant. The extraction of starch and fiber from the plant mostly takes place by using either mechanically by hand or by using decortication machine. The pseudo stem are cut in to the required size and tied with a fixed wood at certain inclination and separate the starch from the fiber. The qualities of the fibers are depending on the setting between the lower and upper cylinder of decortication machine. Sometimes fiber can also extracted from the plant by soaking with water and caustic soda for a certain period of time. These kinds of fiber extraction mechanisms mostly affect the overall mechanical performance of the fiber. Because the microorganism may start to grow and eat the cellulose part of the fibers see figure 3 a

Figure 3. (a) Raw enset fiber (b) Clean enset fiber

3.2. FTIR Analysis of Enset Fiber

The FTIR result of the enset fiber consists for 3331 absorption O-H stretching ,2917 absorption C-H stretching (aliphatic + aromatic) ,1100 absorption band C-O stretching of conjugated ester groups in grass lignin’s and 1242 absorption C=C stretch were observed. FTIR adsorption band indicated that enset fiber has three major chemical compositions: cellulose, hemicellulose and lignin. Like other lignocellulose fibers, the physical and mechanical performance of the fiber as well as the bio composite materials reinforced with enset fibers were significantly affected by three major constituents, especially the percentage of hemicellulose and lignin present in the enset fiber.

Table 1. FTIR absorption of Enset fiber in BUTAL.

Position (cm^{-1})	Band origin
3331.427	O-H stretching
2917.770	C-H stretching (aliphatic + aromatic)
1730.799	C=O stretching (unconjugated ketone, ester or carboxylic groups)
1665.340	C=O stretching in conjugation to aromatic ring
1422.244	Aromatic ring vibrations
1369.212	C-H deformations
1321.964	Syringyl ring breathing
1242.897	C=C stretch
1156.116	C-O-C asymetrical
1100.190	C-O stretching of conjugated ester groups in grass lignins
1028.837	C-C, C-oH, C-H ring and side group vibration
897.701	C-O-C, C-C-O, C-C-H deformation and stretching
662.428	C-H out of plane in p-hydroxyphenyl units

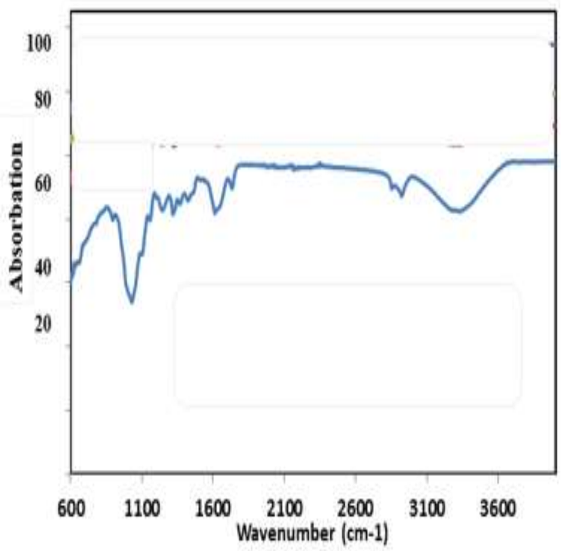

Figure 4: IR Spectra of Enset fiber

3.3. Morphological Properties of Enset fiber

Enset fibers had a hard touch and core fiber like other most bast fiber. We can also observe longitudinal streaks which are characteristics of long vegetable fibers and same starch material which were not removed from the fiber during fiber extraction (figure 5a). Moreover, in a single fiber of enset contains a lot of hole and cross sectional area having a shape of bean, which indicate that in a single enset fiber, there is a possibility to extract a lot of fine fiber (figure 5b)

By examining these technical fibers in SEM (Scanning Electron Microscope) we can see a ″composite″ structure where ultimate fibers are held together by sticky and waxy substances to finally form technical fiber with section forms difficult to define. The ultimate fibers show oval and irregular sections with large lumen (figure 5c).

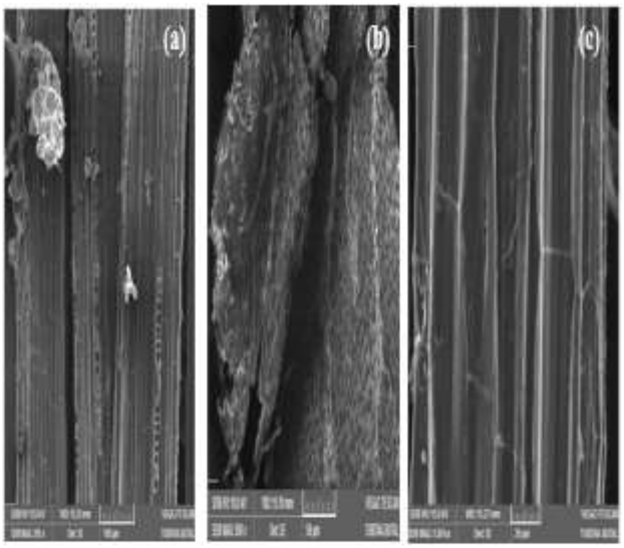

Figure 5: SEM view of Enset fiber (a) Longitudinal View (b) Cross sectional view (c) Number of layers of in a single fiber (natural composite fiber)

From figure 5b and 5c, enset fiber have a lot of whole structure both in the longitudinal as well as transversal direction of the fiber axis. Theses open spaces present on the fiber structure have a significant advantage in the acoustic application and absorbed desired amount of matrix in green composite. Comparison with other textile fibers, fibers are more hydrophilic than cotton, flax, and other lignocellulose vegetable fibers with moisture content of 7- 10%.

CONCLUSION

Their abundance in nature combined with the ease of their processing had an attractive feature, which makes enset fiber an important substitute for synthetic fibers. The test results indicated that , Enset pseudo-stem suggest that this material which is residue after harvesting Kocha can be used as potential source of cellulose fiber to make high valued ecofriendly technical materials like biodegradable composite, geo-textile, agro-textile and packaging mats which gives high strength without any finishing. The agro waste naturally composite fibers were ecofriendly, economically fit as well as disposable material and play a significant role in reduction of carbon emissions. The farmers in Ethiopia are cultivated the plant for food source, but after extraction of the required food the disposal of this agro waste fiber was the major problem for them. Utilization of this agro waste fiber for industrial application helps the poor farmer to generate addition income in their life and poverty alleviation program. Enset fiber had low moisture abortion and good mechanical strength which made the fiber to substitute most of bast and leaf fibers in technical textile application.

FURTHER WORK

Future aim of the research was effetely utilizing agro waste fiber as a new alternative natural fiber for green composite, Agro Textile, Geotextile and packaging application sectors by fiber characterization and designing special processing and manufacturing methods to reduce global warming by reducing using of petrochemical fibers.

ACKNOWLEDGMENTS

This research work was a part of Alhayat Getu TEMESGEN‘s PhD Thesis part doing in Bursa Uludag University, Graduate School of Natural and Applied Sciences, Department of Textile Engineering. The Authors would like to express our deep gratitude and sincere thanks to Mehmet TİRİTOĞLU and Uludag University, department of textile and physics lab assistance helped us directly or indirectly during our research work.

REFERENCES

[1]. TEMESGEN Alhayat Getu and OMPRAKASH Sahu, 2014, Process Ability Enhancement of False Banana Fibre for Rural Development, Journal of Agricultural Economics, Extension and Rural Development: ISSN-2360-798X: Vol. 1, pp.63-73.

[2]. TEMESGEN Getu, A. and Sahu, O., 2014. Green composite material from agricultural waste. International Journal of Agricultural Research and Reviews, 2(5), pp.56-62.

[3]. TEMESGEN A.G., EREN R., AYKUT Y. 2019, Investigation and Characterization of Fine Fiber from Enset Plant for Biodegradable Composites, 17th National 3rd International the Recent Progress Symposium on Textile Technology and Chemistry, ISBNNo.978-605-01-1312-9,pp. 356-361,Turkey.

[4]. A. SHUMBULO, YISHAK Gecho1 and MELESE Tora; 2012. Diversity, Challenges and Potentials of Enset (Ensete ventricosum) Production: Food Science and Quality Management; Vol 7.

[5]. D. FEKADU a, I. Ledin b 1997;Weight and chemical composition of the plant parts of enset and the intake and degradability of enset by cattle; Livestock Production Science ,PP. 249-257.

[6]. GENET Birmeta ,2004;Genetic Variability and Biotechnological Studies for the Conservation and Improvement of Ensete ventricosum, , Department of Crop Science, Alnarp, Doctoral thesis, Swedish University of Agricultural Sciences, Alnarp.

[7]. G. BLOMME, G. Sebuwufu , TEMESGEN Addis and L. F. TURYAGYEND, A Relative Performance Of Root And Shoot Development In Enset And East African Highland Bananas;; African Crop Science Journal, Vol. 16, No. 1, pp. 51 – 57.

[8]. PIEDAD, ROBIN Zuluaga, JUAN MANUEL Velez, 2004, Biological Natural Retting for Determining the Hierarchical Structure of Banana Fibers, Macromol. Biosci, PP.978–98,.

[9]. ROGER M Rowell, RAYMOND A Young and JUDITH Rowell ,1996, Natural Polymers and Agro fibers Based Composites in Paper and Composites from Agro-Based Resources, CRC Press .

[10]. TADESSA Daba, MASAYOSHI Shigeta, 2016; Enset (Ensete Ventricosum) Production in Ethiopia: Its Nutritional and Socio-Cultural Values,; Agriculture and Food Sciences Research; Vol. 3, No. 2, PP. 66-74.

[11]. M.K. Sinha, 1982, A- review of processing technology for the utilization of agro-waste fibers, Agricultural Wastes, 4,PP. 461-475.

[12]. K. MURALI Mohan Rao, K. MOHANA Rao 2007, Extraction and tensile properties of natural fibers: Vakka, date and bamboo, Composite Structures 77, PP. 288–295.

[13]. RYAN Coda, 2005, a Study of Cellulose Based Biodegradable Foams and Sponges, a Thesis Presented to Georgia Institute of Technology May.

[14]. DONG Ruan, LINA Zhang, JINPING Zhou, 2004, Structure and Properties of Novel Fibers Spun from Cellulose in NaOH/Thiourea Aqueous Solution, Macromol. Biosci. 4, PP. 1105–1112.

[15]. SANG K.Y.Lim, TAE W.S, DONG W.L, BONG K.P, Kyu M.C,2001., Novel Regenerated Cellulose Fibers from Rice Straw, Journal of Applied Polymer Science, Vol. 82, PP. 1705–1708.

Thermal Insulation Properties of Glass Fiber Epoxy Composite with Stonewool Fiber, Nanofiber Web, Silica Aerogel Layers

GÜNAL, Sevde Rana[1], SAYAR, Ersin[2], GEYGEL, Berkay[3], ÖZKAN HACIOĞULLARI, Selcen[4], KARACA, Neslihan[5], UÇAR, Mehmet[3], SELVER, Erdem[6], SOLAK, Nuri[1], BAYDOĞAN, Murat[1], ÖNEN, Ayşen[5], UÇAR, Nuray[4]

[1]İTÜ, Malzeme Müh Böl, Maslak, İstanbul, TÜRKİYE
[2]İTÜ, Makine Müh Bölümü, Gümüşsuyu, Taksim, İstanbul TÜRKİYE
[3]Kocaeli Üniversitesi, Otomotiv Müh Bölümü, İzmit, TÜRKİYE
[4]İTÜ, Tekstil Müh Böl, TESENLİF Laboratuvarı, Gümüşsuyu, Taksim,
[5]İTÜ, Kimya Bölümü, Maslak, İstanbul, TÜRKİYE
[6]Kahramanmaraş Sütçü İmam Üniversitesi, Tekstil Müh Böl, Kahramanmaraş

s.ranagunal@gmail.com

ABSTRACT

Thermal insulation is very important for transportation industry including aircraft, train, automobile, etc. Glass fiber epoxy composite with nonwoven containing Polyacrylonitrile nanofiber, silica aerogel, stone wool fiber layers have been evaluated for thermal insulation.

INTRODUCTION

Glass fiber epoxy composite is widely used in transportation industry including aircraft, train, automobile, ship, etc. and other areas such as cryogenic. Heat insulation is very important for these areas. Silica aerogels with its nano porous structure and mass, is a very suitable material to be used as super insulating composite material[1]. Polyacrylonitrile (PAN) is a versatile man-made polymer and has been used in a large array of products. Also, this polymer has the good thermal properties.[2]

Stone wool is a fire-resistant, water-repellent heat and sound insulation material containing 97% natural fibers and produced by melting minerals and inorganic stones derived from volcanic rocks such as basalt, diabase and dolomite between 1400-1500 °C to form fibers[3]. It is used for thermal insulation, sound insulation, acoustic comfort as well as fire safety. In this study, glass fiber epoxy composite structures with insulating properties were developed using these materials. The morphology and thermal insulation have been analyzed. It has been seen that nanofiber, silica aerogel and stone wool blanket used for insulation material result to decrease of heat transfer coefficient due to pores in the structures, compared to reference glass fiber epoxy composite without any insulation layer.

EXPERIMENTAL

Material

Glass fabric (525 g/m^2 , plain weave , 2 weft/cm, 2 warp/cm, 0.4 mm thickness), Epoxy (F-1564), curing agent (F-3486) purchased from Fibermak. Commercial available silica aerogel ENOVA® MT 1200 (Cabot´s Aerogel), nonwoven fabric (spunlace), Polyacrylonitrile, stonewool have been used.

Method

PAN/DMF (%8 PAN) have been used for electrospinning system with set up 14 kV voltage, 14 cm distance, 0,9 ml/h feeding rate and 21 needle gauge. Nanofiber web has been electrospun on nonwoven layer. The thickness of PAN nanofiber web and also each nonwoven layer are approximately 0.085 mm. Silica aerogel particle (0,25 gr) has been placed on nonwoven layer.

Heat flow meter (by using steady heated insulated plate, laboratory type/handmade measurement device) was used to measure heat transfer coefficient.

Glass fiber epoxy composite (ratio of 62/38 %) has been produced by hand laying technique using brush for the 0-0 placement with 6 glass woven fabric.
Each of insulation materials have been layered on glass fiber epoxy composite as given in Table 1.

Table-1. Materials used in this study

No	Material/ Sample Design	Layers type	Thickness (mm)/ Weight (gr/m^2)
1	Reference Glass Fiber Epoxy Composite (RGC)	Glass Fiber Epoxy Composite	3 mm 4600 g/m^2
2	Glass Fiber Epoxy Composite with stone wool fiber blanket layer with 2 mm thickness (GCSW)	Glass Fiber Epoxy Composite + Stone Wool Fiber Blanket Layer with approx. 2 mm Thickness	5 mm 5068 g/m^2
3	Glass Composite+ Silica Aerogel layer with 2 mm thickness (GCS)	Glass Composite+ nonwoven (23 layers) and Silica Aerogel (2 layers) (approx. 2 mm thickness)	5,5 mm 4933 g/m^2
4	Glass Composite+ PAN Nanofiber (GCP)	Glass Composite+ nonwoven (21 layers) and nonwoven with PAN layer (4 layers) (approx. 2 mm thickness)	5,5 mm 4978 g/m^2

EXPERIMENTAL RESULTS

As can be seen from Figure 1, nanofiber is in nanometer range and silica aerogel particle is in micron range. As can be seen from Table 2, nanofiber with 2 layer, silica aerogel with 2 layer and stone wool blanket used for insulation material result to decrease of heat transfer coefficient due to pores in the structures, compared to reference glass fiber epoxy composite without any insulation layer. Even though, heat transfer coefficient of nonwoven with PAN nanofiber is some higher than others, the easy production process and cost of nanofiber may be preferable.

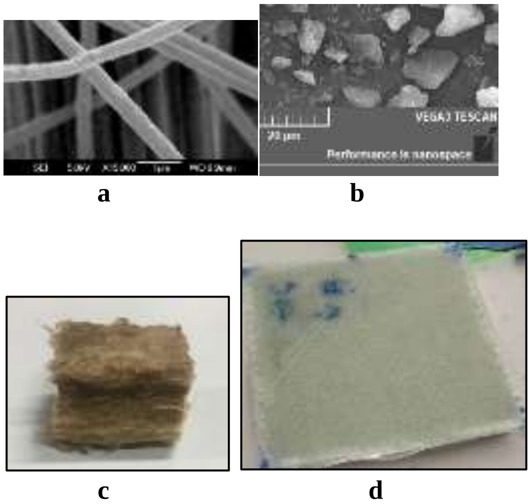

Figure 1. Morphology a-SEM appearance of PAN nanofiber, b- SEM appearance of Silica Aerogel and c-Stone wool blanket, d-glass fiber/epoxy composite

Table 2. Thermal insulation properties

No	Material/ Sample Design	Heat transfer coefficient W/mK
1	Reference Glass Fiber Epoxy Composite (RGC)	0.140W/mK
2	Glass Fiber Epoxy Composite with stone wool fiber blanket layer with approx. 2 mm thickness (GCSW)	0.078W/mK
3	Glass Composite+ Silica Aerogel layer with approx. 2 mm thickness (GCS)	0.088W/mK
4	Glass Composite+ PAN Nanofiber (GCP) with approx.2 mm thickness	0.093W/mK

CONCLUSIONS

Nanofiber, silica aerogel and stone wool blanket used for insulation material result to decrease of heat transfer coefficient due to pores in the structures, compared to reference glass fiber epoxy composite without any insulation layer. Heat transfer coefficient of nonwoven with PAN nanofiber is some higher than others, however, the easy production process and cost of nanofiber may be preferable.

ACKNOWLEDGMENT

This study has been supported by TUBITAK under the project TÜBİTAK COST “218M766. We would like to thank TUBITAK. We also would like to thank producers/ distributors which provides some raw materials.

REFERENCES

[1] Venkataraman, M., Mishra, R., Militky, J. and Hes, L. 2014. “Aerogel Based Nanoporous Fibrous Materials for Thermal Insulation”, Fibers and Polymers, Vol. 15, 1444-1449.

[2] Madakbas¸ S., Çakmakçı, E., Kahraman, M. V. 2013. “Preparation and thermal properties of polyacrylonitrile/hexagonal boron nitride composites”, Thermochimica Acta, 552, 1– 4.

[3]WEB:https://www.bonusyalitim.com.tr/en/products/bonus-stone-wool

Investigation of Wear Properties of Polyethylene/Carbon Fiber Composites

AKGUL, Yasin[1], AHLATCI, Hayrettin[1], SIMSIR, Hamza[2], TOPTAS, Ali[3], ERDEN, Mehmet Akif[4], KILIC, Ali[3]
[1] Department of Metallurgical and Materials Engineering, Karabuk University, Karabuk, Turkey,
[2] TOBB Technical Science Vocational School, Karabuk University, Karabuk, Turkey
[3] TEMAG Labs, Textile Technology and Design Faculty, Istanbul Tech University, Istanbul, Turkey
[4] Department of Biomedical Engineering, Karabuk University, 78050, Karabuk, Turkey
alikilic@itu.edu.tr

PURPOSE

The aim of this study is to improve the wear resistance of linear low-density polyethylene (LLDPE) material. For this purpose, LLDPE matrix composites containing different amounts (1%, 2.5%, %5, 10%, 15%, 20%) of carbon fiber are produced via twin-screw extrusion and injection molding.

INTRODUCTION

Polyethylene (PE) is one of the most used materials for tribology in biomedical applications due to its excellent wear and chemical resistance (Liu et al. 2012). Although it is currently the most frequently used bearing surface, it does not fully provide the expected tribological performance (Goodman and Lidgren 1992). Therefore, in recent years, researchers have conducted studies to improve the wear resistance of PE matrix composites (Liu et al. 2014).

Lahiri et al. (Lahiri et al. 2014) investigated the tribological behavior of graphene nanoplatelets reinforced ultra-high molecular weight polyethylene (UHMWPE) composites. Results show that the coefficient of friction (COF) of UHMWPE decreased by 68% with 1% graphene addition. In another study, Akinci et al. (Akinci, Yilmaz, and Sen 2012) studied wear behavior of basalt filled low-density polyethylene (LDPE) composites. It was observed that 30%Basalt/70%LDPE composite has 90% less wear rate compared to pure LDPE under 20 N load. Also, no change in wear resistance was observed in the reinforcement range from 30% to 70%. In another similar study, Gogoleva et al. (Gogoleva et al. 2015) examined the mechanical and tribological properties of basalt fibers/UHMWPE composites. Wear resistance of 5% basalt fiber reinforced composites was nearly 7 times higher than pure UHMWPE. To sum up, the tribological properties of PE can be increased with different types of fillers.

Carbon fibers (CF) are promising fillers for polymer matrix composites due to their light mass and superior mechanical properties (Akgul et al. 2019). In this study, the effect of content on wear properties PE matrix composites was investigated. Also, the hardness test was performed.

EXPERIMENTAL

Material

LLDPE granules with 17 MFI (ASPUN™ 6834) and carbon fibers with a length of 3-6 mm were purchased from DowAksa LLC., USA.

Method

Carbon fibers and LLDPE granules were mixed using a twin-screw extrusion process. Then, composite samples with dog bone shape were produced via injection molding. Reciprocating wear test was conducted for each sample using simulation body fluid (SBF) under three different loads (20 N, 30 N, 50 N). Also, the Vickers hardness test was performed.

EXPERIMENTAL RESULTS AND DISCUSSIONS

The hardness of the samples was presented in Figure 1. It can be seen that the hardness values of the samples increased with the increase in carbon fiber ratio. The hardness value of PE-20CF has two times greater than pure LLDPE. This can be attributed that polymer chain movement is restricted with the addition of CF and presence of harder CF in the composites (Akgul et al. 2019).

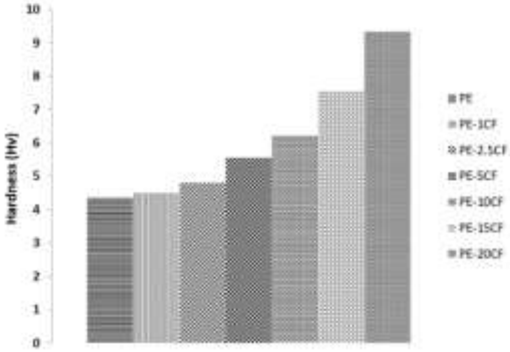

Figure 1. The hardness of composites and pure LLDPE.

Figure 2 shows the wear rates of samples containing carbon fiber up to 5% against different applied loads. It can be observed that composite samples have better wear resistance than pure LLDPE. This is because CF has lubricant effect and stiffer than pure PE. PE-2.5

CF sample has the best wear resistance among the samples.

On the other hand, composites containing more than 5% of carbon fiber have a greater wear rate than pure PE (Figure 3). This can be explained by the agglomeration of CF. The agglomeration caused poor matrix-reinforcement bonding, so higher CF fraction led to lower wear resistance (Akgul et al. 2019).

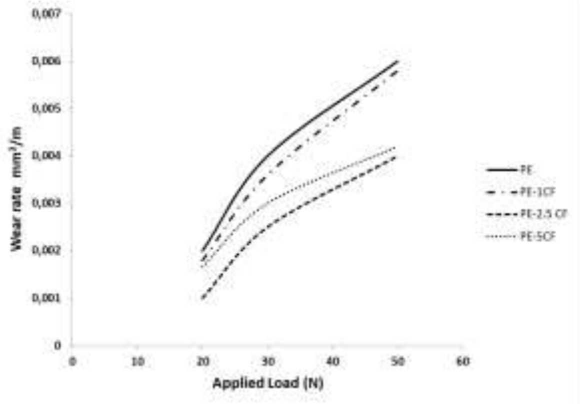

Figure 2. Wear rates of PE, PE-1CF, PE-2.5CF and PE-5CF samples.

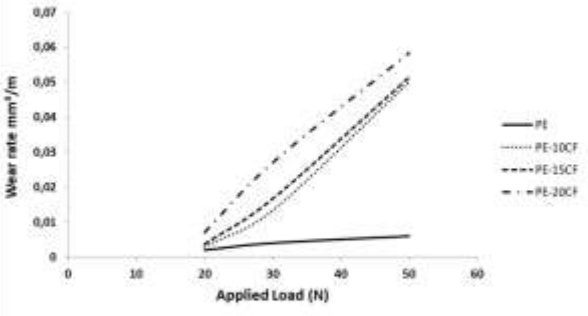

Figure 3. Wear rates of PE, PE-10CF, PE15CF and PE-20CF

CONCLUSIONS

The results show that the hardness of low-density polyethylene increases significantly depending on the carbon fiber content. PE-20CF sample exhibited the highest hardness value, which has nearly 100 % improvement compared to the pure LLDPE. However, the same trend was not observed for wear resistance of composites. PE-2.5CF showed best wear performance in SBF fluid conditions.

SUGGESTIONS FOR FURTHER WORK

In vivo studies will be performed for each sample in future works.

ACKNOWLEDGMENTS

The authors gratefully acknowledge the AREKA ADVANCED LLC. for financial support.

LITERATURE

Akgul, Yasin et al. 2019. “Influence of Carbon Fiber Content on Bio-Tribological Performances of High-Density Polyethylene.” Materials Research Express 6 (12): 125307.

Akinci, Akin, et al. 2012. “Wear Behavior of Basalt Filled Low Density Polyethylene Composites.” Applied Composite Materials 19 (3–4): 499–511.

Gogoleva, O. V., et al. 2015. “Wear-Resistant Composite Materials Based on Ultrahigh Molecular Weight Polyethylene and Basalt Fibers.” Journal of Friction and Wear 36 (4): 301–305.

Goodman, Stuart, and Lars Lidgren. 1992. “Polyethylene Wear in Knee Arthroplasty: A Review.” Acta Orthopaedica Scandinavica 63 (3): 358–364.

Lahiri, Debrupa, et al. 2014. “Nanotribological Behavior of Graphene Nanoplatelet Reinforced Ultra High Molecular Weight Polyethylene Composites.” Tribology International 70: 165–169.

Liu, Tian, et al. 2014. “Enhanced Wear Resistance of High-Density Polyethylene Composites Reinforced by Organosilane-Graphitic Nanoplatelets.” Wear 309 (1–2): 43–51.

Liu, Tian, et al. 2012. “Effect of Reinforcement on Wear Debris of Carbon Nanofiber/High Density Polyethylene Composites: Morphological Study and Quantitative Analysis.” Wear 294: 326–335.

Vollastonit ve Kalsiyum Karbonat Katkılı Polipropilen Kompozitlerde Katkı Malzemelerinin Yüzey Enerjisine Etkisi

SONCU, Serkan[1], AKKOYUN, Meral[2]
[1]Demo Plastik Ürünleri Sanayi ve Ticaret A.Ş. NOSAB Ceviz Cad. No.15/A Nilüfer/Bursa, Türkiye
[2]Bursa Teknik Üniversitesi, Lif ve Polimer Mühendisliği, Yıldırım/Bursa, Türkiye
serkan.soncu@safe-demo.com, meral.akkoyun@btu.edu.tr

AMAÇLAR

Bu çalışmanın amacı düşük yüzey enerjisine sahip polipropilenin (PP) yüzey enerjisinin artmasını sağlayarak yüzeyde oluşan yapışma kuvvetinin geliştirilmesi hedeflenmektedir. Bu amaçla 6 farklı katkı malzemesi ve PP matris malzemesi kullanılarak çift vidalı ekstrüder yöntemi ile kompozit üretimi gerçekleştirilmiştir. Sonrasında basınçlı kalıplama ile plakalar elde edilmiştir ve bu numunelerin temas açısı ölçümleri yapılmıştır.

GİRİŞ

Yüzey enerjisi boya, kaplama vb. işlemlerde yapışma kuvvetinin arttırılması için en önemli etkenlerden biridir. Bu amaçla plazma, flamaj ve korona yöntemleri kullanılmaktadır. Ancak bu yöntemler yeni proses tasarımı ve ilk yatırım maliyeti gerektirmektedir. Kullanılan hammaddenin yüzey enerjisi arttırılarak oluşabilecek bu maliyetlerin önüne geçilebileceği aşikardır.

Yüzey serbest enerjisinin belirlenebilmesi için farklı yöntemler geliştirilmiştir. Mevcut literatürün analizi yapıldığında Owens, Wendt, Rabel ve Kaelble (OWRK) metodunun en yaygın yöntemlerden birinin olduğunu göstermektedir.[1] İki farklı cismin yüzey tabakasında bulunan parçacıklar arasındaki etkileşimlerin, bu cisimlerin parçacıkları arasındaki etkileşimlerin geometrik ortalamasına eşit olduğunu söyleyen bu yöntem, yüzey enerjisinin dağıtıcı ve polar bileşenlerinin belirlenmesinden oluşur.[1]

Yeni malzemeler ve uygulamaları üzerine bilimsel araştırmalar daha çok polimer matrisli kompozit malzemelere ve lifli veya toz yapılı ve farklı büyüklükteki çeşitli organik ve inorganik dolgulara odaklanmaktadır1. Polimer kompozit malzemeler üretmenin temel amacı, reolojik, mekanik, termal ve elektriksel özellikler de dahil olmak üzere uygulanan bir polimer matrisinin özelliklerini arttırmaktır[1]. Kalsiyum karbonat (CaCO3), polimer matrisinde iyi bir dispersiyon sergileyen popüler ve kolayca temin edilebilen bir inorganik dolgu maddesidir.1 Çok iyi özellikleri (kimyasal olarak pasif, toksik olmayan, yüksek derecede saf, kokusuz ve tatsız) nedeniyle kalsiyum karbonat, polimerlerin hem termal mukavemetini hem de çentikli darbe mukavemetini arttırmanın uygun maliyetli bir aracı olarak kullanılır, ürün sertliğini ve yüzey kalitesini iyileştirir.[1]

Polimerlerde kullanılan katkı malzemelerinde iğne yapılı volastonitler artan sertlik ve mukavemetin yanı sıra birçok işleme ve performans avantajı sağalamaktadır. Volastonit, plastiklerde fonksiyonel dolgu maddesi olarak kullanılan bir kalsiyum silikattır (CaSiO3). Tamamen asiküler olan doğal olarak oluşan tek beyaz mineraldir. Volastonit parçacıklarının yapısı, yani en boy oranları, sadece doğal koşullara değil, aynı zamanda büyük ölçüde kullanılan hazırlama ve boyut küçültme tekniklerine de bağlıdır.

Polipropilen kompozitlerin yüzey enejisini arttırmaya yönelik birçok çalışma yapılmaktadır.[1-4] Bu çalışmada, farklı partikül boyutunda olan CaCO3 ve farklı yüzey işlemli volastonit partiküllerinin PP kompozitlerin yüzey enerjisine olan etkileri araştırılmıştır.

DENEYSEL

Malzeme

Bu çalışmada hazırlanan kompozitlerde saf PP matris malzemesine 40% oranında 1 µm ve 2 µm tanecik boyutlarında steraik asit kaplı CaCO3 ve Tremin 939 300 AST, Tremin 939 300 ZST, Tremin 283 010 AST, Tremin 283 400 AST volastonit katkıları kullanılmıştır.

Yöntem

PP/katkı (Tablo 1) karışımları çift vidalı esktrüder ve kesme makinesi kullanılarak kompozit granül haline getirilmiştir. Ardından sıcak pres kullanılarak plakalar üretilmiştir. Temas açısı ölçümü için uygun yüzeyler kesilerek ölçüm yapılmıştır.

Tablo 1. Deney matrisi

Katkı Malzemesi	Katkı Oranı (Kütlece)	PP Oranı (Kütlece)
Tremin 939 300 AST	40%	60%
Tremin 939 300 ZST	40%	60%
Tremin 283 010 AST	40%	60%
Tremin 283 400 AST	40%	60%
$CaCO_3$ (1 µm)	40%	60%
$CaCO_3$ (2 µm)	40%	60%

DENEYSEL SONUÇLAR/TARTIŞMA

Yüzey enerjisi ölçümleri su, formamid, etilen glikol ve diidometan kullanılarak yüzey temas açıları ölçülmüştür. Elde edilen sonuçlar Tablo 2'de verilmiştir.

Tablo 2. Temas açısı ölçüm sonuçları

	Temas Açısı (°)			
	Su	Formamid	Etilen Glikol	Diiodometan
PP	78,533	63,622	69,8	55,09
CaCO3 - 1µm	98,467	85,135	68,68	57,936
CaCO3 - 2µm	80,143	73,704	56,888	50,843
939 300 AST	80,413	87,213	75,747	56,304
939 300 FST	84,505	68,761	57,425	59,778
283 010 AST	101,077	80,078	76,764	54,36
283 400 AST	95,14	81,659	63,697	52,011

Ölçümlerde kullanılan test sıvılarının yüzey gerilimleri Tablo 3' de verilmiştir.

Tablo 3. Test sıvıları yüzey gerilimleri

	Yüzey Gerilimi (mN/m)			
	Su	Formamid	Etilen Glikol	Diiodometan
Dispersive	18,7	39,4	29,3	50,8
Polar	53,6	20	18,2	0
Total	72,3	59,4	47,5	50,8

Yapılan temas açısı ölçümlerinden yola çıkılarak yüzey enerjilerinin hesaplanmasında OWRK metodu kullanılmıştır. Bu metoda göre yapılan hesaplamalar aşağıdaki gibidir.

Yapılan temas açısı ölçümlerinden yola çıkılarak yüzey enerjilerinin hesaplanmasında OWRK metodu kullanılmıştır. Bu metoda göre yapılan hesaplamalar aşağıdaki gibidir.

σ_L = Toplam sıvı yüzey gerilimi
σ_L^D = Sıvı dispersive yüzey gerilimi
σ_L^P = Sıvı polar yüzey gerilimi
θ = Temas açısı
σ_S^D = Dispersive yüzey enerjisi
σ_L^P = Polar yüzey enerjisi

$$\frac{\sigma_L(1+cos\theta)}{2\sqrt{\sigma_L^D}} = \frac{\sqrt{\sigma_S^P}\sqrt{\sigma_L^P}}{\sqrt{\sigma_L^D}} + \sqrt{\sigma_S^D} \qquad (1)$$

$$y = \sqrt{\sigma_S^P}x + \sqrt{\sigma_S^D} \qquad (2)$$

$$y = \frac{\sigma_L(1+cos\theta)}{2\sqrt{\sigma_L^D}} \qquad (3)$$

$$x = \sqrt{\frac{\sigma_L^P}{\sigma_L^D}} \qquad (4)$$

Tablo 4. Farklı test sıvıları için x ve y değerleri

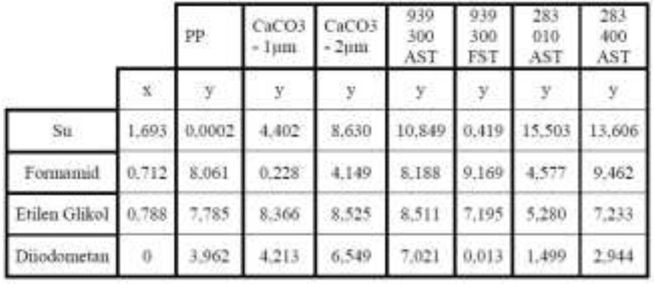

		PP	CaCO3 - 1µm	CaCO3 - 2µm	939 300 AST	939 300 FST	283 010 AST	283 400 AST
	x	y	y	y	y	y	y	y
Su	1,693	0,0002	4,402	8,630	10,849	0,419	15,503	13,606
Formamid	0,712	8,061	0,228	4,149	8,188	9,169	4,577	9,462
Etilen Glikol	0,788	7,785	8,366	8,525	8,511	7,195	5,280	7,233
Diiodometan	0	3,962	4,213	6,549	7,021	0,013	1,499	2,944

Tablo 5. Dispersive ve polar yüzey enerjileri

	σ_S^P	σ_S^D
PP	7,42	50,79
CaCO3 - 1µm	0,10	16,35
CaCO3 - 2µm	1,44	47,72
939 300 AST	5,24	46,44
939 300 FST	0,12	20,02
283 010 AST	71,55	0,001
283 400 AST	39,90	7,31

Toplam yüzey enerjisi polar ve dispersive yüzey enerjilerinin toplamına eşittir.

$$\sigma_S = \sigma_S^P + \sigma_S^D \qquad (5)$$

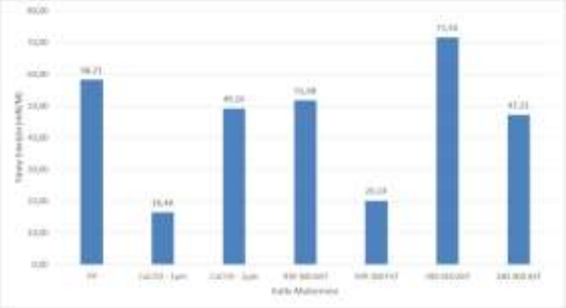

Şekil 1. Katkı malzemelerine göre yüzey enerjisi

GENEL SONUÇLAR

Bu çalışmada en küçük temas açısı ölçümleri ve buradan da en optimum toplam yüzey enerji değerleri $CaCO_3$ ve 283 010 AST katkıları ile elde edilmiştir.

SONRAKİ DÖNEM ÇALIŞMALARI

Bu çalışmanın devamında en uygun katkı miktarı, mekanik dayanımına ve enjeksiyon yöntemiyle kalıplanabilirlik üzerine çalışmalar yapılacaktır.

TEŞEKKÜR/BILGILENDIRME/FON KAYNAĞI

Niğtaş ve Kaolin firmalarına katkı malzemelerinin temini konusunda verdikleri destek için teşekkür ederiz.

KAYNAKLAR

1. Rudawska, A., Jakubowska, P., Kolozinski, 2017. “Surface free energy of composite materials with high calcium carbonate filler content”, Polimery, 62, 434-440.

2. Svab, I., Musil, V., Leskovac, M., 2005. “The Adhesion Phenomena in Polypropylene/Wollastonite Composites” Acta Chim. Slov., 52, 264-271.

3. Nurdina, A.K., Mariatti, M., Samayamutthirian, P., 2009. Effect of single-mineral filler and hybrid-mineral filler additives on the properties of polypropylene composites, Journal of Vinyl & Additive Technology, 15, 20-28.

4. Demjen, Z., Pukanszky, B., Nagy, J., 1998, Evaluation of interfacial interaction in polypropylene/surface treated CaC03 composites, Composites Part A, 29A, 323-329.

Hijyen Ürünlerinde Kullanılabilecek Spunlace Nonwoven Kumaşlarda Lif Tipi ve Karışım Oranının Ürün Performansına Etkilerinin İncelenmesi

ÇELİKTEN, Ebru[1], SATIL, Eyüp Ali[1], YAYLA, Osman[1]
[1]Selçuk İplik San. Ve Tic. A.Ş. Ar-Ge Merkezi, Gaziantep, Türkiye
ebru.celikten@kholding.com.tr

AMAÇLAR

Tek kullanımlık hijyen ürünleri genellikle, spunbond ve meltblown teknolojilerinde poliolefin bazlı liflerin kullanılmasıyla elde edilmektedirler. Bu çalışmada, spunlace teknolojisinde farklı lif içeriklerine sahip alternatif yeni ürünlerin geliştirilmesi amaçlanmıştır.

GİRİŞ

Dokunmamış kumaşlar (nonwoven) gün geçtikçe hayatımızda daha fazla yer almaya başlamıştır. Geleneksel yöntemlerle üretilen kumaşlara alternatif olarak geliştirilen nonwoven üretim teknolojisi, düşük üretim maliyeti ve yüksek üretim kapasitesine sahiptir. Nonwoven yüzeyler çok farklı kullanım alanlarına sahip olmakla birlikte bunların en başında hijyen sektörü yer almaktadır.

Hijyen sektöründe kullanılan ürünlerin bazıları; kadın hijyen pedi, bebek bezi, bebek ıslak ve kuru mendilleri, kişisel mendiller, makyaj temizleme pedleri, yetişkin bezleri, vb. dir [Zamfir, 2010]. Bu ürünlerin birçoğu katmanlı yapılardan oluşmaktadır. Ürünlerin bazı bölgelerinde emici yapılar, yer alırken bazı bölgelerinde sıvıyı geçirmeyen yapılar (bebek bezi kenar katman ve arka katman gibi) yer almaktadır [Das ve ark., 2008]. Bu çalışma kapsamında, tek kullanımlık hijyen pedlerinde spunlace teknolojisi kullanılarak hem hidrofil hem de hidrofob yapıların elde edilebilirliği araştırılmıştır.

DENEYSEL

Malzeme

Çalışma kapsamında kullanılan liflerin özellikleri Tablo 1'de verilmiştir.

Tablo 1. Kullanılan hammaddelerin özellikleri

Özellik / Lif Tipi	Lif Uzunluğu [mm]	Lif İnceliği [dtex]
Polipropilen (PP)	40	1,7
Poliester (PES)	38	1,67
Viskon (CV)	40	1,7
Bikomponent (BICO) PP/PE (50/50)	40	1,7

Yöntem

Numune üretimleri Andritz Spunlace hattında (Şekil 1) gerçekleştirilmiştir. Üretim parametreleri (sıcaklık, su jeti basınçları, makine hızı, tarak çekim oranları, vb.) sabit tutulmuştur.

Şekil 1. Spunlace üretim hattı

Numunelere, 22±2°C sıcaklık ve %60±4 nem'de 24 saat kondisyonlandıktan sonra Tablo 2'de verilen testler uygulanmıştır.

Tablo 2. Numunelere uygulanan test ve standartlar

Uygulanan Testler	Standartlar
Birim Ağırlık (gsm)	NWSP 130.1
Kalınlık (mm)	NWSP 120.6
Kopma Mukavemeti (N/5cm)	NWSP 110.4
Kopma Uzaması (%)	NWSP 110.4
Sıvı Alma Kapasitesi (%)	NWSP 10.01
Sıvı Emme Süresi (saniye)	WSP 70.3
Geri Islatma (%)	WSP 70.8

DENEYSEL SONUÇLAR/TARTIŞMA

Toplamda 6 adet numunenin sahip olduğu lif kompozisyonları Tablo 3'de verilmiştir.

Tablo 3. Numuneler ve özellikleri

Numune No	Kompozisyon
D1	% 100 PP
D2	% 50 PES % 50 PP
D3	% 50 PP % 50 CV
D4	% 100 CV
D5	%25 PES -%50 PP-%25 BICO
D6	% 100 PES

Elde edilen sonuçlar detaylı olarak incelendiğinde;

- D1 numunesindeki PP lifleri nem alımı olmadığından hidrofob yapıdadırlar. Bu yüzden elde edilen ürün, sıvı transferinin olmaması istenilen alanlar için uygundur.
- D2 numunesinde PP ve PES lif karışımı içerdiğinden hidrofob özelliğini korumaktadır.
- D3 numunesinde ise yapıda selülozik bir lif olan CV'nin kullanılmasıyla hidrofil bir yapı elde edilmiştir. Ancak D1 ve D2 numunelerine kıyasla mukavemet ve uzama (ıslak ve kuru) değerlerinde azalma tespit edilmiştir.
- D4 numunesinde ise %100 CV lifi kullanımı (hidrofil yapısından dolayı) özellikle sıvı emme süresinde pozitif bir etki yaratırken, geri ıslatma değerlerinde olumsuz sonuçlar vermiştir.
- Sentetik liflerin karışımından elde edilen D5 numunesinde (%25 PES-%50 PP-%25 BICO) yüksek mukavemet ve uzama değerleri elde edilirken, sıvı performans testlerinde hidrofob yapı özelliğini korumaya kısmen devam etmektedir.
- Son olarak %100 PES lifinden elde edilen D6 numunesinde sıvı performans özelliklerinde D1 numunesine kıyasla olumlu bir artış sağlanırken, son kullanım alanında hidrofil yüzeylerin kullanılmasında tercih edilebilir özellikte olduğu tespit edilmiştir.

Tablo 4. Numuneler ve test sonuçları

Numune **Özellik**	**D1**	**D2**	**D3**	**D4**	**D5**	**D6**
Birim Ağırlık [g/m^2]	35	35	35	35	36	35
Kalınlık [mm]	0,53	0,54	0,4	0,54	0,59	0,57
Mukavemet-Kuru-MD [N/5 cm]	104,5	92,4	45	55,7	94	70
Mukavemet-Kuru-CD [N/5 cm]	38,5	34,6	12	19,7	35,4	25
Mukavemet-Islak-MD [N/5 cm]	109,8	98,5	35	53,1	94,9	-
Mukavemet-Islak-CD [N/5 cm]	38,9	33,3	12	16,4	37,6	-
Uzama-Kuru-MD [%]	48,6	47,5	15	35	55,9	50
Uzama-Kuru-CD [%]	180	171	100	150,3	165,8	170
Uzama-Islak-MD [%]	49,4	48,6	15	40,5	55,1	-
Uzama-Islak-CD [%]	180,8	170	70	140	172,6	-
Sıvı Emme Süresi [sn]	-	-	3,21	1,97	1916	2,98
Geri Islatma [%]	-	-	7,33	24,1	0,44	1,12
Sıvı Emme Kapasitesi [%]	-	-	1035	1040	-	1245

GENEL SONUÇLAR

Tek kullanımlık hijyen ürün üretiminde kullanılan mevcut spunbond ve meltblown teknolojilerinden farklı olarak spunlace teknolojisinde bu çalışma kapsamında üretilen ürünlerde, lif içeriğine bağlı olarak hem hidrofil hem de hidrofob yapılar elde edilmiştir. Bu sayede, herhangi bir kimyasal bitim işlemine gerek kalmadan talep edilen hijyen ürünlerinin özelliklerine göre (emici katmanlar için hidrofil yapı, sıvıyı iletmemesi için hidrofob yapı) alternatif ürünler geliştirilmiştir.

KAYNAKLAR

[1] Zamfir, M., 2009. Composite Nonwovens for Hygiene and Medical Applications. Department of Technology and Design of Textile Products.

[2] Das, A., V. K. Kothari, K. V., Makhija. S., Avyaya, K., 2007. Development of high-absorbent light-weight sanitary napkin. journal of applied polymer science, vol. 107, 1466–1470.

Evaluating the Potential Use of Lightweight Nonwovens as Adhesive Webs

SUVARI, Fatih, KESIMCI, Mahmut Oguz
Bursa Uludag University, Faculty of Engineering, Textile Engineering Department, Bursa, Turkey
kesimci@uludag.edu.tr

PURPOSE

The aim of this work is to investigate the use of lightweight and porous webs as an adhesive for the lamination of fabrics.

INTRODUCTION

Lamination is a process of sticking at least two surfaces into a strong and stable composite material. Dry lamination is the permanent jointing of two surfaces by using powders, plastisols, or melt adhesives. Generally, heat and pressure are also required for the process.

Air-permeable laminated structures are requested in some applications (for instance, upholstery fabrics used for furniture). Adhesives like hot-melt films close the pores of the fabrics completely. The resulting structure does not allow air to pass from one side to the other. In this work, three types of nonwovens are used as adhesive webs for the lamination. Due to the fibrous and porous structure, nonwovens can be an excellent candidate to produce air-permeable laminated structures.

EXPERIMENTAL

Material

Copolyurethan, Copolyester-1, and Copolyester-2 are the three different types of adhesive webs that were used to laminate polyester fabrics in this study. Melting, stick point, and melt flow rate of the polymers used for the production of the webs are given in Table 1. Melt flow rate (MFR) in Table I indicates the ease of flow of melted polymers. 5-gram sample is heated above its melting point and forced to flow through a capillary using 2.16 kg weight [1]. The viscosity of copolyesters can be regarded as high compared to copolyurethan polymer.

Heat resistance values of each polymer are also given in Table I. Thermal stability is the ability of polymers to keep their properties at high temperatures. Heat resistance temperature is the upper limit in which a polymeric material can support a mechanical load without a change in shape [2].

100% polyester woven fabric with plain weave structure is used for the lamination. Warp and weft densities of the fabric are 42 warp/cm and 26 weft/cm, respectively. Yarn counts of both warp and weft yarns are determined as 90 deniers. The thickness is 0.09 mm. The mass per unit area of the polyester fabric is 57.6 g/m^2.

Table 1. Properties of the polymers used

Material	Melting or stick point [°C]	Heat resistance [°C]	Melt flow rate [g/10min]
Copolyurethan	85	60	17
Copolyester-1	95	89	11
Copolyester-2	85	80	12

Method

Three different adhesive webs were used for laminating the polyester woven fabrics at the temperature of 120°C for 5 minutes. Table type press was used to produce laminated fabrics.

The thickness and weights of the adhesive webs were measured. Microscope images were also taken. Air permeability tests were performed using an SDL Atlas M021A. The pressure drop and test area were chosen as 125 Pa and 38 cm^2, respectively. The adhesion strengths of the laminated woven fabrics were measured according to AATCC 136-2009 test method.

EXPERIMENTAL RESULTS AND DISCUSSIONS

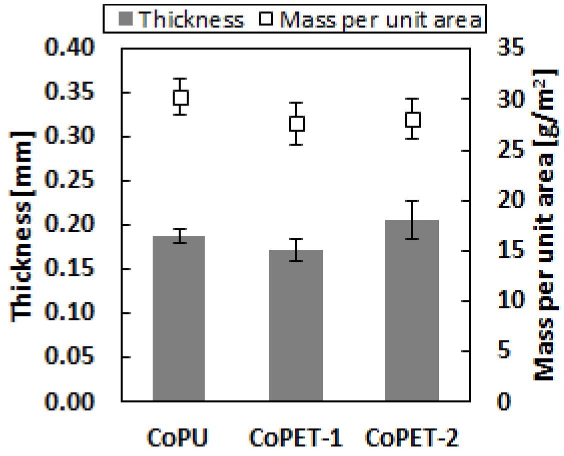

Figure 1. Mass per unit area and thickness of the webs

Thickness and mass per unit area data of the adhesive webs are given in Figure 1. These webs can be considered lightweight and thin structures.

Bending rigidity of the laminated fabrics produced using these webs can be potentially low due to the low values of these two essential fabric properties.

The air permeability results are shown in Figure 2. According to the results, the air permeability values of the webs are extremely high compared to the reference woven fabric due to the porous structure of the adhesive webs (Figure 3). It seems that CoPET-2 web has bigger pores.

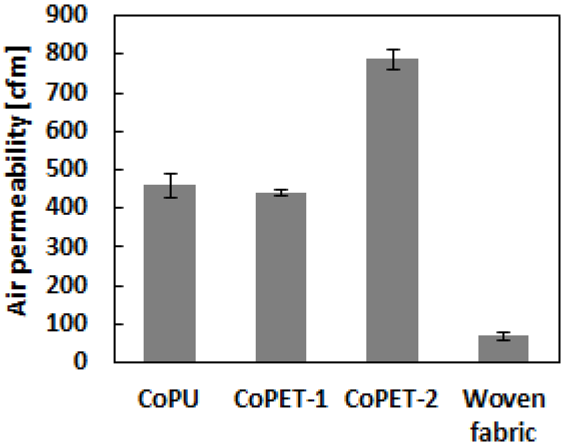

Figure 2. The air permeability of the webs and the reference fabric


CoPU CoPET-1 CoPET-2

Figure 3. The porous structure of the webs

Two reference polyester woven fabrics were laminated using the adhesive webs. The selected temperature was 120°C, and the duration was 5 minutes. The air permeability values of the laminated structures are given in Figure 4. Note that after the lamination, air can pass throughout the laminated structures.

Delamination or bond strength test was also performed to the laminated fabrics. Resistance forces that occurred during the delamination test are recorded. The maximum resistance force results for each type of lamination are given in Figure 5. Structures laminated using CoPET-1 and CoPU adhesive webs are more resistant to delamination. On the other hand, the structure with CoPET-1 is weaker in terms of delamination. It seems big pores of the CoPET-1 adhesive web caused fewer bonding points.

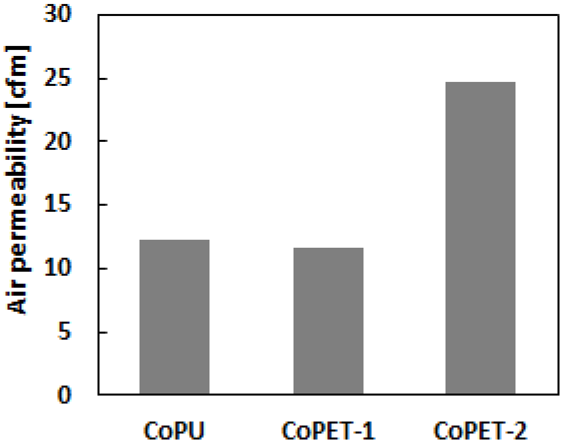

Figure 4. The air permeability of the laminated structures

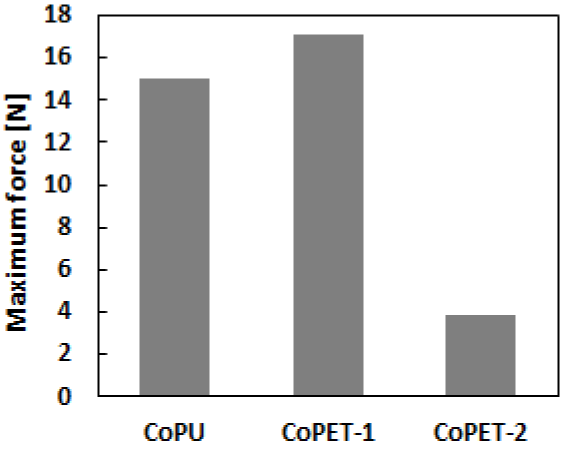

Figure 5. Maximum resistance forces of the laminated structures

CONCLUSIONS

Three different lightweight adhesive webs were used to laminate the polyester woven fabrics. After the lamination, air can pass throughout the laminated structures for all adhesive types. Moreover, structures laminated using CoPET-1 and CoPU adhesive webs are more resistant to delamination.

REFERENCES

[1] https://polymerdatabase.com/polymer%20physics/Melt%20Flow.html

[2] Heat Resistance and Thermal Stability of Polymers. (n.d.) The Great Soviet Encyclopedia, 3rd Edition. (1970-1979).

Improving flame retardancy of PE with halogen-free materials

GUNAYDIN, Beyza Nur[1], SEYHAN, Aybeniz[1], POLAT, Yusuf[1,2], KILIC, Ali[1,3], DEMIR, Ali[1,3], UREYEN, Mustafa Erdem[4,5], AVCI, Huseyin[1,4]
[1]TEMAG Labs, Textile Tech. and Design Faculty, Istanbul Tech. Uni., Istanbul, Turkey
[2] Mechanical Engineering, Faculty of Engineering, Marmara Uni., Istanbul, Turkey
[3] Textile Engineering, Textile Tech. and Design Faculty, Istanbul Tech. Uni., Istanbul, Turkey
[4]Advanced Technologies Research Centre (ITAM), Eskisehir Tech. Uni., Eskisehir, Turkey
[5]Department of Fashion and Textile Design, Eskisehir Tech. Uni., Eskisehir, Turkey
[6] Metallurgical and Materials Engineering, Engineering - Architecture Faculty, Eskisehir Osmangazi Uni., Eskisehir, Turkey
havci@ogu.edu.tr

PURPOSE

Flame retardancy (FR) properties of linear low density polyethylene (LLDPE) has been studied with different halogen-free flame retardants of aluminium trioxide (ATH), nanoclay and nanocrystalline cellulose. The samples were produced by twin screw extruder. In addition, to reveal the synergistic effect of phosphorous-mineral containing additives with ammonium polyphosphate (APP) and ATH (30% ATH-10% APP) were used. Limiting oxygen index (LOI) and micro combustion calorimeter (MCC) tests were performed to compare untreated and treated samples.

INTRODUCTION

Polyethylene (PE) is the most used polymer type in the world. The ignition time of PE is relatively low compared to other thermoplastics. It is classified as a low smoke emission polymer but considering the high peak heat release rate, it can be dangerous in the real fire situations[1]. The ongoing combustion reactions in the form of ignited droplets play a critical role in accelerating fire. Therefore, flame retardancy and thermal properties of PE should be improved in order to widen the application areas. Flame retardant additives are used to reduce or stop the ignition of polymeric materials. Flame retardant property gains importance especially in composite applications of high performance fibers[2]. Although halogen based flame retardants and combinations with antimony trioxide are conventionally used in polymer applications because of their low cost, acceptable efficiency and no significant change in the physical performance of a polymer, there are important problems in practice due to their performance limitations, environmental and toxic effects[3]. Thus, demand and studies on using halogen-free flame retardants are rapidly grown[4]. Moreover, decreasing the FR amount used in the polymer and nano sized additive applications are becoming popular subjects, recently[4].

In this study, ATH, nanoclay and nanocrystalline cellulose were used as halogen-free FRs and the samples were produced by the twin screw extruder. All the samples were subjected to LOI and MCC tests to analyze and compare the flammability and heat characteristics. At the last part, according to test results, ATH-APP hybrid masterbatch was studied with different ratios via melt spin line. The aim of using the APP with ATH together is to decrease the high amount requirements of ATH to obtain sufficient flame retardancy properties for high performance PE fibers by synergistic activity between ATH and APP.

EXPERIMENTAL

Material

The ASPUN™ 6000 linear low-density polyethylene (LLDPE) (MFI, 19 and density, 0.935 g/cm^3) was obtained from Dow Chemical Company. 99.95% pure ATH having a grain size of 20-25 µm from Entekno Industrial Company; Cloisite-20 nanoclay with an organic intercalated dry particle size <10µm and a density of 1.77g/cm^3 was Feza Chemical Company; nanocrystalline cellulose (CNC) from Nanografi Company having a density of 1.49 g/cm^3 and diameter of 10-20 nm and a length of 300-900 nm and Acar Kimya ve Sanayi Tic. Ltd. Ltd. Şti., EXOLIT AP 422 APP were purchased.

Method

Micro-compounder with twin screw (DSM Xplore) were used to produce samples according to TS 11162 EN ISO 4589 standard for LOI tests (Concept Equipment). Hybrid filaments were produced by a single screw extruder melt spin line with 0.6 mm spinneret diameter. For the determination of thermal behaviors of PE, MCC test was also performed to all samples.

EXPERIMENTAL RESULTS AND DISCUSSIONS

LOI results of samples prepared with different ATH concentration demonstrated the addition of ATH slowed down the burning at the same oxygen concentration. But LOI value could not be improved satisfactorily. Maximum LOI value (22.17%) was obtained by 40% ATH.

Table 1. Comparison of the limiting oxygen index of PE and PE-ATH with different additive amounts.

Samples	**ATH (wt %)**	**PE (wt %)**	**LOI (%)**
PE	0	100	**19.00**
PE-1	10	90	**19.91**
PE-2	20	80	**20.91**
PE-3	30	70	**21.29**
PE-4	40	60	**22.17**

Also, for other additives such as nanoclay and CNC, the best LOI values were determined 20.30 and 19.30 at 10 wt%, respectively. In MCC test, heat release rate (HRR), peak of heat release rate (pHRR), pHRR temperature, heat release capacity (HRC) and total heat release (THR) values were represented in Fig. 1. According to the given MCC results, it is seen that the amount of ATH positively affects the HRR of PE and reduces HR capacity. Although the addition of nanoclay had no effect on the LOI value, it was observed that the combustion behavior and melt dripping property of the polymer material was improved. Moreover, significant char formation and flameless dripping were observed in the burned polymer with the addition of cellulose compared to the samples produced with nanoclay and ATH.

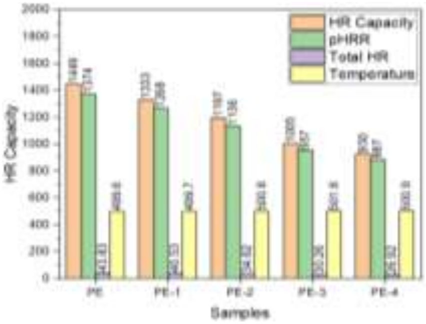

Figure 1. Comparison of the MCC test results of PE and PE-ATH with different additive amounts.

To reduce the ATH amount, APP was mixed with ATH and ATH-APP hybrid in different ratios (5 wt%, 3 wt% and 2 wt%) were added to the system during extrusion. APP is added in sufficient amounts, it has the formation of charcoal, reduces the combustion time of the polymers and prevents dripping.

CONCLUSIONS

Samples were separately made from flame retardant additives by twin screw extruder. According to given results, it was seen that nano additives did not affect the LOI test results, unlike lowered the values instead of raising them. ATH can show positive effect when amounts to increased 40 wt.%. Thus, because of requiring the high amounts, ATH alone is not effective to produce high performance PE fibers. Depending on the initial results, ATH-APP hybrid was only feed to the melt spin line. The result of adding APP, synergistic affect was observed and ATH-APP hybrid structure demonstrated LOI values of 20.

SUGGESTION FOR FURTHER WORK

Different hybrid studies will be investigated to improve FR effects. After the optimization, the high performance PE fibers with having FR properties will be produced by our modified melt-spin line.

ACKNOWLEDGEMENTS OF FUNDING

The authors thank TUBITAK (Project Number: 117Z673) for financially support to this research. The authors also gratefully acknowledge Dow Chemical Company for providing ASPUN™ 6000 and Mimtek Makine San. Tic. A.Ş to provide APP additive.

LITERATURE

1. Agwuncha, S. C., Ibrahim, I. D., & Sadiku, E. R. (2017). Improving the thermal and flame resistance properties of polyolefins. In Polyolefin Fibres (pp. 421-448). Woodhead Publishing.
2. Bourbigot, S., & Flambard, X. (2002). Heat resistance and flammability of high performance fibres: A review. Fire and materials, 26(4-5), 155-168.
3. Avcı, H., Üreyen, M. E., Kiliç, A., Sağlam, A. E., & Demir, A. Güç Tutuşur Polipropilen Polimeri Ve Lif Uygulamalarinda Son Gelişmeler Ve Gelecek Beklentileri. Uludağ University Journal of The Faculty of Engineering, 24(2), 609-632.
4. Rault, F., Giraud, S., Salaün, F., & Almeras, X. (2015). Development of a halogen free flame retardant masterbatch for polypropylene fibers. Polymers, 7(2), 220-234.

REAKTİF BOYALI PAMUKLU KUMAŞLARDA KULLANILAN FİKSATÖR TİPLERİ VE KOMPOZİSYONLARININ RENK HASLIĞI ÜZERİNE ETKİSİ

OĞUZ, Damla[1], YILDIRIM, Kenan[2]

[1]Rudolf Duraner Kimyevi Mad. Tic. A.Ş., Bursa/Türkiye

[2]Bursa Teknik Üniversitesi, MDBF, Lif ve Polimer Mühendisliği Bölümü, Bursa/Türkiye

damla.tunaa@hotmail.com, kenan.yildirim@btu.edu.tr

AMAÇLAR

Bu çalışmanın amacı literatürde eksik olan fiksatör tipleri ve karışımlarının reaktif boyarmaddeler ile boyanmış pamuklu örme kumaşlara ait haslık değerleri üzerine etkisinin incelenmesidir.

GİRİŞ

Pamuk lifi emiciliği ve konfor özellikleri sayesinde oldukça tercih edilen ve tekstil üretiminin %50'den fazlasında kullanılmakta olan bir lif tipidir. Tekstil sektörü hayatımızın vazgeçilmezleri arasında yer almakta olup üretilen mamüllerin renk haslık özellikleri ürün kalitesi için önemli parametrelerden biridir.Tecrübeler gösterir ki reaktif boyarmaddelerin özellikle ışık haslık değerleri oldukça iyidir ancak yaş haslık değerleri reaktif gruba ve substantifliğe bağlı olarak orta dereceli olarak değerlendirilmektedir.[1]

Bu durumu iyileştirmek adına haslık özelliklerini geliştirmekte kullanılan fiksatör olarak tanımlanan polimerler ile ard işlemler yapılmaktadır. Fiksatörler, selüloz ve boyarmadde arasında güçlü köprü oluşturur ve bu sayede boyarmadde molekülleri elyaf yüzeyine sabitlemektedirler.Fiksatörlerin haslık üzerine etkisinin incelenmesine yönelik bir çok çalışma mevcuttur.[2-5]

DENEYSEL

Malzeme

Çalışmada bordo, siyah ve turkuaz olmak üzere 3 farklı renkte %100 pamuklu örme kumaşlar kullanılmıştır.

Yöntem

Örme kumaşlar kısa ve uzun zincirli quaterner poliamonyum, poliamin, poliamid, poliüretan ve epiklorhidrin bazlı 6 adet fiksatör ile ard işleme tabi tutulmuştur. Uygulama işleminde fiksatörlerin kendileri ve karışım (%50+%50) halleri kullanılmıştır. Banyo konsantrasyonu 15 g/l, pH değeri 5-5.5 ve kumaşın çözeltiyi alma oranını ise %85 olacak şekilde ayarlanmıştır. Emdirme yöntemi ardından işlem gören kumaşlar ramda 140ºC' de 2 dk fikse işlemine tabi tutulmuştur. Sonuçlar hem göz ile subjektif olarak hem de spektrofotometre cihazı ile objektif olarak değerlendirilmiştir. Fiksatörün etkisi görmek üzere Evsel ve Ticari Yıkamaya Karşı Renk Haslığı (ISO 105 C06), ve Sürtmeye Karşı Renk Haslığı (ISO 105 X12) testleri uygulanmıştır.Renk haslık analizlerinin değerlendirilmesi refekat bezine akma durumuna göre yapılmıştır. Akma seviyesi ise refekat bezindeki pamuk lifine akma seviyesi olarak ölçülmüştür.

DENEYSEL SONUÇLAR/TARTIŞMA

Bordo, siyah ve turkuaz renkte olan kumaşlar koyu tonda oldukları için renk değişimi parametresi bazında değerlendirme yapılamamıştır. Üç farklı renkteki işlemli kumaşlara ait yıkamaya karşı renk haslığı değerlerinin poliamin bazlı fiksatör ve karışımlarında oldukça geliştiği gözlenmiştir.

Poliamin fiksatör ve karışımlarında ortalama olarak bordo renkte 1,5 birim, turkuaz renkte 0,5 birim ve siyah renkte ise 0,5 birim iyileştirdiği görülmüştür. Sürtmeye karşı (yaş) haslık değerlerinde ise poliüretan ve poliüretan/epiklorhidrin bazlı fiksatörler, bordo rengi 2 birim, turkuaz rengi 0,5 birim, siyah rengi ise 1,5 birim iyileştirmiştir.

Tablo 1: Kumaşların renklendirilmesinde kullanılan boyar maddeler.

Bordo	Reactive Red 239 Cosmos Red S-C (Bezaktiv)
Turkuaz	Reactive Blue 181 Reactive Blue 21
Siyah	Yellow ED (Everzol) Red ED- 7BN (Everzol) Setz. Black SNN (Everzol)

Tablo 2: Kumaşların renklendirilmesinde kullanılan boyar maddeler.

Fiksatör tipleri	**1**	**2**	**3**	**4**	**5**	**6**
Epiklorhidrin bazlı	15	-	-	-	-	-
Poliamin reçine bazlı	-	15	-	-	-	-
Poliamid bazlı	-	-	15	-	-	-
Kuaternar amonyum tuzları bazlı (uzun zincirli)	-	-	-	15	-	-
Poliüretan bazlı	-	-	-	-	15	-
Kuaternar amonyum tuzları bazlı (kısa zincirli)	-	-	-	-	-	15
pH	5-5,5	5-5,5	5-5,5	5-5,5	5-5,5	5-5,5
Banyo alımı	%85	%85	%85	%85	%85	%85
Kurutma sıcaklığı	140ºC	140ºC	140ºC	140C	140ºC	140ºC
Kurutma süresi	2 dk	2 dk	2 dk	2 dk	2 dk	2 dk

GENEL SONUÇLAR

Bordo renkli kumaşların poliamin bazlı fiksatör ve bu fiksatörün diğer fiksatörler ile karışımları ile fikse edilmesi (ard işlem yapılması) durumunda; yıkamaya karşı renk haslık değerlerini gözle yapılan değerlendirmede 2-3' den 4' e yükselttiği, cihazla yapılan değerlendirmede ise sadece poliamin bazlı fiksatörün 3' ten 4-5' e, diğer fiksatör tipleri ile olan karışımlarının ise 3'ten 4' e yükselttiği gözlenmiştir. Uzun zincirli kuaternar poliamonyum bazlı fiksatör ise akma değerini 2-3' ten 3-4' e, cihazla değerlendirmede ise 3' ten 4' e yükseltmiştir. Bu fiksatör tipi ile epiklorhidrin, poliamin ve kısa zincirli kuaternar poliamonyum bazlı fiksatör karışımlarının uygulanması durumunda ise hem göz hem de cihaz ile değerlendirmede haslık değerlerini +1-1,5 birim arasında iyileştirdiği görülmüştür. Epiklorhidrin, poliamid, poliüretan, kısa zincirli kuaternar poliamonyum bazlı fiksatörlerin ise, yıkama haslık değerlerinin gelişmesine olumlu yönde bir katkı sağlamadıkları gözlenmiştir.

Turkuaz renkli kumaşların poliamin bazlı fiksatör ve karışımları ile fikse edilmesi durumunda yıkamaya karşı renk haslık değerlerini gözle değerlendirmede 4'ten 4-5'e yükselttiği ancak cihaz değerlendirmesinde herhangi bir farkın oluşmadığı görülmüştür. Diğer fiksatörler ve birbirleri ile olan karışımlarının ise haslık değerleri gelişmesine olumlu ya da olumsuz yönde herhangi bir katkı sağlamadıkları gözlenmiştir.

Ard işlem öncesi siyah renkli kumaşa ait multifiberdaki akma değeri 4-5 olup bu değer üst sınırdadır. Ard işlemler sonrası fiksatörlerin yıkamaya karşı renk haslık değerleri üzerine olumlu ya da olumsuz yönde etkisi gözlenmemiş olup ard işlem öncesi değer korunmuştur.

Bordo, turkuaz ve siyah her üç renkte de sürtmeye karşı renk haslık analizinin kuru sürtme değerleri gözle yapılan değerlendirme 4-5, cihaz ile yapılan değerlendirme ise 5 olarak ölçülmüştür. Bu değerler haslık değerleri olarak yüksek kabul edilen değerlerdir ve tüm fiksatör tipleri ile yapılan ard işlemler sonrasında da herhangi bir değişim göstermemiştir.

Bordo rengin yaş sürtme değerlerinde ise, poliüretan bazlı fiksatör ve poliüretan/epiklorhidrin fiksatör karışımları, haslık değerini gözle yapılan değerlendirmede 2' den 4' e, cihazla yapılan değerlendirme de ise 3' ten 4-5'e, yükselterek, +2-2,5 birim artış sağlamıştır. Poliamid/poliüretan karışımı ise haslık değerini gözle yapılan değerlendirmede 2' den 3' e çıkarırken cihazla yapılan değerlendirmede ise 3'ten 3-4'e yükseltmiştir. Diğer fiksatör ve karışımları ise gözle değerlendirmede haslık değerini 2'den 2-3'e yükseltirken cihazla değerlendirmede genel olarak ciddi bir değişim göstermemiştir.

Turkuaz rengin yaş sürtme değerlerinde ise poliüretan bazlı fiksatör ve poliüretan/epiklorhidrin karışımının haslık değerini gözle yapılan değerlendirmede 4' ten 4-5' e yükselttiği görülmüştür ancak cihaz ile yapılan değerlendirmede herhangi bir değişim izlenememiştir. Diğer fiksatör ve karışımlarının sürtme haslık değerleri üzerine olumlu ya da olumsuz herhangi bir katkısı bulunmadığı tespit edilmiştir.

Siyah rengin yaş sürtme değerlerinde ise, poliüretan bazlı fiksatör ve poliüretan/epiklorhidrin karışımının haslık değerini hem göz hem de cihaz ile yapılan değerlendirmede 2-3'ten 4'e yükselttikleri görülmüştür. Diğer fiksatörler ve karışımların gözle yapılan değerlendirmede haslık değeri üzerinde olumlu ya da olumsuz bir etkisinin olmadığı, cihaz ile yapılan değerlendirme de ise, poliamid/uzun zincirli kuaternar poliamonyum ve poliamid/kısa zincirli kuaternar poliamonyum karışımlarının yaş sürtme değerini 2-3' ten 2' ye düşürdükleri görülmüştür.

SONRAKİ DÖNEM ÇALIŞMALARI

Fiksatör tür ve karışımlarının yünlü kumaşlara etkisinin incelenmesi ve farklı boyarmaddeler üzerindeki etkisi yine pamuklu kumaşlarda denenmesi kumaş renk haslıklarındaki gelişmelere katkısı olacaktır

TEŞEKKÜR/BILGILENDIRME/FON KAYNAĞI

Çalışmaların yapılması için firma alt yapısının kullanımına izin verdiği ve proje masraflarını karşıladığı için Rudolf Duraner Kimyevi Mad. Tic. A.Ş., Bursa/Türkiye firmasına teşekkür ederiz.

KAYNAKLAR

[1] Jamadhar, R., Daberao, A., Nadiger M., Chandrakar, K. 2017. "Effect of Dyeing of Cotton Fabric by Using Dye Fixing Agent", International Journal on Textile Engineering and Processes, 3 (1), 51-53.

[2] He, W., Xu, H., Hu, Z. 2002. "Synthesis and Application of Reactive Pre-polyurethane Resin Dye Fixing Agent", Dye Printing, (6), 6-9.

[3] Hu, Y., Guo, R., Jia, S.T. 2009. "Synthesis and Application of Waterbased Polyurethane Dye Fixing Agent", Polyurethane Industry, 24 (1), 26-29.

[4]https://tr.scribd.com/document/352385349/Dye-Fixing-Problems [08Kasım 2018].

[5] Mughal, J. M., Saeed, R., Naeem, M., Ahmed, A.M., Yasmien, A., Siddiqui, Q., Iqbal, M. 2013. "Dye Fixation and Decolourization of Vinyl Sulphone", Journal of Saudi Chemical Society, 14, 23-26,. doi:10.1016/j.jscs.2011.02.017.

[6] Yakartepe, M., Yakartepe, Z. 1995. "Tekstil Terbiye Teknolojisi Kasardan Apreye" İstanbul.

Örme Kumaşlarda Lif Türünün Isıl Konfora Etkisi

KERTMEN Mehmet[1], TANDOĞAN Gökhan[1], GÖRKEM Gamze Rabia[1]
[1]İskur Tekstil Enerji Ticaret ve Sanayi A.Ş., Kahramanmaraş, Türkiye
mehmet.kertmen@iskur.com

AMAÇLAR

Son yıllarda giysi konforu konusunun tüm dünyada önemi ve dolayısıyla müşteri beklentileri giderek artmaktadır. Giysilerde ısıl konforu etkileyen çeşitli parametreler söz konusudur ve bunların en önemlilerinden birisi elyaf cinsidir. Çalışmanın amacı, doğal ve sentetik esaslı farklı lif türlerinin (pamuk, viskon, modal, poliester, akrilik) giysilerin ısıl konfor özellikleri üzerindeki etkisini incelemektir. Elde edilen sonuçlar ışığında kullanım yerine ve amacına uygun olarak yüksek konforlu giysi tasarımları yapmak mümkün olacaktır.

GİRİŞ

Çevre ve insan arasındaki fizyolojik, psikolojik ve fiziksel etkileşimin memnuniyet derecesini gösteren konforun tekstil malzemelerinde incelenen en önemli parametesi ısıl konfordur[1].

İnsan vücudu, besin ve oksijen kullanarak mekaniksel ısı oluşturan termodinamik bir sistemdir. Isıl konfor hissinin devamı için vücut sıcaklığının dengede kalmasına olanak sağlanmalıdır[2]

Isıl konfor, tekstilde ısı ve nem geçirgenlik özelliklerinin tespit edilmesi ile belirlenmektedir. Isıl açıdan konforlu giysiler, farklı çevre şartları ve vücut aktivitelerine bağlı olarak, değişen sıcaklığı ve vücut nemini transfer ederek mikroklimadaki ısı ve nem dengesinin korunmasını sağlayan giysiler olarak tanımlanmaktadır[1-2-3-5]. Örneğin uzun süre aşırı soğuk veya sıcak hava şartlarında çalışan kişiler için vücut sıcaklığını korumak, bedenin nefes alabilmesini sağlamak, teri hızla dışarı atarak kuru kalabilmek hayati önem taşımaktadır7.

Önceki yapılan çalışmalarda, iplik numarası arttığında (inceldiğinde), büküm katsayısı arttığında, ilmek iplik uzunluğu arttığında, kumaş sıklığı azaldığında, ısıl direnç değerinin azaldığı; ayrıca kumaşta elastan kullanıığında, veya elastan oranı arttırıldığında ve iplik tüylülüğü (h) değerleri yükseldiğinde ise ısıl direnç değerinin arttığı belirtilmiştir.[2-3-4-5-6] Ayrıca yüksek ısıl direnç özelliği açısından interlok gibi çift katlı ve sık yapılı kumaşların daha avantajlı olduğu görülmektedir[3--6.] Pike yapısında kumaşlar ile %100 özel poliester ipliklerden üretilmiş yapıların daha yüksek hava geçirgenliği ve ısıl direnç sağladığı ve daha sıcak temas hissi verdiği ortaya konmuştur[4].

Bu çalışmada ise iplik ve kumaş performansını doğrudan etkileyen elyaf özelliklerinin ısıl konfor üzerindeki etkisi incelenmiştir. Bu doğrultuda, doğal ve sentetik esaslı tek tip veya karışım lifler kullanılarak üretilen ipliklerden örülmüş kumaşların ısıl konfor özellikleri karakterize edilmiştir. Kumaşların, ısıl direnç ve su buharı geçirgenliği gibi ısıl konfor özellikleri ölçülmüştür.

DENEYSEL

Malzeme

Tablo 1. Kullanılan lif özellikleri

Lif Tipleri	**Lif Tanımı**
Pamuk	3,7 mic.
Viskon	1,3 dtex, 40 mm
Poliester Kanallı	1,4 dtex, 38 mm
Poliester Coolmax	1,6 dtex, 38 mm
Poliester Thermolite	1,6 dtex, 38 mm
Modal	1,3 dtex, 40 mm
Bambu	1,33 dtex, 38mm

Yöntem

Bu çalışmada Tablo 1'de verilen farklı lif tipleri kullanılarak ring eğirme metodu ile tüm numuneler Ne 30 inceliğinde ve **(αe=3.6)** olacak şekilde iplik üretimi gerçekleşmiştir. Bu iplikler ile yuvarlak örme makinalarında süprem kumaş üretimleri yapılmıştır. Bu üretim adımlarının tamamı İskur Tekstil Enerji Ticaret ve Sanayi A. Ş. bünyesinde gerçekleştirilmiştir.

Süprem kumaşların örme işlemi E 28 inceliğinde ve 32" çaplı yuvarlak örme makinesinde sabit ayar değerleri ile üretilmiştir. Numuneler relaksasyon işlemleri için 24 saat boyunca standart atmosfer koşullarında bekletilmiştir. Isıl direnç ve Su Buharı

Geçirgenliği değerleri ISO 11092 standardına göre Permetest cihazında ölçülmüştür.

DENEYSEL SONUÇLAR/TARTIŞMA

Tablo 2. Gramaj, ısıl direnç ve su buharı geçirgenliği ölçüm sonuçları

Numune	*Gramaj (g/m2)*	*İlmek İplik Uzunluğu*	*Isıl Direnç (m2 K/W)*	*Su Buharı Geçirgenliği (%)*
%100 Cotton	*150*	*32*	*0,0104*	*63,79*
%100 Bamboo	*145*	*31*	*0,0075*	*68,51*
%100 Modal	*140*	*31*	*0,0074*	*68,36*
%100 Viscose	*145*	*31*	*0,0089*	*64,15*
%100 PES	*154*	*32*	*0,0110*	*54,97*
% 100 Kanallı PES	*155*	*32*	*0,0116*	*61,74*
% 100 Hallow PES	*144*	*32*	*0,0139*	*59,45*
%50 Cotton %50 Viscose	*140*	*31*	*0,0099*	*58,28*
%50 Cotton %50 Bamboo	*148*	*32*	*0,0084*	*61, 27*
%50 Cotton %50 Modal	*150*	*32*	*0,0089*	*65,08*
%50 Cotton %50 Polyester	*150*	*32*	*0,0124*	*54,97*
%13 Cotton %75 Polyester %12 Viscose	*150*	*32*	*0,0121*	*58,62*

GENEL SONUÇLAR

Bu çalışma sonunda lif seçiminin ısıl konfor üzerinde çeşitli etkileri olduğu gözlenmiştir.

- Hem rejenere selülöz lifleri ve hem de kanallı poliester lifleri ile örülen kumaşların su buharı geçirgenliği değerlerinin daha yüksek olduğu saptanmıştır.
- en yüksek ısıl direnç değerinin içi boşluklu polyester (hollow fiber) liflerinden örülen kumaşa ait olduğu görülmüştür. Bu liflerin içerisinde bulunan durgun hava ısıl direncin yüksek olmasını sağlamıştır.
- Rejenere selüloz (%100 viskon, %100 modal, %100 bambu) ile üretilen kumaşlar ile daha düşük termal direnç ölçülmüştür,
- Boşluklu poliester lifleri ile standart poliester liflerine göre daha yüksek termal direnç sağlanmıştır.
- Bu verilere dayanarak, ısıl konfor açısından kışlık kıyafetlerde boşluklu poliester ve % 100 pamuklu ya da pamuklu karışım kıyafetler önerilirken, yazlık kıyafetlerde rejenere selüloz ve karışımları ile kanallı poliester yapısı önerilmektedir.

KAYNAKLAR

[1] Aydın I S, Kertmen M., Marmaralı A., 2017 "Evaluating the effect of spinning systems on thermal comfort properties of modal fabrics" Journal of Biological and Chemical Research, ISSN 2319-3077, Vol.4, Issue 11, p265 – 27

[2] Ertekin, G., Oğlakcıoğlu, N., Marmaralı A., 2015 “Thermal Transmission Attributes of Knitted Structures Produced by Using Engineered Yarns” Journal of engineered fibers and fabrics. 72. 4-2015. 10.1177/155892501501000418.

[3] Gülsevin, N., 2005 Spor Giysilerin Konfor Özellikleri Üzerine Bir Araştırma, Yüksek Lisans Tezi, Ege Üniversitesi Fen Bilimleri Enstitüsü, İzmir

[4] Marmaralı A., Kadoğlu H., Oğlakcıoğlu N., Çelik P., Blaga M., Ursache M., Loghin C., 2009, “Thermal comfort properties of some new yarns generation knitted fabrics”, In: Proceedings of the AUTEX 2009 World Textile Conference, 26–28 May 2009.

[5] Marmaralı A., Özdil N., Dönmez S., 2006, "Giysilerde Isıl Konfor", Tekstil Teknik, No:9, 163-167.

[6] Oğlakçıoğlu N., Marmaralı A., 2010 “Rejenere Selüloz Liflerinin Kompresyon Çoraplarının Isıl Konfor Özelliklerine Etkisi”, Tekstil ve Mühendis, 17(77), 6-12.

[7] Üte Bedez T., Çelik P., Kadoğlu H., ,Üzümcü B., Ertekin G., Marmaralı A., 2018 , Farkli Doğal Liflerin İç Giysilerde Kullaniminin Konfor Özellikleri Açisindan Araştirilmasi, Tekstil ve Mühendis, Yıl 2018/4, Cilt : 2, Sayı: 112.

KARIŞIM KUMAŞLARDA PİLLİNG DEĞERLERİNİ İYİLEŞTİREN FONKSİYONEL POLİMERİN TASARIMI, SENTEZİ ve TEKSTİL UYGULAMALARI

BÜYÜKKORU, Burcu [1,2], KARA, Ali [1]
[1]*Fen Fakültesi, Kimya Bölümü, Uludağ Üniv., Bursa, Türkiye*
[2]*Rudolf-Duraner, Bursa, Türkiye*
burcub@rudolf-duraner.com.tr,akara@uludag.edu.tr

AMAÇLAR

Tekstil pazarında kullanılmak üzere kumaşların pilling değerlerini iyileştiren, karışım kumaşlarda da etkili, uygulandığı kumaşlardaki tuşeyi ve hidrofiliteyi arttıran fonksiyonel polimerin tasarlanması ve sentezlenmesi hedeflenmiştir. Sentezlenen polimerin tekstil uygulamalarında başarı sağlamasının ardından Rudolf-Duraner ürün gamında yer alması ve pazar beklentisini karşılayacak bir ürün olarak satışa sunulması amaçlanmıştır. Tekstil pazarında bu alanda eksikliğin olması sebebiyle projede geliştirilen fonksiyonel polimer ile yüksek satış rakamlarına ulaşılacağı öngörülmektedir.

GİRİŞ

Tekstil yardımcı kimyasalları üreten firmaların efekt bölümlerindeki başlıca çalışma konularından biri; pilling azaltıcı ürünler tasarlamak, üretmek ve satışını gerçekleştirmektir. Tekstil pazarında oldukça ilgi gören bu alana yönelik epey çalışma ve ürün vardır. Bu ürünler genellikle enzim ya da poliüretan içeren kimyasallardır. Ancak söz konusu kimyasallar, pazar beklentilerini yeterince karşılayamamaktadır. Bunun temel sebebi, bu kimyasalların karışım kumaşlarda istenilen pilling iyileştirme değerlerini sağlayamamasıdır. Karışım olmayan kumaşlarda etkili olup pilling değerlerini iyileştiren enzimlerin hem fiyatının pahalı kalması hem de istenilen yumuşaklık efektini kumaşlara kazandıramaması sebebiyle piyasada alternatif ürün arayışları devam etmektedir. Enzim içermeyen bazı kimyasallar literatürde ve pazarda mevcuttur. Bu kimyasallar genellikle poliüretanlardır. Pilling değerlerini iyileştirmeye katkı sağlayan bu alanda kullanılabilen poliüretanlar kimyası gereği kumaşlara sert bir tuşe vermektedir. Ayrıca enzimlerin ve poliüretanların kumaşa aplikasyonundan sonra kumaşların hidrofiliteleri de geriye gitmektedir. Bu sebeple, hem hidrofilitesi ve tuşesi iyi hem anti-pilling özelliği olan alternatif ürüne piyasada ihtiyaç duyulmaktadır.

Bu çalışma kapsamında, enzim veya poliüretan kullanmadan fonksiyonel bir polimer ile istenilen özellikleri kumaşlara kazandıran ürün piyasaya sunulacaktır.

Piyasadaki anti-pilling ürünleri fular ya da kaplama teknikleri ile kumaşa aplike edilmektedir. Projede geliştirilen fonksiyonel polimer de bu yöntemlere uygun olup fular ve kaplama aplikasyonları ile kumaşa uygulanabilecektir.

Yün, pamuk, viskoz gibi kopma ve aşınma dayanımı düşük olan liflerde boncuklar daha yüksek kopma mukavemeti, esneme mukavemeti ve aşınma direncine sahip sentetik liflere kıyasla sürtünme ile yüzeyi daha kolay terk ederler.

Hidrofil elyafa nazaran hidrofobik lifler elektrostatik özelliklerine bağlı olarak yabancı maddeleri çekmeye daha yatkındırlar. Kumaş yüzeyine tutunan liflere göre kopmuş ve karmaşıklaşmış lifler daha kısadırlar. Tutucu lifler en güçlü lifler iken kopmuş ve karmaşıklaşmış lifler en ince ve esnek liflerdir. Örme kumaşlar, dokuma kumaşlara göre daha fazla boncuklanma eğilimindedirler.

Kumaşın kötü görünmesinin yanı sıra, boncuklanma bazen delik oluşumuna kadar giderek giysilerin yıpranması nedeniyle kullanma süresinin kısalmasına neden olmaktadır.

Kumaşların pilling oluşumlarının tespit edilmesi için bir çok yöntem geliştirilmiştir. ISO 12945-2 standardı esas alınarak Martindale Pilling cihazının kullanımı çok yaygındır. Yöntemde 150 mm çapında kumaş numuneleri kullanılır. Lissajous hareketi ile test gerçekleştirilir. Bu harekette, üst numunelerin hareketi, dairesel hareketle başlayıp, yavaş yavaş daralan elips şeklinden doğrusal hale gelinceye kadar devam eden ve sonra da ters yönde genişleyen elips şeklindeki hareketle devam eder. Programlanmış hareket ve sabit basınç test sonuçlarına yüksek tekrarlanabilirlik güvencesi sağlamaktadır.

Kumaşların pilling değerlerinin notlandırılmasında iki çeşit yöntem vardır.
1. Yöntem: Standart ışık kabininde boncuklanma derecesini standart fotoğraflarla karşılaştırarak subjektif şekilde karar verilebilmektedir. Fotoğraflı standartlarla karşılaştırmada, EMPA tarafından geliştirilmiştir ve üç adet dokuma, üç adette örme kumaşlar için olmak üzere toplam altı kategoriye ayrılan fotoğraflar kullanılmaktadır. Her alt kategoride dört fotoğraf bulunmakta ve beş dereceli skala kullanılmaktadır.

Boncuklanma Derecesi ve Açıklaması;
5: Hiçbir değişiklik yok
4: Çok az miktarda tüy veya boncuk
3: Orta derecede tüylenme veya boncuk
2: Açıkça görülebilecek miktarda
1: Çok yoğun miktarda

2. Yöntem: Pillgrade ile değerlendirme;

Gözle değerlendirmek yerine otomatik okutma sisteminde kumaşlar birkaç defa okutularak ortalama bir değer alındığında daha kesin ve tekrarlanabilir sonuçlar elde edilebilir. Bu amaçla pilling değerlendirilmesinde diğer yöntem Pillgrade ile kumaşların notlandırılmasıdır. Pillgrade 3 boyutlu bir kumaş tarama sistemidir. Numune kumaşlardaki yüzey özelliklerini nesnel olarak değerlendirilmek üzere kullanılır. Sistem boncuklanma detaylarını tespitleyerek ISO standartlarına göre 1-5 arası değeri monitöre aktarır. Her kumaş türü ve kalınlığına uygun bir ölçüm cihazıdır.

Pillgrade boncuklanma değerlendirme test cihazı

Boncuklanmayı azaltmak için alınabilecek önlemler şöyle sıralanabilir;

- İplik ile ilgili önlemler: büküm katsayısını arttırmak, Kalın iplik kullanmak, karışım yerine %100 tek cins iplik kullanmak, daha az tüylü iplikleri tercih etmek, katlı iplik kullanmak,
- Örgü yapısı ile ilgili önlemler: Sıklığı arttırmak, çift katlı yapıları tercih etmek, kumaşın gramajını arttırmak.
- Çok kuvvetli temas kuvvetleri veya bağlantılarla liflerin birlikte çok sıkı bir şekilde tutulması sağlanarak oluşan boncuklanmaya karşı dirençli kumaşlar üretmek kolaydır. Ancak bu durum estetik ve konfor açıdan olumsuzluklara sebep olabilmektedir.

Kumaşlardaki pilling değerlerini azaltmak adına kullanılan en etkin yöntemlerden biri anti-pilling kimyasallarının kullanılmasıdır. Bu kimyasalların özellikleri, film oluşturucu, yüzeyi etkileyici, lifin kayma yeteneğini önlemesi, kullanımı ile pürüzsüz bir lif yüzeyi meydana getirmesi ve lif uçlarının saç tokası şeklinde bükülmelerini sağlamalarıdır.

DENEYSEL

Malzeme

Kumaş olarak piyasada pilling değerlerinin iyileştirilmesi en zor olan karışım kumaşlar tercih edilmiştir. Öncelikle, çalışmada 5 adet kumaş incelenmiştir. Boncuklanma değerleri özellikle kötü olan, derecesi 3 olarak adlandırılan 2 çeşit kumaş ile çalışılmıştır. Aşağıdaki tabloda bu kumaşlara ait veriler yer almaktadır.

Çalışılan kumaş	**Pilling değeri (İşlemsiz)**
Beyaz Pamuk	5
Beyaz Poliester/Pamuk	3
Beyaz Poliester	5
Beyaz Poliester/Viskon	3
Beyaz Viskon	4

Tablodan da görüleceği üzere pilling değeri 3 olarak notlandırılan 2 çeşit kumaş vardır. Beyaz renkte karışım kumaş olarak temin ettiğimiz bu kumaşları detaylı inceledik. Kullanılan kumaşlar, ışık mikroskop (markası: OLYMPUS, modeli: BX51) altında incelenerek CO, PES, CV lifleri belirgin şekilde tespit edilerek kumaş içerikleri detaylı bir şekilde analiz edilmiştir.

Kumaş tanımı	**Elyaf cinsi**
Beyaz Poliester/Pamuk	68 PES/ 32 CO
Beyaz Poliester/Viskon	45 PES/ 55 CV

Çalışmada kullanacağımız kumaşların mümkün olduğunca poliester ve viskon içermesi de bizim için önemliydi. İstediğimiz özelliklerde PES ve CV içeren kumaşlar ile tekstil uygulamaları gerçekleştirilmiştir.

Tasarlanan polimerin elde edilmesi için RD Mon 2 tedarik edilerek bu monomer, uygun başlatıcı ve çözücü kullanılarak serbest radikal polimerizasyonuna tabii tutulmuştur. Burada kullanılan kimyasalların neler olduğunu şirket gizliliği için burada paylaşamıyoruz. Özetle monomer, çözücü ve katalizör ile fonksiyonel polimer sentezlenmiştir.

Yöntem

Pilling azaltıcı etki sağlayacağı düşünülen polimer tasarlanarak sentezlenecektir. Polimer sentezinin başarı ile gerçekleştirilmesinin ardından tekstil uygulamaları için gereken miktarda polimer sentezlenerek ürün çoğaltılacaktır.

Polimerin çeşitli kumaşlarda fular aplikasyonu yapılacaktır. Fularda kullanılacak kimyasal çeşitli konsantrasyonlarda hazırlanarak optimum uygulama miktarı belirlenecektir. Aplikasyon sırasında kullanılacak fular makinasındaki basınç kumaşlarda %65 pick-up değeri elde edilecek şekilde ayarlanacaktır. Fular makinasından çıkan kumaşlar ram yardımıyla 130°C'de kurutulacak ve şartlandırma odasında bir gün bekletilecektir.

Hazırlanan kumaşlar pilling testine tabii tutulacaktır. Pilling değerinde olumlu sonuç alınan kumaşların tuşe ve hidrofiliteleri de değerlendirilecektir. Bu testlerden de başarı ile geçen kumaşlara optik beyazlık testi uygulanararak polimerin kumaşlarda sararmaya yol açıp açmadığı görülecektir.

Bütün bu çalışmalar piyasada mevcut olan muadil ürünlerle de gerçekleştirilerek sonuçlar kıyaslanacak ve geliştirilecek fonksiyonel polimerlerin etkisi net bir biçimde ortaya konmuş olacaktır.

Yapılan tüm testlerin ardından başarı sağlanırsa fonksiyonel polimer firmanın ürün gamında yer alarak satışa sunulacaktır. Her zaman aynı kalitede ürün elde etmek amacıyla polimerin kalite kontrol spektleri belirlenecektir. Ayrıca FT-IR, NMR, TGA, GPC analizleri yapılarak ürün karakterize edilecektir.

DENEYSEL SONUÇLAR/TARTIŞMA

Sentez: RD Mon 2 kullanılarak uygun başlatıcı ve çözücü ile serbest radikal polimerizasyonu ile polimer elde edildi. Polimere EPW 18042 kodu verilmiştir.

Stabilite testi: Polimerin sulu çözeltilerinin hazırlanarak ürün haline getirilmesinden sonra, oda koşullarında kavanoz içerisinde bekletilerek ayrışıp ayrışmadığı gözle takip edilmiştir, ürün stabildir.

pH değeri ölçümleri: Hedefimiz, nihai polimerin ürün haline geldikten sonra pH değerinin 5,0-5,5 civarında olması idi. Reçetelere asetik asit eklenerek pH ayarlanmıştı. pH metre ile yapılan kontroller ile ürünün pH değeri istenilen aralıkta çıkmıştır.

FTIR analizleri: Ar-Ge merkezimizde bulanan FTIR cihazı ile sentezlenen polimerin analizi yapılarak istenilen pikler cihazda görülmüştür.

Viskozite ölçümü: Polimerin sulu çözeltilerinin hazırlanarak ürün haline gelmesi aşamasında eklenen su miktarına bağlı olarak viskozite epey değişmektedir. Genel olarak ürünlerin viskozitesi 20-500 mPa·s arasındadır.

Gel permeation chromatography (GPC): Rudolf-Duraner Ar-Ge merkezindeki GPC cihazı ile polimerin analizleri gerçekleştirilerek istenilen piklerin elde edildiği görülmüştür.

Çevresel etkilere yönelik analiz çalışmalarında, Rudolf-Duraner Ar-Ge merkezi ürün güvenliği bölümü altında çalışan personelimizden destek alınarak bu çalışmalar yapılmıştır. Polimerlerin sentezinde kullanılan tüm kimyasallar kendilerine iletilmiş ve çevresel etkilere yönelik analiz çalışmaları sonuçları alınmıştır. Polimerin sentezi için kullanılacak kimyasalların ve elde edilen polimerin tekstil uygulamalarında kullanılmasında bir sakınca yoktur.

Polimerin sentezinden sonra 5, 20, 40 g/l konsantrasyonlarda EPW 18042 hazırlanarak kumaşlara fular aplikasyonu yapılmıştır. Bu kumaşlar, Martindale cihazı ile pilling testine tabii tutulmuştur. Elde edilen pilling değerleri aşağıdaki tablodaki gibidir.

Uygulanan	Kumaş	Sonuç	İşlemsiz
EPW 18042 (40 g/l)	PES/CO	4-5	3
EPW 18042 (20 g/l)	PES/CO	4	3
EPW 18042 (5 g/l)	PES/CO	3-4+	3

EPW 18042'nin PES/CO kumaşlara farklı miktarlarda fular aplikasyonu sonucu kumaşlardaki pilling değerleri

Uygulanan	Kumaş	Sonuç	İşlemsiz
EPW 18042 (40 g/l)	PES/CV	4	3
EPW 18042 (20 g/l)	PES/CV	3-4	3
EPW 18042 (5 g/l)	PES/CV	3	3

EPW 18042'nin PES/CV kumaşlara farklı miktarlarda fular aplikasyonu sonucu kumaşlardaki pilling değerleri

Tablodan da görüleceği gibi işlemsiz kumaşlara göre pilling değerlerinde olumlu iyileşme görülmüştür. PES/CO kumaşlarda elde edilen iyileşme daha fazladır. Ancak polimerin fular aplikasyonunda uygulama miktarı arttırıldığında PES/CV kumaşlarda da 1 birim artış sağlanmaktadır.

Optik beyazlık testi Bu dönemde çalıştığımız kumaşlardan iki tanesi beyaz renkte idi (beyaz poliester/pamuk, beyaz poliester/viskon). Bu kumaşlara uygulanan polimerlerin fular aplikasyonlarında ram makinasında 130 °C ile çalıştık ve hiç bir çalışmada kumaşlar sararmamıştır. Dolayısıyla, kumaşların bu polimerler ile aplike edildiğinde optik beyazlık açısından sıcaklıktan etkilenmediğini söyleyebiliriz.

Uygulanan	Beyaz PES/Pamuk Hidrofilite	Beyaz PES/Viskon Hidrofilite
İşlemsiz	20 - 30 sn.	3-4 sn.
EPW 18042 (40 g/l)	2 sn.	2 sn.
EPW 18042 (20 g/l)	2-3 sn.	2-3 sn.
EPW 18042 (5 g/l)	5-6 sn.	2-3 sn.

EPW 18042'nin 5, 20, 40 g/l fular aplikasyonu sonucu 2 çeşit kumaşta ***hidrofilite değerleri***

- **Hidrofilite:** İyileşmektedir. 5 g/l bile hidrofilitesi açısından iyi olup 20 g/l ve 40 g/l de alınan sonuçlar çok iyidir.

- **Tuşe:** İşlemsize göre iyileşmiştir. Miktar arttıkça tuşe daha yumuşak ve kaygan olmaktadır.

- **Yorum*:*** Pilling, hidrofilite ve tuşe açısından değerlendirildiğinde EPW 18042 ile alınan sonuçlar hedeflendiği gibidir.

GENEL SONUÇLAR

- Uygulama sonuçlarında başarı sağlanan fonksiyonel polimer sentezlenerek bu polimerin pilling azaltıcı etkisine patent başvurusunda bulunulmuştur (Başvuru numarası: 2019/03389, Başvuru tarihi: 06.03.2019).

- Bu proje ile UTIB (Uludağ Tekstil İhracatçı Birliği) kurumunun düzenlemiş olduğu Techxtile Start-up Challenge Proje Yarışması kapsamında ilk 3 proje arasına girerek proje ödülü kazanılmıştır.

- Patent başvusurunda bulunulan fonksiyonel polimer için üretim hazırlıkları başlamıştır. Ürün EPW 18042 kodu ile Rudolf-Duraner ürün gamında yer alarak satışa sunulacaktır.

- Kumaşa anti-pilling özelliği, yumuşak tuşe ve hidrofilite kazandıran, çeşitli karışım kumaşlarda etkili ürün elde edilerek tekstil pazarının beklentisine uygun ürün geliştirebilmiştir.

SONRAKİ DÖNEM ÇALIŞMALARI

Tekstil uygulamalarında başarılı olan anti-pilling ürünü piyasaya sunulacaktır. Bu anti-pilling ürünü kendi tasarladığımız ve sentezlediğimiz fonksiyonel polimerdir. EPW EPW 18042 kodu ile Rudolf-Duraner ürün gamında yer alacaktır. Bu polimerin sentezi için gerekli monomerin daha uygun fiyata alınabilmesi adına tedarikçi arayışı gerçekleştirilecektir. Monomer uygun fiyata bulunduktan sonra polimerin başlangıçta 600 kg üretimi gerçekleştirilecektir. Pazarda zaten bu konuda bir ürün beklentisi olduğundan hangi müşterilerde ürünün deneyeceğimiz belirlidir. Müşterilerin arasından seçim yapılarak 600 kg üretilen polimerin pilling uygulamları işletmelerde denenecektir. Başarılı sonuçların elde edilmesinden sonra ürünün performansı kanıtlanmış olacaktır. Ardından müşterilerde derinleşmeye giderek ürünün teksil pazarında yaygınlaştırılması hedeflenmektedir.

Ayrıca sentezlenen polimerin karakterizasyonlarında ek analizlere ihtiyaç duyulmaktadır. Bu açıdan lif-polimer termal özellikleri için TGA/DTA analizleri de gerçekleştirilecektir.

TEŞEKKÜR/BİLGİLENDİRME/FON KAYNAĞI

Bu çalışma Rudolf Duraner ve Uludağ Üniversitesi iş birliğinde yürüyen TÜBİTAK-TEYDEB projesidir. Bu iş birliğine katkı sağlayan TÜBİTAK'a desteklerinden dolayı teşekkür ederiz.

KAYNAKLAR

Aksoy, S.A., Genç, E. 2015. Functionalization of cotton fabrics by esterification cross-linking with 1,2,3,4-butanetetracarboxylic acid (btca), *Cellulose Chemistry And Technology*, 49 (5-6): 405-413.

Annis, P.A., 1996. "Pilling Evaluation of Laboratory Abraded, Laundered, and Worn Fabrics Using Image Analysis", *Book of papers International Conference and Exhibition American Association of Textile Chemists and Colorists*, 465-479.

Dalbaşı, E. S., Kayseri, G.Ö. 2015. Research About The Effect Of The Antipilling Treatments On Different Structured Cotton Knitted Fabrics. *Tekstil Ve Konfeksiyon*, 25: 54-60.

Furferi, R., Governi, L., Volpe, Y., 2012. "A novel method for ring spinning performance evaluation based on Computer Aided analysis of yarn geometry", *International Journal of Mechanics*, 6 (4), 212-221.

Kowalczyk, D., Brzezinski, S., Kaminska, I. 2015. Multifunctional bioactive and improving the performance durability nanocoatings for finishing PET/CO woven fabrics by the sol-gel Method. *Journal of Alloys and Compounds*, 649: 387-393.

Li L., Jia G., Zhou W., 2009. Effect of Yarn Properties on the Pilling of Cashmere Knitted Fabric. Fibres & Textiles in Eastern Europe, Vol. 17, No. 6 (77) pp. 76-79.

Lv, H.N., Chen, Z.J., Xue, Y., Cai, Z.S. 2010. Synthesis and application of waterborne polyurethane on the anti-pilling finishing of wool fabrics, Proceedings Of The 12th International Wool Research Conference (IWRC 2010), Shanghai, China.

Man, L. W., Raymand, 2009. Mechanisms of pilling formation and reduction by attrition methods, The Hong Kong Polytechnic University Institute of Textiles & Clothing.

Schidler, W.D., Houser, P.J., 2004. Chemical Finishing of Textiles, Wood Head Publishing, Cambridge, England, 129.

Ukponmwan, J.O., Mukhopadhyay, A., Chatterjee, K.N. 1998. Pilling, Textile Progress, *The Textile Institute*, 28: 1-57.

Wang, X.Y., Gong, R.H., Dong, Z., Porat, I. 2007. Abrasion resistance of thermally bonded 3D nonwoven fabrics. *Science Direct*, Wear, 262: 424–431.

Zilz, L., Rau, M., Budag, N., Scharf, M., Cavaco-Paulob, A., Andreausa, J. 2012. Nonionic surfactants and dispersants for biopolishing and stonewashing with Hypocrea jecorina cellulases. *Society of Dyers and Colourists, Color. Technol.*, 129: 49–54.

Zia, K.M., Zubera, M., Rizwana, A., Jamilb, T., Tabasuma, S., Shahidc, M. 2012. Modification of cellulosic fabric using polyvinyl alcohol. *Carbohydrate Polymers*, 87: 2063– 2067.

Mikroemülsiyon Yöntemi ile Limon Yağı İçeren Aromatik Mikrokapsül Üretimi ve Tekstil Uygulaması

KOPTUR TASAN, Perinur[1], YILDIRIM, Filiz[2], ELİBÜYÜK ARAS, Sultan, YUMRU, Şaban, ÇÖREKCİOĞLU, Mustafa, ALAY AKSOY, Sennur
[1,2,3,4,5]Ozanteks Tekstil, [6]Süleyman Demirel Üniversitesi Tekstil Mühendisliği Bölümü
perinur.koptur@ozanteks.com.tr

AMAÇLAR

Tekstil ürünlerine hoş koku, aroma terapi gibi özellikler kazandırmak amacıyla biyo uyumlu doğal içerikli maddelerin mikroemülsiyon yöntemi ile kapsüllenmesi ve tekstil ürünlerine aplikasyonu amaçlanmaktadır.

GİRİŞ

Günümüzde tüketiciler, tekstil ürünlerinden temel özelliklerinin yanında sağlık ve güzelliği koruması, yaşam kalitesini arttırması, doğal olması gibi ekstra fonksiyonlara da sahip olmasını, tüm bunları gerçekleştirirken, insana ve çevreye zarar vermemesini beklemektedir. Ayrıca küreselleşen dünya pazarında artan rekabet, tekstil sektörünü katma değeri yüksek fonksiyonel ürünlerin üretimine zorlamaktadır. Tekstil materyallerine fonksiyonellik lif üretiminde yapılabildiği gibi çoğunlukla da bitim işlemleri ile kazandırılmaktadır. Mikrokapsülasyon teknolojisi tekstillerin fonksiyonelleştirilmesinde kullanılan teknolojilerden birisidir. Mikrokapsülasyon teknolojisinden yararlanılarak farklı bileşenler ihtiva eden mikrokapsüllerin üretimi ve tekstil materyallerine aplikasyonu ile farklı fonksiyonel özelliklerde tekstillerin üretimi mümkündür.

Mikrokapsüller, boyutları 1 µm ile 1 mm arasında değişen, çekirdek ve duvar maddesinden oluşan partiküllerdir[1]. Farklı tür maddeler farklı pek çok amaç için mikrokapsüllenebilmektedir. Koku maddesinin mikrokapsüllenmesindeki amaç onu uygun olmayan çevre koşullarına karşı korumak, kontrollü ve yavaş salınımını sağlamaktır[2].Koku maddeleri uçucu özelliklerinden dolayı tekstil materyaline direkt olarak aplike edilememektedir. Bu maddeler ısı, nem ve diğer dış etkenler nedeniyle buharlaşarak uzaklaşmalarını önlemek, kokunun uzun süre kullanılması ve yavaş salınımı amacıyla polimerik duvar materyali içerisine kapsüllenmektedirler[1,3]. Aromatik mikrokapsül içeren tekstil ürünleri giysi, ev tekstilleri vb. ürünlerde aromaterapi özellikleri nedeniyle ilgi görmektedirler.

Bu çalışmada, aromatik mikrokapsüllerin üretimi ve kumaşa aplikasyonu çalışmaları gerçekleştirilmiştir. Mikrokapsül üretimi mikroemülsiyon yöntemi ile gerçekleştirilmiştir. Üretilen mikrokapsüllerin emdirme yöntemi ile pamuklu kumaşlara aplikasyonu sağlanmıştır. Kapsül oluşumu ve morfolojisini incelemek için mikrokapsüllerin optik mikroskop görüntüleri alınmıştır. Pamuk elyafına kapsüllerin tutunma özelliğini incelemek için mikrokapsülasyon aplikasyonu ve 5 yıkama sonrası kumaş SEM (Taramalı Elektron Mikroskobu) görüntüleri alınmıştır.

DENEYSEL

Malzeme

Çalışmalarda çekirdek malzeme olarak limon yağı, duvar yapısı için doğal polimer olan arap zamkı (Merck), emülsiyon oluşturmak için yüzey aktif madde olarak Triton X, çapraz bağlayıcı olarak gluteraldehit çözeltisi (%25) ve pH ayarlaması için sodyum karbonat kullanılmıştır. Mikrokapsüllerin tekstil ürününe aplikasyonunda %100 pamuklu dokuma kumaş ve binder olarak Crilotan 300 (Bozzetto Group) kullanılmıştır.

Yöntem

Mikrokapsül üretiminin ilk aşaması kapsüllenecek çekirdek maddenin su fazını oluşturan polimer çözeltisi için de emülsiyonlaştırılması sağlanmıştır. Bu amaçla arap zamkı çözeltisi içinde kapsüllenecek limon yağı, bir emülsiyonlaştırıcı (Triton X 100) varlığında yağ damlaları halinde dağıtılarak su içinde yağ emülsiyonu elde edilmiştir. Emülsiyon sistemi Oluşan çekirdek damlaları etrafına çözelti halindeki polimerin depozite edilebilmesi için $CaCl_2$ reaksiyon ortamına ilave edildi. Ardından, çözelti sıcaklığı 4°C'ye, pH da 8-9 aralığına ayarlanarak oluşan mikrokapsül duvar yapısının stabilitesini artırmak için polimer molekülleri arasındaki çapraz bağlanma reaksiyonlarının gerçekleştirecek gluteraldehit reaksiyon ortamına ilave edilmiştir. Reaksiyonun tamamlanmasından sonra mikrokapsül sulu çözeltisi kumaşlara uygulanmak üzere hazırlanmıştır.

Mikrokapsüllerin kumaşa bağlanması için 110^0C'de 2 d kurutma ve 120^0C'de 2 d fikse uygulaması yapılmıştır.

DENEYSEL SONUÇLAR/TARTIŞMA

Mikrokapsül oluşumunu gözlemlemek için oluşturulan emülsiyon çözeltisinden mikroskop altında görüntüler alınmıştır. Şekil 1'de mikrokapsüllerin optik mikroskop ile alınan görüntüleri verilmiştir. Görüntülerden küresel yapılı, tanecikli mikrokapsül yapısının oluşumu görülmektedir.


Şekil 1: Mikrokapsüllerin 100x büyütme oranında optik mikroskop görüntüsü.

Mikrokapsüllerin pamuklu kumaşa aplikasyonu sonrası kumaşlardan SEM görüntüsü alınmıştır. Şekil 2'de mikrokapsüllerin pamuk lifi üzerindeki görüntüleri verilmiştir. SEM görüntüsü incelendiğinde mikrokasüllerin küresel morfolojili oldukları, parçacık boyutlarının 10 µm'den daha küçük ve homojen boyut dağılımlarına sahip olduğu görülmektedir.

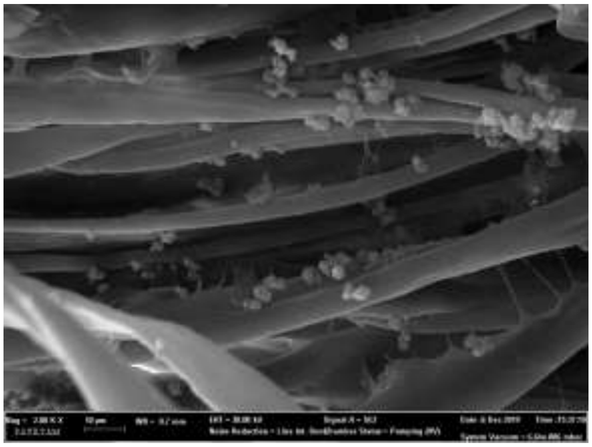
Şekil 2: Mikrokapsüllerin pamuklu kumaşa aplikasyonu sonrası SEM görüntüsü.

Kumaşlara mikrokapsül aplikasyonu sonrası sübjektif olarak koku varlığı belirlenmiştir. Ancak tekrar eden 5 yıkama sonrası kumaşlardaki koku miktarının azaldığı belirlenmiştir. Ayrıca, kumaşa mikrokapsül aplikasyonu sonrası ve yıkama sonrası alınan SEM görüntüleri incelendiğinde 5 yıkama sonrası mikrokapsüllerin büyük oranda kumaş yapısından uzaklaştığı belirlenmiştir (Şekil 3).

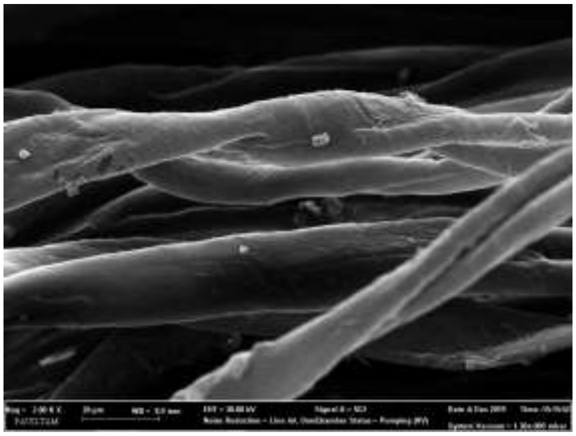
Şekil 3: 5 yıkama sonrası mikrokapsüllerin kumaş üzerindeki SEM görüntüleri.

SONRAKİ DÖNEM ÇALIŞMALARI

Bu çalışma mikroemülsiyon yöntemi ile doğal duvar yapılı aromatik mikrokapsüllerin ve tekstillerin üretimi üzerine odaklanılmış bir projeye ait çalışmaların bir bölümünü kapsamaktadır. Projede, mikrokapsüllerin koku salım davranışlarının incelenmesi, koku salma sürelerinin uzatılması için uygun mikrokapsül duvar yapısının geliştirilmesi, mikrokapsüllerin kumaş yapısında yıkama dayanımlarının arttırılması üzerine araştırmalara devam edilmektedir.

TEŞEKKÜR/BILGILENDIRME/FON KAYNAĞI

Bu çalışma, Ozanteks Tekstil Ar-Ge merkezi tarafından, TÜBİTAK 3190195 proje numarası ile desteklenmiştir.

KAYNAKLAR

[1] Rodrigues, S.N., Fernandes, I., Martins, I.M., Mata, V.G., Barreiro, F., Rodrigues, A. E. 2008. Microencapsulation of Limonene for Textile Application. Industrial & Engineering Chemistry Research, 47, 4142–4147.

[2] Aydın, N. Öztürk, G., Karaboyacı, M., Alay, S. 2011. Koku İçeren Mikrokapsül Uygulanmış Akrilik El Örgüsü İpliklerden Örülen Kumaşların Karakterizasyonu. Süleyman Demirel Üniversitesi Fen Bilimleri Enstitüsü Dergisi, 15-1,67-74.

[3] Kebapçı, K. 2012. Kokulu Mikrokapsüller. Süleyman Demirel Üniversitesi Fen Bilimleri Enstitüsü Yüksek Lisans Tezi Kimya Anabilim Dalı, Isparta.

[4] Li, S., Lewis, J. 2008. Effect of Finishing Methods on Washing Durability of Microencapsulated Aroma Finishing. Institute of Textile Technology, North Carolina State University, 99, 177-183.

[5] Ertürk, R., Çelik, C. 2010. Ticari Olarak Satılan Kekik ve Nane Uçucu Yağlarının Antimikrobiyal Aktiviteleri. Cumhuriyet Tıp Dergisi, 32, 281-286.
[6] Liakos, I., Rizzello, L. 2013. All-Natural Composite Wound Dressing Films of Essential Oils Encapsulated in Sodium Alginate with Antimicrobial Properties. International Journal of Pharmaceutics, 463, 137-145.
[7] Ghayempour, S., Mortazavi, S. M. 2014. Antibacterial Activity of Peppermint Fragrance Micro–Nanocapsules Prepared with a New Electrospraying Method. Journal of Essential Oil Research, 26, 492-498.

Investigation of Structural Changes after Texturizing of Acrylic Filament Yarn

MUTLU, Aras[1,2], DEMİR, Ali [1]
[1]Istanbul Technical University, [2] Aksa Akrilik Kimya Sanayi A.Ş.
mutluar@itu.edu.tr

PURPOSE

Consumption of textile fibers gradually increase by population growth, changing consumer behavior and widespread use of textile materials in different end uses. Filament yarns are becoming more and more popular in various applications of textile industry with a share of 50% among all textile fibers. Polyester, nylon, polypropylene which are the most common synthetic fibers are mostly used as filament yarn (73%). Unlike other synthetic fibers acrylic fiber is entirely used as staple fiber. Recently developed acrylic filament yarn with its higher tenacity, better abrasion resistance, excellent UV resistance, considerable resilience properties has potential to be used in a wide range of application such as awning, sewing thread, carpet industry, knitted products etc. However as-spun acrylic filament yarn is an undesirable product for some of aforementioned applications due to its shininess, harsh touch and lack of bulkiness. Texturizing is the method to impart textural features to synthetic fibers and since 1950s various texturizing methods has been developed for different purposes. As acrylic filament yarn has not been commercialized, there is no significant experience on texturizing with traditional methods. Purpose of this work is to investigate effects of texturizing process on structural properties of acrylic filament yarn and determine optimum process parameters to obtain appropriate properties.

INTRODUCTION

Synthetic filament yarns are texturized to create a bulky structure for better insulation, lightweight with good cover properties, more natural appearance and softer touch[1]. Although various texturizing methods have been developed since 1950s, false twist texturizing is the most common method especially in apparel market. This method is based on three major parameters: temperature, twist and tension[2]. Yildirim et al. commented that dye sorption and crimp properties of polyester yarns are effected by draw ratio and D/Y ratio whereas they do not have a significant influence on crystallinity[3]. Final yarn tenacity can also be adjusted by setting overfeed, D/Y ratio and first heater temperature[4]. On the other hand, it is found that first heater temperature also effects crystallinity of polyester and nylon 6.6 yarn[5,6]. It is also reported that crystal size of polyester yarn also increases by increasing temperature whereas increasing texturing speed results the opposite[7]. Cross sectional shape of polyester yarn has been observed and is mentioned that it significantly changes after texturizing process. It is also commented that disk type twisting unit results more yarn deformation compared to belt type twisting unit[8].

Air-jet texturizing is the method which is used to obtain yarns more similar to that made of staple fiber[1]. Acar and Wray studied parameters effecting air-jet texturized yarn properties and listed parameters as polymeric and physical properties of supply yarn, single filament denier, number of filaments, cross-sectional shape of the yarn, jet type, overfeed ratio, air pressure, take-up speed, processing conditions (wet/dry) and use of an impact element [9]. It is claimed that coarser filaments result lower tenacity and bulkiness in air-jet texturing process[10]. Overfeed ratio is the main process parameter which effects instability of texturized yarn and also wetting during texturizing plays an important role to improve quality of texturizing[11]. Tenacity of texturized yarn decreases by increasing air jet pressure as filaments are more disrupted[12].

Structure of acrylic fiber has not been fully revealed yet. Liu and Ruland suggested planar zigzag conformation of polyacrylonitrile chains and has not observed an evidence of two phase model in their studies[13]. On the other hand, it is also claimed that molecular structure of highly oriented acrylic fiber is consisted of amorphous and ordered regions with two times longer size that of amorphous regions[14]. One of most recent studies was carried out by Kunzmann et al. which state that acrylic fiber structure has two different types of fibrils. One type has smooth surface and homogenous volume structure whereas the other type was having shish-kebab structure[15].

X-ray diffractometry is a method to determine crystallinity of textile materials. Studies that investigate crystallinity of acrylic fibers state that crystalline peaks are observed at 2ϴ= 17° and 2ϴ=29°. Crystallinity of acrylic fibers is effected by process parameters and thermal treatment[16].

EXPERIMENTAL

Material

In this work, two different wet spun acrylic filament yarns were used. Yarn count was 600 dtex / 200f for air jet texturizing trials whereas it was 225 dtex / 100f for false-twist texturizing. Both types were raw white yarns.

Method

Air-jet texturizing trials are carried out at SSM DP5-TC texturizing machine and Barmag FK6 V-1000 was used for false-twist texturizing trials. Process parameters are shown at Table 1 and Table 2.

Table 1. Air-Jet Texturizing Process Parameters

Process Parameters	
Supply Yarn	600 dtex / f200 acrylic
Take-Up Speed (m/min)	300
Overfeed (core)	5%
Overfeed (effect)	-
Air Pressure (bar)	4
Jet Type	D32
Heater Temperature (°C)	170

Table 2. False-Twist Texturizing Process Parameters

Process Parameters	
Supply Yarn	225 dtex / f100 acrylic
Take-Up Speed (m/min)	350
Draw Ratio	1,10
Disk Type	Polyurethane
Heater Temperature (°C)	210

Cross sectional images were taken by Carl Zeiss Evo MA scanning electron microscope and X-ray diffraction patterns were generated and crystallinity is measured by Bruker D8 Discover. Minitab 17 is used for statistical analyses.

EXPERIMENTAL RESULTS AND DISCUSSIONS

Both air-jet texturizing and false-twist texturizing caused decrease in yarn tenacity. This can be considered as an indicator of deformation of filaments and change in macromolecular structure. Figure 1 and Figure 2 show comparison yarn tenacity variation of as-spun and texturized yarns. In each case p-value was 0.000 which shows tenacity significantly changes after texturizing process.

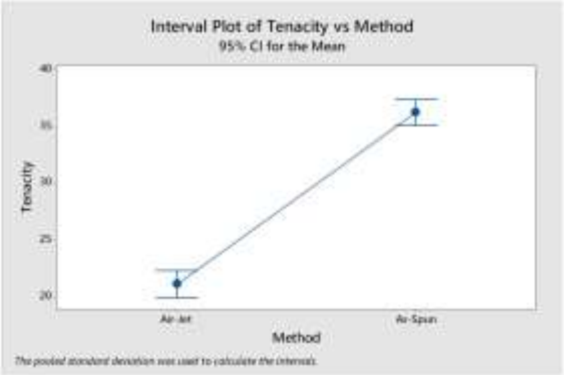

Figure 1. Comparison of the tenacity of as-spun and air texturized yarn

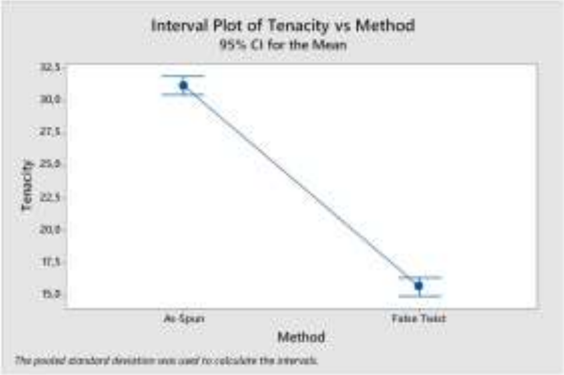

Figure 2. Comparison of the tenacity of as-spun and false twist texturized yarn

Figure 3 shows x-ray diffractograms of as-spun, airjet texturized and false twist texturized yarns. It can be seen that intensity of peaks at 2ϴ= 17° and 2ϴ=29° significantly decrease after both texturizing processes indicating reduction of crystallinity. As-spun yarn had a crystallinity of 71.8% whereas air-jet texturized yarn was having 60.8% and it was 60.4% with false twist texturized yarn. Crystallite size also decreased from 103.49 Å to 67.45 Å and 72.89 Å respectively.

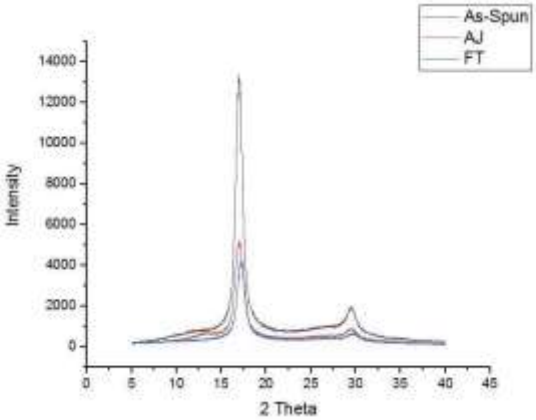

Figure 3. X-ray diffractograms of as-spun and texturized yarns

SEM images of texturized yarns are observed after fracture in order to understand structural defects after texturizing processes. Figure 4 shows that air-jet texturized yarn has been fractured almost homogenously along cross section. On the other hand, a layered fracture occurred with false-twist texturized yarn due to radial variation in shear stress level[17].

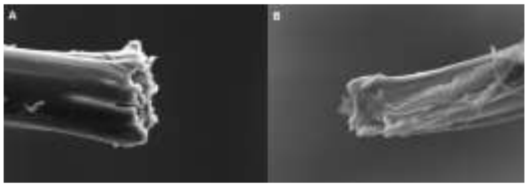

Figure 4. SEM images after fracture
(A) Air-jet texturized, (B) False twist texturized

CONCLUSIONS

Texturizing processes have an influence of structural changes of acrylic filament yarn. Crystalline size and orientation are disturbed by both methods and resulted decrease in yarn tenacity. Better yarn tenacity may be obtained by precisely created design of experiment and optimizing texturizing process parameters. Shininess and bulkiness of yarn has also improved after both texturizing techniques which may bring opportunities for particular end uses. Processability of yarns in further textile processes should also be taken into consideration. False-twist texturized yarn could be knitted and woven appropriately after it was intermingled to keep filament together. It was needed to impart twist to air-jet texturized yarn as shedding problem occurred during weaving. It should comparatively be studied with as-spun and texturized yarns to investigate effects of texturizing on fabric properties.

SUGGESTIONS FOR FURTHER WORK

Optimum process parameters for both air-jet and fakse-twist texturizing should be determined considering yarns properties and processability. Fabrics made of as-spun and texturized yarns should also be investigated in terms of strength, bulkiness, abrasion resistance etc.

LITERATURE

1. Lord, P. R. 2003. Handbook of Yarn Production. Cambridge: Woodhead Publishing
2. Hearle, J. W. S. 2001. Yarn Texturing Technology. Cambridge: Woodhead Publishing
3. Yildirim, K. et al. 2009. “Relationship between yarn properties and process parameters in false-twist textured yarn”, Journal of Engineered Fibers and Fabrics, 4(2), 26-32.
4. Azimi, B. 2013. “Prediction of False Twist Textured Yarn Properties by Artificial Neural Network Methodology”, Journal of Engineered Fibers and Fabrics, 8(3), 97-101.
5. Deilamani, M. T. et al. 2016. “Effect of major false-twist texturing parameters on tensile properties and crystallinity of polyester microfilament yarn and optimized by RSM”, Bulgarian Chemical Communications, 48, 55-64.
6. Savic, M. et al. 2016. “The influence of the variation of texturing process parameters on structural characteristics of polyamide textured yarns in the false twist”, Advanced Technologies, 5(2), 64-72.
7. Karakas, H. and Dayioglu, H. 2005. “Influence of false-twist texturing parameters on the structural properties of polyester yarns”, Indian Journal of Fibre & Textile Research, 30, 37-41.
8. Canoglu, S. 2009. “Effect of first heater temperature variations on the polyester yarn properties of false-twist texturing techniques”, Fibres & Textiles in Eastern Europe, 17(4), 35-39.
9. Acar,M. and Wray, G.R. 1986. “An analysis of the air-jet yarn texturing process part 7: the effects of processing parameters on yarn properties”, Journal of the Textile Institute, 77(6), 377,385.
10. Baldua, R.K. et al. 2015. “Effect of Feeder Yarn Paramters on Air-Jet Textured Yarn Properties”, Fibers and Polymers, 16(2), 463-470.
11. Demir, A. et al. 1986. “Air-Jet Textured Yarns: The effects of process process and supply yarn parameters on the properties of textured yarns”, Textile Research Journal, 318-328.
12. Rengasamy, R.S. et al. 2004. “Effect of Process Variables and Feeder Yarn Properties on the Properties of Core-and-Effect and Normal Air-Jet Textured Yarns”, Textile Research Journal, 74(3), 259-264.
13. Liu, X.D. and Ruland, W. 1993. “X-ray Studies on the Structure of Polyacrylonitrile Fibers”, Macromolecules, 26, 3030-3036.
14. Warner, S.B. et al. 1979. “Oxidative stabilization of acrylic fibers Part 3: Morphology of polyacrylonitrile”, Journal of Materials Science, 14, 1893-1900.
15. Kunzmann, C. 2018. “Microscopic investigation of polyacrylonitrile fiber fibrils separated by ultrasonic etching”, Journal of Materials Science, 53, 4693-4704.
16. Lee, S. et al. 2012. “Structural Evolution of Polyacrylonitrile Fibers in Stabilization and Carbonization”, Advances in Chemical Engineering and Science, 2, 275-282.
17. Miraftab, M. 2009. Fatigue Failure of Textile Fibres. Cambridge: Woodhead Publishing

PVA ve PVP ultra ince lif kaplı Yün/PVA kumaşlardan hidrojel kompozitlerin üretimi ve zamanla su kaybı tayini

BULGURCUOĞLU, Emre[1], BOSTANCI, Ayşe[1], KOÇ, Ümit[1], EREN, Recep[1,2] , AYKUT, Yakup[1,2]
[1]Bursa Uludag University, Engineering Faculty, Department of Textile Engineering, 16059, Gorukle, Nilufer, Bursa, Turkey
[2]Bursa Uludag University, Graduate School of Natural and Applied Sciences, Textile Engineering, 16059, Gorukle, Nilufer, Bursa, Turkey
aykut@uludag.edu.tr

AMAÇLAR

Çözgüsü yün, atkısı ise PVA ve yünden oluşan dokuma kumaş yapılarının üzerlerini elektro çekim metoduyla poli (vinil alkol) (PVA) ve poli (vinil pirolidon) (PVP) ultra ince lifler ile kaplayıp ardından sulu boraks çözeltisi ile muamele edilerek yapının farklı özelliklerde kumaş takviyeli hidrojel kompozit formuna dönüşmesini sağlamak ve kumaş yapıların PVA ve PVP ultra ince lif lerin kaplanması sonrası elde edilen hidrojel kompozitlerdeki suyun uzaklaşma hızına olan etkisini incelemektir.

GİRİŞ

Yapısı gereği bol hidroksil gruplarına sahip olan polivinil alkol (PVA) suda iyi çözünen bir polimerdir[1]. PVA, biyouyumluluk, işlenebilirlik, mukavemet, toksik olmayan yapısı sayesinde gıda ve ilaç endüstrilerinde de yaygın olarak kullanılan hidrofilik bir polimerdir[1,2]. Polivinil alkol (PVA) kimyasal çapraz bağlama[3], ışınlama[4] ve donma-çözülme tekniği [5] gibi çeşitli yöntemlerle çapraz bağlı hidrojeller oluşturabilen sentetik bir polimerdir. PVA hidrojelleri özellikle biyomedikal alanda kullanılmaktadır[5]. Polivinil pirolidon (PVP), suda çözünür polimerdir[6]. PVP aynı zamanda PVA polimeri gibi biyouyumlu olup toksik olmayan yapıya sahiptir [7]. Viskoziteyi arttırmak, fiziksel ve mekanik özellikleri değiştirmek için PVP çapraz bağlanabilir.

Uygun molekül ağırlığında polimerler kullanıldığında PVA[8] ve PVP[9] elektro çekim metoduyla nanolif formuna dönüştürülebilen polimerlerdir. Elektro çekim metoduyla yüzeyler nanoliflerle kaplanabilmektedir. Elektroçekim metodu da işleme dahil edilerek PVA[10] ve PVP[11] nanoliflerden hidrojeller üretilmiştir. PVA[12] ve PVP[13] çapraz bağlayıcılar ile hidrojel formuna dönüştürülebileceğinden, elektro çekim metoduyla istenen incelikte nanolif web yapısından oluşan ince filmler yüzeye kaplanabilmekte ve ardından çapraz bağlayıcılarla muamele edilerek ince film hidrojel yüzeylerlerin oluşumu sağlanabilmektedir.

Bu çalışmada, yün ve PVA ipliklerden üretilmiş kumaş yüzeyi PVA ve PVP ultra ince lifler ile ayrı ayrı elektro çekim metoduyla kaplanmış, ardından sulu boraks çözeltisi ile muamele edilerek yapıdaki PVA ve PVP'lerin çapraz bağlanmak suretiyle hdirojel matrisli kumaş takviyeli kompozit yapıların eldesi sağlamak ve nanolif kaplamanın bünyede tutulan suyun uzaklaşma süresine olan etkisi incelenecektir.

DENEYSEL

Materyal

Elektro çekim malzemeleri: Poli (vinil alkol) (PVA) toz formunda (MA~85.000-124.000, PVA) (%87-89 hidrolize edilmiş) Sigma Aldrich firmasından, poli (vinil pirolidon) (PVP) toz formunda (MA~1.300.000, PVP) Acros Organics firmasından satın alınmıştır. PVA distile suda, PVP ise etanolda çözdürülmüştür.

Kumaş malzemeleri ve özellikleri: Atkı iplikleri ile hem alt hem de üst yüzeylerden çözgüsünü sıkıca tutmak ve örtmek için 10 çözgü ve 30 atkıdan oluşan dokuma raporu hazırlanmıştır. PVA iplik numarası: Ne40/2, yün iplik numarası: Nm56/2. Bu kumaş yapısında çözgü yönünde yün ipliği, atkı yönünde ise 2PVA+ 1 hibrit (1PVA+1Yün) kullanılmıştır. Kumaşlar 400 mm genişliğinde bir örnek dokuma makinesinde dokunmuştur.

Yöntem

Elektro çekim metoduyla kumaşların ultra ince lif yüzeylerle kaplanması: Molekül ağırlığı 85.000-124.000 g/mol olan poli (vinil alkol) (PVA) polimeri %10 ağırlık oranında distile edilmiş suda çözünmüştür. Molekül ağırlığı 1.300.000 g/mol olan poli (vinil pirolidon) (PVP) polimeri içerisinde çözünmüştür (1 gr PVP/8ml etanol). Elektro çekim işlemi için boyutlarında 2,5*2,5 cm kesilen kumaşlar toplayıcı plakaya yerleştirilmiştir. Elektro çekim işlem parametreleri her iki solüsyon için de aynı olmak üzere akış oranı 1,5 mL/sa, şırınga ile toplayıcı plaka arası mesafe 10 cm, uygulanan voltaj 15 kV olarak belirlenmiştir.

Sulu Boraks Çözeltisinin hazırlanması: Ağırlıkça %1 lik boraks/su çözeltisi, 50ºC'de manyetik karıştırma işlemi ile hazırlanmıştır.

Hidrojel matrisli kumaş takviyeli kompozit yapının oluşturulması: Hidrojel matrisli kumaş takviyeli kompozit yapının oluşturulması aşamasında, PVA'nın çapraz bağlanmayla hidrojel oluşumu gerçekleştirilmiştir. Hazırlanan %1 boraks-su çözeltisi kumaşa dökülmüştür ve 24 saat bekletilmiştir. Yapı suda çözündükten sonra boraks gibi fonksiyonel moleküllerle çapraz bağlanıp suda çözünmeyen hidrojel yapılarına dönüşmektedir.

Su kaybı testi: Numunelerin ilk önce kuru ağırlıkları hassas terazide tartılmış ve "kuru ağırlık" olarak not edilmiştir. Aynı numuneye belli ve sabit oranlarda pipet yardımıyla saf su eklenir. Saf su eklendikten sonra ortalama 15 dakika beklenir. Bu beklemenin sebebi kumaşların bünyesine homojen bir şekilde alımını sağlamak içindir. 15 dakika sonunda hassas terazide tekrar ölçüm yapılmış ve "yaş ağırlık" olarak not edilmiştir. Yaş ağırlıktan kuru ağırlık çıkarılarak yapıdaki su miktarı tespit edilmiş ve ölçümlere devam edilerek yüzde su kaybı grafikleri çizilmiştir.

DENEYSEL SONUÇLAR/TARTIŞMA

PVA ve PVP ultra ince lif kaplı yün/PVA kumaş yapılarının optik mikroskop resimleri Şekil 1'de verilmiştir. Kumaş üzerindeki PVA ultra ince lif yüzeylerin arka taraftaki kumaşın deseni belirgin şekilde görülmektedir (Şekil 1A ve 1B). Diğer taraftan PVP ultra ince liflerle kaplı kumaş yüzeyinde PVP film formunda toplanmış olup kumaşın deseninin görünmesine engel olmuştur.

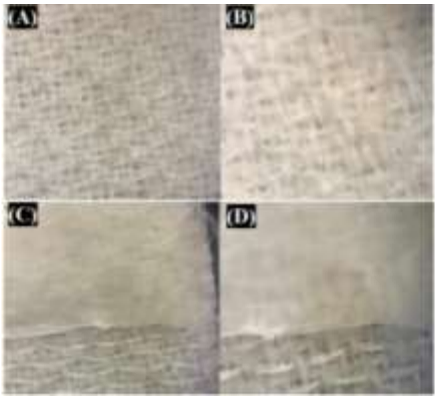

Şekil 1. (A, B) PVA ultra ince lif kaplı yün/PVA kumaş, ve (C, D) PVP ultra ince lif kaplı yün/PVA kumaşların optik mikroskop resimleri.

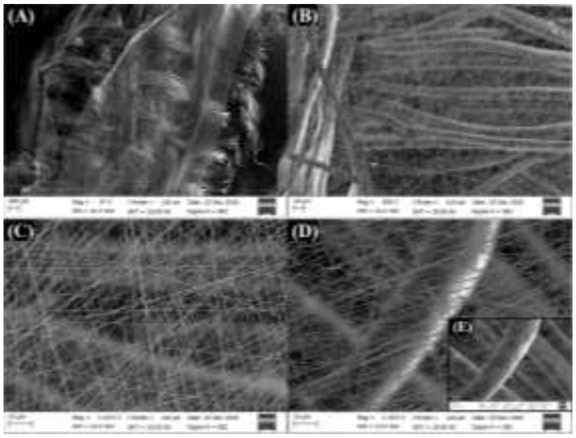

Şekil 2. PVA ultra ince lif kaplı yün/PVA kumaşların farklı büyütme oranlarındaki SEM resimleri.

PVA ve PVP ultra ince lif kaplı yün/PVA kumaş yapılarının SEM resimleri Şekil 2 ve Şekil 3'te verilmiştir. Kumaş üzeriende PVA ultra ince lif yüzey belirgin olarak Şekilde 2A'da görülmektedir. SEM görüntü derinliği arttırıldığında yüzeydeki ultra ince lif ler daha belirginleş altta kalan kumaş yapısındaki kalın lifler üzerindeki PVA ultra ince lifler net görülmektedir.

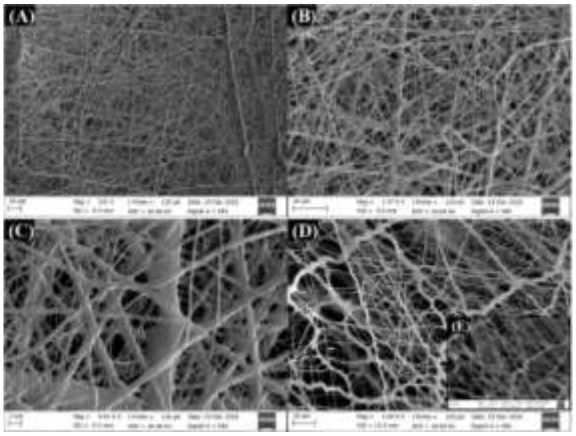

Şekil 3. PVP ultra ince lif kaplı yün/PVA kumaşların farklı büyütme oranlarındaki SEM resimleri.

Şekil 3'de ise kumaş yüzeyindeki PVP ultra ince lifler SEM ile incelenmiştir. PVA ultra ince lifler kumaş üzerinde toplandığında tam kurumamış olduğundan ultra ince lifler birbirine temas ettiği noktalarda birleşmiştir.

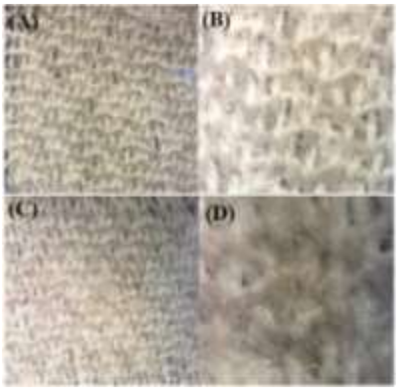

Şekil 4. Sulu boraks çözeltisi ile işlem görmüş: (A, B) PVA ultra ince lif kaplı yün/PVA kumaş, ve (C,D) PVP ultra ince lif kaplı yün kumaşların optik mikroskop resimleri.

Sulu boraks çözeltisi ile işlem görmüş PVA ve PVP ultra ince lif kaplı yün/PVA kumaşların optik mikroskop resimler Şekil 4'te verilmiştir. Yapıdaki PVA moleküllerinin jelleşmesi sonucu Şekil 1'de kumaştan jel matris içeririnde bulunan sadece yün ipliklerin kaldığı kumaş formuna dönmüştür.

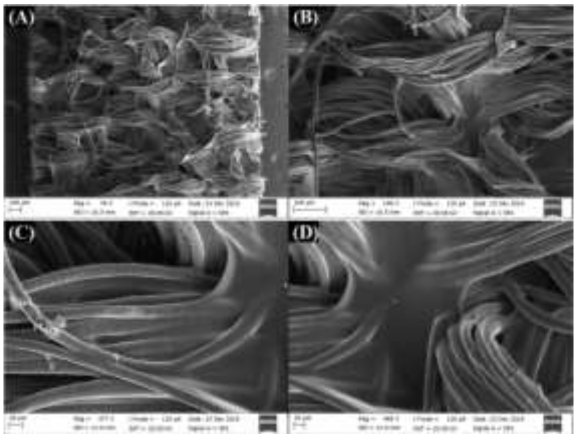

Şekil 5. Sulu boraks çözeltisi ile işlem görmüş PVA ultra ince lif kaplı yün/PVA kumaşların farklı büyütme oranlarındaki SEM resimleri.

Sulu boraks çözeltisi ile işlem görmüş PVA ultra ince lif kaplı yün/PVA kumaşların SEM resimler Şekil 5'te verilmiştir. Jel yapıların özellikle kumaş yapısındaki ipliklerin bağlantı noktalarında toplandığı gözlemlenmiştir. Yün liflerinin pulçuklu yüzey yapısı net bir şekilde görülmektedir.

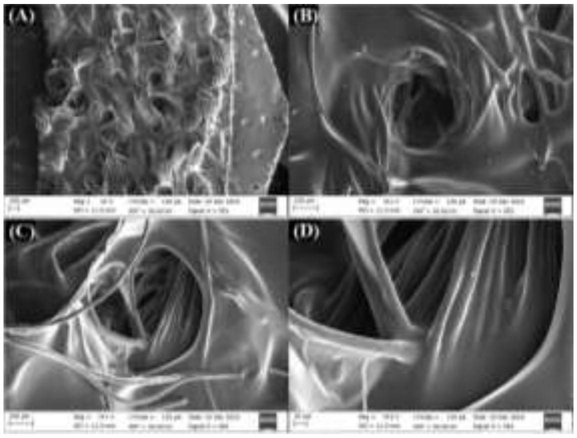

Şekil 6. Sulu boraks çözeltisi ile işlem görmüş PVP ultra ince lif kaplı yün/PVP kumaşların farklı büyütme oranlarındaki SEM resimleri.

Sulu boraks çözeltisi ile işlem görmüş PVP ultra ince lif kaplı yün/PVA kumaşların SEM resimler Şekil 6'da verilmiştir. Yün iplikleri ve liflerinin arasında jelleşen veya çözündükten sonra kuruyarak kalan PVA (kumaşın kendi yapısından gelen) ve PVP görülmektedir. Bu kısım Şekil 5'e kıyasla Şekil 6'da daha fazladır. Buda eğer çapraz bağlanma oranı fazla ise yapının daha fazla su almasında, eğer az ise yapının su ile temasında çözülerek yapıdan uzaklaşmasına sebep olacaktır.

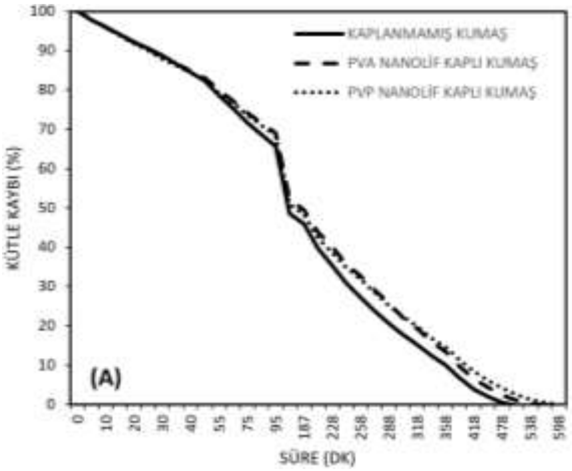

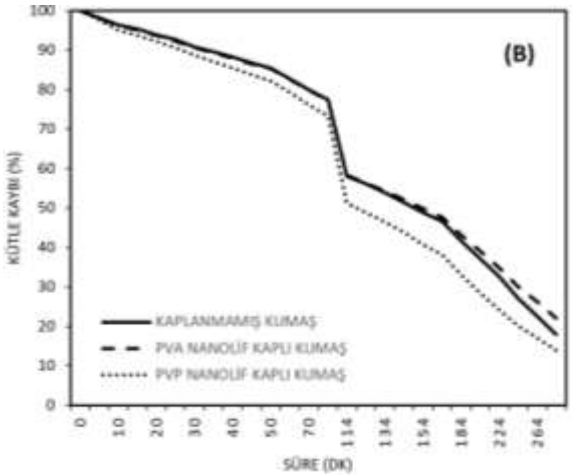

Şekil 7. PVA ve PVP ultra ince lif kaplı yün/PVA kumaşların sulu boraksla işleminden sonra zamana bağlı buharlaşarak yüzde su kaybetme oranı. (A) ilk tekrar, (B) ikinci tekrar.

Sulu borak çözeltisi ile muamele edilen kumaşlar kurumaya terkedilmiş, kumaşlar kurutulduktan su içerisinde 15 dk bekletilerek üzerlerine aldıkları su miktarı %100 kabul edilerek zamana bağlı laboratuvar ortamında buharlaşarak numuneden uzaklaşan su miktarı Şekil 7A'da verilmiştir. Aynı işlem kurutulan kumaşaların yine 15 dk. su içerisinde bekletildikten sonra ikinci tekrar olarak ölçüm yapılmıştır ve sonuçlar Şekil 7B verilmiştir.

Şekil 7A'da görüldüğü gibi tüm numunelerde başlangıçta hızlı olan suyun uzaklaşması zamanla yavaşlamıştır. Yine ilk tekrarda ilerleyen zamanlarda ölçülen bünyedeki su miktarı nanolif kaplı numunelerde sadece kumaştan elde edilen yapıya kıyasla daha fazladır.

Şekil 7B'de görüldüğü gibi ikinci tekrarda ise PVP ultra ince lif kaplı kumaşın boraksla işlemi ile elde edilen yapıdaki suyun buharlaşarak uzaklaşması diğer iki numuneye kıyasla bir miktar daha fazla olmuştur, buda başlangıçtaki PVP ultra ince liflerdeki moleküllerin tamamen çapraz bağlanmanın gerçekleşmediği ve su ile temasta bu moleküllerin bir kısmının uzaklaşmasından kaynaklanmış olabilmektedir.

GENEL SONUÇLAR

Yapısında çözgü yönünde yün atkı yönünde ise yün ve PVA bulunan ipliklerden oluşmuş dokuma kumaş yapılarının yüzeyleri PVA ve PVP ultra ince lifler elektro çekim işlemi ile kaplanmıştır. Hazırlanan numuneler sulu boraks çözeltisi ile muamele edilerek yapıdaki PVA ve PVP moleküllerinin çapraz bağlanması sağlanarak hidrojel matrisli ve kumaş takviyeli kompozit yapılar elde edilmiştir. Boraksla işlem öncesi ve sonrası yapılan mikroskobik incelemelerde PVA ve PVP lif yapılarının dönüşümü gözlemlenmiştir. İlk tekrarda ultra ince lif kaplı numunelerde suyun uzaklaşması bir miktar daha yavaş iken, PVP ultra ince lif kaplı kumaştan elde edilen yapıdan suyun uzaklaşması ikinci tekrarda diğer numunelere kıyasla daha hızlı gerçekleşmiştir.

SONRAKİ DÖNEM ÇALIŞMALARI

PVA ve PVP ultra ince lif kaplamanın boraksla işlemden sonra suyun uzaklaşması üzerine olan etkisini daha net gözlemleyebilmek için bir sonraki çalışmada kumaş yapısında sadece yün ipliklerin bulunduğu dokuma kumaşlar kullanılarak aynı ölçümler tekrar edilecektir. Aynı şekilde ultra ince lif kaplama miktarları farklılaştırılarak sonuçlar değerlendirilecektir.

TEŞEKKÜR/ FON KAYNAĞI

Bu çalışma Bursa Uludağ Üniversitesi (BUU) Bilimsel Araştırma Projeleri Birimi tarafından OUAP(MH)-2018/11 nolu proje ile desteklenmiştir. Çalışma Emre Bulgurcuoğlu'nun BUU Tekstil Mühendisliği Bölümü Bitirme Projesidir.

KAYNAKLAR

1. Marin, E., Rojas, J., Ciro, Y. 2014. "A review of polyvinyl alcohol derivatives: Promising materials for pharmaceutical and biomedical applications", African Journal of Pharm Pharmacol, 8(24), 674-684.
2. Bajpai, A. K., Saini, R. 2005. "Preparation and characterization of biocompatible spongy cryogels of poly(vinyl alcohol)-gelatin and study of water sorption behaviour", Polymer International, 54(9), 1233-1242.
3. Nuttelman, C. R., Mortisen, D. J., Henry S. M., Anseth K.S. 2001. "Attachment of fibronectin to poly(vinyl alcohol) hydrogels promotes NIH3T3 cell adhesion, proliferation, and migration", Journal of Biomedical Materials Research, 57(2), 217-223.
4. Schmedlen, R. H., Masters, K. S., West J. L. 2002. "Photocrosslinkable polyvinyl alcohol hydrogels that can be modified with cell adhesion peptides for use in tissue engineering", Biomaterials, 23(22), 4325-4332.
5. Hassan, C. M., Peppas, N. A. 2000. "Structure and applications of poly(vinyl alcohol) hydrogels produced by conventional crosslinking or by freezing/thawing methods", Advances in Polymer Science, 153, 37-65.
6. Zheng, M., Gu, M., Jin, Y., Jin, G. 2001. "Optical properties of silver-dispersed PVP thin film", Materials Research Bulletin, 36(5-6), 853-859.
7. Singh, B., Pal, L. 2011. "Radiation crosslinking polymerization of sterculia polysaccharide-PVA-

PVP for making hydrogel wound dressings", International Jornal of Biological Macromoleculs, 48(3):501-10.

8. Koski, A., Yim, K., Shivkumar, S. 2004. "Effect of molecular weight on fibrous PVA produced by electrospinning", Materials Letters, 58(3-4), 493-497.
9. Chuangchote, S., Sagawa, T. 2009. "Yoshikawa S. Electrospinning of poly(vinyl pyrrolidone): Effects of solvents on electrospinnability for the fabrication of poly(p-phenylene vinylene) and TiO2 nanofibers", Journal of Applied Polymer Science,. 114(5), 2777-2791.
10. Cay, A., Miraftab, M. 2013. "Properties of electrospun poly(vinyl alcohol) hydrogel nanofibers crosslinked with 1,2,3,4-butanetetracarboxylic acid", Journal of Applied Polymer Science, 129(6), 3140-3149.
11. Lubasova, D., Niu, H., Zhao, X., Lin, T. 2015. "Hydrogel properties of electrospun polyvinylpyrrolidone and polyvinylpyrrolidone/poly(acrylic acid) blend nanofibers", RSC Advances, **5**, 54481-54487.
12. Kumar, A., Han, S. S. 2017. "PVA-based hydrogels for tissue engineering: A review", *International Journal of Polymeric Materials and Polymeric Biomaterials*. 159-182.
13. Roy, N., Saha, N. 2012. "PVP-based hydrogels: Synthesis, properties and applications", In: Hydrogel synthesis, characterization, and applications, ed. F.V. Câmara, L.J. Ferreira, Nova Science, New York, 227–252.

Pamuk Lifindeki Hasar Seviyesinin FT-IR Cihazı Kullanarak Tespit Edilebilirliği

PARIN, Fatma Nur[1], ŞEN, İbrahim[2], YILDIRIM, Kenan[1]

[1]Bursa TeknikÜniversitesi, MDBF, LifvePolimerMühendisliğiBölümü, Bursa/Türkiye

[2]Bursa TeknikÜniversitesi, MerkeziAraştırmaLaboratuvarı, Bursa/Türkiye

kenan.yildirim@btu.edu.tr

AMAÇLAR

Bu çalışmanın amacı çevresel kirliliğe neden olan kimyasal madde kullanımı olmadan pamuk lifine verilen zararın kantitatif olarak Fourier transform infrared (FT-IR) ve Termogravimetrik (TGA) analizi ile tespit etmektir.

GİRİŞ

Pamuk elyafından üretilmiş tekstil materyalleri kullanım konfor ve estetiği açısından daha elverişli olmasına yönelik olarak terbiye ve boyama işlemine maruz bırakılır. Bu işlemler kimyasal maddeler eşliğinde yapılan uygulamalar olup, ekseriyetle bazik ortamda işlem görmesine rağmen asidik ortamda işleme de maruz kalabilmektedir. Özellikle kumaş bileşeninde pamuk+asidik ortamda terbiye ve boya işlemine tabi tutulan elyaf olması durumunda pamuk lifi asitle temas edebilmektedir. Pamuk lifinin moleküler yapısı oksijen köprüleri üzerinden selüloz makromoleküllerini oluşturan β glikoz monomeri olup, inert bir yapısı yoktur. Bu nedenle asidik ve alkali ortamda hidroliz ve oksidasyon reaksiyonları verebilmektedir [1,2]. Bu reaksiyonlar sonucu selüloz makromoleküllerinde zincir kopuşları, glikoz halkasının açılması veya her ikisi birden oluşabilmektedir. Pamuk lifinin doğal olması ve moleküler yapıtaşının glikoz olması nedeniyle mikroorganizmalar tarafından da bozunma riski olan bir elyaf çeşididir. Her iki bozunma durumunda da lif yapısındaki değişim benzerdir. Bu reaksiyonlar sonucu pamuk lifinin özelliği değişmektedir. Zincir kopması pamuk lifinin mukavemetini düşürürken, halkanın açılması lifin reaksiyon özelliğini değiştirmektedir. Mukavemet ürünlerin kullanım ömrünü belirleyen bir parametredir. Bu parametrenin kontrol altında tutulması gerekmektedir. Mukavemet kaybına ise hidroliz olan selüloz makromolekül ağırlığındaki azalma (polimerizasyon derecesinin düşmesi) neden olmaktadır. Terbiye ve boyam işleminde pamuk lifinin ne seviyede hasar görmüş olduğunun bilinmesi bu nedenle önemli bir durumdur. Halihazırda bir çok metotla pamuğa verilen hasar seviyesi sübjektif metotlarla yapılmaktadır [3].

Pamuk elyafının, pamuk elyafından üretilmiş hem iplik hem de kumaş halindeki ürünlerin hasar görüp görmediğinin, kimyasal hasar var ise hasar derecesinin tespiti hem üretim sonrasında hem de bekleme sonrasında önemli bir durumdur. Pamuk lifi gördüğü işlemlerde hasar göreceği gibi bekleme şartlarının uygun olmaması durumunda da hasar görmektedir. Pamuk veya pamuklu mamul alım satımlarından önce, pamuklu ürünlerin her bir terbiye işleminden önce ve sonra pamuk elyafının hasar görüp görmediğinin, hasar var ise seviyesinin ne olduğunun bilinmesi nihai ürünün kalitesi açısından önemli ve zorunlu bir durumdur [4,5].

DENEYSEL

Malzeme

Ham pamuk, H_2O_2, sodium sülfat, NaOH, yüzey aktif malzeme, H_2SO_4, distile su.

Yöntem

500 mL distile su içerisine stokiyometrik oranda H_2O_2, sodyum sülfat, NaOH, yüzey aktif malzeme konarak homojen bir karışım hazırlanır. Bu karışım pH 11-12 olacak şekilde 40-50°C sıcaklıkta tutulur ve ardından ham pamuk bu karışım içine daldırılır ve sıvının pamuğun her tarafına tamamen girmesi sağlanarak hidrofilikleşmesi işlemi gerçekleşmiştir. Hem ham pamuk hem de hidrofilik muamele görmüş pamuk 3,10,30 ve 60 dk zaman aralıklarında belli sıcaklık altında seyreltik H_2SO_4 çözeltisi içine batırılır ve hemen ardından nötralizasyonu için derişik NaOH çözeltisinde 30 dk bekletilir.

Tablo 1. Numunelerin işlem süreci.

Numune kodu	Işlem süreci
H1	hidrofilleştirilmiş
H3	Hidrofilleştirilmiş ve 3 dk asitle muamele edilmiş
H10	Hidrofilleştirilmiş ve 10 dk asitle muamele edilmiş
H30	Hidrofilleştirilmiş ve 30 dk asitle muamele edilmiş
H60	Hidrofilleştirilmiş ve 60 dk asitle muamele edilmiş
P1	Ham pamuk
P3	3 dk asitle muamele edilmiş
P10	10 dk asitle muamele edilmiş
P30	30 dk asitle muamele edilmiş
P60	60 dk asitle muamele edilmiş

DENEYSEL SONUÇLAR/TARTIŞMA

Tüm numunelerin FTIR spektrumları (Şekil 1 ve Şekil 2) incelendiğinde selülozun karakteristik pikleri olduğu açıkça görülmektedir. 3333cm^{-1}'deki yayvan pik selülozun yapısındaki ve su moleküllerinden kaynaklanan -OH grubu ile alakalıdır [6]. 2920 ve 2850 cm^{-1} selülozun yapısındaki -CH_2 grubunun gerilim titreşiminden kaynaklanmaktadır. 1162, 1103, 1051, 1030 ve 999 cm^{-1}'deki pikler ise selülozun yapısındaki C-O-C grubunun gerilim titreşiminden kaynaklanmaktadır [6-8]. 878 cm^{-1}'de ham pamukta pik olmaz iken, hidrofil hale getirilen pamuk numunesinde pik oluştuğu ve pik şiddetinin asitle muamele derecesine bağlı olarak arttığı görülmüştür. Hidrofilleşen pamuk numunelerinde görülen 878 cm^{-1}'deki bu pik $(CO_3)^{-2}$'tan kaynaklanmaktadır [9]. Asitle muamele işleminde pamuk lifi yüzeyinde radikal grupların oluştuğu spektrumdaki baseline düşüşünden görülmektedir. Asitle muamele görmüş pamuk liflerinin OH grubu pik oluşumundan sonraki baselinede genel bir düşme olduğu görülmektedir. Bunun ise lifte oluşan radikallerden kaynaklandığı düşünülmektedir. 1103 cm^{-1}'deki pik sadece asitle işlem görmeyen hidrofilik hale gelmiş pamuk numunesinde bulunmaktadır. H1, H3 ve H10 numunelerinde pik yükseklikleri sıralamaya göre azalmaktadır ve H30 ve H60 numunelerinde bu pik kaybolmuştur. 1103 cm^{-1}'deki pik selüloz makromolekülündeki monomerler arası köprü olan C-O-C yapıyla ilgili olduğundan bozunma oksiselülozdan ziyade hidroselülоz olarak oluştuğu ve zincir kopması reaksiyonu olduğu görülmektedir [10,11]. Asitle muamele sonrasında 1425 cm^{-1}'de pik oluştuğu bununda yapıya bağlanan SO_x grubundan kaynaklandığı düşünülmektedir. SO_x bu pikin SO_x grubuna ait olduğuna TGA thermogramında %50 kütle kalıntısı kalmasında ilave bir delil teşkil etmektedir. SO_x grubundan dolayı pamuk lifleri yanmazlık özelliği kazandığından bozunma yeterli seviyede olamamıştır.

Tablo 2. Numunelerin ısıl olayı.

kod	1.l Isıl olay	2.l Isıl olay	3.l Isıl olay	% Kül
P1	215°C'de, %7.39 kütle kaybı, su çıkışı	488°C'de, %71 kütle kaybı, piroliz	709°C'de, %19.6 kütle kaybı, bozunma	0.008
P10	275°C'de, %38.68 kütle kaybı, bozunma	-	-	52.88
P60	194°C'de, %9.44 kütle kaybı, su çıkışı	536°C'de %48.23 kütle kaybı, piroliz	686°C'de %14.86 kütle kaybı, bozunma	26.12
H1	178°C'de %7.20 Kütle kaybı, su çıkışı	496°C'de %68 kütle kaybı, piroliz	703°C'de %19.22 kütle kaybı, bozunma	3.77
H10	341°C'de %39 kütle kaybı, bozunma	-	-	59.85
H60	279°C'de %45.38 kütle kaybı, bozunma	-	-	54.82

Bilindiği gibi SO_x grupları malzemelere güç tutuşurluk özelliği kazandırmaktadır. 878 cm^{-1}'deki pik yükseklikleri Tablo 3'teki gibi hesaplanmıştır. Asitle hasar görmemiş P1 numunesi haricinde tüm numunelerde bu pike rastlanmaktadır. Söz konusu pik yükseklik değerleri pamuk lifinin görüdüğü hasara bağlı olarak artmakta olup, hasar miktarı ile pik yüksekliği arasında bir ilişki olduğu görülmüştür. buna ilave olarak 1103 cm^{-1} deki pik yüksekliği ise pamuk lifinin gördüğü hasara bağlı olarak düştüğü görülmüştür. pik yüksekliğindeki düşüş yine hasar miktarı ile orantılı olduğu görülmüştür. tüm asitler SO_x grubu içermediğinden hasar için bu pikin bir anlamı yoktur. Ancak hem 1103cm^{-1} hem de 878 cm^{-1} deki piklerdeki değişim ile pamuk hasar miktarı korelasyonu yapılabileceği görülmüştür. Hem hidrofilleştirilmiş hem de ham pamuğun %100 ağırlık kaybettiği ve organik yapının tamamen bozunduğu görülmüştür (TGA thermogramı) ancak sülfürik asitle muamele gören pamuk liflerinin %50 kütle kaybına uğradığı, yapıya bağlanmış olan SO_x gruplarının organik yapıyı oksijenli ortamda 800ºC sıcaklıkta yanmasını engellediği görülmüştür.

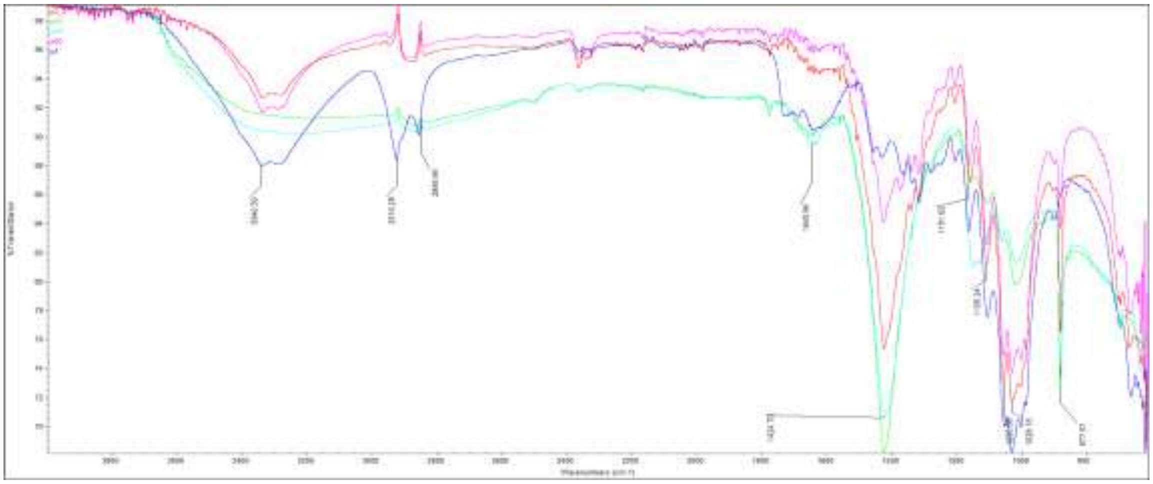

Şekil 1. Asitle işlem görmüş ham pamuk liflerinin FTIR spektrumları.

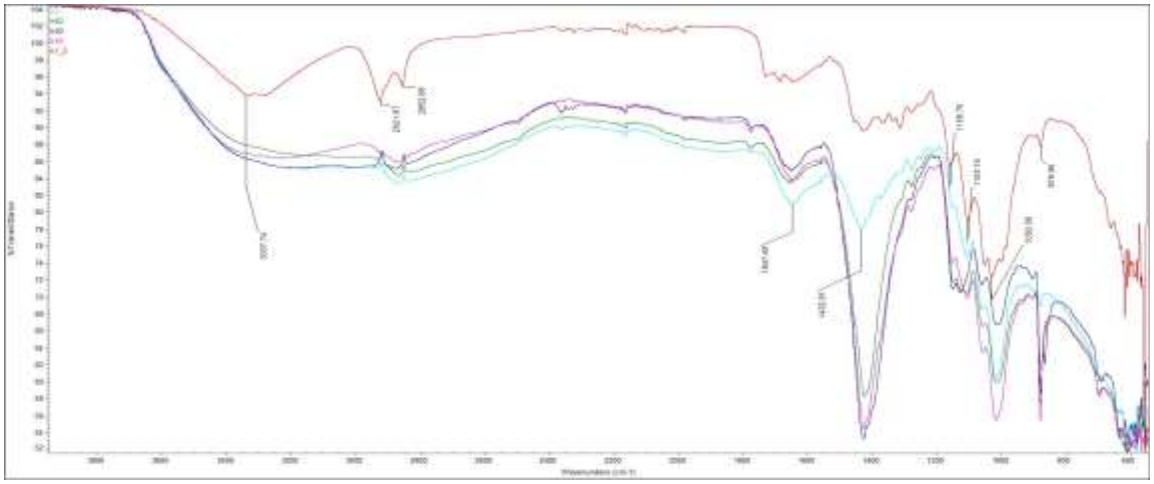

Şekil 2. Asitle işlem görmüş hidrofilleşen pamuk liflerinin FTIR spektrumları.

Hasar görmüş pamuk liflerinde bozunma şeklinde bir tane ısıl olaya olurken, normal pamuk liflerinde su çıkışı, 1. Isıl olay, organik yapının azot ortamında pirolizi, 2. Isıl olay, oksijenli ortamda piroliz olan kısmın bozunması 3.ısıl olay şekilde 3 farklı ısıl olayın olduğu görülmüştür.

Tablo 3. Numunelerin verilen dalga boyundaki kantitatif değerleri.

Numune kodu	**Frekans (cm^{-1})**	**Pik yüksekliği**
H1	1103	4.67
H3		4.42
H10		3.64
H30		-
H60		-
P1	878	-
P3		9.98
P10		28.09
P30		23.69
P60		5.12

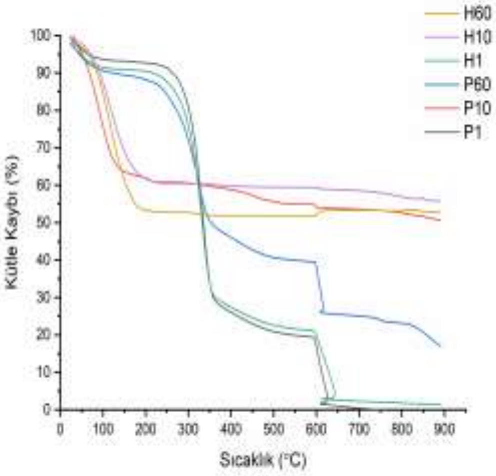

Şekil 3. Pamuk liflerinin TGA termogramı.

GENEL SONUÇLAR

Pamukta oluşan hasar miktarı FT-IR analizi ile tespit edilmektedir. 1103 cm^{-1} ve 878 cm^{-1} deki piklerden bu hasar açıkça görülmektedir. Aynı zamanda asitle hasar sonucunda pamuk liflerine tutunan SO_x yapıya bağlanmıştır ve yanmazlık özellik kazanabilmektedir.

SONRAKİ DÖNEM ÇALIŞMALARI

Pamuk lifindeki hasar miktarının FTIR ile tespitine yönelik metot geliştirilmesi ve pik yüksekliği ile hasar seviyesinin optimizasyounun yapılarak yeni bir analiz metodunun literature kavuşturulması çalışması düşünülmektedir.

TEŞEKKÜR/BİLGİLENDİRME/FON KAYNAĞI

Ham pamuğun temin edilmesine katkı sağlayan Nazilli Pamuk Araştırma Enstitüsü'ne teşekkür ederiz.

KAYNAKLAR

[1] Harris, M. 1954. Handbook of Textile Fibers, Interscience Publishers, p. 226-253.

[2] Garner, W. 1966. Textile Laboratory Manual, Vol.1, Qualitative methods, Heywood Boks, American Elsevier, 3rd edition.

[3] Fan, Q. 2008. Fabric Chemical Testing in Fabric Testing (ed. J. Hu), Wood Head Publishing, p.143.

[4] Gordon S. and Hsieh, Y.L. 2007. Cotton Science and technology, Wood Head Publishing, p.6.

[5] Laurence A. 2003. ‘’Dupont, Cellulose in lithiumchloride/N;N-dimethylacetamide, optimisation of a dissolution method using paper substrates and stability of the solutions’’, Polymer, 44, 4117–4126.

[6] Manasoğlu, G., Kanık, M., Yıldırım, K. 2019. ‘’Effect of fixation conditions on yellowing behavior of cellulose powder–coated fabrics’’, JEFF, 14, 1-14.

[7] Matheus, P., Heitor, L.O.J., Ademir, J.Z. 2014. ‘’Native cellulose: structure, characterization and thermal properties’’, Materials, 7, 6105–6119.

[8]Jiangtao, S., Dong, X., Jian, L. 2012. ‘’FTIR studies of the changes in wood chemistry from wood forming tissue under inclined treatment’’, Energ Proc 16, 758–762.

[9] Andersen, F.A., Brecevic, L. 1991. ‘’Infrared Spectra of Amorphous and Crystalline Calcium Carbonate’’, Acta Chemica, 45,1018-1024.

[10] United States Patent Application Publication, Pub. No.: US 2014/0225051 A1, Naskar et al. Pub. Date: Aug. 14, 2014.

[11] Yıldırım, K. 2013. ’’Polimerik malzeme Karekterizasyonunda İleri Metotlar’’ Ders Notu.

Microwave energy-based approach for carbonization and characterization of conducting polymers covered by simultaneously grown carbon nanotubes and metal oxide nanowires

POYRAZ, Selçuk[1]
[1]Department of Textile Engineering, Faculty of Engineering, Adıyaman University, 02040, Adıyaman/TURKEY
spoyraz@adiyaman.edu.tr

PURPOSE

Carbonized conducting polymer, e.g. polypyrrole (PPy), nanostructures (nCCPs) with simultaneously grown carbon nanotube (CNT) and metal oxide nanowire (MONW) coverage on their surface were manufactured, with a great potential as a building material for advanced engineering applications such as energy storage, via a microwave (MW) energy-based approach.

INTRODUCTION

As a result of their uniquely blended morphological, spectroscopic and electrochemical features, nanostructured hybrid materials (nHMs), which contain different types of active species with relevant functional groups, have attracted intense research interest of numerous research institutes from a wide variety of science fields and industry.[1-15] Since its discovery at the beginning of 1990's,[16] CNTs, in either their single or multi-walled forms, have been significantly investigated as one of the most common building block materials in affordable and high performance value added nHM production for sensory,[3,4,8,17] energy storage,[6,10,13-15,18-27] and magnetic resonance imaging (MRI)[28] applications due to their extraordinary thermal, electrical, mechanical and electrochemical properties. Nanostructured metals[15] or MOs[7,10] made up of Fe_2O_3,[14,28-30] Fe_3O_4,[2] ZnO,[6] MnO_2,[3,8,31] and TiO_2[1,14] have been commonly utilized, by means of filling[6] or attaching via spontaneous self-assembly,[5] along with CNTs in order to both enhance and diversify their above mentioned inherent properties and to optimize their use in nHM production.[26] As one of the most well-known and well-studied members of CP family, owing to its advantageous properties such as facile and low-cost synthesis at ambient conditions with high yield, relatively high electrical conductivity, long-term environmental stability, and high electrochemical performance, PPy is chosen as the active host material to prepare the targeted nHM together with the simultaneously grown CNT and Fe_2O_3 NW guest materials on its carbonized surface via MW energy-based approach.[1,2,6,7,12,13,22,32-40] Thus, the targeted nHMs' preparation in 3D composite form, via MW energy-based approach along with the utilization of nCCP as the host and the simultaneously grown CNTs and MONWs as the "surface decoration" guest, would result in combination of both the advantageous nanostructured material design and unique electrochemical properties of all the individual components in one structure.[1,3-15,26,29,31,41,42] With that, in current study, a well-established, in-situ polymerization/coating method and a simple and straightforward ex-situ MW energy-based carbonization approach, i.e. PopTube, are systematically combined to prepare the targeted novel nHM composites.

EXPERIMENTAL

Material

Following chemicals and reagents, including ammonium peroxydisulfate (APS, $(NH_4)_2S_2O_8$, 98% min.), ferrocene (99%), acetone, and pyrrole (98%), were all purchased from Alfa Aesar and used for the synthesis reactions. Iron pentacarbonyl ($Fe(CO)_5$, 99.5% and 99%-Fe) was purchased from Strem Chemicals and used for MW energy-based nHM preparation.

Method

In order to obtain the targeted nHM samples; 50 mg of PPy/ferrocene powder was placed in a glass vial and soaked with 0.1 mL of $Fe(CO)_5$ until its surface became completely wet. After the partial evaporation of the liquid phase, the damp sample was placed into a standard kitchen MW oven (Panasonic Inverter, NN-SN936B) chamber for the quick heating process as shown in Figure 1.

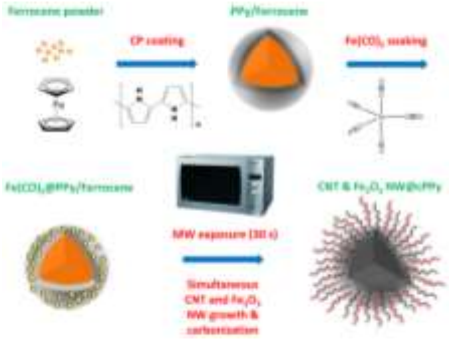

Figure 1. Schematic illustration of the combined nHM synthesis approach.

RESULTS AND DISCUSSION

Based on the measurements taken from these SEM images, couple of microns long CNTs with ~200 nm average diameters (Figure 2A and 2A'), and noodle-like MONWs with more than 10 µm in length and ~500 nm in average diameters (within 300-700 nm distribution range) were densely grown on the relevant nHM sample's surface (Figure 2B and 2B').

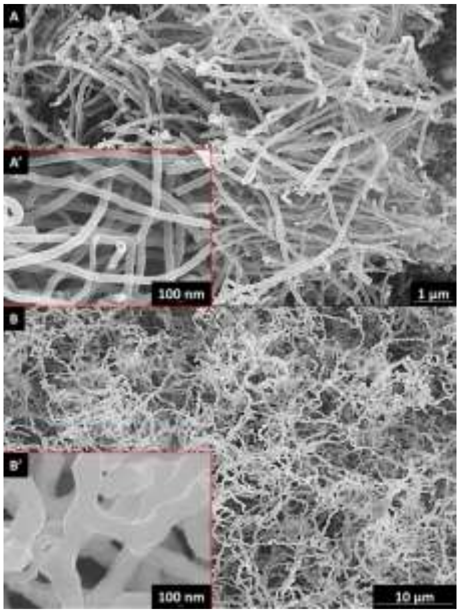

Figure 2. SEM images of the simultaneously grown; (A, A') CNTs, and (B, B') MONWs on nHM sample.

These results are in good agreement with the ones from the previous literature,[6,8,12,28,43-50] and thus, the as-obtained nHM's previously mentioned potential use in electrochemical energy storage-related applications becomes highly expected along with its carbonized ultra-high surface area that is homogenously decorated with the as-grown CNTs and MONWs.

Last but not the least; the as-prepared nanostructured materials' potential energy storage application performances were evaluated via CV in a comparative manner and the relevant results are shown in Figure 3.

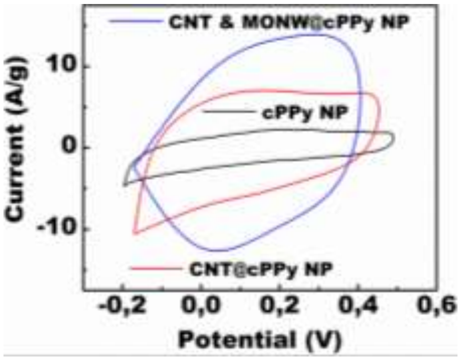

Figure 3. CV voltammograms of; (black line) cPPy NP, (red line) CNT@cPPy NP, and (blue line) CNT&MONW@cPPy NP samples.

The analyzed nanostructured samples' voltammograms exhibit dominant EDLC-based electrochemical characteristics, since majority of the samples were carbonized and/or contain high amount of C in their structures. In terms of shape and symmetry, cPPy NP and CNT@cPPy NP sample electrodes' voltammograms exhibit ideal capacitive property with quasi-rectangular characteristic and no obvious redox peaks, but in terms of size, i.e. current density, approximately two folds of difference can be observed between them. Here, the reason can be attributed to the high abundance of CNTs, which significantly contributes the above mentioned interface formation through their effective contact area with the electrolyte.[50] Expectedly, CNT & MONW@cPPy NP sample exhibits a two times larger voltammogram compared to that of CNT@cPPy NP sample. Here, the intra-/inter-tube pores on and among the CNTs enable both facilitated electron diffusion and rapid ion transfer between the electrolyte and MONW surface. This can be considered as a major proof of a similar electrochemical characteristic with much higher capacitive performance difference between these samples.

CONCLUSION

Well-organized experimental procedures, i.e. in-situ polymerization/coating of nCP on a metallocene precursor material, and the ex-situ MW energy-assisted PopTube, were systematically combined to develop nHMs, e.g. simultaneously grown CNTs and MONWs decorated nCCPs, with a promising potential for electrochemical energy storage applications. Throughout this study, the effective mechanisms involved in nHM production were also revealed as a route to optimize its potential application performance. Thus, along with these accomplishments it is envisaged that the as-prepared nHMs would soon become a material of preference and would be effectively used for various advanced applications such as electrochemical energy storage, MRI imaging, water treatment and so on.

REFERENCES

Çelik, E. J. 1986. “Crystallinity of PET fibers”, Textile Research Journal, 104, 269-274.

1. de Oliveira H. P. 2015. “Synthesis and dielectric characterization of multiwalled carbon nanotubes/polypyrrole/titanium dioxide composites”, Fullerenes Nanotubes Carbon Nanostructures, 23 (4), 339-345.

2. Ghashghaei, E., Kheirjou, S., Asgari, S, Kazerooni, H. 2018. “Nanostructured ternary composites of PPy/CNT/NiFe2O4 and PPy/CNT/CoFe2O4: Delineating and improving microwave absorption”, Comptes Rendus Chimie, 21 (9), 862-871.

3. Hou, Y., Cheng, Y. W., Hobson, T., Liu, J. 2010. “Design and synthesis of hierarchical MnO2 nanospheres/carbon nanotubes/conducting polymer ternary composite for high performance electrochemical electrodes”, Nano Letters, 10 (7), 2727-2733.

4. Hu, Y., Guo, C. 2011. Carbon Nanotubes - Growth and Applications. Rijeca, CROATIA: INTECH.

5. Li, J., Tang, S. B., Lu, L., Zeng, H. C. 2007. “Preparation of nanocomposites of metals, metal oxides, and carbon nanotubes via self-assembly”, Journal of the American Chemical Society, 129 (30), 9401-9409.

6. Liu, Y., Zhang, X. Y., Poyraz, S., Zhang, C., Xin, J. H. 2018. “One-step synthesis of multifunctional zinc-iron-oxide hybrid carbon nanowires by chemical fusion for supercapacitors and interfacial water marbles”, ChemNanoMat, 4 (6), 546-556.

7. Lokhande, V. C., Lokhande, A. C., Lokhande, C. D., Kim, J. H., Ji, T. 2016. “Supercapacitive composite metal oxide electrodes formed with carbon, metal oxides and conducting polymers”, Journal of Alloys and Compounds, 682, 381-403.

8. Luo, Y., Wang, K., Luo, S., Zhao, F., Wu, H., Jiang, K., Li, Q., Fan, S., Wang, J. 2018. “Three-dimensional carbon nanotube/transition-metal oxide sponges as composite electrodes with enhanced electrochemical performance”, ACS Applied Nano Materials, 1, 2997-3005.

9. Mao, X. W., Simeon, F., Achilleos, D. S., Rutledge, G. C., Hatton, T. A. 2013. “Metallocene/carbon hybrids prepared by a solution process for supercapacitor applications”, Journal of Materials Chemistry A, 1 (42), 13120-13127.

10. Mazloumi, M., Shadmehr, S., Rangom, Y., Nazar, L. F., Tang, X. W. 2013. “Fabrication of three-dimensional carbon nanotube and metal oxide hybrid mesoporous architectures”, ACS Nano, 7 (5), 4281-4288.

11. Motshekga, S. C., Pillai, S. K., Ray, S. S., Jalama, K., Krause, R. W. M. 2012. “Recent trends in the microwave-assisted synthesis of metal oxide nanoparticles supported on carbon nanotubes and their applications”, Journal of Nanomaterials, 691503, 1-15.

12. Poyraz, S., Cook, J., Liu, Z., Zhang, L., Nautiyal, A., Hohmann, B., Klamt, S., Zhang, X. Y. 2018. “Microwave energy-based manufacturing of hollow carbon nanospheres decorated with carbon nanotubes or metal oxide nanowires”, Journal of Materials Science, 53 (17), 12178-12189.

13. Xiong, P., Zhu, J. W., Wang, X. 2015. “Recent advances on multi-component hybrid nanostructures for electrochemical capacitors”, Journal of Power Sources, 294, 31-50.

14. Zheng, W., Zhang, P. G., Chen, J., Tian, W. B., Zhang, Y. M., Sun, Z. M. 2019. “Microwave-assisted synthesis of three-dimensional MXene derived metal oxide/carbon nanotube/iron hybrids for enhanced lithium-ions storage”, Journal of Electroanalytical Chemistry, 835, 205-211.

15. Zheng, W., Zhang, P. G., Yang, L., Chen, J., Tian, W. B., Zhang, Y. M., Sun, Z. M. 2018. “A fast approach to the synthesis of MO/CNT/Fe hybrid nanostructures built on MXene for enhanced Li-ion uptake”, Ceramics International, 44 (18), 22456-22461.

16. Iijima, S. 1991. “Helical microtubules of graphitic carbon”, Nature, 354 (6348), 56-58.

17. Lota, G., Fic, K., Frackowiak, E. 2011. “Carbon nanotubes and their composites in electrochemical applications”, Energy and Environmental Science, 4 (5), 1592-1605.

18. Bose, S., Kuila, T., Mishra, A. K., Rajasekar, R., Kim, N. H., Lee, J. H. 2012. “Carbon-based nanostructured materials and their composites as supercapacitor electrodes”, Journal of Materials Chemistry, 22 (3), 767-784.

19. Chen, C., Fan, Y. Q., Gu, J. H., Wu, L. M., Passerini, S., Mai, L. Q. 2018. “One-dimensional nanomaterials for energy storage”, Journal of Physics D: Applied Physics, 51 (11).

20. De Adhikari, A., Oraon, R., Tiwari, S. K., Saren, P., Maity, C. K., Lee, J. H., Kim, N. H., Nayak, G. C. 2018. “Zn-doped SnO2 nano-urchin-enriched 3D carbonaceous framework for supercapacitor application”, New Journal of Chemistry, 42 (2), 955-963.

21. Jiang, L. B., Yuan, X. Z., Liang, J., Zhang, J., Wang, H., Zeng, G. M. 2016. “Nanostructured core-shell electrode materials for electrochemical capacitors”, Journal of Power Sources, 331, 408-425.

22. Meng, Q. F., Cai, K. F., Chen, Y. X., Chen, L. D. 2017. “Research progress on conducting polymer

based supercapacitor electrode materials", Nano Energy, 36, 268-285.

23. Syarif, N., Ivandini, T. A., Wibowo, W. 2012. "Direct synthesis carbon/metal oxide composites for electrochemical capacitors electrode", International Transaction Journal of Engineering, Management, & Applied Sciences & Technologies, 3 (1), 21-34.

24. Wang, X. M., Wang, W. W., Zhu, Z. H., Yan, C., Zhang, Q. T. 2017. "Metal oxide-embedded porous carbon nanoparticles as high-performance anode materials for lithium ion batteries", Ionics, 23 (12), 3255-3263.

25. Xia, C., Chen, W., Wang, X. B., Hedhili, M. N., Wei, N. N., Alshareef, H. N. 2015. "Highly stable supercapacitors with conducting polymer core-shell electrodes for energy storage applications". Advanced Energy Materials, 5 (8), 1401805-1401813.

26. Yu, G., Xie, X., Pan, L., Bao, Z., Cui, Y. 2012. "Hybrid nanostructured materials for high-performance electrochemical capacitors", Nano Energy, 2, 213-234.

27. Zhang, L. L., Zhao, X. S. 2009. "Carbon-based materials as supercapacitor electrodes", Chemical Society Reviews, 38 (9), 2520-2531.

28. Xie, H., Poyraz, S., Thu, M., Liu, Y., Snyder, E. Y., Smith, J. W., Zhang, X. Y. 2014. "Microwave-assisted fabrication of carbon nanotubes decorated polymeric nano-medical platforms for simultaneous drug delivery and magnetic resonance imaging", RSC Advances, 4 (11), 5649-5652.

29. Zhao, Y., Li, J. X., Wu, C. X., Guan, L. H. 2011. "A general strategy for synthesis of metal oxide nanoparticles attached on carbon nanomaterials", Nanoscale Research Letters, 6, 71-75.

30. Zhang, G. D., Shi, Y. H., Wang, H. R., Jiang, L. L., Yu, X. D., Jing, S. Y., Xing, S. X., Tsiakaras, P. 2019. "A facile route to achieve ultrafine Fe2O3 nanorods anchored on graphene oxide for application in lithium-ion battery", Journal of Power Sources, 416, 118-124.

31. Yan, J., Fan, Z. J., Wei, T., Cheng, J., Shao, B., Wang, K., Song, L. P., Zhang, M. L. 2009. "Carbon nanotube/MnO2 composites synthesized by microwave-assisted method for supercapacitors with high power and energy densities", Journal of Power Sources, 194 (2), 1202-1207.

32. Liu, Z., Zhang, L., Poyraz, S., Smith, J., Kushvaha, V. Tippur, H., Zhang, X. Y. 2014. "An ultrafast microwave approach towards multicomponent and multi-dimensional nanomaterials", RSC Advances, 4 (18), 9308-9313.

33. Fong, K. D., Wang, T. S., Smoukov, S. K. 2017. "Multidimensional performance optimization of conducting polymer-based supercapacitor electrodes", Sustainable Energy Fuels, 1 (9), 1857-1874.

34. Liu, Z., Liu, Y., Poyraz, S., Zhang, X. Y. 2011. "Green-nano approach to nanostructured polypyrrole", Chemical Communications, 47 (15), 4421-4423.

35. Liu, Z., Zhang, X. Y., Poyraz, S., Surwade, S. P., Manohar S. K. 2010. "Oxidative template for conducting polymer nanoclips", Journal of the American Chemical Society, 132 (38), 13158-13159.

36. Lu, X. F., Zhang, W. J., Wang, C., Wen, T. C., Wei, Y. 2011. "One-dimensional conducting polymer nanocomposites: Synthesis, properties and applications", Progress in Polymer Science, 36 (5), 671-712.

37. Poyraz, S., Flogel, M., Liu, Z., Zhang, X. Y. 2017. "Microwave energy assisted carbonization of nanostructured conducting polymers for their potential use in energy storage applications", Pure and Applied Chemistry, 89 (1), 173-182.

38. Raza, W., Ali, F. Z., Raza, N., Luo, Y. W., Kim, K. H., Yang, J. H., Kumar, S., Mehmood, A., Kwon, E. E. 2018. "Recent advancements in supercapacitor technology", Nano Energy, 52, 441-473.

39. Reddy, K. R., Sin, B. C., Ryu, K. S., Kim, J. C., Chung, H., Lee, Y. 2009. "Conducting polymer functionalized multi-walled carbon nanotubes with noble metal nanoparticles: Synthesis, morphological characteristics and electrical properties", Synthetic Metals, 159 (7-8), 595-603.

40. Zhang, L., Du, W. Y., Nautiyal, A., Liu, Z., Zhang, X. Y. 2018. "Recent progress on nanostructured conducting polymers and composites: synthesis, application and future aspects", Science China Materials, 61 (3), 303-352.

41. Lakshmi, A., Gracelin, D. L., Vigneshwari, M., Karpagavinayagam, P., Veeraputhiran, V. C. V. 2015. "Microwave synthesis and characterization of multiwalled carbon nanotubes (MWCNT) and metal oxide doped MWCNT", Journal of Nanoscience and Technology, 1, 19-22.

42. Lin, Y., Baggett, D. W., Kim, J. W., Siochi, E. J., Connell, J. W. 2011. "Instantaneous formation of metal and metal oxide nanoparticles on carbon nanotubes and graphene via solvent-free microwave heating", ACS Applied Materials and Interfaces, 3 (5), 1652-1664.

43. Liu, Y., Guo, N., Yin, P., Zhang, C. 2019. "Facile growth of carbon nanotubes by microwave ovens: The emerging application of the highly efficient domestic plasma reactors", Nanoscale Advances, 1, 4546-4559.

44. Liu, Z., Wang, J. L., Kushvaha, V., Poyraz, S., Tippur, H., Park, S., Kim, M., Liu, Y., Bar, J., Chen, H., Zhang. X. Y. 2011. "Poptube approach for ultrafast carbon nanotube growth", Chemical Communications, 47 (35), 9912-9914.

45. Liu, Z., Zhang, L., Poyraz, S., Smith, J., Kushvaha, V., Tippur, H., Zhang, X. Y. 2014. "An ultrafast microwave approach towards multicomponent and multi-dimensional nanomaterials", RSC Advances, 4 (18), 9308-9313.

46. Poyraz, S., Liu, Z., Liu, Y., Zhang, X. Y. 2013. "Devulcanization of scrap ground tire rubber and successive carbon nanotube growth by microwave irradiation", Current Organic Chemistry, 17 (20), 2243-2248.

47. Schwenke, A. M., Hoeppener, S., Schubert, U. S. 2015. "Synthesis and modification of carbon nanomaterials utilizing microwave heating", Advanced Materials, 27 (28), 4113-4141.

48. Zhang, X. Y., Liu, Z. 2012. "Recent advances in microwave initiated synthesis of nanocarbon materials", Nanoscale, 4 (3), 707-714.

49. Poyraz, S., Zhang, L., Schroder, A., Zhang, X. Y. 2015. "Ultrafast microwave welding/reinforcing approach at the interface of thermoplastic materials", ACS Applied Materials and Interfaces, 7 (40), 22469-22477.

50. Liu, Z., Chen, L., Zhang, L., Poyraz, S., Guo, Z. H., Zhang, X. Y., Zhu, J. H. 2014. "Ultrafast Cr(VI) removal from polluted water by microwave synthesized iron oxide submicron wires", Chemical Communications, 50 (59), 8036-8039.

Electro-solution Blown Polyacrylonitrile Nanofibers for Air Filtration Application

CALISIR Mehmet D[1,2]., GUNGOR Melike[1], KILIC Ali[1]
[1]TEMAG Lab, Istanbul Technical University, Istanbul, Turkey
[2]Recep Tayyip Erdogan University, Faculty of Engineering, Rize, Turkey
alikilic@itu.edu.tr

PURPOSE

Production of PAN-based nanofibrous mats as filter material via electro-solution blowing method is the main purpose of this study. The effect of applied voltage on fiber morphology and filtration performance will be investigated.

INTRODUCTION

Air quality on the earth is decreasing day by day due to the increasing human population and consequently increasing industrialization. Among the pollutants, particulate matters (PM) based air pollution contributes to increased risk of cardiopulmonary and lung cancer mortality[1]. Filtration is one of the direct solutions to air pollution by preventing spread the pollutants to the atmosphere from the source. Porous membrane and fibrous filters are the main types of filters.

Nonwoven fibrous membrane filters have been widely used in filtration applications. Glass, polyethylene (PE), polypropylene (PP), polyester, and aramid fibers are some of the fibers used in these filters [2]. However, these filters often complain from the issues like non-uniform fiber diameter and pore size, relatively low filtration efficiency, high basis weight, and poor high-temperature resistance[3]. Compared to conventional microfiber-based filters, nanofiber-based filters have significantly improved filter efficiency, filter life, and exhibited lower pressure drops. The main reason for the higher performance of nanofiber-based filters is the lower airflow resistance of nanofibers as a result of the 'slip effect'[4]

Solution Blowing (SB) is a highly efficient micro – or nanofiber production method that used the compressed air as the driving force for fiber production. In this method, the polymer solution is fed through the inner channel of the nozzle while the compressed air flows through the outer channel. With the high airflow formed at the nozzle tip, the solution is blown towards the collector surface, the solvent in the solution evaporates during its way to the collector and the blown solution is collected as a fibrous structure on the collector surface[5]. The system is known to be safe and cost-effective among other nanofiber production systems[6].

The difference of the electro-solution blowing (ESB) system from the SB is the presence of an electrical field. The electrical field produces an additional driving force on the solution to able to produce finer fibers by additional stretching of the polymer chains [7]. In this way, it is possible to produce nano-sized and aligned fibers with high production speeds.

Depending on the application area, the physical and chemical stability of the filter materials against moisture, temperature, chemicals, and other effects must be provided. Polymer-based nanofibrous filters such as polyamide-6 (PA-6), polyacrylonitrile (PAN), poly (vinyl alcohol) (PVA), polyurethane (PU) are generally used in applications such as vehicle cabin filters, building filters, and personal is used [2]. Among them, PAN has strong chemical bonds with nitrogen groups, thus, the fibers obtained from PAN show high stability against weather conditions.

In this study, the production of PAN-based nanofibrous mats as filter material via electro-solution blowing method is aimed. The effect of applied voltage on fiber morphology and filtration performance will be investigated.

EXPERIMENTAL

Material

Polyacrylonitrile copolymer (PAN, Mw 225,000 g.mol^{-1}) was purchased from Aksa and dimethylformamide (DMF, 99.99% purity) was purchased from Merck.

Method

To prepare a homogeneous spinning solution, PAN was added into dimethylformamide (DMF) at 8 wt.% concentration and stirred at 80ºC for 4h. Nanofibrous PAN filter samples were then fabricated by using E-Aerospinner L1.0 (Areka Group LLC). The basic components of the machine are schematically given in Figure 1. The prepared solution was blown with pressurized air (2 bar) using a 22 gauge needle and 5 ml/h feeding rate. Electrical voltage (0kV, 15kV, and 30kV) was applied during production. The blown fibers were collected on a rotating collector covered with a 25 gsm PP nonwoven. During the process, the rotational speed of the collector fixed to 60 rpm.

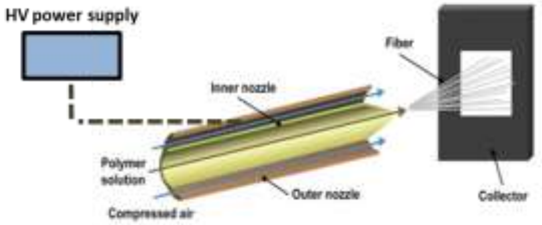

Figure 1. Schematic presentation of the ESB system.

RESULTS AND DISCUSSIONS

SEM images and fiber diameter distributions of PAN NFs are shown in Figure 2. Accordingly, regardless of the presence or not voltage, all samples had lots of droplets. However, the number and size of the droplets were lower with increasing the applied voltage. The finest fibers with the lowest droplets and standard deviation were obtained from the sample blown with 30 kV. Additionally, the diameters of the produced fibers were 80, 70 and 60 nm.

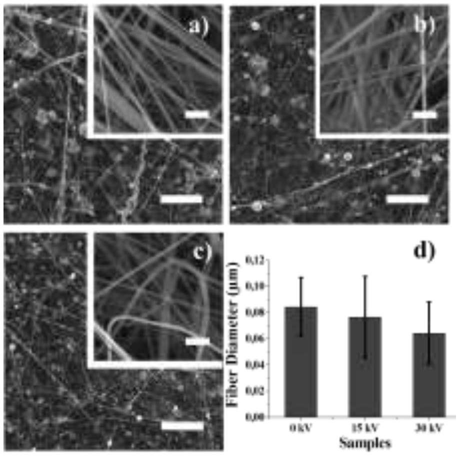

Figure 2. The SEM images and fiber distribution (d) of the PAN samples which were produced with a) 0kV, b) 15kV, c) 30kV.

In .

Table 1, the air permeability results of the samples were given. Accordingly, the air permeability of the fibers has decreased with increasing electric field as a result of the finer fibrous structure. When the fibers get finer, the gaps between the fibers reduce and airflow rate decreases.

Table 1. Air permeability test results of the samples

Samples	Area (cm^2)	Pressure (Pa)	Air Permeability (mm/s)
0 kV	38	125	25.4
15 kV			22.2
30 kV			13.4

The filter performances of the samples were measured as a single and double layer. In the case of double-layer measurement, the filtration efficiency was improved. Additionally, the finer fibers as a result of the increased electric field also resulted in higher filtration performance. However, the pressure drop of this fiber was higher since the airflow through the filter media was decreased as a result of reduced porosity.

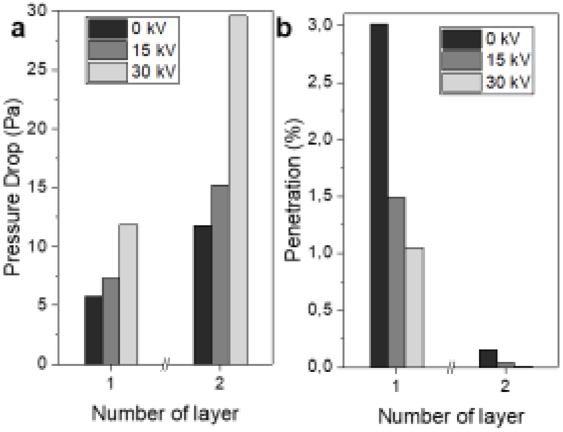

Figure 3. % Penetration and pressure drop versus the number of the layer of fibrous samples.

CONCLUSIONS

The PAN-based nanofibrous mat was produced successfully with electro-solution blowing. With the applied electric field, fiber diameters were reduced and the finest fibers produced with 30 kV electric field showed 99.993% filter performance.

SUGGESTION FOR FURTHER WORK

Different concentrations of the solution and also fibers from different MW PAN polymers will be produced to obtain defect-free fibrous mats.

ACKNOWLEDGMENTS

The authors grateful Areca LLC for providing the E-Aero Spinner L1.0 system.

LITERATURE

1. Miller, K. A. *et al.New England Journal of Medicine* 356, 447–458 (2007).
2. Wang, N., Mao, X., Zhang, S., Yu, J. & Ding, B. 299–323 (Springer, Berlin, Heidelberg, 2014). doi:10.1007/978-3-642-54160-5_12.
3. Zhu, M. *et al.* 302, 1600353 (2017).
4. Choi, H.-J. *et al. Journal of Aerosol Science* 114, 244–249 (2017).
5. Polat, Y. *et al. Journal of Applied Polymer Science* 133, (2016).
6. Zhang, X. & Lu, Y. *Polymer Reviews* 54, 677–701 (2014).
7. Longo, E. & Porta, F. de A. L. (Springer, 2017).

İzotaktik Polipropilen/Poli(etilen tereftalat) Karışımlarının SEM İle İncelenmesi

EKİNCİ, Aysun[1], ÖKSÜZ, Mustafa[2]
[1] Yalova Üniversitesi, Fen Bilimleri Enstitüsü, 77200, Yalova, Türkiye
[2] Yalova Üniversitesi, Polimer Mühendisliği Bölümü, 77200, Yalova, Türkiye
ekinci_aysun@hotmail.com

AMAÇLAR

Bu çalışmanın amacı, termodinamik açıdan uyumsuz olan izotaktik polipropilen/poli(etilen tereftalat) (iPP/PET) karışımlarının morfolojik özelliklerine maleik anhidrit aşılanmış polipropilen (PP-g-MA) ile uyumlaştırmanın etkisini incelemektir.

GİRİŞ

Polipropilen düşük maliyet, işleme kolaylığı ve sahip olduğu fiziksel ve kimyasal özellikleri sayesinde pek çok uygulama alanında kullanılan bir termoplastiktir[1,2,3,4]. Ancak, polipropilenin mekanik özellikleri bazı uygulamalarda yetersiz kalmaktadır[1]. Son zamanlarda yüksek performans[2], düşük maliyet[3] ve uygulama alanlarının[5,6] geliştirilmesi amacıyla polipropilen (PP) karışımlarının hazırlanması ve karakterizasyonun üzerine hem akademik hem de endüstriyel alanda çeşitli çalışmalar yapılmaktadır. Polipropilen karışımları, istenilen özelliklere sahip yeni malzeme oluşturma avantajı sunmaktadır[6].

PP karışımlarının termodinamik açıdan uyumlu ve uyumsuz karışım olmak üzere iki sınıfa ayrılmaktadır[5,6]. PP karışımlarının özellikleri, karışım bileşenlerinin türü ile karışımdaki yüzdeleri ve morfolojisine göre değişim göstermektedir[6,7,8]. PP/PET karışımları uyumsuz yani çok fazlı bir polimerik karışımdır[7,8,9,10]. PP/PET karışımında ara yüzeyler kontrol edilerek karışımın morfolojisi kararlı hale getirilmektedir[11,12]. PP karışımlarında ara yüzey özellikleri ve morfoloji kararlılığı uyumlaştırma işlemi kontrol edilebilmektedir[7,13]. PP karışımlarının ara yüzey özelliklerinin iyileştirilmesinde genellikle maleik anhidrit (MA), akrilik asit (AA) ve glisidil metil metakrilat (GMA) gibi fonksiyonel gruplara sahip kopolimerler tercih edilmektedir[7,14,15,16,17,18].

Bu çalışmada, izotaktik polipropilen/ poli(etilen teraftalat) karışımının morfolojisine karışımı uyumlaştırmanın etkisi taramalı elektron mikroskobu kullanılarak araştırılmıştır. Mikro yapı analizlerinde, iPP/PET karışımlarını PP-g-MA ile uyumlaştırmanın dağılan fazın tanecik boyutunda düşme sağladığını ve karışımın uyulaştırıcı varlığında homojenleştiği görülmüştür.

DENEYSEL

Malzeme

Bu çalışmada, iPP/PET (70/30) karışımlarının kırık yüzeyleri kullanılmıştır. Uyumlaştırıcı olarak PP-g-MA (ağırlıkça %0,1,5) kullanılmıştır.

Yöntem

iPP/PET (70/30) karışımları eriyik harmanlama yöntemi ile çift vidalı ekstrüderde hazırlandıktan sonra TS EN ISO 294 standardına uygun olarak enjeksiyon makinesinde kalıplanmıştır. iPP/PET karışımlarındaki polimerlerin etkileşimi ve dağılım özelliklerine PP-g-MA'nın etkisi taramalı elektron mikroskobu (SEM) ile incelenmiştir. Numuneler vakum altında altın ile kaplandıktan sonra Inspect/S50 model SEM cihazında analiz edilmiştir.

DENEYSEL SONUÇLAR/TARTIŞMA

Şekil 1'de iPP/PET karışımlarının kırılma yüzeylerine ait SEM görüntüleri verilmiştir. iPP/PET/PP-g-MA 70/30/0 karışımında iPP matrisi içerisindeki PET fazının homojen bir şekilde dağılmadığı görülmektedir. Bu durum, iPP ve PET polimerinin ara yüzey etkileşiminin kötü olduğunu kanıtlamaktadır. iPP/PET karışımlarında artan uyumlaştırıcı oranına bağlı olarak iPP matrisi içerisinde dağıtılan PET fazının geometrisinin dağılımının ve boyutlarının değiştiği görülmüştür.

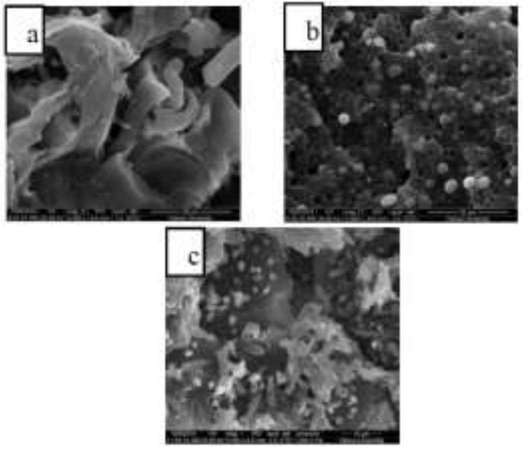

Şekil1. a)iPP/PET/PP-g-MA 70/30/0 b)iPP/PET/PP-g-MA 70/30/1 c)iPP/PET/PP-g-MA 70/30/5 ait x5000 büyütmedeki SEM görüntüleri

Uyumlaştırıcı oranındaki artış PET'in daha homojen dağılmasını sağlayarak iPP matrisi ile PET fazının ara yüzey etkileşimini artırmıştır (Şekil 2).

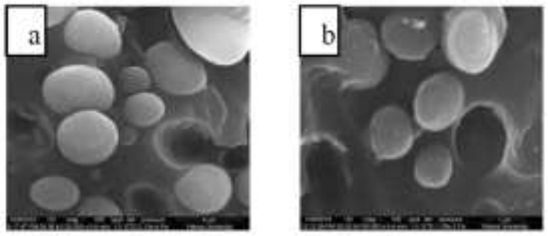

Şekil 2. a) iPP/PET/PP-g-MA 70/30/1 b) iPP/PET/PP-g-MA 70/30/5 ait x50000 büyütmedeki SEM görüntüleri

GENEL SONUÇLAR

Bu çalışmada iPP/PET (70/30) karışımlarının morfolojik özelliklerine uyumlaştırmanın etkisi SEM ile incelenmiştir. Artan uyumlaştırıcı oranına bağlı olarak, iPP'nin PET fazının ara yüzey özelliklerinin iyileştiği görülmektedir. Bu durumun PP-g-MA'nın fonksiyonel uç grubunun PET'in fonksiyonel uç gruplarının etkileşiminin kanıtıdır. Hazırlanan karışımların mikro yapıları kıyaslandığında, en küçük ortalama tanecik boyutu iPP/PET/PP-g-MA 70/30/5 karışımında gözlenirken, en büyük ortalama iPP/PET/PP-g-MA 70/30/0 karışımında tanecik boyutu gözlenmiştir.

TEŞEKKÜR/BILGILENDIRME/FON KAYNAĞI

Bu çalışma Yalova Üniversitesi Bilimsel Araştırma Projeleri Komisyonu Tarafından Desteklenmiştir.
Proje Numarası:2018/DR/0005

KAYNAKLAR

[1] Berktaş M. E., Ekinci A., Karagöz İ. ve Öksüz M., 2019. The Effect Of Nucleating Additives on the Thermal and Mechanical Properties of Polypropylene, Tam Metin, The Internatinonal Conference on Materials Science, Mechanical and Automotive Engineerings and Technology in Cappadocia/Turkey (IMSMATEC'19).

[2] Öz E. K., Karagöz İ. ve Öksüz M., 2015. Poliamid 6/Polipropilen (PA 6/PP) Karışımlarının Yapı ve Özellikleri, I. Ulusal Plastik Teknolojileri Sempozyumu, İstanbul, Türkiye.

[3] Ekinci A., Karagöz İ. ve Öksüz M., 2019. Modification of Thermoplastics with Chain Extender, Tam Metin, The Internatinonal Conference on Materials Science, Mechanical and Automotive Engineerings and Technology in Cappadocia, Turkey (IMSMATEC'19), 1098 –1100.

[4] Karagöz İ. ve Öksüz M., 2018. Microstructures occurring in the joined thermoplastics sheets with friction stir welding, Journal of the Faculty of Engineering and Architecture of Gazi University 33:2, 503-515.

[5] Lin J. H., Pan Y. J., Liu C. F., Huang C. L., Hsieh C. T., Chen C. K., Lin Z. I. ve Lou C. W., 2015. Preparation and Compatibility Evaluation of Polypropylene/High Density Polyethylene Polyblends, Materials 8, 8850–8859; doi:10.3390/ma8125496.

[6] Nwabunma D. ve Kyu T., 2007. Polyolefin blends, John Wiley & Sons, Inc., ISBN 978-0-471-79058-7.

[7] Oyman Z. O. ve Tincer T., 2003. Melt Blending of Poly(ethylene terephthalate) with Polypropylene in the Presence of Silane Coupling Agent, Journal of Applied Polymer Science, Vol. 89, 1039–1048.

[8] Jayanarayanan K., Thomas S. ve Joseph K., 2011. In situ microfibrillar blends and composites of polypropylene and poly (ethylene terephthalate): Morphology and thermal properties, Journal of Polymer Research, 18:1–11 doi: 10.1007/s10965-009-9384-6.

[9] Oromiehie A., Ebadi-Dehaghani H., ve Mirbagheri S., 2014. Chemical Modification of Polypropylene by Maleic Anhydride: Melt Grafting, Characterization and Mechanism, International Journal of Chemical Engineering and Applications, Vol. 5, No. 2.

[10] Yi X., Xu L., Wang Y., Zhong G., Ji X. ve Li Z., 2010. Morphology and properties of isotactic polypropylene/poly(ethylene terephthalate) in situ microfibrillar reinforced blends: Influence of viscosity ratio, European Polymer Journal 46, 719–730.

[11] Lima M. S., Matias Á. A., Costa1 J. R. C., Fonseca A. C., Coelho J. F. J. ve Serra A. C., 2019. Glycidyl methacrylate-based copolymers as new compatibilizers for polypropylene/ polyethylene terephthalate blends, Journal of Polymer Research 26:127, doi: 10.1007/s10965-019-1784-7.

[12] Fakırov S., Bhattacharyya D., Lın R. J. T., Fuchs C. ve Frıedrıch K. 2007. Contribution of Coalescence to Microfibril Formation in Polymer Blends during Cold Drawing, Journal of Macromolecular Science, Part B, 46:1, 183-194, doı: 10.1080/00222340601044375.

[13] Çavuş F. K., Özcanlı Y., Beken M., 2019. The effect of PET additive on mechanical and morphological properties of PP, Journal of the Faculty of Engineering and Architecture of Gazi University 34:1, 319-326.

[14] Mi D., Wang Y., Kuzmanovic M., Delva L., Jiang Y., Cardon L., Zhang J. ve Ragaert K., 2019. Effects of Phase Morphology on Mechanical Properties: Oriented/Unoriented PP Crystal Combination with Spherical/Microfibrillar PET

Phase, Polymers, 11, 248; doi:10.3390/polym11020248.

[15] Mirjalili F., Moradian S. ve Ameri F., 2013. Enhancing the Dyeability of Polypropylene Fibers by Melt Blending with Polyethylene Terephthalate, The Scientific World Journal, Article ID 468542, P. 10, doi:10.1155/2013/468542.

[16] Zadhoush A., Akbari M. ve Haghighat M., 2007. PET/PP blending by using PP-g-MA synthesized by solid phase, Journal of Applied Polymer Science, Vol. 104, 3986–3993.

[17] Mantia F. P. L., Ceraulo M., Giacchi G., Mistretta M. C. ve Botta L., 2017. Effect of a Compatibilizer on the Morphology and Properties of Polypropylene/Polyethylentherephthalate Spun Fibers, Polymers, 9, 47; doi:10.3390/polym9020047.

[18] Razak N. C. A., Inuwa I.M., Hassan A. ve Samsudin S.A., 2013. Effects of compatibilizers on mechanical properties of PET/PP blend, Composite Interfaces, Vol. 20, No. 7, 507–515, doi: 10.1080/15685543.2013.811176.

Atık Haldeki Ayçiçeği Gövdesi Kullanılarak Selüloz Esaslı, Isıl Yalıtım Özellikli Elyaf Eldesi

ÇAVUŞLAR, Ersin [1], BOZAR, Deniz [2], ERGÜL, Eren[3], Leyla GİRGİNTAŞ [4]
[1] Beybi İş Güvenliği Malzemeleri San.Tic.A.Ş. Ar-Ge Merkezi
Yukurı Dudullu Organize Sanayi Bölgesi 1. Cadde No:27 Ümraniye / İstanbul

ersin.cavuslar@beybi-is.com.tr

AMAÇLAR

Sürdürülebilir atık yönetimini sağlayabilmek için sisteminin her bir elemanının çevresel ve ekonomik yüklerini irdelemek ve bu mekanizmayı sürekli olarak işletmek gereklidir. En ekonomik ve işletme maliyeti en düşük olan atık yönetimi sistemi en az atığın üretildiği sistemdir. Atık miktarını azaltmak için ise minimum atık üretecek tekniklerin uygulanması, atıkların enerji ve/veya materyal olarak geri kazanımının sağlanması gereklidir. (Yaman ve ark.)

Üretimin ardından ortaya çıkan ayçiçeği sapı çiftçimiz içinde büyük sorun oluşturmaktadır. Yılda yaklaşık 2.500.000 ton ayçiçeği sapı atık olarak bulunmaktadır. (Binici ve ark.)

Çalışma dahiliden atık halde bulunan ayçiçeği saplarının fiziksel parçalama prosesini takiben kimyasal havuzlama işlemi ile tekstilde kullanılabilir elyaf haline getirilmesi amaçlanmaktadır.

GİRİŞ

Çalışma kapsamında atık halde bulunan ayçiçeği saplarının geri dönüşümü sağlanarak üretime ve ekonomiye tekrar kazandırılması amaçlanmaktadır. Ayçiçeği sapı içerisinde yaklaşık olarak % 54 – 55 oranında selüloz, % 12-13 oranında lignin barındırmaktadır. En yakın selüloz madde miktarı yapısı % 70 ile keten lifinde mevcuttur (Mengeloğlu ve ark.). Keten lifinin teknik özellikleri ve havuzlanarak elyaf halinde kullanımına ilişkin yapılan araştırmalarda keten yapısında bulunan lignin polimerinin havuzlama ve elyaf kalitesini belirlemede olumsuz etki oluşturmadığı tespit edilmiştir (Doğan vd ark.) Bu da göstermektedir ki ayçiçeği sapı kullanılarak keten yapısına benzer kimyasal yapıda elyaf eldesi mümkün olabilmektedir.

Gövdede bulunan liflerin sert yapıdan ayrıştırılması için mekanik, kimyasal ve biyolojik birçok yöntem bulunmaktadır.(Körlü ve ark.)

Çalışma dahilinde ayçiçeği saplarının dekortikasyon (kırma) işlemini takiben, hızlı bir üretim tekniği olan kimyasal havuzlanaya tabi tutulması öngörülmektedir. [6] Giderek tükenen ham madde kaynaklarınıan alternatif oluşturması planlanan biyobozunur bu ham madde kaynağı sayesinde pamuk, keten, bambu gibi oldukça yaygın kullanılan bitkisel esaslı liflere çevresel yük oluşturmayan bir lif çeşidi eklenmesi öngörülmektedir.

Güler ve ark.(2005), yaptıkları çalışmada ayçiçeği sapları ve akkavak yongalarından üç tabakalı yonga levhalar üretilmiştir. Çalışmada elde edilen sonuçlara göre ay çiçeği sapı esaslı yongaların üre formaldehit ile uyumlu olduğu ve ay çiçeği saplarının tek başına ya da kavak yongaları ile karıştırılarak yonga levha üretiminde hammadde olarak kullanılabileceğini vurgulamıştır.

Ayçiçeği sapının içerisinde bulunduğu bir yapının ısıl yalıtım özelliği gösteren yeni bir malzeme halinde kullanıldığı tespit edilmiştir. Üretilen blok ve panel yalıtım malzemelerinde ayçiçeği sapı katkılı malzemelerin ısı ve ses yalıtım özellikleri araştırılmıştır. Ayçiçeği sapı bulunduran yapıların konvansiyonel strafor yapılara göre daha üstün performans özelliği sağladığı tespit edilmişir. (Mengeloğlu ve ark.)

Bu çalışmalar doğrultusunda keten selülozik yapısına benzer bir yapıda olduğu tespit edilmiş ve özellikle ısıl yalıtım özelliği olan ayçiçeği sapının pamuk, keten, yün gibi ham maddelerle kullanılarak termal performans özelliği bulunan iplik ve kumaş yüzeyleri elde edilebileceği öngörülmüştür.

DENEYSEL

Malzeme

Ham madde olarak kullanılması öngörülen ayçiçeği sapları % 50’den fazla selüloz içermesi sayesinde ve yapısındaki mukavemeti sağlayan lignin polimeri sayesinde mukavim yapılı, fiziksel perormans özellikleri yüksek olan bir alternatif konumundadır (Doğan ve ark.).

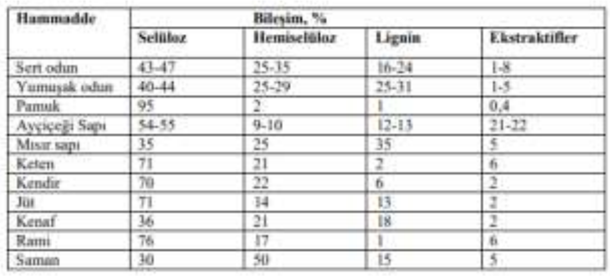

Hammadde	Bileşim, %			
	Selüloz	Hemiselüloz	Lignin	Ekstraktifler
Sert odun	43-47	25-35	16-24	1-8
Yumuşak odun	40-44	25-29	25-31	1-5
Pamuk	95	2	1	0,4
Ayçiçeği Sapı	54-55	9-10	12-13	21-22
Mısır sapı	35	25	35	5
Keten	71	21	2	6
Kendir	70	22	6	2
Jüt	71	14	13	2
Kenaf	36	21	18	2
Rami	76	17	1	6
Saman	30	50	15	5

Şekil 1.Yapısında Selüloz Bulunan Bazı Ham Maddelerin Kimyasal Bileşimi

Yöntem

Ayçiçeği sapına ait dış katmanlar soyulduktan sonra, dekortikasyon (kırma) işleminde geçirilecektir. (Şekil 2)

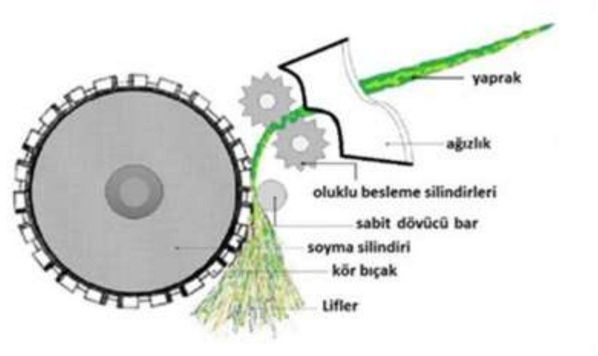

Şekil 2. Dekortikatör Kullanımı İle Liflerin Ayrılması

Kırma işlemini takiben yapının elyaf formuna getirilmesi için alkali ile işlenmesi prosesine geçilecektir. Alkaliler özellikle hemiselüloz ile reaksiyona girebildiğinden en sık tefcih edilen ve etkili zamk giderme prosesidir. Kimyasal yardımıyla zamk giderme prosesi boyunca sırasıyla sırasıyla; sülfürik asit (H2SO4) gibi bir asit içerisinde daldırıp bekletme, yıkama, sodyum hidroksit (NaOH) çözeltisi ile kaynatma, yıkama, ağartma, suyun uzaklaştırılması, yağlama ve kurutma şeklindedir. Zamk giderme işleminde dikkat edilmesi gereken noktalardan biri de işlem sırasında tek liflerin birbirlerine bağlanmasını sağlayacak miktarda zamkın bırakılmasıdır. Aksi halde lifler birbirlerinden bağımsız konumda tek tek lifler halinde kalacaktır. Tek liflerin uzunluğunun kısa olmasından dolayı zamkı tümüyle giderilmiş lifler eğrilememektedir (Franck ve ark.).

DENEYSEL SONUÇLAR/TARTIŞMA

Yapılan literatür araştırmaları gerek içerisinde barındırdığı selüloz ve lignin miktarı gerekse atıl halde bulunan bitkisel yapının bazı fiziksel ve kimyasal proseslerden geçirilerek kullanılabileceği tespit edilmiştir.

GENEL SONUÇLAR

Yıllık yaklaşık 2.500.000 ton civarında oluşan ve hiçbir şekilde ekonomik ve üretim süreçlerinde değerlendirilmeyen ayçiçeği gövdesi yapılan hazırlama prosesleri neticeisnde termal, fiziksel performans özellikleri bulunanan katma değerli bir elyaf haline getirilebilecektir. Hızla tükenen doğal ham madde kaynaklarına alternatif sunması öngörülen yapıyla öncelikli olarak iç piyasada sonrasında ihracat anlamında ülke ekonomisine katkı sağlanabileceği düşünülmektedir.

SONRAKİ DÖNEM ÇALIŞMALARI

Yapılan literatür araştırmaları neticesinde kullanılabileceği görülen ayçiçeği saplarının ilerleyen zamanlarda belirlenen proseslerde ve parametrelerde laboratuvar ölçekli olarak üretilmesi amaçlanmaktadır. Sonrasında yapılacak performans testleri ile mekanik ve termal etkiler gözlemlenecektir. Elde edilen ürünün yumuşak bir doku sağlanması için tek başına değil, pamuk, yün, bamboo gibi diğer elyaf Kaynakları ile berlili oranlarda karıştırılarak kullanılması öngörülmektedir.

KAYNAKLAR

Binici H., Sevinç A.H., Eken M., 2012, Ayçiçek Sapı Ve Tekstil Atıkları İle Yalıtım Malzemesi Üretimi, SAÜ Fen Bil Der 20. Cilt, 2. Sayı, s. 203-221, 2016.

Doğan, H. ve Sezer, S. (2013). Doğal bir polimer olan selüloz ve türevleri, Türkiye Kimya Sanayicileri Derneği e-Bülteni, 16-28.
Son Erişim Tarihi : 30.12.2019.

Gardetti, M. A. ve S. S. Muthu, 2015, "Handbook of Sustainable Luxury Textiles and Fashion", cilt 1, ed: Springer .

Güler C., Bektas, Ġ. and Kalaycıoglu H., 2006. The experimental particleboard manufacture from sunflower stalks (Helianthus annuus L.) and Calabrian pine, (Pinus brutia Ten.) Forest Prod. J. 56:56-60

Körlü, A.,E., Gümüştürkmen B., 2006, Ketenin genel özellikleri ve havuzlanmasi properties of flax and retting of flax, Tekstil Ve Konfeksiyon Dergisi,1, 276 – 280.

Mengeloglu F., Alma M.H., 2002, Buğday Saplarının Kompozit Levha Üretiminde Kullanılması, Ksü Fen Ve Mühendislik Dergisi 5 37-48.

R. R. Franck, 2005, Bast ve Other Plant Fibres, cilt 39: Crc Press.

YAMAN K., 2012 Bitkisel Atıkların Değerlendirilmesi ve Ekonomik Önemi,., Kastamonu Üni., Orman Fakültesi Dergisi, 12 (2), 339.

Effects of HALS and Nano-TiO_2 on the Flammability of Cyclic Phosphonate-based Flame Retardant/Polypropylene System

YÜKSEL, Gamze[1], ÜREYEN, Mustafa Erdem[2,3]

[1]Eskişehir Technical University Institute of Graduate Programs, Department of Materials Science and Engineering, İki Eylül Campus Eskişehir 26555, TURKEY
[2]Eskişehir Technical University, Department of Fashion and Textile Design, Yunusemre Campus, Eskişehir, 26473, TURKEY
[3]Eskişehir Technical University, Advanced Technologies Research Centre (ITAM), Eskisehir, 26555, TURKEY

g_yuksel@eskisehir.edu.tr

PURPOSE

The main aim of the study is to investigate the effect of N-alkoxy hindered amine based light stabilizing (HALS) agent and nano-sized titanium dioxide particles on the flammability of a cyclic phosphonate-based flame retardant (FR)/polypropylene (PP) system.

INTRODUCTION

Polypropylene (PP) is one of the most widely used thermoplastic polymers in several industries[1] due to its low cost, environmental friendliness and easy processability[2]. High mechanical strength and chemical resistance[3] are also advantageous of PP. However, due to its aliphatic hydrocarbon structure, it is highly flammable and burns quickly without leaving any residue[4]. PP, which is also very sensitive to UV, decomposes by photo-oxidation as a result of long-term UV exposure, especially in outdoor applications. These disadvantages can be overcome by using flame retardants (FRs) and UV stabilizers. Phosphorus compounds are proposed as halogen-free flame retardants for polymeric materials. The flame-retardant mechanism of phosphorus compounds alone and in combination with other flame retardants has been studied by Schartel[3]. It was explained that phosphorus flame retardants can act in the condensed phase by enhancing char, by yielding intumescence or inorganic glass formation; and in the gas phase through flame inhibition. In the study of Hoang and Kim[4], they proved that the flame-retardant additives containing phosphorus compounds decompose before the polymer and thus show the flame-retardant effect in the gas phase by thermogravimetric analysis.

The effect of N-alkoxy hindered amine light stabilizers on the flammability, UV stability and mechanical properties of polypropylene systems were studied in several papers[5]. Xie et. Al[6], found out that N-alkoxy hindered amine (NOR116) promoted char formation. Cao et. al.[7] synthesized N-alkoxy hindered amine and used it as a synergist with an intumescent flame-retardant system (APP/PER/MEL) in polypropylene.

TiO_2 inorganic UV stabilizers are used in polymeric materials. Particularly when used in nano sized or combination with HALS is very effective[8,9] Qi et al.[8] used TiO_2 nanoparticles with conventional HALS (Chimassorb 944) and demonstrated that these two additives exhibited a strong synergistic effect during the photooxidation of PP composites. Wang et al.[10] observed that nano-sized TiO_2 increased thermal stability and flame retardancy in acrylic polymers and coatings.

In this study, N-alkoxy hindered amine based light stabilizing agent and nano-sized titanium dioxide particles were added to the FR/PP system in different ratios. The effect of HALS and TiO_2 on the thermal stability and flame retardancy of FR/PP containing systems were investigated. The maximum total additive ratio of the samples was adjusted to be less than 10% by weight to check their usability for polypropylene fiber spinning in future studies.

EXPERIMENTAL

Materials

The isotactic polypropylene (Ecolen HZ40S) with a melt flow index (MFI) of 25g/10min (230°C, 2.16 kg; 0.91 g/cm^3) was supplied by Hellenic Petroleum, Greece. Organic phosphorus/cyclic phosphonate-based flame-retardant (FR) additive (Aflammit PCO-900) was supplied by Thor GmbH, Germany. A monomeric N-alkoxy hindered amine light stabilizer (Flamestab NOR-116) was supplied by BASF, Switzerland. Titanium dioxide (99.7% purity, d <25 nm nano-powder) was supplied by Sigma-Aldrich (MERCK), Germany.

Methods

Samples were prepared in different compositions as indicated in Table 1. Firstly, additives were mixed with the polymer in a mechanical mixer. After mechanical stirring, it was fed into a twin-screw micro-compounder (DSM Xplore, The Netherlands), which was set at a temperature of 180 °C. The mixtures blended in the compounder for 2 minutes. The homogeneous composition obtained was transferred to an injection molding unit (DSM Explore, The Netherlands) at 175 °C and appropriate sample size molds were prepared.

Limit oxygen index values of samples were measured in LOI tester (Concept Equipment, UK) according to ASTM D2863-10 test standard. Before testing, the samples were conditioned for at least 24 hours in a climate chamber (Binder, Germany) with 20°C, 50% humidity. The thermal behavior of the doped polypropylene molds was analyzed by a simultaneous thermal analyzer (SDT Q600, TA Instruments, USA). Approximately 10 mg of sample was placed in an open alumina pan and heated to 800°C at a heating rate of 10°C/min under a nitrogen flow of 100 ml/min.

Table 2. Compositions of the samples and LOI test results.

Sample Code	PP (wt%)	FR (wt%)	HALS (wt%)	TiO_2 (wt%)	LOI (%O_2)
RefPP	100.0	-	-	-	19.0
PPFR	95.0	5.0	-	-	21.7
PPFRH	95.0	3.5	1.5	-	25.0
PPFRHT-1	94.5	3.5	1.5	0.5	25.5
PPFRHT-2	94.0	3.5	1.5	1	26.3
PPFRHT-3	93.5	3.5	1.5	1.5	26.3

RESULTS AND DISCUSSION

The LOI value of the pure PP sample was determined as 19.03%. By the addition of 5 wt% FR additives, the LOI value of the pure PP increased to 21.7%. When 1.5 wt.% of cyclic phosphonate in PPFR was substituted by NOR-116, the LOI increased from 21.7% to 25.0% (PPFRH). The LOI of PPFRH was further increased to 25.5% (PPFRHT-1) and 26.3% (PPFRHT-2) by the addition of 0.5 wt. % and 1wt% nano-sized TiO_2 respectively. However, the LOI was not further improved by the addition of the higher nano-sized TiO_2 content than 1.0% (PPFRT-3).

Thermal stability of the samples was investigated by TG/DTG under nitrogen and the corresponding curves are shown in Figure 1 and Figure 2 respectively. TGA curves revealed that a single stage decomposition had occurred for all samples. As indicated in Table 2, the results of the mass loss temperatures at 10% by weight and 50% by weight showed that all additives reduced the initial decomposition temperature. The thermal decomposition temperature values of the samples containing FR and HALS additives were lower than the decomposition temperature of RefPP. It was evaluated that FR and HALS additives degraded at lower temperatures and changed the degradation behaviour of PP positively. At the end of the analysis, there is no residue left from RefPP. In contrast, an increase in the amount of residue at 500°C and 700°C was observed in samples containing nano-sized TiO_2.

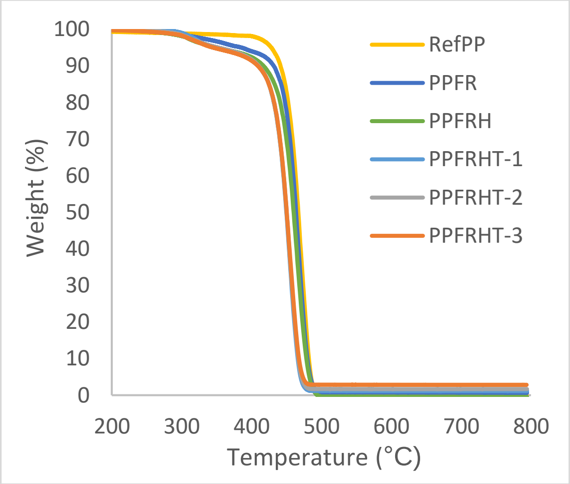

Figure 4. TGA curves of samples

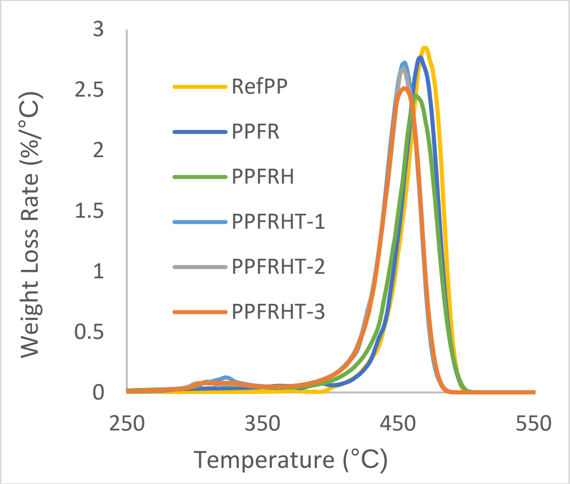

Figure 5. DTG curves of samples

Table 3. Thermogravimetric analysis results of the samples

Sample Code	$T_{(\%10)}$	$T_{(\%50)}$	Residue at 500°C (%)	Residue at 700°C (%)
RefPP	441.41	466.93	0.00	0.00
PPFR	431.67	463.72	0.78	0.67
PPFRH	416.93	460.31	0.00	0.00
PPFRHT-1	409.15	449.88	1.16	1.14
PPFRHT-2	410.00	450.25	1.68	1.66
PPFRHT-3	409.08	450.32	2.87	2.83

CONCLUSION

In this work, HALS and nano-sized TiO_2 added to the flame retardant polypropylene system. HALS and TiO_2 nanoparticles increased the FR/PP system's LOI value synergistically. TGA results showed that the addition of all additives reduced the onset temperature of the neat PP. FR and HALS additives decreased the decomposition temperature of PP led to the conclusion that it can show activity in the gas phase. In contrast, an increase in the amount of residue at 500°C and 700°C was observed, especially in samples containing nano-sized TiO_2. At the end of the analysis, the formation of residues also showed that the condensed phase activity.

FUTURE WORK

Pyrolysis and heat release mechanism will be evaluated by using Micro Combustion Calorimetry and Cone Calorimetry. The availability of the compositions for fibre spinning will be investigated.

REFERENCES

1. Du, B., Guo, Z. and Fang, Z. 2009. "Effects of organo-clay and sodium dodecyl sulfonate intercalated layered double hydroxide on thermal and flame behavior of intumescent flame retarded polypropylene", Polymer Degradation and Stability, 94(11), 1979-1985.

2. Maddah, H.A. 2016. "Polypropylene as a promising plastic: A review", American Journal of Polymer Science, 6(1), 1-11.

3. Schartel, B. 2010. "Phosphorus-based Flame Retardancy Mechanisms Old Hat or a Starting Point for Future Development?", Materials, 3, 4710-4745.

4. Hoang, D. And Kim, J. 2008. "Synthesis and applications of biscyclic phosphorus flame retardants", Polymer Degradation and Stability, 93, 36-42.

5. Üreyen, M.E., Kaynak E., Yüksel G., 2020, "Flame-retardant effects of cyclic phosphonate with HALS and fumed silica in polypropylene", J. APPL. POLYM. SCI. 137(4), 2020, p. 1-8.

6. Xie, H., Lai, H., Zhou, R., Li, H., Zhang, Y., Zeng, X., Guo, J. 2015. "Effect and mechanism of N-alkoxy hindered amine on the flame retardancy, UV aging resistance and thermal degradation of intumescent flame retardant polypropylene", Polymer Degradation And Stability, 118, 167-177.

7. Cao, K., Wu, S.-l., Qiu, S-I., Li, Y.,Yao Z. 2012 "Synthesis of N-Alkoxy Hindered Amine Containing Silane as a Multifunctional Flame Retardant Synergist and Its Application in Intumescent Flame Retardant Polypropylene",Industrial & Engineering Chemistry Research 52, 309-317.

8. Qi, L., Ding, Y., Dong, Q., Wen, B., Wang, F., Zhang, S., Yang, M. 2014. "Photostabilization of polypropylene by surface modified rutile-type TiO_2 nanorods", Journal of Applied Polymer Science, 131(16), 1-9.

9. Miyazaki, K. and Nakatani, H. 2009. "Preparation of degradable polypropylene by an addition of poly(ethylene oxide) microcapsule containing TiO_2", Polymer Degradation and Stability, 94 (12), 2114-2120.

10. Wang, Z., Han, E., Liu, F., Ke, W. 2007. "Thermal behavior of nano-TiO2 in fire-resistant coating", Journal of Materials Science and Technology, 23(4), 547-550.

Investigation of Polymer Foams (Expanded Polymers) and Their Use in Textile

CELEN, Rumeysa[1], ULCAY, Yusuf[1]
[1]Bursa Uludag University, Faculty of Engineering, Department of Textile Engineering
rumeysa@uludag.edu.tr

INTRODUCTION

Nowadays, the application of polymeric components is increasing in scientific and industrial fields. Therefore, the saving in the consumption of these materials is an environmental requirement.[1] There are two different ways to respond to demands to reduce the consumption of fossil fuels:

- ✓ The development of renewable energies and
- ✓ Saving and maintaining energy

Despite the special investments, renewable energies have not been proven profitable as expected because they currently account for almost 15% of total global energy demand.[2-4] Therefore, the development of energy-saving methods is a fundamental way for researchers.

One of the effective ways to save consumable polymer materials is foaming. While reducing the amount of material consumed, this method can improve the properties such as mechanical[5,6] physical[7] and chemical[8] properties as well as sound[9] and thermal[10] insulation.

POLYMER FOAMS

Polymer-based foam materials can be defined as cellular or expanded plastics.[11]They consist of two phases, one of which is the solid polymeric matrix and the other is the gas phase obtained with the foaming agent.[12]

The voids in the polymer reduce the density of the material and allow the use of less raw materials. Besides, the polymer density can be adjusted by controlling the void ratio in the polymer. Thus, polymer foams which has different properties can be produced.[12]

Polymer foams are found virtually everywhere in our modern world. Polymer foams are widely used because they have many advantageous features.[13] Polymeric foams are widely used due to their low thermal conductivity, high strength, excellent thermal and sound insulation properties in comparison to conventional plastic materials.[14,15] The most used polymer foams are PU (Polyurethane), PS (Polystyrene), PE (Polyethylene), PP (Polypropylene), PVC (Polyvinyl chloride) and PC (Polycarbonate).[16]

Polymer foams were classified in Table 1.

Table 1. Classification of polymer foams

Polymer Matrix Material	Cell Morphology	Glass Transition Temperature	Expansion Rate	Foam Cell Size
Thermoplastic	Closed-cell	Rigid	Low density	Macro cell
		Semi-rigid	Medium density	Micro cell
Thermosetting	Open - cell	Flexible	High density	Ultra micro cell
				Nano Cell

POLYOLEFIN POLYMER FOAMS

Polyethylene Polymer Foams

Polyolefin foams have a diverse range of applications, and there are few, if any, industries where these foams are not used.[17] Most polyolefin foams have a closed-cell structure.[18]

PE foam is one of the largest volumetric thermoplastic foams, commercially produced in the early 1940s.[18,19]

PE has a significant worldwide usage due to its chemical resistance, good process ability, low cost, impact resistance and high ductility.[20]

PE foams are used in thermal insulation, electronic packaging, toys, auto parts, household appliances. PE foams have better impact resistance and comfort properties than PP foams in low-temperature applications.[21]

Polypropylene Polymer Foams

Polypropylene foam which was developed by JSP, is one of the most produced polymer foams in the world after polystyrene (PS) foam. It has not only the good properties of polypropylene but also has its own and good mechanical properties.[22,23]

PP foams have a homogenous and closed-cell structure.[24] Resistant to water, oil, chemicals and abrasion.[17,24] Stable thermal conductivity, even in humid environments. Therefore it is an excellent heat-preserving material.[24] It is an environmentally friendly polymer, fully recyclable. Recyclable and reusable, degradation performance is better than PE and PS foams.[17,24] It has outstanding properties such as energy absorption, insulation, heat resistance, impact resistance, immersion and acoustic properties.[17]

PP foams are used in different areas such as the vacuum cleaner body, dishwashers, washing machines, hand mixers and dryers, and the use of household electric appliances. PP foam is a suitable material for vehicle seats, replacing metal structures and simplifying the vehicle platform.

PP foams are ideal for personal protective equipment such as helmets. It is used for console fillings and acoustic applications in buildings and construction sector. It is also ideal for packaging applications of pharmaceuticals, prosthetics and hygienic products. PP foams are also used in sports equipment.[17,24]

RECENT STUDIES ON THE USE OF POLYMER FOAMS IN TEXTILE

Razzaz et al.[25] produced porous hollow fibers made of polymer foam for membrane applications. Azodicarbonamide and low density polyethylene were combined by extrusion. In order to achieve high cell density and uniform cell size distribution, the blowing gas quantity and temperature profile are optimized. It was concluded that membranes with higher cell density had higher gas permeability.

Zhu et al.[26] compared the acoustic properties of conventional open cell PU foams with PE fiber added PU foams. It was aimed to improve the sound absorption properties of PE fiber doped PU foams, ranging in PE fiber content (0.1-0.6 g). The effect of fiber additive on sound absorption and the relationship between additive and absorption coefficient were investigated. With the addition of PE fiber to the PU foam, sound absorption was significantly increased, especially in the low-frequency region (100-630 Hz). 0.1 g PE fiber additive provides optimum sound absorption capability. PE fiber reinforced PU composites showed a higher sound absorption coefficient than PU foam.

Wu et al.[27] produced composite fabrics which were composed of polyester nonwoven fabric, carbon fabric and flexible polyurethane foam. The effect of the weight ratio of polyester nonwoven and the additive ratio of the flame retardant material on the mechanical properties and flame retardant properties of the composite structures were investigated. Mechanical properties improved with increasing weight. The increase in the rate of flammable material also positively affected the flammability of the composite structure. The composite structure is considered as fireproof.

Yan et al.[28] produced composite foam using carbon black, single-walled carbon nanotube and LDPE to obtain low-density polyethylene foam with high electrical conductivity. The electrical conductivity, mechanical properties, microstructure, density and crystallinity of the foam were examined in detail. Carbon black and single-walled carbon nanotubes have been found to have a synergistic effect when used together. 2.88×10^{-5} S/cm electrical conductivity was obtained with the additive of 19% CB and 0.05% SWCNT.

CONCLUSION

With the rapid consumption of energy resources, all states have sought to control their energy needs and use energy effectively. In our country, energy consumption, especially in the industrial and residential sectors, increases every year; most of the energy used in the houses is consumed for heating and cooling purposes.

Since the 1920s, "noise problem" has arisen with the development of industry and lightening of building elements. One of the most effective ways of fighting noise is sound insulation. When investigating sound insulation materials, it has been found out that some of the known thermal insulation materials can also be used in sound insulation. Although not all thermal insulation materials can be used as sound insulation materials, almost all sound insulation materials can also be used as thermal insulation materials.[29]

Polymeric foams are also used in both heat and sound insulation due to their porous structure.[1] Textile materials are frequently used in heat and sound insulation applications due to their porous structure and economical. However, when the literature is examined, limited studies have been found regarding the use of foam polymers in textiles.

Studies have focused on composite structures and composite fabric structures. It can be said that the use of foam polymers in textiles is a subject that is open to research and development.

REFERENCES

1. Hasanzadeh, R., Azdast, T., Doniavi, A., & Eungkee Lee, R. 2019. "Thermal-insulation performance of low density polyethylene (LDPE) foams: Comparison between two radiation thermal conductivity models". Polyolefins Journal, *6*(1), 13-21.
2. Glicksman L., Schuetz M., Sinofsky M. 1987. "Radiation heat transfer in foam insulation." International Journal of Heatand Mass Transfer, , 30(1): 187–197.

3. Campo-Arnáiz R.A., Rodríguez-Pérez M.A., Calvo B.,
4. De Saja J.A. 2005. "Extinction coefficient of polyolefin foams." Journal of Polymer Science Part B: Polymer Physics, 43(13): 1608–1617.
5. Alvarez-Lainez M., Rodriguez-Perez M.A., De Saja J.A. 2008. "Thermal conductivity of open-cell polyolefin foams." Journal of Polymer Science Part B: Polymer Physics, 46(2): 212–221.
6. Cuce E., Cuce P.M., Wood C.J., Riffat, S.B. 2014. "Toward aerogel based thermal superinsulation in buildings: a comprehensive review." Renewable and Sustainable Energy Reviews, , 34: 273–299.
7. Hasanzadeh R., Azdast T., Eungkee Lee R., Afsari Ghazi,A. 2017. "Experimental polymeric nanocomposite material selection for automotive bumper beam using multicriteria decision making methods." Iranian Journal of Materials Science and Engineering, , 14(3): 1–10.
8. Gao K., van Dommelen J.A.W., Geers M.G.D. 2017. "Investigation of the effects of the microstructure on the sound absorption performance of polymer foams using a computational homogenization approach. European Journal of Mechanics-A/Solids," 61: 330–344.
9. Gwon J.G., Kim S.K., Kim J.H. 2016. "Sound absorption behavior of flexible polyurethane foams with distinct cellular structures." Materials & Design, 2016, 89:448–454.
10. Hasanzadeh R., Azdast T., Doniavi A., Lee R.E. 2019."Multi-objective optimization of heat transfer mechanisms of microcellular polymeric foams from thermal-insulation point of view." Thermal Science and Engineering Progress, 9: 21–29.
11. Ünal, H., Yetgin, S. H. 2011. "Enjeksiyonla Kalıplama Yöntemiyle Üretilen PP Köpük Malzeme Özelliklerine Kimyasal Köpük Ajanının Etkisinin İncelenmesi." 6 th International Advanced Technologies Symposium (IATS'11), 16-18 May 2011, Elazığ, Turkey.
12. Yetgin S. H., Ünal H. 2008. "Polimer Esaslı Köpük Malzemeler" Dumlupınar Üniversitesi Fen Bilimleri Enstitüsü Dergisi, Sayı:17, ISSN-1302-3055.
13. Sivertsen, K. 2007. "Polymer Foams". https://ocw.mit.edu/.../3...polymer. .. /-polymer_ foams.pdf (Last Access: 10.08.2017).
14. Sauceau, M., Nikitine, C., Rodier, E., Fages, J., 2008. "Effect of supercritical carbon dioxide on polystyrene extrusion," J. of Supercritical Fluids, 43 (2).
15. Gautam, R., Bassi, A. S., Yanful, E. K. 2007. "A review of biodegradation of synthetic plastic and foams." Applied Biochemistry and Biotechnology, 141(1), 85-108.
16. Jiong S. M. S. 2006. "Application of nanoparticles in polymeric foams" Degree of Doctor of Philosophy, Graduate School of the Ohio State University.
17. Srivastava V., Srivastava R. 2014. "A Review on Manufacturing, Properties and Application of Expanded Polypropylene", MIT International Journal of Mechanical Engineering, Vol. 4, No. 1, January 2014, pp. 22–28.
18. Zhang, Y. Rodrigue, D., Ait-Kadi, A. 2003. "High-density polyethylene foams. I. Polymer and foam characterization." Journal of applied polymer Science, 90(8), 2111-2119.
19. Burillo, G., Adem, E. 1996. In Polymeric Materials Encyclopedia; CRC: Boca Raton, FL, 1996; Vol. 8.
20. Moore SJ and Wanke SE. 2001. "Solubility of ethylene, 1-butene and 1-hexene in polyethylenes". Chem Eng Sci, 56(13): 4121–4129.
21. Nofar, M. Guo, Y.;Park, C. B. 2013. "Double Crystal Melting Peak Generation for Expanded Polypropylene Bead Foam Manufacturing". Ind. Eng. Chem. Res. 52, 2297.
22. Liu, H., Chuai, C., Iqbal, M., Wang, H., Kalsoom, B. B., Khattak, M., Qasim Khattak, M. 2011. "Improving foam ability of polypropylene by crosslinking." Journal of Applied Polymer Science, *122*(2), 973-980.
23. Viot, P., Beani, F., Lataillade, J. L. 2005. "Polymeric foam behavior under dynamic compressive loading." Journal of Materials Science, 40(22), 5829-5837.
24. Yu, L., Zhu, Q., Yu, J. 2013. "Development and application of expanded polypropylene foam." Journal of Wuhan University of Technology-Mater. Sci. Ed., 28(2), 373-379.
25. Razzaz, Z., Mohebbi, A., Rodrigue, D. 2018. "Effect of processing conditions on the cellular morphology of polyethylene hollow fiber foams for membrane applications." Cellular Polymers, 37(4-6), 169-188.
26. Tongtong, Z. H. U., Shuming, C. H. E. N., Wenbo, Z. H. U., Yebin, W. A. N. G., & Jiang, Y. 2019. "Sound Absorption Property

of Polyurethane Foam with Polyethylene Fiber.” Materials Science, 25(1), 85-

27. Wu, L., Ban, J., Jiang, Q., Li, T. T., Shiu, B. C., Huang, S. Y., ... & Lin, J. H. 2019. “Polyethylene Terephthalate/Carbon Fabric/Polyurethane Foam Sandwich Composites: Flame Retardance and Mechanical Properties.” Fibers and Polymers, 20(6), 1277-1283.
28. Yan, Y., Iqbal, A., Wu, C., Wang, Y., Li, G., & Qi, R. 2020. “Electrical conductivity of carbon black/single-wall carbon nanotube/low-density polyethylene ternary composite foam.” Journal of Applied Polymer Science.
29. Binyıldız E. 2017.” Isı Yalıtımı ve Faydaları.” https://www.mmo.org.tr. (Last Access: 27.01.2017).

Comparative Study on the Mechanical Properties and Potential Uses of Enset Yarn in Bio Composite and Technical Textile

TURŞUCULAR, Ömer Fırat.[1*], TEMESGEN, Alhayat Getu. [1], ULCAY, Yusuf. [1]

[1]Textile Engineering Department, Faculty of Engineering, Bursa Uludag University, Bursa, Turkey

Corresponding Authors: omerfirattursucular@gmail.com*

PURPOSE

Enset yarn was low density, abundant, biodegradable and low coat yarn, which were very common agro waste raw material in Ethiopia. Enset yarn's mechanical and morphological properties were studied. Moreover, rupture (Fracture) mechanics were studied to compare with Flax/Linen yarn. Also, to show the potential application of enset yarn would had been used in Bio composite, textile and technical textiles.

Key words: Enset yarn, Flax/Linen yarn, Mechanical properties, Technical textile.

INTRODUCTION

Today, it is known that man made products (synthetic) from petroleum and petroleum derivatives, which are consumable sources, cause harm to health, environment and ecosystem. In addition, scientists are focused their research on natural resources as an alternative of petrochemical materials. They are focusing on unutilized natural fibers that can provide new and similar functions like other bast natural fibers. In this context; Enset fiber, which is a new and effectively non utilized lignocellulose fiber obtained from bast and mid rib of enset plant found in Ethiopia. It has high production possibility in all environmental condition and soil type most part of Ethiopia.

In Atmakuri's research[1]; 5 samples of composite materials with two different natural fibers (Flax/Linen and Hemp) reinforcing materials and one type of matrix material were prepared. Contact angle, flexural strength and shear forces of inter laminar were examined in accordance with ASTM standards. The test result shown that; hybrid composites had higher bending strength and inter laminar shear values compared to pure composites.

In Ayele's research[2]; more than 20 percent of the Ethiopian population; food raw materials, fiber, animal feed, construction materials, access to medicines, etc depending on southern and south eastern Ethiopia have been concentrated for living, In additional, Ethiopia is a country, which has high production of Enset plantation. Enset facility is easy to use as raw material and can be produced for large scale industrial production. It was found that average 6146 Kg/ha Enset was yield in 2012. Enset is one of the potential indigenous crops for food production and can be grown everywhere in Ethiopia. Cultivation is estimated to cover more than 224,400 hectares of land. It which has 53.5 kg enset fiber can be produce after some processes from Enset plant which has about 1000 kg.

In Foulk's research[3]; he stated that the materials that were usually used to meet daily household needs from plastic and metallic materials had negative effects on the ecology and the customers. Therefore, various samples were produced by emphasizing the importance of green composites and three point bending, shear strength and water repellency were investigated. He stated that natural fibers used as reinforcing elements require pretreatment in order to increase their strength. Ecological and cost advantages of using natural fibers were emphasized.

In Liu's research[4]; natural fiber reinforced composite materials had been studied to increase their usage area due to various advantages. The aim of the study; cost, performance improvement, weight reduction and environmental pollution reduction. High performance Flax/Linen fiber had been reported due to its potential to replace glass or carbon as reinforcement. The reinforcing element was made with Flax/Linen fiber by compression molding and the matrix element was epoxidized soybean oil in green composite materials manufacturing. As the concentration of the curing agent increased, the tensile and bending strengths of the fiber / volume ratio increased up to % 10. As a result; the length of the Flax/Linen fiber affected the mechanical properties of the composites. The longer the fiber length, the better the mechanical properties have been observed.

In Romhány's research[5]; the tensile strength of technical linen fibers was determined by applying single fiber tensile test in various fiber lengths (20, 40 and 80 mm) and the results were compared with the literature data. It had been shown that the breaking force of Flax/Linen fibers of each different length corresponds to the two-parameter were manipulated by Fracture mode. According to this model, the technical axial splitting of fibers, mainly owned by the fibers; chemical structure components, radial cracking of the first fibers and fiber breaks. These result reflects the aggregation Flax/Linen fibers from the base structure.

In Temesgen's research[6]; the suitability of linen fiber for the textile sector was mentioned. He emphasized that it was an alternative to glass fibers in terms of cost. It was stated that, it is an innovative and alternative fiber, since it provides most of the various properties expected from composite materials and with its cost advantage. The harvesting methods of Flax/Linen fiber had been mentioned and mentioned several advantages of a combine harvester developed in the United States over the European method. He stated that this harvesting method was called curled enzymatic withdrawal system (CER). High productivity was emphasized. The raw Flax/Linen fibers have a lower density. However, it had similar tensile strength values at a lower cost than glass fibers, and is therefore indicated to provide an environmentally friendly alternative to composites. While the raw linen fibers had various uses for composite materials, it had been emphasized that the optimization studies of the fibers pretreated with enzyme should be done and researches should be done on their usage areas. Flax/Linen fiber had some economic, environmental and mechanical advantages over glass fiber. It had been suggested that these Flax/Linen fibers are thought to be used in place of glass fibers in the composites later.

In Temesgen and Omrakash's research[7]; morphology and characterization of Enset fibers (FBF) modified by pretreatment process were studied. One of the components of the research; Process ability enhancement Enset (False banana fiber(FBF) or yarn has been developed by softening mechanism for the production of a variety of FBF products such as sacks, mats or carpets with a soft touch and industrial application. It has been observed that the properties of these fibers after the pretreatment process are changed due to the chemical and biochemical processes were adapted to the research. Physico-chemical changes in the main structures of the fiber was observed due to pretreatment processes include: weight loss, moisture content/recovery, tensile strength, fineness, bending and torsional stiffness. The results showed that the pretreated FBF had a good elasticity and a good moisture absorbance and was thinner than the untreated FBF. In addition, the treated FBF is a cost-effective alternative to natural jute and sisal in the Ethiopian sack production industry.

In Temesgen's research[8]; he mentioned the origin of the Enset fiber. The research work stated that, how it can be extracted and used in technical textiles, green composites, geotextiles and packaging industry. It was a new alternative fiber to existing bast fibers used in technical textile application. Moreover fiber morphology, physical and mechanical properties of enset fibers were characterized. According to the Study the fiber had; low density (1.2g/cm^3), good moisture absorbance (% 10.85) and low elongation (% 6.39) and moderate tensile strength (428.67 MPa) values. Due to their light weight, abundantly available and low cost use of enset fibers would increase by decreasing the widespread use of synthetic fibers in the bio composite and packaging sector without affecting the desired mechanical properties of products as well as structure.

EXPERIMENTAL

Material

For the comparative study of Physico-mechanical properties of natural fiber, Enset and Flax/Linen yarns were used. Yarn types were determined as independent variables. Yarn counts were determined as fixed variables, 5 repetitions of test were made and their arithmetic averages were taken. As a result of the arithmetic mean, Both Enset and Flax/Linen yarns used for the study had 4.4 Tex number.

Method

Tensile strength tests for the yarns were performed on Shimadzu AG-X Plus under standard atmospheric conditions. Tensile Strength Test (Yarn) Technical Data: Distance between jaws (cm): 20, Load cell (N): 5000, Tensile speed (mm/min): 100 '. It was performed 5 times and the arithmetic averages were taken. Yarn types were considered as independent variables and yarn counts were considered as constant variables. Tensile strength test (Yarn) was applied on the yarns in 4.4 Tex yarn counts. Experimental studies on surface morphology were performed with optical microscope images (x15). In addition, experimental studies on fracture mechanics were carried out by means of photographs taken by camera during tensile strength test (Yarn).

EXPERIMENTAL RESULTS AND DISCUSSIONS

1. Enset yarn

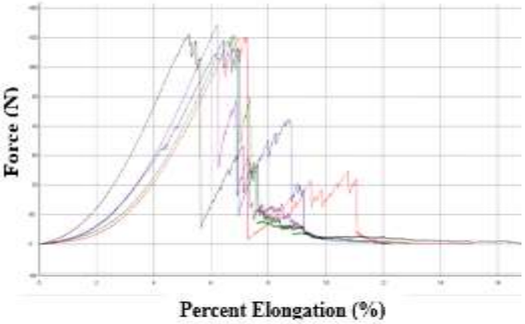

Figure 1. Graphical test results of Enset yarn tensile strength

Table 1. Enset yarn tensile strength test results

Name	Length	Max Force	Max Percent Elongation	Max Gerilme	Max Elongation	Max Shape Change	Max Strain	Max time
Unit	**mm**	**N**	**%**	**N/mm^2**	**mm**	**mm**	**%**	**sec**
1 _ 1	200	421,798	7,17228	421,798	14,3446	14,3446	7,17228	8,67
1 _ 2	200	445,448	6,2307	445,448	12,4614	12,4614	6,2307	7,54
1 _ 3	200	425,467	6,80563	425,467	13,6113	13,6113	6,80563	8,23
1 _ 4	200	423,966	6,5557	423,966	13,1114	13,1114	6,5557	7,93
1 _ 5	200	426,718	5,2306	426,718	10,4612	10,4612	5,2306	6,34
A.M	**200**	**428,6794**	**6,398982**	**428,6794**	**12,79798**	**12,79798**	**6,398982**	**7,742**

- Table 1 was shown that, Enset yarn could be used as an alternative to Flax/Linen yarn in any technical textile areas.
- The maximum breaking force of Enset yarn was 428.67 N.
- Maximum breaking elongation of Enset yarn was 12.79 mm.
- Percent elongation of Enset yarn was % 6.39.
- Percent elongation percentage of Enset yarn for the test was 6.39% at Breaking times of 7.74 seconds.

Figure 2. Optic Microscopic view of enset yarn (x15)

When the optical images (x15) of enset yarn were examined in microscope, it had been observed that the fibers of the set yarn had little parallelism in the direction of the fiber axis.

Breaking mechanics of Enset yarn depending on the results of tensile test. Breaking Mechanics of Enset Yarn; Because the weak distribution of lignocellulose contain of the fiber, non-uniformly distribution of fiber in enset yarn with respect to the direction of the fiber axis, and the impurities had relatively high effect on the overall effect of the yarn Physico-mechanical performance. It was observed that, the yarn was broke in the upper and lower region of the yarn instead of breaks from the most central regions.

In addition, it was observed that a same number of large diameter fibers in the yarn was perpendicular to the fiber axis and relatively heterogeneous due to their higher pack ability. The angle in the y - axis direction is often close to 30 - 45 degree and observed protrude longer fibers.

Enset fiber had some advantages over linen fiber as follows; low density (lightness), cheapness, ease of cultivation and draught tolerance (can be grown in areas where water is low), Although Flax/Linen fiber can grow in sandy soil, while Enset fiber can grow in all kinds of soil. Having longer fibers, linen was usually mechanical in the yarn production stages but chemical processes were available in the decay stage, while Enset fiber had mechanical processes in all stages. (Peeling process).

2. Flax/Linen yarn

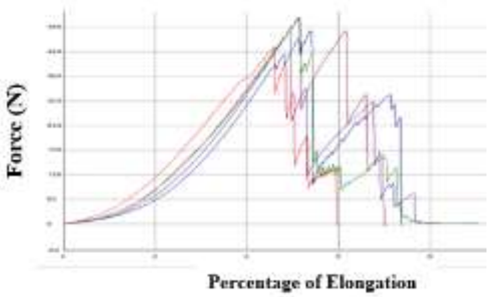

Figure 3. Graphical test results of Flax/Linen yarn tensile strength

Table 2. Flax/Linen yarn tensile strength test results

Name	Length	Max Force	Max Percent Elongation	Max Gerilme	Max Elongation	Max Shape Change	Max Strain	Max time
unit	**mm**	**N**	**%**	**N/mm^2**	**mm**	**mm**	**%**	**sec**
2 _ 1	200	505,432	5,15563	505,432	10,3113	10,3113	5,15563	6,25
2 _ 2	200	472,291	4,93898	472,291	9,87795	9,87795	4,93898	5,99
2 _ 3	200	522,9	5,53903	522,9	11,0781	11,0781	5,53903	6,71
2 _ 4	200	503,151	5,11393	503,151	10,2279	10,2279	5,11393	6,2
2 _ 5	200	471,953	5,4057	471,953	10,8114	10,8114	5,4057	6,55
A.M	**200**	**495,1454**	**5,230654**	**495,1454**	**10,46133**	**10,46133**	**5,230654**	**6,34**

As shown Table 2;

- Maximum value of breaking force for Flax/Linen yarn was 495.14 N.

- Maximum value of breaking elongation was 10.46 mm for Flax/Linen yarn.

- Percent elongation of Flax/Linen yarn was % 5.23.

- Times for breaking Flax/Linen yarn for this test was 6.34 seconds.

Figure 4. Optic Microscopic view of Flax/Linen yarn (x15)

When the optical microscope view (x15) was observed, it has been that the fibers of the Flax/Linen yarn had a considerable degree of parallelism in the direction of the fiber axis.

Based on the tensile test results: the breakage mechanics of Flax/Linen yarn are examined; due to the weak spot effect, the Flax/Linen yarn had relatively light brown in the color and the impurities were relatively low as compared with Enset fiber. The fractures from the most central regions were generally observed. In addition, it was observed that a large number of small diameter fibers perpendicular to the fiber axis. Like enset fiber it was observed that the yarn was relatively homogeneous and the angle in the y - axis direction is close to 90 degree. Form this result, it was generalized that the two yarn could be used alternatively so enset yarn could be substitute most yarn obtained from most natural fiber like Flax/Linen, jute, sisal and banana fibers.

CONCLUSIONS

- Because of environmentally friendly, biodegradable nature of the materials; Enset fiber/yarn was could be used in various textile and technical textile fields.

- Enset yarn could be considered as an alternative to Flax/Linen and cotton yarn after pretreatment with a certain concentration of NaOH in technical textiles and in extra-bodily medical textile applications such as face masks, surgical gowns and bandages.

- In conventional textiles; can be used in home textiles for ornamental and decorative purposes. It was envisaged that in winter garment fabrics, the mixture will be used in winter garments by increasing the thermal insulation by increasing the heat insulation with the air to accumulate in the spaces between the fibers by using a low proportion of the yarn.

- The yarn had similar mechanical properties like most natural fibers such as jute, ramie and sisal, which are used in agricultural textiles (Big bags) and packaging textiles (Food packaging), and automotive textiles (Floor coverings) bottom panel, side panel or ceiling coverings). Because of its abundantly available, light weight, drought tolerance and low production cost, set fiber/yarn was used without affect the desired all properties.

SUGGESTION FOR FURTHER WORK

- Some future work in connection with experimental research;

- Enset fiber, which is agricultural waste will be used in different areas by designing special production methods to reduce the increasing environmental pollution and global warming. Also will be used in various forms of textile structures (woven, knitted, nonwoven surfaces, braiding).

- By measuring and comparing heat conduction coefficients with other natural fibers used for thermal insulation in winter garments such as wool.

- Some physical quality control tests such as UV, water repellency and air permeability can be carried out on various physical performance values.

ACKNOWLEDGEMENT

The authors gratefully acknowledge and express our sincere thanks to High Textile Engineer Mehmet TİRİTOĞLU for his supporting and allowing to use all the necessary laboratory equipment's for this study.

LITERATURE

[1]. Atmakuri, A. Palevicius, A. Griskevicius, P. Janusas, G. 2019. ‘’Investigation of Mechanical Properties of Hemp and Flax Fibers Hybrid Composites for Biomedical Applications‘’. MECHANICA. 25 (2), 149-155. Ayele,

[2]. A. Sahu. O. 2014. ‘’ Extension of Enset Plant Product for Rural Development in Ethiopia ‘’. Journal of Agricultural Economics, Extension and Rural Development, 2 (3), 031-040.

[3]. Foulk. J. A. Akin. D. E. Dodd. R. B. 2000. ‘’ New Low Cost Flax Fibers for Composites ‘’, SAE 2000 World Congress Detroit, Michigan, 1-13.

[4]. Liu, Z. Sevim. Z. E. Akın. D. E. Barton. F. E. 2006. “Green Composites from Renewable Resources: Preparation of Epoxidized Soybean Oil and Flax Fiber Composites‘’, J. Agric. Food Chem, 54 (1). 2134−2137.

[5]. Romhány, G. Karger-Kocsis, J. Czigány, T. 2003. ‘’Tensile fracture and failure behavior of technical flax fibers‘’. Journal of Applied Polymer Science. 90 (13), 3638-3645.

[6]. Temesgen, A. G. Sahu, O. 2014. ‘’Green Composite Material from Agricultural Waste‘’, International Journal of Agricultural Research and Review. 2 (5). 056-062.

[7]. Temesgen, A. G. Sahu, O. 2014. ’’Process Ability Enhancement of False Banana Fibre for Rural Development‘’, Journal of Agricultural Economics, Extension and Rural Development, 1 (6). 064-073.

[8]. Temesgen, A. G. Eren, R. Aykut, Y. 2019. ‘‘Investigation and Characterization of Fine Fiber from Enset Plant for Biodegradable Composites‘’, 17th National 3rd International the Recent Progress Symposium on Textile Technology and Chemistry, Bursa, Turkey. 356-361.

Şerbetçi otu ((Humulus lupulus L.)Bitkisi Gövde Lif Özelliklerinin İncelenmesi

TURAN CANDAN Nurcan, ALBAYRAK Mert, DESTİCİ İrem, EVREN Ayşegül,
BALKAN Berk, CANDAN Alp Eren
Eskişehir Emine Emir Şahbaz Bilim ve Sanat Merkezi
nurcancandan26@gmail.com.tr

AMAÇLAR

Şerbetçi otu((*Humulus lupulus L.*)bitkisi gövde lif özelliklerinin incelenerek kullanım alanlarının araştırılması

GİRİŞ

Şerbetçiotu bitkisi ekimi yapıldıktan sonra 2 yıl boyunca ürün alınamamaktadır devamında yirmi hatta otuz yıla kadar ürün alınabilmektedir. Bitkinin çok yıllık olan kısmı kökleridir. Yaklaşık 8 – 10 m.'ye uzanan sarılıcı gövdesi ve yaprakları hasat sonrası ölür, ertesi yıl yeni gövdeler sürer. Bu yüzden hasattan üç – dört hafta sonra toprağın üzerinden sürgünler budanır. (Bağcı ve ark.., 2008) Hasat sonrası bu gövdeler kurur ve toplanır. Çoğu kez atıl durumda olan gövdeler ekonomik yönden değerlendirilememektedir.. Bu çalışma da şerbetçi otu bitkisinin gövdesinden lif eldesi ve lif özelliklerinin incelenmesi açısından önemlidir. Tarımsal atıkların değerlendirilmesi, ekonomik ve çevre dostu özelliklerinden dolayı şerbetçi otunun gövde lifleri önemli bir hammadde kaynağı olacaktır. Konu ile üniversite, özel sektör arasında ARGE çalışmalarının yapılması önerilir.

DENEYSEL

Malzeme

Şerbetci otu (*Humulus lupulus L*) gövde lifleri

Yöntem

- Liflerde
- Havuzlama
- Zamk çıkarma
- Kırma ve temizleme
- Mikroskop görüntüsünün alınması
- Fiziksel özelliklerinin belirlenmesi
- Su tutma kapasitesinin ölçülmesi testi
- Kimyasal reaktiflere karşı özelliklerinin belirlenmesi:

Işlemleri yapılmıştır.

DENEYSEL SONUÇLAR/TARTIŞMA

Lif özelliklerinin belirlenmesi

- Lif Uzunluğu (mm) 8,48 ± 0,41
- Lif Genişliği (µm) 23,08 ± 3,54
- Lümen Genişliği (µm) 18,2 ± 2,84
- Lif Çeper Kalınlığı (µm) 11,7 ± 0,33
- Elastiklik Oranı 78.85
- **Lineer yoğunluk ölçümü**
  - Lifin Numarası (Tex) = Ağırlık (g)×100000 / Uzunluk (cm)
  - Tex= 1000 metre elyafın gram cinsinden uzunluğudur
  - Lif uzunluğu(ort):100 cm
  - Lif ağırlığı(ort):0,00944
  - 9,4

Zaman dk	Isırgan	Keten	Kenevir	Şerbetçiotu
5	29	26	27	24
10	39	29	30	32
15	47	32	36	38
20	49	38	42	41
25	49	38	42	44

Tablo 1 Diğer liflerin nem iletkenliği (mm)

Isırgan bitkisinden elde edilen liflerin nem iletkenliğinin ve su tutma kapasitesinin en iyisi olduğu gözlemlenirken, şerbetçi otunun nem iletkenliği ve su tutma kapasitesinin kenevirden büyük olması yine şerbetçiotunun gövdesinden elde edilen liflerin tekstil alanında kullanılabileceğini göstermektedir.

GENEL SONUÇLAR

Şerbetçiotunun gövde liflerinin doğal bir endüstriyel hammaddesi olması, ısırgan ve kenevir lifleri ile benzer özellik taşıması, lif çıkarma işleminin ekonomik ve kolay olması, ülkemiz de bitki için hammadde ihtiyacının olması önemli ekonomik kazanımlar sağlanacaktır.Tarımsal atıkların değerlendirilmesi, ekonomik ve çevre dostu özelliklerinden dolayı şerbetçi otunun gövde lifleri önemli bir hammadde kaynağı olacaktır

SONRAKİ DÖNEM ÇALIŞMALARI

Şerbetçiotundan elde edilen liflerden yararlanarak el yapımı doğal kağıt yapımı denemeleri yapılmıştır.

TEŞEKKÜR/BILGILENDIRME/FON KAYNAĞI

Çalışma da Eskişehir Orman Bölge Fidanlığı Müdürlüğünden destek alınmıştır.
Lifler Bilecik Pazaryerinden elde edilmiştir.

KAYNAKLAR

1. Akgül, Mehmet, Et Al. "Isırgan Otu (Urtica Dioica L.) Saplarının Kimyasal Analizi." Ulusal Akdeniz Orman Ve Çevre Sempozyumu (2011).)
2. Bağcı, İlker, Er, Celal Ve Gürbüz, Bilal. (2008). Şerbetçiotu Yetiştiriciliği. Ziraat Mühendisliği Dergisi, (350), S. 8 – 13, Ankara
3. Başkaya, Zafer. "Bilecik İlinde Şerbetçiotu Üretiminin Coğrafi Esasları/The Geographical Foundations Of Hops Production İn Bilecik." Doğu Coğrafya Dergisi 16.25 (2011).
4. Baytop, T., 1984, Türkiye'de Bitkiler İle Tedavi (Geçmişte Ve Bugün), İstanbul Üniversitesi Yayınları No: 3255, İstanbul.
5. Baytop, T., 1999. Türkiye'de Bitkiler İle Tedavi, Geçmişte Ve Bugün (İkinci Baskı). Nobel Tıp Kitapevi, S. 480, İstanbul
6. Bellmann Ve Ark,2005. Bellmann, C., A. Caspari, V. Albrecht, T.T. Loan Doan, E. Mader, T. Luxbacher And R. Kohl, (2005). Electrokinetic Properties Of Natural Fibres. Colloids And Surfaces A: Physicochem. Eng. Aspects, 267: 19–23.
7. Brink, M. And R.P. Escobin, (2003). Plant Resources Of South-East Asia: Fibre Plants. P.301–333. Backhuys Publishers, No: 17, Leiden
8. Bulut, Yasemin; Erdoğan, Ümit Halis. Selüloz Esaslı Doğal Liflerin Kompozit Üretiminde Takviye Materyali Olarak Kullanımı. Tekstil Ve Mühendis, 2011, 18.82
9. Çelik, S., Konkan, R., Erkmen, H., Tabo, A., & Erkıran, M. (2007). Bitkisel İlaçlar Ve Psikiyatride Kullanımı. Düşünen Adam, 20, 186-95.
10. Doğanay, H., 1998, Türkiye Ekonomik Coğrafyası . Çizgi Kitabevi Yayınları, Konya
11. Gedik, Görkem, Osman Ozan Avinç, And Arzu Yavaş. "Kenevir Lifinin Özellikleri Ve Tekstil Endüstrisinde Kullanımıyla Sağladığı Avantajlar." Tekstil Teknolojileri Elektronik Dergisi 4.3 (2010): 39-48.
12. Gücüş, Mehmet Onurhan, And Hüdaverdi Eroğlu. "Türkiye'de Doğal Olarak Yetişen Titrek Kavak Odununun (Populus Tremula L.) Lif Morfolojisi Ve Kimyasal Yapısının İncelenmesi." 55.
13. Kalaycı, Ece, Et Al. "Tarımsal Atıklardan Elde Edilen Sürdürülebilir Tekstil Lifleri: Ananas Yaprağı Lifleri." Sakarya Üniversitesi Fen Bilimleri Enstitüsü Dergisi 20.2 (2016): 203-221
14. Kireççi, M.,"Farklı Ortamlardan İzole Edilen Bakterilerle Lignin Biyodegradasyonunun Araştırılması", Yüksek Lisans Tezi, Kahramanmaraş Sütçüİmam Üniversitesi Fen Bilimleri Enstitüsü, Biyoloji Anabilim Dalı, Kahramanmaraş,(2006).
15. Konak, Sema. Bamya Bitkisinden Suda Çürütme Yöntem İle Lif Elde Edilmesi Ve Elde Edilen Lifin Çeşitli Fiziksel Kimyasal Ve Mekanik Özelliklerinin Ölçümü. Diss. Pamukkale Üniversitesi Fen Bilimleri Enstitüsü, 2014.
16. Kurban, Mutlu, Et Al. "Isırgan Otu Lifi Ve Özellikleri." Tekstil Teknolojileri Elektronik Dergisi 5.1 (2011): 84-106.
17. Mangut, M.,Karahan, N., Tekstil Lifleri, Ekin Basın Yayın Dağıtım, 36-62-63, (2008).
18. Saatçioğlu, Kenan. "Geleneksel Bir Türk El Dokuması: Rize Bezi (Feretiko)." Atatürk Üniversitesi Güzel Sanatlar Fakültesi Sanat Dergisi 25 (2014): 93-105.
19. Sönmez, A.E., (2007). Kâğıt Ürünleri Sanayi. T.C. Başbakanlık Dış Ticaret Müsteşarlığı, _İhracatı Geliştirme Etüt Merkezi.
20. Şafak, Bora. Türk Bira Sektörü Analizi Ve Türk Bira Firmalarının İhracat Olanakları. 2006. Phd Thesis. Deü Sosyal Bilimleri Enstitüsü.
21. Şahin, Güven; Üçışık Erbilen, Süheyla. Türkiye'de Yetiştirilen Keyf Bitkiler İçerisinde Özel Bir Tür: Şerbetçiotu (Humulus Lupulus L.). Zeitschrift Für Die Welt Der Türken/Journal Of World Of Turks, 2012, 4.3: 237-258.
22. Yaman,B Trabzon Koşullarında Yetiştirilen Kiwi (Actinidia Deliciosa (A. Chev.) C. F. Liang & A. R. Ferguson)'Nin Lif Morfolojisi Süleyman Demirel Üniversitesi Orman Fakültesi Dergisi Seri: A, Sayı: 2, Yıl: 2005, Issn: 1302-7085, Sayfa: 14

Tekstil Uygulamaları İçinTDI-PEG400, PG400 Etkileşimi ile Üretilen Poliürütan Koku Kapsülleri ve Salım Davranışları

ÖZSEVİNÇ,Ali[1] , ALKAN, Cemil[2]
[1]Gaziosmanpaşa Üniversitesi, Tekstil Programı,Taşlıçiftlik Kampüsü, 60240 Tokat
[2]Gaziosmanpaşa Üniversitesi, Kimya Bölümü, Taşlıçiftlik Kampüsü, 60240 Tokat
ali.ozsevinc@gop.edu.tr

AMAÇLAR

Tekstil malzemelerinde kullanılmak üzere, kontrollü salım mekanizması ile koku salımı yapabilen mikrakapsül-parçacıklar, arayüzey polimerizasyon tekniği kullanılarak TDI-PEG400, PG400 etkileşimi ile uçucu lavanta yağı kapsüllenmiştir. Mikrokapsül-parçacıkların karakterizasyonu FTIR, parçacık büyüklüğü, polarize optik mikroskop (POM) ve taramalı elektron mikroskop (SEM) analizi ile yapılmış, ayrıca düzenli ağırlık takibi ile kontrollü salım, özellikleri belirlenerek, tekstil uygulamaları için kullanılabilirliği araştırılmıştır.

GİRİŞ

Mikrokapsülleme teknikleri sayesinde de küçük boyuttaki mikrokapsüllerin üretimi yapılarak, tekstil sanayinde kumaşlara uygulanması ile konfor özellikleri iyileştirilebilmekte ve ekstra özellikler sağlanabilmektedir. Mikrokapsülleme tekniği yaygın olarak faz değiştiren maddelerin kapsülenmesi ile tekstilde termal konforun iyileştirilmesi üzerine yoğunlaşmaktadır[1]. Koku maddeleri tekstil materyallerine uçucu özelliklerinden dolayı direk olarak uygulanamamaktadır. Bu yüzden koku maddelerinin bir duvarla kapsülleyerek dış etkilerden korunması sağlanarak tekstil malzemelerine aplike edilmektedir[2,3]. Dış kabuk olarak poliüretan ve poliüre sistemlerinde en etkili yöntem iyi mekanik özelliklerinden dolayı ara yüzey polimerizasyonudur. Ara yüzey polimerizasyonun da birbirine karışmayan su ve organik fazın kesişme noktalarında, monomerler arasındaki reaksiyondan dolayı çekirdek maddesinin yüzeyinde polimer bir zar oluşur. Birbirine karışmayan su ve organik faz karıştırılarak temas eden yüzey alanı artırılır. Çekirdek maddesindeki monomer, içine jelleştirici bir monemer çözündürülmüş sıvı faza dispers edilir, daha sonra sıvı faz ve organik faz karıştırılarak kapsül üretilir. Reaksiyon çok hızlı gerçekleşir ve karıştırıcı hızına göre kapsül büyüklükleri değişir[4].

Poliüretanlar tekstil endüstrisinde elastomerik liflerin üretiminde kullanılmaktadır. Poliüretan elastomerlerin üretiminde farklı isosiyanat ve dioller kullanılarak yapıda sert ve yumuşak birimlerin beraber bulunması sağlanır. Yumuşak bölgeler uzama yeteneğinin oluşmasını sağlar ve amorf yapıda olup kolaylıkla deforme olurlar. Sert bölgeler ise kısadır ve polimer zincirleri arasında çapraz bağ oluşturarak yapının birarada kalmasını teşkil eder[5].

Çalışma kapsamında , arayüzey polimerizasyon tekniği kullanılarak lavanta koku maddesinin, toluen diizosiyanat ve PEG 400 PG400 ile kapsül üretimi gerçekleştirilmiştir. Koku salan kapsüllerin kimyasal karakterizasyonu Fourier transform infared (FTIR), parçacık boyutu analizi, optik mikroskop (POM), taramalı elektron mikroskop (SEM) görüntüleri ve konrollü salınım hızı ölçülerek yapılmıştır.

DENEYSEL

Malzeme

Toluen 2,4-diiziosiyanat (TDI), Acros Organics, Propilen glikol 400 (PG400) ve Polietilen glikol 400 (PEG400), Sigma Aldrich, Polivinil alkol (Moviol 3-96), Sigma Aldrich, Dibütiltindilaurat (DBDTL), Merck ve Lavanta uçucu yağı, Tokat ilinde doğal olarak yetiştirilen lavanta çiceğinden elde edilerek katkısız olarak (Kocatürk eczanesi) çalışmada kullanılmıştır.

Yöntem

Tablo 1' de belirtilen kimyasal miktarları ile arayüzey polimerizasyon tekniği kullanarak ceketli cam reaktörde 70 °C' de, 200 d/dk karıştırma hızında, 2 saat karıştırılarak mikrokapsül üretimi gerçekleştirilmiştir. Daha sonra % 30 'luk etanol ile yıkama yapılarak oda sıcaklığında kurutulmuş ve kimyasal karekterizasyonları yapılarak, salım hızları tespit edilmiştir.

Tablo1. Yağ ve su fazlarının yapı ve kimyasal sistemi

	Faz	Koku(mL)	Su(mL)	İzosiyanat (mL)	PVA(gr)	PEG_{400}-PP_{400}(mL)	DBDTL (mL)
PEG_{400}	Yağ	20		7,5 TDI			
	Su_1		120		2		
	Su_2		60			18,7 PEG	0,5
PP_{400}	Yağ	20		7,5 TDI			
	Su1		120		2		
	Su2		60			10,4	0,5

DENEYSEL SONUÇLAR/TARTIŞMA

Parçacık Büyüklüğü Sonucu: Parçacık boyutu ölçümü öncesinde mikrokapsüller su ve yüzey aktif madde (Triton- X 100, 2-3 damla) ile homojenizatör ile 10000 dev/dk hızda 15 dk karıştırılarak Malvern marka parçacık ölçerde yapılmıştır.

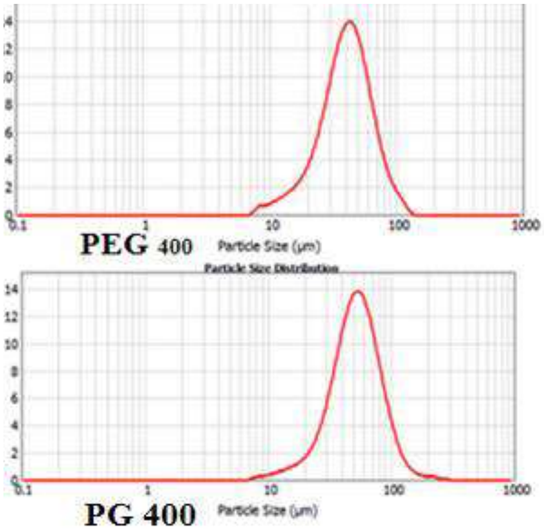

Şekil 1. Parçacık büyüklüğü sonuçları

Ortalama parçacık büyüklüğü PEG 400 ile üretilen mikrokapsüllerde 40,94 µm olarak bulunmuş olup, mikrokapsüllerin parçacık boyutu 20,77 µm ile 70,49 µm arasında değişmektedir. PG 400 ile üretilen kapsüllerde ise ortalama 50,23 µm olarak bulunmuş ve 27,64 µm ile 90,89 µm arasında değiştiği tespit edilmiştir. Parçacık büyüklüğü dağılımı Şekil 1'de gösterilmiştir.

Optik Mikroskop Görüntüleri (POM): Koku kapsüllerinin polarize optic mikrokop görüntüleri 1200 kat büyütme yapılarak, Leica marka polarize optik mikroskopta görüntüleme yapılmış ve Şekil 3'de gösterilmiştir.

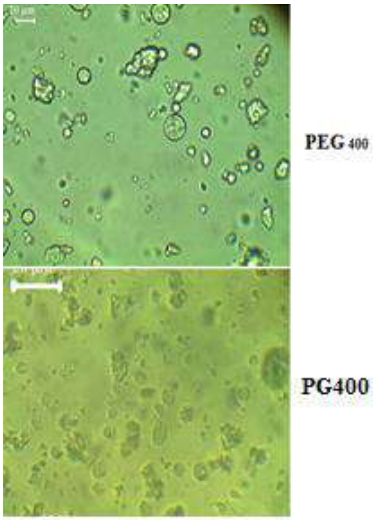

Şekil 3. Polarize optik mikroskop görüntüleri.

SEM Görüntüleri: Koku kapsülerinin FE-SEM, MİRA III, TESCAN marka cihazda görüntülenerek kapsül şekil, kabuk yapısı ve kapsül büyüklükleri Şekil 4'de gösterilmiştir.

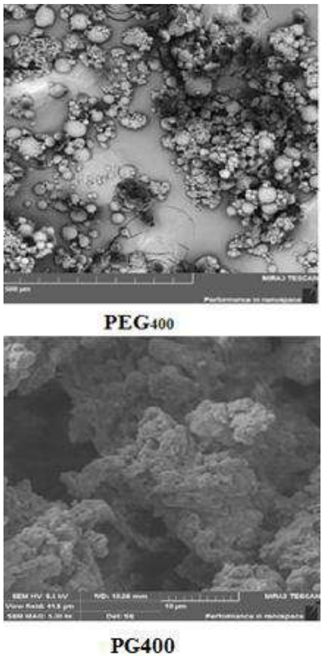

Şekil 4. Kontrol salım önce ve sonrasında SEM görüntüleri.

SEM görüntülerine göre PEG 400 ile üertilen mikrokapsüllerin dairesel olarak ve parçacık sonucuna parelel olarak ortalama 50 µm üretildikleri tesbit edilmiştir. PG400 ile üretilen kapsüllerin ise kapsülden ziyade mikroparçaçık olarak üretildikleri görüntülenmiştir.

FTIR Sonucu: FTIR spektroskopisi ile kimyasal yapı analizinde mikrokapsüller, mikrokapsül üretiminde kullanılan duvar ve çekirdek maddelere ait spektrumlar incelenmiş ve mikrokapsül yapısında koku ve duvar polimerinin mevcut olup olmadığı araştırılmıştır.

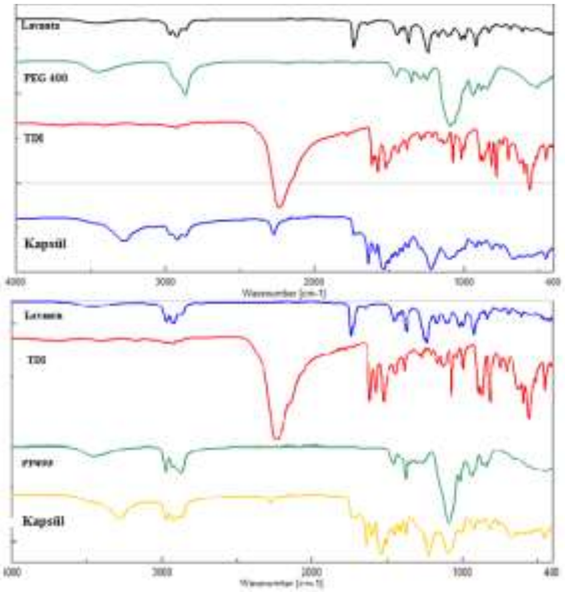

Şekil.5 FTIR analiz sonucu.

Tablo 2. Kapsüllerin pik cinsi ve dalga numarası

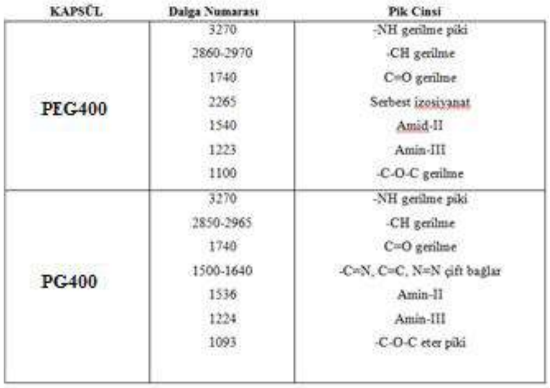

KAPSÜL	Dalga Numarası	Pik Cinsi
PEG400	3270	-NH gerilme piki
	2860-2970	-CH gerilme
	1740	C=O gerilme
	2265	Serbest izosiyanat
	1540	Amid-II
	1223	Amin-III
	1100	-C-O-C gerilme
PG400	3270	-NH gerilme piki
	2850-2965	-CH gerilme
	1740	C=O gerilme
	1500-1640	-C=N, C=C, N=N çift bağlar
	1536	Amin-II
	1224	Amin-III
	1093	-C-O-C eter piki

Kontrollü Salınım Sonucu: Üretilen koku kapsülleri hassas terazide 24 saatte bir 30 gün boyunca ağırlık ölçümü yapılmış ve koku maddesinin kapsül duvarından uzaklaşarak ortama koku salması ağırlık kaybı ile araştırılmıştır.

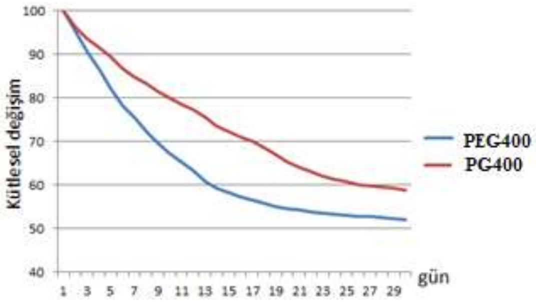

Şekil 6. Kontollü salınımın kütlesel değişimi.

Koku kapsülleri 30 gün boyunca düzenli olarak koku salımı yaparak ağırlığının yaklaşık % 40-50'sini kaybettiği görülmektedir. PEG400 ile üretilen kapsüller daha hızlı salım yaparken, PG400 ile üretilen kapsüller daha düzenli salım yapmıştır.

GENEL SONUÇLAR

Lavanta koku maddesini TDI-PGetkileşimi ile poliüretan kabuk ile kapsülleyerek tekstil malzemelerinde kullanılmak üzere mikro boyutta kapsül üretimi gerçekleştirilmiştir. Kapsüllerin parçacık boyutu analizlerinde mikro boyutta olduğu ve zamana bağlı olarak kontrollü salım ve kırılma mekanizması ile koku maddesinin kapsülden uzaklaşarak ortama koku verdiği görülmüştür.

KAYNAKLAR

[1] Nelson, G. 2002. ''Application of microencapsulation in textiles'',International Journal of Pharmaceutics, 242(1) 55-62.

[2] Rodrigues, S.N. Fernandes, I. Martins, I.M. Mata, V.G. Barreiro, F. Rodrigues, A. E. 2008. ''Microencapsulation of Limonene for Textile Application'', Industrial & Engineering Chemistry Research, 47, 4142–4147.

[3] Hong, K., Park, S., 1998. ''Preparation of polyurethane microcapsules with different soft segment and their caharacteristics'', Reactive & Functional Poymers, 42, 193-200

[4] Bouchemal, K., Briancon, S., Fessi, H., Chevallier, Y., Bonnet, I., Perrier, E., 2006. Simultaneous emulsification and interfacial polycondensation for the preparation of colloidal suspensions of nanocapsules. Materials Science & Engineering C-Biomimetic and Supramolecular Systems 26, no. 2-3, 472-480.

[4] Petrovic, Z.S. Ferguson, J. 1991. ''Polyurethane elastomers '', Progress in Polymer Science, 16 (5),695-836.

Surface modification of polyethylene by a simple post-treatment method

SEYHAN, Aybeniz[1], GUNAYDIN, Beyza Nur[1], POLAT, Yusuf[1,2], KILIC, Ali[1,3], DEMIR, Ali[1,3], AVCI, Huseyin[4,5]
[1]TEMAG Labs, Textile Tech. and Design Faculty, Istanbul Tech. Uni., Istanbul, Turkey
[2] Mechanical Engineering, Faculty of Engineering, Marmara Uni., Istanbul, Turkey
[3] Textile Engineering, Textile Tech. and Design Faculty, Istanbul Tech. Uni., Istanbul, Turkey
[4] Metallurgical and Materials Engineering, Engineering - Architecture Faculty, Eskisehir Osmangazi Uni., Eskisehir, Turkey
[5]AvciBio Research Group, Eskisehir Osmangazi University, Eskisehir, Turkey www.avcibio.com
havci@ogu.edu.tr

PURPOSE

Corona discharge method has been studied to increase the adhesive property of the polyethylene surface. Different sets of design parameters were applied to investigate the effect of atmospheric plasma treatment onto linear low-density polyethylene (LLDPE) fibers produced by our modified melt-spinning line.

INTRODUCTION

Polyethylene (PE) has a leading usage portion in polymer industries including filament production and composite materials. Performance fibers having high tensile strength can be used alone or as a composite material in thermoset or thermoplastic resins. Due to its simple chain structure, lack of functional groups and non-polar nature, polyethylene surfaces show poor adhesion and incompatible fiber-resin interface which significantly affects the mechanical properties of composites. Therefore, the surface properties of PE fibers to be produced in a modified melt spinning line need improvement. For this purpose, corona discharge, which is counted as a physical modification method, provides an environmentally friendly and effective treatment[2]. Studies reveal that plasma treatment effectively increases surface roughness and functionality, and then various grafting and silane coatings may be applied to it for further improvement on the adhesive behavior of polyethylene[1].

EXPERIMENTAL

Material

The ASPUN™ 6000 linear low-density polyethylene (LLDPE) MFI, 19 and density, 0.935 g/cm^3 was received from Dow Chemical Company.

Method

Polyethylene films were prepared by a laboratory scaled film extrusion machine with 0.07 mm thickness. Monofilament fibers were produced by a single screw extruder melt spinning line with 0.6 mm spinneret diameter at 2250 m/min take-up speed. SIMCO ION CM5 device with point to plane geometry was used for discharge. The effect of electrostatic charge application was detected by SIMCO ION TM FMX-003 electrostatic field meter. Contact angle measurements were done according to the static sessile drop method at temperature 23°C with a KSV Attension Theta Lite optical tensiometer.

EXPERIMENTAL RESULTS AND DISCUSSIONS

Prior to applying corona discharge on melt-spun LLDPE filaments, 0.07 mm thick film samples of the same polymer have been prepared. They have been processed in atmospheric conditions according to parameters described in Table 1. The working distance between the electrodes and the PE surfaces was set to 6 cm for all samples. Achieved surface modification is showed to be time-dependent. Electrostatic field measurements indicate that higher voltage applications are efficient in the short run. Nevertheless, the application of relatively lower voltage (20 kV) peaks in a longer time period.

Table 1. Electrostatic field measurements (FM) of identical LLDPE film samples with the various voltage applications.

Sample	Applied Voltage (-kV)	FM (kV, t=0 min)	FM (kV, t=5 min)	FM (kV, t=10 min)	FM (kV, t=15 min)
1	20	0.1	-1.0	-0.4	-2.0
2	25	0.1	-1.0	-2.9	-2.5
3	30	0.1	-2.0	-4.2	-3.7

Contact angle with the water on the film samples has been investigated. Regarding to the primary experiment, discharge voltage has been decreased to 15 kV, and working distance has been set to 5 mm. As given in Table 2, the wettability of PE samples has been improved gradually as the discharge duration increased. A drop of 14.5% surface tension between the control and treated sample has been achieved, which is an indication of surface energy increase.

Table 2. Electrostatic field measurements (FM) of identical LLDPE film samples with the various voltage applications at 5 mm working distance.

Sample	Applied Voltage (-kV)	Duration (min)	Contact Angle (°)
Control	-	-	77.1±0.3
1	15	5	68.3±1.9
2	15	10	65.9±0.7

According to the literature, the experimental design has been rearranged for fiber application. Working distance was kept at strictly 5 mm, which has been proved to be efficient. The literature has shown that voltages applied in the range of 10-15 kV have an increasing effect on PE surface wettability and adhesion performance[1,3,4].

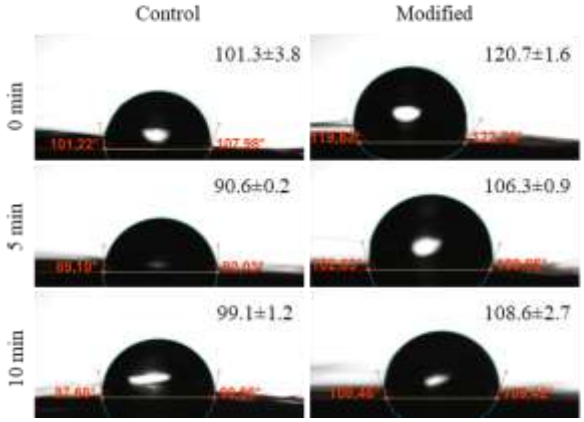

Figure 1. Comparison of the contact angle measurements of 10 kV charged both control and modified filament samples.

The modification in the melt-spinning line results in a straighter fiber alignment and higher surface tension. Line-modified fibers showed a higher degree of hydrophobicity in comparison with the control sample. When control and modified fibers are exposed to corona treatment at 10kV, their hydrophobic character weakens, and contact angles have been decreased for both sets of fibers. Longer process time results slightly worse than the 5-min procedure. In a short interval of application time, modified fiber's wettability behavior (CA 106.3°) resembles the one of untreated control samples (CA 101.3°) with an 12% increase.

CONCLUSIONS

Film and melt-spun filament samples have been produced with LLDPE. Corona treatment on film surfaces showed that lower voltage with a shorter distance between electrodes and surface results in a longer-lasting charge effect. Applications on filaments demonstrated that better hydrophilicity can be achieved with a narrow time window. Modified melt-spinning line allows fibers to be produced with higher tensile properties in comparison with conventional melt-spinning production. However, it decreases the LLDPE fibers' wettability. Corona treatment restores and advances its adhesive behavior in measure of hydrophilicity. Same to better results with shorter treatment duration enables the possibility of in-line plasma modification of fibers along the melt-spinning line.

FUTURE STUDIES

The effect of corona discharge on fibers will be investigated for medium and high-density PE. Upon reaching the optimum wettability, mechanical performance of the fibers, which are produced by our modified melt-spin line, are planned to be evaluated in composite applications.

ACKNOWLEDGMENTS

The authors are grateful to TUBITAK (Project Number: 117Z673) for the financial support of this research. The authors also thankfully acknowledge Dow Chemical Company for providing ASPUN™ 6000 LLDPE.

LITERATURE

1. Iwata, H., Kishida, A., Suzuki, M., Hata, Y. and Ikada, Y. 1988. "Oxidation of polyethylene surface by corona discharge and the subsequent graft polymerization", Journal of Polymer Science: Part A: Polymer Chemistry, 26, 3309-3322.
2. Li, C., Shi, Y., Zhang, R., Wang, G., Jia, J. 2019. "Effect of surface modifications on the properties of UHMWPE fibres and their composites", e-Polymers, 19, 40-49.
3. Kim, C. Y. and Goring, D. A. I. 1971. "Surface morphology of polyethylene after treatment in a corona discharge", Journal of Applied Polymer Science, 15, 1537-1364.
4. Novak, I, Pollak, V. and Chodak, I. 2006. "Study of surface properties of polyolefins modified by corona discharge plasma", Plasma Processes and Polymers, 355-364.

Flame Retardant and UV Resistant Polypropylene: A Study of Phosphorus and NOR HALS Compounds

KAYNAK Elif[1], ÜREYEN Mustafa E.[2,3], YÜKSEL Gamze[4], KARABULUT Deniz[5], KOPARAL A. Savaş[6]

[1]Eskisehir Technical University, Department of Chemical Engineering, İki Eylül Campus Eskişehir 26555, TURKEY
[2]Eskişehir Technical University, Department of Fashion and Textile Design, Yunusemre Campus, Eskişehir, 26473, TURKEY
[3]Eskişehir Technical University, Advanced Technologies Research Centre (ITAM), Eskisehir, 26555, TURKEY
[4]Eskişehir Technical University Institute of Graduate Programs, Department of Materials Science and Engineering, İki Eylül Campus Eskişehir 26555, TURKEY
[5]Eskişehir Technical University- Institute of Graduate Programs, Department of Chemical Engineering, İki Eylül Campus Eskişehir 26555, TURKEY
[6]Anadolu University, Open Education Faculty, Eskişehir 26473, TURKEY

elifkaynak@eskisehir.edu.tr

PURPOSE

This study aims to develop an additive formulation to improve the flame retardancy and UV stability of polypropylene. For this reason, the possible interaction between a phosphorus based flame retardant compound and N-alkoxy hindered amine based light stabilizer has been studied in terms of flammability.

INTRODUCTION

The ease-of processing, low cost, excellent resistance to chemicals and lightweight features of polypropylene (PP) have led to a wide range of end uses[1]. The injection moulded products is the major field in terms of PP consumption and is followed by the textiles which account for the 23% of the global consumption[2]. Though polypropylene is widely used in home textiles (carpets, floor coverings), automotive textiles, outdoor and protective clothing, the applications may well be extended to other technical and industrial products (i.e.; filtration products, geotextiles)[3]. In applications where high technical standards are required, polypropylene suffers from two major drawbacks; it has high flammability and it tends to degrade by UV[1].

Induced by heat or UV energy, in the presence of oxygen the autoxidation occurs which involve the following steps[4]:

- The hydrogen from the polymer chain is stripped to form alkyl free radicals (R●).
- The free radicals react to form new reactive species (i.e.; peroxy radicals and hydroperoxides) and other fragment species (H_2O, H_2, H_2O_2).
- The hydroperoxides (ROOH) react to form new free-radical species such as hydroxyl and alkoxy radicals. The peroxy and alkoxy radicals lead to the decomposition of polymer.

The UV stabilization mechanism of a hindered amine light stabilizer (HALS) is based on its ability to produce nitroxyl radicals (NO●) which then react with polymer radicals or other free radicals (R●) and block the chain scission reaction forming an alkoxy amine (NOR)[4,5]. Upon heating, halogen and some phosphorus-based flame retardant (FR) compounds also decompose into radical quenchers and interfere with the combustion[6]. On the other hand, the acidic decomposition products of halogen-based FRs were found to acidify the HALS that is of basic nature and thus lead to the deactivation of HALS. Therefore, the use of non-basic N-alkoxy hindered amine based light stabiliser (NOR HALS) has been proposed[7]. Moreover, NOR HALS compound was found to improve both flame retardancy and UV stability of PP containing an intumescent flame retardant (APP/PER)[8].

In this study the effects of a phosphorus-based FR and NOR HALS on the flammability and thermal stability of PP were investigated. Lower additive contents (max. 10 wt. %) were studied as they are favourable in terms of fibre drawing.

EXPERIMENTAL

The phosphorus compound containing 11% P was kindly supplied by Setaş Kimya A.Ş., Turkey. A monomeric N-alkoxy hindered amine (Flamestab

NOR-116) was supplied by BASF, Switzerland. The polypropylene chips (melt flow rate=25 g/10 min) were supplied by Hellenic Petroleum, Greece.

Polypropylene and additives were compounded by a twin-screw extruder operated with a constant temperature profile of 170°C and moulded by injection (T_{melt}=175°C, $P_{injection}$=8 bar) (Microcompounder, DSM Xplore, The Netherlands). The compositions of the prepared samples are presented in **Error! Reference source not found.**. UV aging test was performed following TS EN ISO 4892-3/Method A using UV Test Instrument (Atlas, USA). Flammability of specimens (80mm x 10mm x 4mm) was measured according to ASTM D2863 in terms of limit oxygen index (LOI) using an oxygen index module (Concept Equipment, UK). The flammability parameters of thin plate samples were measured by the cone calorimeter (Fire Testing Technology, UK) according to ISO 5660 under a heat flux of 35 kW/m^2. Simultaneous thermal analysis (STA) were performed (SDT Q600, TA Instruments, USA) using approximately 10 mg sample, up to 800°C at a heating rate of 10ºC/min under nitrogen flow (100 ml/min). The real time spectra of the evolved gases were collected by a FTIR (Cary 600, Agilent Technologies) coupled to the SDT with a heated transfer line (T=270ºC).

Table 1. Sample compositions and LOI test results (LOI% (t=0), (t=240h) and (t=480h) correspond to the LOI values before test, after 240 hours and 480 hours of UV exposure).

Code	**FR (wt.%)**	**NOR HALS (wt.%)**	**LOI% (t=0)**	**LOI% (t=240h)**	**LOI% (t=480h)**
PPref	-	-	19.0	-	-
PP-F	10	-	24.8	24.7	24.7
PP-FH	8	2	25.7	25.7	25.7

Table 1. Cone calorimeter test results

Code	**PHRR (kW/m^2)**	**THR (MJ/m^2)**	**MARHE (kW/m^2)**	**CO yield (kg/kg)**	**TSP (m^2)**
PPref	1302.5	105.8	550.2	0.048	11.6
PP-F	963.6	102.1	429.0	0.085	17.9
PP-FH	839.5	101.2	406.3	0.079	18.3

EXPERIMENTAL RESULTS AND DISCUSSIONS

The LOI test results of the samples are presented in **Error! Reference source not found.**. The incorporation of 10% phosphorus-based FR increased the LOI of neat PP from 19.0% to 24.8%. When 2 wt. % of FR in PP-FR was substituted by N-alkoxy hindered amine compound, the LOI increased to 25.7% (PP-FH). The flammability of PP-F and PP-FH samples were not affected by UV exposure.

The cone calorimeter data are presented in Table 1 and the heat release rate (HRR) curves are given in Figure 1. In comparison to neat PP, the peak rate of heat release (PHRR) values PP-F and PP-FH were 26% and 36% lower as measured by the cone calorimeter. The carbon monoxide yield and total smoke production (TSP) values were increased by the incorporation of 10 wt.% FR and further increased when 2 wt.% FR was substituted by NOR HALS. The increase in the quantity of smoke and CO addresses the flame inhibition in the gas phase[9,10].Therefore further analysis of the evolved gases are necessary to identify the flame retardant mechanism.

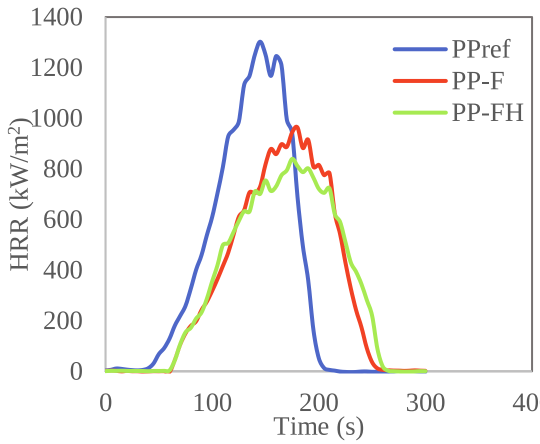

Figure 1. HRR curves obtained by the cone calorimeter

CONCLUSIONS

The flammability of polypropylene was significantly improved when 10 wt.% phosphorus-based FR was incorporated. The further increase in LOI and decrease in PHRR by the substitution of 2 wt.% NOR HALS by phosphorus based FR may be attributed to the synergistic activity between the FR and NOR HALS. The LOI of the PP-FH (25.7%) didn't change even after 480 h exposure to UV light.

SUGGESTIONS FOR FURTHER WORK

The study of UV degradation and mechanical properties of polypropylene containing the phosphorus based flame retardant and the N-alkoxy hindered amine compound is suggested as a future work.

SOURCES OF FUNDING

This study was financially supported by The Scientific and Technological Research Council of Turkey (Grant no: 218M109).

LITERATURE

1. Maddah HA. Polypropylene as a Promising Plastic: A Review. American Journal of Polymer Science 2016;6:1-11.

2. Genis AV. Analysis of the global and Russian markets of polypropylene and of its main consumption areas. Russian Journal of General Chemistry 2017;87:2137-50.

3. Jambrich M, Hodul P. Textile applications of polypropylene fibers. In: Karger-Kocsis J, ed. Polypropylene: An A-Z reference. Dordrecht: Springer Netherlands; 1999:806-12.

4. Tolinski M. Ultraviolet Light Protection and Stabilization. In: Tolinski M, ed. Additives for Polyolefins: William Andrew Publishing; 2015:32-4.

5. Pfaendner R. How will additives shape the future of plastics? Polymer Degradation and Stability 2006;91:2249-56.

6. Salmeia K, Fage J, Liang S, Gaan S. An Overview of Mode of Action and Analytical Methods for Evaluation of Gas Phase Activities of Flame Retardants. Polymers 2015;7:504-26.

7. Tolinski M. Flame-Retarding Additives In: Tolinski M, ed. Additives for Polyolefins William Andrew Publishing; 2015:44-56.

8. Xie H, Lai X, Zhou R, et al. Effect and mechanism of N-alkoxy hindered amine on the flame retardancy, UV aging resistance and thermal degradation of intumescent flame retardant polypropylene. Polymer Degradation and Stability 2015;118:167-77.

9. Braun U, Schartel B, Fichera MA, Jäger C. Flame retardancy mechanisms of aluminium phosphinate in combination with melamine polyphosphate and zinc borate in glass-fibre reinforced polyamide 6,6. Polymer Degradation and Stability 2007;92:1528-45.

10. Li H, Ning N, Zhang L, Wang Y, Liang W, Tian M. Different flame retardancy effects and mechanisms of aluminium phosphinate in PPO, TPU and PP. Polymer Degradation and Stability 2014;105:86-95.

Cam Fiber/Epoksi Çatlaklı Kompozit Borularda Yama Analizi

AVCI, Ahmet[1]
[1] Necmettin Erbakan Üniversitesi Müh-Mim. Fakültesi Biyomedikal Bölümü, Konya
ahmetavci@erbakan.edu.tr

AMAÇLAR

Flaman sarım kompozit borular yüksek basınca ve korozif ortamlara dayanıklı olup sıvılaştırılmış petrol gazı ve doğalgaz nakliyesinde, su ve kimyasal madde tankları gibi olarak ayrıca askeri alanda roketatar namlusu olarak kullanılırlar. Bu çalışmada üzerinde çatlak bulunan flaman sarımla üretilmiş cam elyaf takviyeli kompozit bir boruda çatlak üzeri yama ile tamir edilerek kuvvetlendirilmiş ve iç basınç testi ile yamanın etkisi incelenmiştir. Borular altı tabakalı ve sarım açısı ±55° olarak üretilmiştir. Yama malzemesi olarak yine cam elyaf kullanılmış ve yamalar çatlağı tamamen kaplayacak şekilde dıştan yapılmıştır. Yamalı borulara serbest uçlu iç basınç testine uygulanmış ve patlama basınçları ve yamanın etkisi incelenmiştir.

GİRİŞ

Muhtelif şekillerde çatlaklar ve hasarların oluştuğu kompozit levhaların ve boruların hasar davranışları mühendislik açısından çözülmesi gereken önemli bir problemdir[1]. Kompozit malzemeler genel olarak imalattan kaynaklanan veya statik ve dinamik yük altında oluşan hatalara karşı oldukça duyarlıdır. Bu sebeple kompozit malzemelerde çatlak ilerlemesi ve hasar analiziyle ilgili geniş araştırmalar yapılmıştır[2-6]. Bu hasar ve çatlakların yama ile tamir edilmesi malzeme mühendisliğinin önemli bir konusudur[7]. Flaman sarım yöntemiyle üretilen kompozit yapılar endüstriyel alanda; proses boru ve tankları, depolama tankları, basınçlı borular, basınçlı tanklar, yer altı tankları, gaz yıkama kuleleri, bacalar, otomobil ve kamyon şaftları gibi, askeri alanda ve havacılıkta; roketatar gövdesi, roket gövdesi, roket muhafazaları, uçak ve planör gövdeleri, uçak havalandırma kanalları gibi çok geniş sahalarda kullanılırlar. Kompozit borular ve tanklar iç basınç altına statik veya dinamik yüklere maruz kalarak çalıştıklarından bunların dayanımlarının ve yorulma ömürlerinin belirlenmesiyle kullanıma uygun tasarım yapılmasına yol açmıştır[8-9]. Kompozit borularda üretim sırasında, dış etkilerin altında ve kullanım sırasında birçok hasarlar ve çatlaklar oluşmaktadır. Bu hasarların yama ile tamir edilmesinden sonra boruların tekrar kullanılabilmesine olanak sağlanmaktadır. Bundan dolayı yamanın şekli, büyüklüğü, kalınlığı ve kullanılan malzemeler kompozit yapının tamirden sonraki ömrünü etkilemektedir. Hasarlanmış boruların tamirinde kompozit yamaların kullanılması uzun süreden beri yapılmakta ve bu sahada literatürde azımsanmayacak kadar çok çalışma bulunabilir ve halen devam etmektedir[19-12]. Yamanın en çok gerektirdiği yerler korozyona maruz kalan deniz kıyıları boru sistemleridir. Çünkü deniz kıyılarındaki borular iç basıncın tesiriyle çevresel gerilmeleri etkilemekte ve hasarlar oluşmaktadır. Boruların kompozit yamayla onarılması boruların çevresel yönde oluşan gerilmelerini iyileştirir. Literatürde bunu açıkça görmekteyiz [13-14].

Bu çalışmada altı tabakalı, ±55° sarım açısına sahip, E-cam elyaf takviyeli plastik (CTP) borular kullanılmıştır. Üzerine eksenel doğrultuda 15mm uzunluğunda kalınlık boyunca boruyu delen bir çatlak açılmıştır. Bu çatlağın üzerine farklı kalınlıklarda yamalar yapılarak tamir edilmiştir. Açık uçlu statik iç basınç testine tabii tutulan yamasız ve yamalı buruların patlama basınçları ve hasarları incelenmiştir. Çam kumaş kullanılarak yapılan yama malzemesinin yama katsayısının mukavemete etkileri değerlendirilmiştir.

DENEYSEL

Malzeme

Bu makalede kullanılan ±55° filaman sarım cam takviyeli plastik (CTP) borular, İZOREEL San. ve Tic. Ltd. Şti. İzmir firmasına ürettirilmiştir. Kompozit borularda 17 mm çapında Vetrotex 1200 tex E-cam elyafı ile CIBA-GEIGY CY 225 Bisfenol-A 100: 90: 0.5 ağırlık oranlarına sahip epoksi reçine sistemi kullanılmıştır. Kompozit boruların iç çapı 72 mm ve ortalama duvar kalınlığı 2,3 mm olup altı tabakadan oluşmaktadır.

Yöntem

Times new roman 10
En çok 150-250 karakter

DENEYSEL SONUÇLAR/TARTIŞMA

Borunun hasar davranışını incelemek amacıyla 300 mm boyutlarında kesildikten sonra üzerlerine 15 mm uzunluğunda eksenel yönde boyuna çatlaklar açıldı. Çatlakların uçları bistürü ile keskinleştirildi. Çatlaklı bölgenin üzerini örtecek şekilde borular cam-epoksi kumaş ile sarılarak yama oluşturuldu. Hazırlanan borular ASTM D 2992 standardı doğrultusunda içten basınca maruz bırakılarak çatlaklı bölgenin hasar oluşumu ve dayanıklılığı izlendi. Öncelikle çatlaksız boruların sonrada yamalı buruların mukavemetleri tespit edildi. Çatlaksız borularda patlama basıncı 19.50 MPa, Elastiklik Modülü 23.10 GPa, ve Poisson Orano 0.81 olarak bulunmuştur. Kompozir boruların yakma testi sonucunda elyaf hacım oranı 0.35 olarak bulunmuştur. Şekil 1de kompozit borunun şematik resmi verilmiştir.

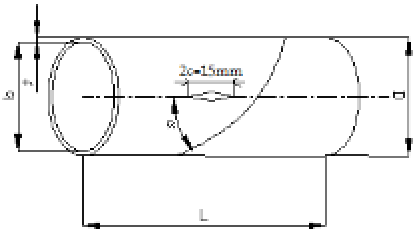

Şekil 1. Kompozit borunun şematik görüntüsü. L = 300 mm, D = 76.3 mm, d = 72 mm, t = 2.15mm

GENEL SONUÇLAR

Çatlaksız borular iç basınca maruz bırakıldığında boruların çapında arma ve boyunda kısalma olmuştur. İç basınç arttıkça zorlanan borularda öncelikle en zayıf bölgesinde beyazlaşma oluştığu gözlendi. Beyazlaşmayı sızıntı takip etti. Sızıntılar su jetine ve nihayi hasara kadar devam etti. Beyazlaşma elyaf-matriks aray yüzey ayrılmasından kaynaklanmaktadır. Bu aralardan iç basıncı oluşturan sıvı ilerleyerek iki tabaka arasına oradan da yüzeye çıkmıştır. Borulardaki hasar tabaka ayrılması ve elyaf kopmasıyla tamamlanmıştır.

Yama yapılmış borularda hasar oluşumu daha farklıdır. Öncelikle borunun çapının artmasıyla yama ile ana boru arasında oluşan kayma gerilmesi burada tabaka ayrılmasına zorlamıştır. Çatlaktan giren sıvının ve iç basıncın etkisiyle yamada kılcal çatlaklar oluşmuştur. Zorlanan yama ve boru birlikte aniden koparak nihai hasara ulaşmıştır. Yamanın tabaka sayısı arttıkça nihai hasar için daha yüksek basınca gerek duyulmuştur. Bu çalışmada yamanın tabaka sayısı çatlaksız borunun mukavemetine ulaşıncaya kadar artırılmıştır. Şekil 2 de çatlaksız ve dört katlı cam-epoksi kumaş ile yamanmış boruların iç basınç altında oluşan nihayi hasarlarının fotoğrafları verilmiştir. Burada çatlaksız borunun elyaf doğrultusunda hasar oluşurken yamalı numunede yama tabakaları çatlak bölgesinin üzerinde ve çatlak doğrultusunda koparak ayrıldığı görülmektedir.

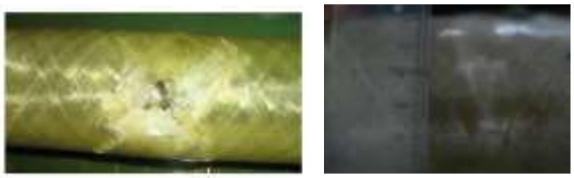

Şekil 2. Çatlaksız ve dört kat yama ile tamir edilmiş yapılan boru numunelerinin nihai hasarlarının görüntüsü.

Yamanın tabaka sayısı borunun iç basınç etkisindeki mukavemetini etkilediğinden kaç tabakada borunun çatlaksız mukavemete eriştiğini görmek gerekmektedir. Yapmış olduğumuz çalışmada bir tabakadan beş tabakaya kadar yama tabakasını artırdık. Beş katmanda çatlaksız numunenin patlama basıncına erişilmiştir. Şekil 3 te yamanın katman sayısına göre patlama basıncının değişimi verilmiştir.

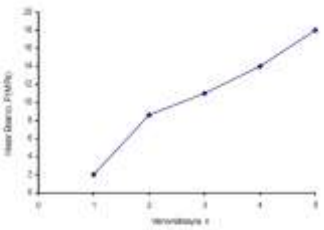

Şekil 3. Çatlaklı borularda tabaka sayısına göre patlama basınçlarının değişimi.

Beş katlı yama uygulaması 4MPa basınçta çıtırtı sesleri vermeye başlamıştır. 6 MPa basınçta beyazlaşmaların yoğunlaştığı görülmüştür. Kat sayısının artması boruyu saran yama borunun şekil değişimini azaltmaya çalışmıştır. İç basınç 18 MPa basınca ulaşınca nihai patlama meydana gelmiştir. Bu değer çatlaksız numunenin patlama basıncına çok yakın bir değer olan 19.50 MPa değere yakındır. Hasar sonrası yama kaldırılmış ve boruya açılan çatlakta kalınlık boyunca çatlakta ilerlemenin olmadığı gözlenmiştir.

SONUÇLAR

Kompozit yama ile onarılmış (±55°) filaman sarım açılı 6 tabakalı ve kalınlık boyunca çatlaklı CTP boruların serbest uçlu statik iç basınç deneyleri yapılarak hasar davranışı gözlenmiştir. Cam elyaf-epoksi sargı kumaş ile beş kata kadar yama yapılmış ve yamanın çatlaklı borulardaki direncinin belirlendiği çalışmada şu sonuçlara ulaşılmıştır.

1- Çatlaksız ±55° sarım açılı CTP borunun serbest uçlu statik iç basınç deneyi sonucunda patlama basıncı 19,5 MPa olarak bulunmuştur. Hasar mekanizmasının oluşumu ve gelişimi; sırasıyla elyaf matriks ayrılması, matriks çatlaması, tabaka ayrılması ve elyaf kopması şeklinde gözlenmiştir.
2- Yama katmanı 2 olduğunda patlama basıncı 8.6 MPa da nihayi hasar olurken 3 tabakalı yamada bu basınç 11. MPa olmuştur. Katman sayısı dörde çıkınca 14 MPa ve son olarak 5 katmanlı yamada 18 MPa iç basınçta nihai hasar olmuştur.

Eğer yama katmanı beşten fazla olsaydı borulardaki hasar yama dışında borunun en zayıf bir bölgesinde oluşacaktı.

3- Beş katmanlı yama ile tamir edilmiş çatlaklı borundan hasar sonrası yama kaldırılınca çatlağın boyuna yönde ilerlemediği gözlenmiştir. Çatlağın boyuna yönde ilerlememesinin sebeplerinden biri fleman sarım borularda çatlak uçları elyaflar tarafından durdurulmakta ve farklı açılarda yönlendirilmelerindendir.

SONRAKİ DÖNEM ÇALIŞMALARI

CTP Flaman sarım kompozit borularda çatlak ilerlemesi, gerilme şiddet faktörleri ve darbe hasarları çalışılabilir.

KAYNAKLAR

1- Gning PB, Tarfaoui M, Collombet F, Davies P. Prediction of damage in composite cylinders after impact. J Compos Mater 2004;39:917–28.

2- Wang, Q.Y., Pidaparti, R.M., 2002, Static Characteristics and Fatigue Behaviour of Composite-Repaired Aluminum Plates, Composite Structures, Vol. 56, pp. 151-155.

3- Xia, M., Takayanagi, H., Kemmochi, K., 2001, Analysis of multilayered filament wound composite pipes under internal pressure, Composite Structures 53: 483-491

4- Perreux, D. and Joseph, E., 1996, The effect of frequency on the fatigue performance of filament wound pipes under biaxial loading: experimental results and damage model, Composite Science and Technology, 57: 353-364

5- Richard, F., and Perreux, D., 2000, A reliability method for optimization of f fiber reinforced composite pipes, Reliability Engineering and System Safety, 68: 53-59

6- Hosseini-Toudeshky, H., Sadeghi, G., Daghyani, H.R., 2005, Experimental Fatigue Crack Growth ad Crack-Front Shape Analysis of Asymmetric Repaired Aluminium Panels with Glass/Epoxy Composite Patches, Composite Structures, Vol. 71, pp. 401-406.

7- Soutis, C., Duan, D-M., Goutas, P., 1999, Compressive Behaviour of CFRP Laminates Repaired with Adhesively Bonded External Patches, Composite Structures, Vol. 45, pp. 289-301.

8- Martens, M., and Ellyin, F., 2000, Biaxial monotonic behaviour of a multidirectional filament-wound glass-fiber/epoxy pipe, Composites Part A, 31: 1001-1014

9- Ellyin, F., and Martens, M., 2000, Biaxial fatigue behaviour of a multidirectional filament-wound glass-fiber/epoxy pipe, Composite Science and Tecnology, 61: 491-502

10- Luka´cs J, Nagy G, To¨ro¨k I, et al. (2010) Experimental and numerical ınvestigations of external reinforced damaged pipelines. Procedia Engineering 2: 1191–1200.

11- Duell JM, Wilson JM and Kessler MR (2008) Analysis of a carbon composite overwrap pipeline repair system. International Journal of Pressure Vessels and Piping 85: 782–788.

12- Gunaydın B., Daghan B.,Avci A., Fatigue behavior of surface-notched composite pipes repaired by composite patches, International Journal of Damage Mechanics, 22(4) 490–498

13- Kuhlman, C. J., Lindholm, U. S., Stephens, D. R., Kilinski, T. J., and Francini, R. B., 1995, “Long-Term Reliability of Gas Pipeline Repairs by Reinforced Composites,” Final Report, Gas Research Institute, Chicago, IL, GRI95/0071.

14- Alexander, C. R., and Wilson, F. D., 2000, “Recent Test Results and Field Experience With Armor Plate Pipe Wrap Repairing Corroded and MechanicallyDamaged Pipes,” 2000 Pigging Conference, Houston, TX.

AHP Yöntemi ile En İyi Fiziksel Özellikli Kumaş Seçimi

ERCAN, Emel[1], YILDIRIM, F. Filiz[1], KOPTUR TASAN, Perinur[1], ARAS ELİBÜYÜK, Sultan[1], ÇÖREKCİOĞLU, Mustafa[1]
[1]Ozanteks Ar-Ge Merkezi
emel@ozanteks.com.tr

AMAÇLAR

Bu çalışma da kumaşlara uygulanan bazı objektif konfor testlerinden elde edilen değerlerin AHP karar analizi ile değerlendirilmesi anlatılmıştır.

GİRİŞ

Konfor birçok fiziksel, psikolojik ve fizyolojik faktörü içeren karmaşık bir kavramdır ve genel olarak da çevre ve vücut arasındaki psikolojik, fizyolojik ve fiziksel uyumun sonucunda ortaya çıkan memnuniyettir. Konfor, termofizyolojik, dokunsal vücut hareket ve estetik konfor olara ayrılmaktadır(Güney ve Kaplan, 2016). Giysilerin konforlu sayılabilmesi için birçok özelliği taşıması yanında esneklik ve deri-kumaş sürtünme gibi değerlerinin de iyi olması beklenmektedir. Bu değerler kullanılarak en iyi fiziksel özelliklere sahip kumaşların seçiminden Analitik Hiyerarşi Prosesi(AHP) yönteminden faydalanılabilmektedir.

Analitik Hiyerarşi Prosesi (AHP)

Analitik Hiyerarşi Prosesi, ölçme ve karar verme problemlerinde kullanılan matematiksel bir teori olup 1970'li yıllarda Thomas L. Saaty tarafından geliştirilmiştir (Saaty ve Niemira, 2006). AHP yöntemin anlaşılabilirliğinin ve uygulanmasının kolay olması nedeniyle literatürde uygulama alanları oldukça fazladır (Ho, 2008: 211).

Uygulamada izlenmesi gereken akış şu şekildedir (Supçiller ve Çapraz, 2011):

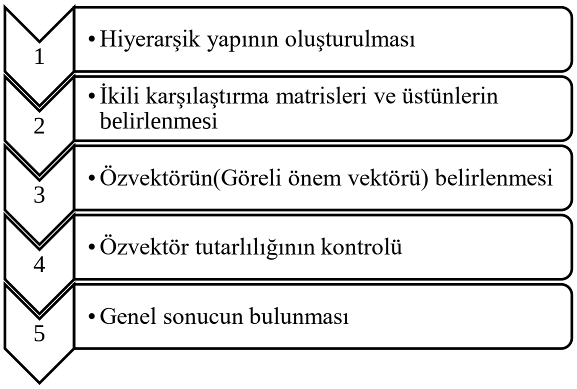

Şekil 2. AHP yöntemi işlem akışı

DENEYSEL

Malzeme

Çalışmalarda parlak, estetik ve güzel efektler oluşturmak için kullanılan bir iplik türü olan FDY naylon iplik, polyesterin aksine atmosfer şartlarında boyanabilme özelliğine sahip elastik bir poliester lifi olan PBT, cilt ile temas durumunda cildin sıcaklığını 1.2 C dereceye kadar azaltabilen Xcool ipliği, sıcaklık yükselmeye başladığında serinlik hissi sağlayan ve içerdiği mikron boyutundaki polimerler sayesinde yüzey alanı artıran ve serinlemeyi sağlayan küçük kanallar oluşan Breze ipliği, başka bir elastik lif olan PTT ve parlak, estetik ve güzel efektler oluşturmak için kullanılan Britex ipliğinden üretilmiş süprem atkılı örme kumaşlar kullanılmıştır. Kumaşların iplik numaraları ve konstrüksüyonlarının aynı olmasına dikkat edilmiştir.

Yöntem

Çalışmada kumaşların fiziksel özelliklerinin objektif olarak değerlendirilebilmesi için çeşitli standartlara uygun testler gerçekleştirilmiştir ve AHP yöntemine göre seçim uygulanmıştır. Bu testler; Kumaşlarının Elastikiyet Özelliklerinin Ölçülmesi (EN 14701-1), Kumaşların Patlama Mukavemeti Ölçümü (ASTM D3787), Kumaş-deri Sürtünme Testi (ASTM D1894) olarak sayılabilir.

DENEYSEL SONUÇLAR/TARTIŞMA

En iyi fiziksel özelliğe sahip kumaş seçimi probleminde kullanılacak kriterler ve alt kriterlerin hiyerarşik yapısı şu şekilde belirlenmiştir:

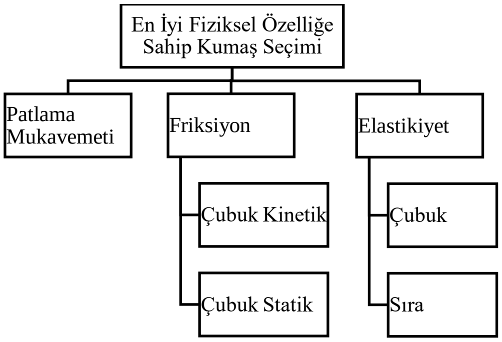

Şekil 3. En İyi Fiziksel Özelliğe Sahip Kumaş Seçimi Kullanılan Kriter ve Alt Kriterler

Patlama Mukavemeti: Bir kumaşın patlamaya karşı direncini (yani patlama mukavemetini) ölçmek için gerçekleştirilir.
Friksiyon: Bir kumaşın sürtünmeye karşı direncini ve buna bağlı olarak da yüzey pürüzlülüğünü ölçmek için gerçekleştirilmiş bir testtir
Elastikiyet: Vücudu saran tüm giysiler için olduğu gibi mayo kumaşlarında da elastikiyet ve elastik geri dönüş özellikleri hayati önem taşımaktadır.

Seçim kriterleri ağırlıklarının elde edilmesi için AHP yöntemi Super Decisions 2.10.0 programı kullanılarak uygulanmıştır. Programda en iyi fiziksel özelliğe sahip kumaş seçimi için oluşturulan hiyerarşik yapı Şekil 2'deki gibi oluşturulmuştur.

Şekil 4. Super Decisions 2.10.0 programında oluşturulan hiyerarşik yapı

Şekil 2'de verilen Super Decisions 2.10.0. programında en iyi fiziksel özelliğe sahip kumaş seçimi problemi hiyerarşisinin ikili kıyaslamalara dayalı karşılaştırılması sonucunda elde edilen kriter ağırlıkları Tablo 1'de verildiği gibidir.

Tablo 1. Kriter ağırlıkları

Kriterler	Ağırlıklar
Patlama Mukavemeti	36,89%
Elastikiyet Cubuk	20,63%
Elastikiyet Sira	20,63%
Cubuk Kinetik	10,93%
Cubuk Statik	10,93%

Her bir kriter bazında seçeneklerin iki kıyaslanması sonucunda en iyi fiziksel özelliğe sahip kumaş seçeneklerinin sıralanması Tablo 2'de görüldüğü gibi elde edilmiştir.

Tablo 2. Kumaş seçenekleri sıralaması

Sıra No	Kumaş Seçenekleri	Ağırlıklar
1	PTT Kumaş	0,2522
2	X-Cool Kumaş	0,1748
3	Breeze Kumaş	0,1580
4	Britex Kumaş	0,1516
5	PBT-Poliamid Kumaş	0,1395
6	FDY Kumaş	0,1239

GENEL SONUÇLAR

Bu çalışma kapsamında en iyi fiziksel özelliğe sahip kumaşın belirlenmesinde, çok kriterli karar verme yöntemlerinden biri olan ve literatürde sıklıkla kullanılan AHP yöntemi kullanılmıştır. Kumaş seçim probleminin uygulanabilmesi için öncelikle kumaşın fiziksel özelliklerini gösteren kriterler belirlenmiştir. Bu kriterler bazında kumaş seçenekleri ikili kıyaslanmış ve seçenekler sıralanmıştır. Sıralama sonucunda en iyi fiziksel kumaş PTT olarak belirlenmiştir.

SONRAKİ DÖNEM ÇALIŞMALARI

En iyi fiziksel kumaş seçimi diğer çok kriterli karar verme yöntemlerinden olan TOPSIS, ELECTRE ve ARAS gerçekleştirilerek, AHP sonucunda elde edilen sıralama ile karşılaştırılabilir.

TEŞEKKÜR/BILGILENDIRME/FON KAYNAĞI

Bu çalışma, Ozanteks Tekstil Ar-Ge merkezi tarafından, TÜBİTAK 3171008 proje numarası ile desteklenmiştir.

KAYNAKLAR

Güney, S., & Kaplan, S. 2016. Basinç Konfor Performasini Etkileyen Parametreler Ve Basinç Konforunun Ölçümü. Journal of Textiles & Engineers/Tekstil ve Mühendis, 23(102).
Ho, W. (2008). "Integrated analytic hierarchy process and its applications-A literature review", European Journal of Operational Research, 186, p.211-228.
Saaty, T.L., Niemira, M.P. 2006. "A framework for making a better decision" Research Review, 13(1).
Supçiller, A.A., Çapraz, O. 2011. "AHP-TOPSIS Yöntemine Dayalı Tedarikçi Seçimi Uygulaması", İstanbul Üniversitesi İktisat Fakültesi Ekonometri Ve İstatistik Dergisi, Ekonometri ve İstatistik Sayı:13, 1-22.

On the use of micromilling for the development of thermoplastic-based microfluidic devices

SEYED ALI MOUSAVI SHAEGH[1,2*], AMIRHESAM BANEJAD[1,3], MOHAMMAD PASANDIDEH-FARD[3],
[1]Orthopedic Research Center, Mashhad University of Medical Sciences, Mashhad, Iran.

[2]Clinical Research Unit, Ghaem Hospital, Mashhad University of Medical Sciences, Mashhad, Iran.

[3]Department of Mechanical Engineering, Ferdowsi University of Mashhad, Mashhad, Iran.

[*]Contact Information: mousavisha@mums.ac.ir

PURPOSE

Nowadays, several fabrication methods have been proposed to develop thermoplastic-based microfluidic microdevices. In this paper, for the fabrication of such devices, a micromilling method is presented as an appropriate candidate for the development of microfluidic actuators. To this end, a pneumatically actuated micropump is designed, fabricated, and characterized. Furthermore, the impact of micromilling process is investigated by investigating the surface quality of micromilled pattern via Atomic Force Microscope (AFM) and Field Emission Scanning Electron Microscope (FESEM) of micormilled surfaces.

INTRODUCTION

Thermoplastics represent excellent capabilities to be exploited as based materials in the fabrication of microfluidic devices [1, 2]. These stem from the benefits of thermoplastic materials including but not limited to viability [3], the ease of accessibility, and mass production features [4, 5]. Moreover, based on the variety in the fabrication methods of such materials that consist of hot embossing, micromilling, injection molding, laser ablation and sterolithography, these materials have attracted the attention of many researchers [1, 6]. In this way, the use of micromilling and Co2 laser ablation methods have outpaced every other method because they are cost-efficient [6]. However, the use of Co2 laser ablation makes researchers apply several post-processing procedures like chemical surface treatment leading to the increase of fabrication time and cost [7]. By contrast, the micromilling approach has the ability to create a wide range of cross-section shapes without the requirement of applying any post processing steps.

In this research, the use of micromilling in the fabrication of thermoplastic-based microfluidic devices is studied. To this end, a peristaltic, gas-actuated micropump is designed and fabricated. The presented microump consists of various layers that are assembled with the aid of the thermal fusion bonding method. Furthermore, the effect of micromilling on the fabrication procedure is investigated using the FESEM and AFM.

EXPERIMENTAL

Material

Commercial Poly(methyl methacrylate) (PMMA) sheets (Calvin, Vietnam) are exploited to fabricate the micropump. A high-tech CNC micro milling (DSP, China) machine is used for micromachining purposes of the PMMA sheets. Various software such as the SOLIDWORKS® and MASTERCAM® are employed to design and fabricate the different layers of micropump. Due to the rigidity of PMMA, for actuating aim, a (Thermoplastic Poly Urethane) TPU film (Covestro LLC, MA, USA) with a certain thickness of 25µm is exploited as a thin and flexible membrane in micropump. A research laboratory oven (ATRA, IRA) is utilized in thermal treatment and bonding of micropump layers. A commercial controller system is leveraged to operate the presented micropump. The system includes some FESTO® fast switch valves (MH1-24V DC) handled by the WAGO® microcontroller. The CODESYS® software is used to command the controller system. A nitrogen gas tank and some pressure regulators are employed to apply and control gas pressure on the membrane.

Design and Fabrication

The presented micropump is peristaltic, including five serial gas-actuated microvalves. Each valve is constituted from liquid channel, gas channel and diaphragm (Figure 1). The compressed air, which is moved through gas channel, forces the diaphragm, and pushes the liquid situated in the liquid channel. By the operation of all valves, based on a certain pattern, the liquid is pumped.

After the design of layers via SOLIDWORKS®, the CNC micromilling is used to engrave the desired features in PMMA sheets. During milling procedure, the feed rate and spindle velocity are controlled accurately owing to their great impact on the surface quality of micromilled channel. After the preparation of layers, the thermal fusion method, which is based on the glass transition temperature of PMMA, is used to bond different layers. In this method, some controllable parameters such as pressure, temperature and bonding time are controlled precisely. Initially, layers are cleaned by water-soap and ethanol, followed by a thermal treatment at 90° C and the vacuum pressure of 80 kPa for not less than 8 hours. After the cooling procedure, all layers (TPU and PMMA) are sandwiched between two clamps. Then, they are kept in the oven at the temperature and vacuum pressure of 142° C and -80 kPa for one hour. Afterward, they are cooled down to 50° C in 50 min.

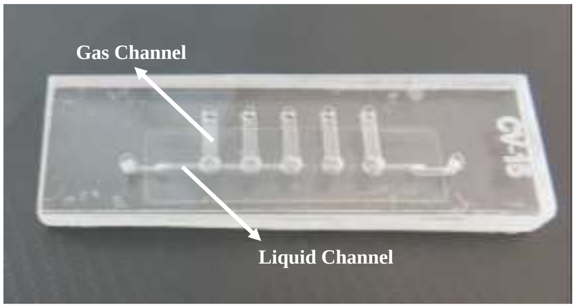

Figure 1. The image of fabricated micropump.

EXPERIMENTAL RESULTS AND DISCUSSIONS

In order to scrutinize the micromilled surface quality, the FESEM and AFM images are shown (Figures 2 and 3). In this way, the surface roughness of various positions in the channel is measured, and the maximum value is reported as the surface roughness of channel. Based on results, the maximum average roughness is measured to be 11.43 nm which is considered appropriate for microfluidic applications.

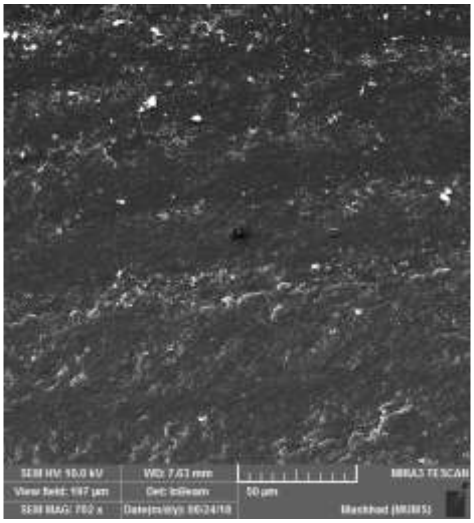

Figure 2. The FESEM image of micromilled surface.

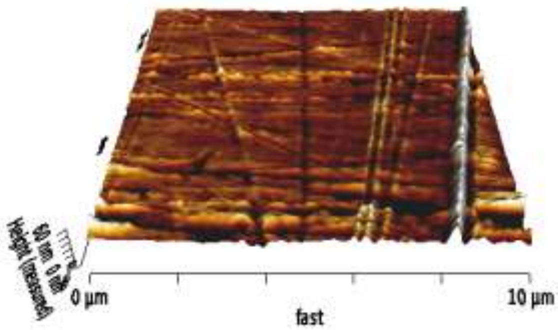

Figure 3. The AFM image of micromilled surface.

Regarding micropump, the impacts of physical parameters including gas actuation pressure on the generated flow rate of micropump are investigated. As shown in figure 4, the increase of gas actuation frequency consistently rises the generated flow rate, in which the maximum flow rate is obtained at the gas actuation frequency of 15 Hz. Regarding gas actuation pressure, an optimum gas pressure of 160 kPa is observed where the maximum flow rate of 345.29±10 µL/min is obtained. Moreover, at 15 Hz, with increasing gas actuation pressure from 160 kPa to 220 kPa, the generated flow rate decreases to 325.99±10 µL/min.

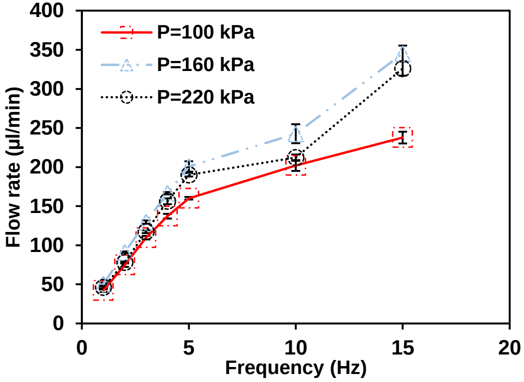

Figure 4. The effects of different gas actuation pressures and frequencies on the performance of the micropump.

CONCLUSIONS

In this paper, the capability of micromilling method for the fabrication of thermoplastic-based microfluidic micropump from the PMMA and TPU is studied. Thanks to the micromilling fabrication method, there is no surface chemical treatment to improve the surface quality of surface. The obtained surface quality implies that this method is appropriate for the fabrication of a wide range of thermoplastic-based microdevices. Furthermore, a thermoplastic micropump was fabricated and characterized. The fabricated micropump can generate a maximum flow rate of about 350 μL/min at an actuation gas pressure and frequency of 160 kPa and 15 Hz, respectively. In comparison with other fabrication methods, the introduced one is more effective in terms of time and cost. Therefore, it can be used for making various microfluidic actuators in a research laboratory for biomedical applications.

ACKNOWLEDGEMENTS/SOURCES OF FUNDING

S. A. M. S. gratefully acknowledges funding by National Institute for Medical Research Development (NIMAD) under grant number 957144.

References

1. Weerakoon-Ratnayake, K.M., et al., Thermoplastic nanofluidic devices for biomedical applications, Lab on a Chip. 17 (2017) 362-381. DOI: https://doi.org/10.1039/C6LC01173J.
2. Voicu, D., et al., Thermoplastic microfluidic devices for targeted chemical and biological applications, RSC Advances. 7 (2017) 2884-2889. DOI: https://doi.org/10.1039/C6RA27592C.
3. Berthier, E., E.W. Young, and D. Beebe, Engineers are from PDMS-land, Biologists are from Polystyrenia, Lab on a Chip. 12 (2012) 1224-1237. DOI: https://doi.org/0.1039/C2LC20982A.
4. Tsao, C.-W., Polymer Microfluidics: Simple, Low-Cost Fabrication Process Bridging Academic Lab Research to Commercialized Production, Micromachines. 7 (2016) 225-236. DOI: https://doi.org/10.3390/mi7120225.
5. Chin, C.D., V. Linder, and S.K. Sia, Commercialization of microfluidic point-of-care diagnostic devices, Lab on a Chip. 12 (2012) 2118-2134. DOI: https://doi.org/10.1039/C2LC21204H.
6. Banejad, A., et al., Design, fabrication and experimental characterization of whole-thermoplastic microvalves and micropumps having micromilled liquid channels of rectangular and half-elliptical cross-sections, Sensors and Actuators A: Physical. 301 (2020) 111713. DOI: https://doi.org/10.1016/j.sna.2019.111713.
7. Shaegh, S.A.M., et al., Rapid prototyping of whole-thermoplastic microfluidics with built-in microvalves using laser ablation and thermal fusion bonding, Sensors and Actuators B: Chemical. 255 (2018) 100-109. DOI: https://doi.org/10.1016/j.snb.2017.07.138.

The Effect of Pique Weave Pattern on the Poisson’s Ratio of Woven Fabric

AKGUN, Mine[1], EREN, Recep[1], SUVARİ, Fatih[1], YURDAKUL, Tuğba[2], SERİNÇAY, Harun[2]
[1] Bursa Uludag University, Faculty of Engineering, Textile Engineering Department, Bursa, Turkey,
[2] Bursa Uludag University, Institute of Natural Science, Textile Engineering Department, Bursa, Turkey
akgunm@uludag.edu.tr

PURPOSE

In this study, in order to investigate the weave patterns which could be used in designing auxetic woven fabric structures, it was aimed to investigate the Poisson’s ratio of the pique structures because of the structural properties of weave pattern having a large number of crossing points and long yarn floats together.

INTRODUCTION

When a material is subjected to tensile force, it is subjected to elongation in the force axis, contraction occurs in other axes, or when a material is subjected to compressive force, expansion occurs in other axes while it is subjected to shortening in the force axis[1]. Poisson's ratio (v) (Equation 1), i.e. the coefficient of elasticity, is the negative ratio of transverse deformation to longitudinal deformation[1].

$$v = -(\text{axial strain} / \text{extensional strain})$$

Although most of the materials used in engineering have a positive Poisson’s ratio, a limited number of materials have a negative Poisson’s ratio. Materials with a negative Poisson’s ratio are also referred to as auxetic materials. Auxetic materials, as opposed to materials with a positive Poisson’s ratio (Figure 1), expand laterally when stretched and contract laterally when compressed[1].

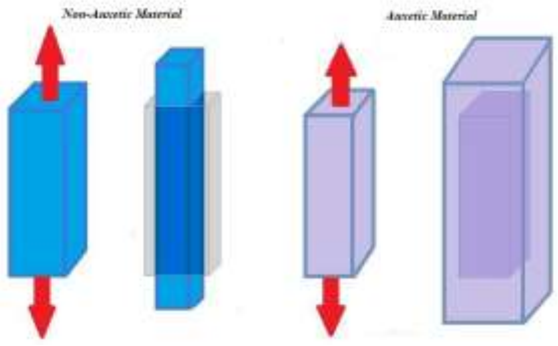

Figure 1. Tensile behavior of non-auxetic (conventional material) and auxetic material

Materials with a negative Poisson’ ratio have significant advantages. These advantages include increased surface area, extra friction resistance, breaking strength, improved acoustic behavior, superior energy absorption (thermal impact resistance, ultrasonic and sonic strength), wet efficiency, adhesion (interface / matrix) strength, tensile strength and better slip module[2-4]. An increased indentation resistance makes auxetic fabrics suitable for use in protective equipment. The improved acoustic properties are suitable for sound insulation applications[2-5].

Since Poisson's ratio is a physical parameter independent of material scales, auxetic behavior can be obtained at different levels from molecular level to macroscopic level[2,6,7].

A potential application of auxetic materials is the usability of the release ability, such as anti-perspirant containing garments, due to increased pore opening as a result of stretching[2,8,9]. Due to the expansion and contraction behavior of auxetic materials, it can be said that these structures have variable permeability. The variable permeability of auxetic materials can be used to produce intelligent filters that can be designed with different sizes and special geometries to control the transition pressure in filtration. One area of application of auxetic materials is biomedical engineering. The evolution of these materials will allow the production of blood vessels that expand their walls when blood is pumped, or the development of new surgical instruments and mechanisms[10].

In general, there are two approaches to producing auxetic fabrics. The first approach is to use conventional fibers and yarns to create a Negative Poisson’s Ratio (NPR) effect through knitting or weaving in a special geometric configuration. With this approach, various weft knitting and warp knitting auxetic fabrics were produced[9,11-13].

In this study, it was aimed to investigate various pique patterns in order to guide the weave designs having negative Poisson's ratio which can give an auxetic effect to create pore opening with tensile effect.

EXPERIMENTAL

Material

In the study, 100 % cotton pique fabrics with different weave structures were used. Fabric constructional properties were presented in Table 1. Microscopic images with 10 times magnification of pique fabrics were presented in Figure 2.

Table 1. Constructional properties of fabrics

Fabric Code	Yarn Count [Nm]		Yarn Density [Thread/cm]		Fabric Weight [g/m^2]
	Warp	Weft	Warp	Weft	
F1	26	22	28	26	208,4
F2	15	15	18	20	255,7

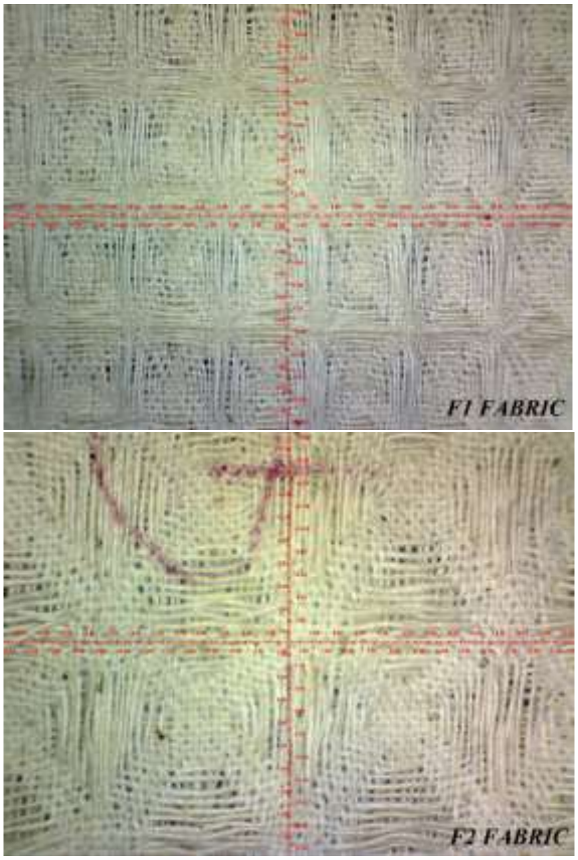

Figure 2. Microscopic images of F1 and F2 fabrics

Method

Tensile measurements of fabrics were made in Shimadzu AG-X plus strength device according to ASTM D2256 standard for warp and weft direction. The images of the fabrics taken under tension were taken simultaneously at certain intervals and image analyzes were performed and Poisson's ratios were calculated.

EXPERIMENTAL RESULTS AND DISCUSSIONS

The Poisson's ratio - elongation graphs of the fabrics are presented in Figures 3 and 4. Changes in Poisson's ratios were evaluated for 1cm elongation.

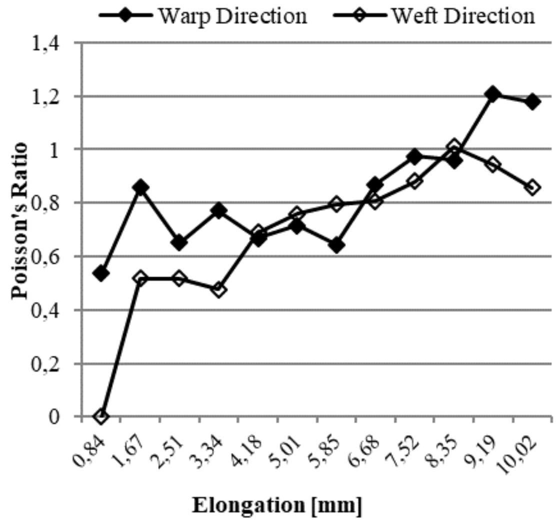

Figure 3. Poisson's ratio - elongation curve of F1 fabric

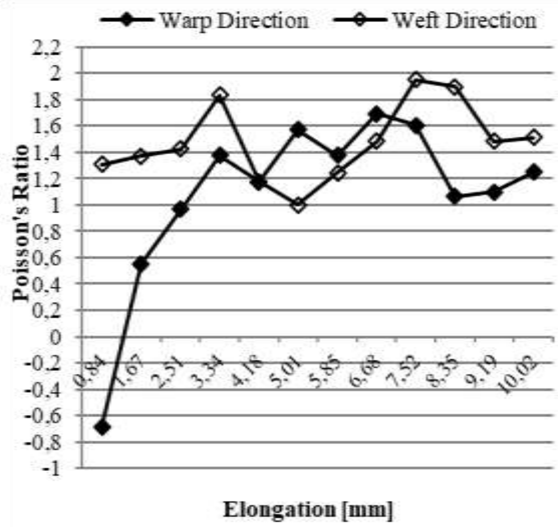

Figure 4. Poisson's ratio - elongation curve of F2 fabric

Negative Poisson's ratio was obtained in the warp direction of F2 pique structure and under 1mm elongation. Under the extension of 1 mm, in which the negative Poisson's ratio was obtained, there was an expansion in the transverse direction in the fabrics subjected to tension in the warp direction.

This might indicated that such structures could be used under conditions of stretching, where the pore opening due to stress was desired (such as medical gauzes, as well as use where moisture, air and water vapor permeability may be desired).

When the structural properties of F2 fabric in which negative Poisson’s ratio was obtained, it was observed that this fabric has thicker yarns and lower fabric density values than F1 fabric.

In addition, the yarn count and density as well as the weave pattern structure must be taken into account. When the weave structure of the F2 fabric was examined, it was observed that there were large yarn intersection regions connected one-to-one between the long warp and weft yarn floating regions.

Although a similar weave structure was also in F1 fabric, it was thought that the negative Poisson's value could not be obtained in F1 fabric because it could be caused both by the effect of yarn counts and density values, and also because of the narrow yarn intersection regions connected one-to-one between the long warp and weft yarn floating regions in the weave structure.

The fact that the one-to-one intersection zones were located in a narrow area indicated that it could not produce an expansion due to the applied tensile in the areas where the long yarn floating areas were dominant.

CONCLUSIONS

As a result of this study which examined pique pattern structures that can be used in auxetic fabric design, it was observed that auxetic effect was obtained in an applied tension of approximately 1mm with proper placement of the yarn connection areas.

SUGGESTIONF FOR FURTHER WORK

Work continues on fabric constructions with different structural parameters and pique pattern structures.

ACKNOWLEDGEMENTS/SOURCES OF FUNDING

This research has been supported by TUBITAK 1001 project (Project No. 119M358). The authors would like to thank TUBITAK for their support.

LITERATURE

1. Uzun, M. 2010. “Negatif Poisson Oranına Sahip (Auxetic) Malzemeler ve Uygulama Alanları”, Tekstil ve Mühendis, 77, 13-18.
2. Darja R., Tatjana R., Alenka, P. C. 2013. “Auxetic Textiles”, Acta Chim. Slov., 60, 715–723.
3. Evans, K., Alderson, A. 2000. “Auxetic Materials: Functional Materials and Structures from Lateral Thinking”, Advanced Materials, 12, 617– 628.
4. Yang, W., Li, Z. M., Shi, W., Xie, B. H., Yang, M. B. J. 2004. “Review on auxetic materials”, Journal of Materials Science,39, 3269–3279.
5. Grima, J. N., Attard, D., Gatt, R., Cassar, R. N. 2009. “A novel process for the manufacture of auxetic foams and for their reconversion to conventional form”, Adv. Eng. Mater., 11, 533-535.
6. Grima, J. N., Farrugia, P. S., Gatt, R., Attard, D. 2008. “On the properties of auxetic meta-tetrachiral structures”, Phys. Stat. Sol. (b), 245, 521–529.
7. Liu, Y., Hu, H. 2010. “A review on auxetic structures and polymeric materials”, Scientific Research and Essays, 5,1052-1063.
8. Alderson, K. L. 2007. “Positive development in negative materials”, Mater. World,15, 32–34.
9. Ugbolue, S. C., Kim, Y. K., Warner, S. B., Fan, Q., Yang, C., Kyzymchuk, O., Feng, Y. 2010. “The formation and performance of auxetic textiles. Part I: theoretical and technical considerations”, J. Text. Inst., 101, 660–667.
10. Carneiro, V. H., Meireles, J., Puga, H. 2013. “Auxetic Materials – A Review”, Materials Science, 31, 561-571.
11. Liu, Y., Hu, H., Lam, J. K. C., Liu, S. 2010. “Negative Poisson’s ratio weft-knitted fabrics”, Text. Res. J., 80, 856–863.
12. Hu, H., Wang, Z. Y., Liu, S. 2011. “Development of auxetic fabrics using flat knitting technology”, Text. Res. J., 81, 1493–1502.
13. Ugbolue, S. C., Kim, Y. K., Warner, S. B., Fan, Q., Yang, C., Kyzymchuk, O., Feng, Y., Lord, J. 2011. “The formation and performance of auxetic textiles. Part II: geometry and structural properties”, J. Text. Inst., 102, 424–433.

RECYCLED CARBON FIBER FOR PROTECTIVE CLOTHING APPLICATIONS

KAYNAK, İdris
Uşak University
idris.kaynak@usak.edu.tr

ABSTRACT

Recycled carbon fibers was carried out using with converted into cheesecloth sheet using standard-universal carding machine processing to obtain technical textile products as a first step. This product was converted to tow profile form as an intermediate process step to obtain yarn. These forms were subjected to tensile-bending-folding process by combining 6 pieces. The yarn had been subjected to the lubrication and holding process for obtaining the one-way spin of orientation fibers process. Open-end machine was used to obtain yarn and the machine velocity was chosen approximately 12,000 rev / min. Using the conventional glove knitting machine, 6 of these yarns were used together to obtain protective gloves. With the use of carbon fibers from recycling, it was observed that the knitted glove endured to a temperature of approximately 400 degrees and remained in the form of knitting and did not burn in laboratory experiments. The total weight of the single glove was determined to be 20 grams.

Keywords: Recycled carbon fibers, Protective clothing, Non-flammable yarn, Knitting, Glove, Light yarn.

A Study on Particulates Release when Machining Nano-structured Polymeric Composites

SHYHA, Islam[1]*, DEARY, Michael[1], HUO, Dehong[2]
[1]Faculty of Engineering and Environment, Northumbria University, Newcastle upon Tyne, UK
[2]School of Mechanical and Systems Engineering, Newcastle University, Newcastle upon Tyne, UK
*islam.shyha@northumbria.ac.uk

PURPOSE

This paper presents a quantitative assessment of particulates released when machining nano-structured composite materials (graphene/epoxy and halloysite nanoclay/polyester) under different cutting conditions.

Current technologies are only able to produce composite parts in near-net shapes. Micromachining is needed to attain higher surface quality, dimension accuracy, and generate additional features such as holes for assembly. Micromachining processes are also feasible for wide ranges of materials. Main challenges when micromachining composites include the excessive generated heat, unexpected variations in cutting forces and dimension accuracy, high rate of tool wear and small particulates (airborne chips) released when machining dry (i.e. without the use of cutting fluids). Machining allowance (the part to be removed from the work material) is transformed during the removal process to chips which rest on machine beds while the finer particulates become airborne. This is mainly occurring when dry machining is employed. Dry machining is unavoidable because the use of cutting fluids can have a high adverse impact on human health, expensive disposal & waste management costs, high consumption rate (EU alone consumes approximately 320,000 tons of cutting fluids per year), and the potential chemical interaction between cutting fluid and workpiece.
Throughout their lifecycle nanocomposites will undergo machining with safety concerns relate to the rate and volume of nanomaterial release from the matrix. Research into nanomaterial safety has expanded alongside their use in research and industry but few studies focus on the release of nanomaterials from nanocomposites. Lack of studies into nanomaterial release from nanocomposites makes rigorous risk assessment and management of occupational exposure impossible. Available studies do show release of nanomaterials from the composite matrix during a variety of machining activities. Froggett et al. reviewed the nanomaterials release and found that studies to date do not indicate a high propensity for discreet nanomaterial release, but rather composite particles of matrix with partially or fully embedded nanomaterials (Froggett et al., 2014).

EXPERIMENTAL WORK

Material

The research aims to evaluate the small/nano-particulates release when micro slotting graphene/epoxy and halloysite nanoclay/polyester nano-structured composites. Constant nano-filler weight percentage of 0.3% was used throughout experiments. Two flutes uncoated micro-grain tungsten carbide end mills with nominal cutting diameter of 1 mm, 3 mm flue length and helix angle of 20° were used. Tool wear was found negligible when cutting nano-composites (Shyha, et al., 2018) and therefore tools were used until fracture. Dry cutting was employed throughout all experiments to allow the capture of airborne chips.

Method

Micro milling experiments were performed on an ultra-precision desktop micro-machine tool (Nanowave MTS5R) equipped with a high speed spindle (max 80,000rpm). Experimental setup is shown in Figure 1. The evaluated process variables and their corresponding levels are shown in Table 1.
The collection of the particulates released was performed using Turnkey Dustmate, laser light scattering monitor at 4 locations away from the point of cutting including 10, 30, 50 and 100 cm. The released PM_{10}, $PM_{2.5}$, PM_1 concentrations (size <10, <2.5 and <1 µm, respectively, with a lower limit of 0.5 µm) was measured. Following the collection of particulates during each cutting experiment, Robust Highest Concentration (RHC) for each size fraction was calculated. RHC is a statistical parameter used in ambient air quality studies (worst case parameter) and can be computed using the following equation.

$$RHC = X_n + (\overline{X}_{n-1} - X_n)\ln\left(\frac{(3n-1)}{2}\right)$$

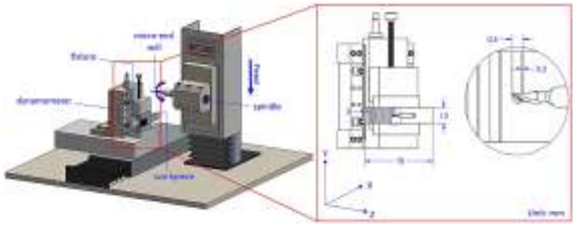

Figure 1. Micro-milling experimental setup

Table 1. Process variables and their levels

Variable/Level	1	2	3	4
Workpiece material	Graphene/ epoxy	Nanoclay/ polyester		
Cutting Speed (m/min)	31.4	94.2	157	
Feed rate (µm/rev)	5	15	25	
Depth of cut (mm)	50	100	150	
Location of Dustmate (cm)	10	30	50	100

RESULTS AND DISCUSSIONS

UK EH40 work exposure limit (WEL) for respirable dust (i.e. <4µm) is 4,000 µg/m^3, which is above all of the experimental conditions tested in this study. However, a small number of trials at different cutting conditions exceeded the IOM recommended limits of 1000 µg/m^3, see Figure 2. For almost all of the experiments, the peak of particulates concentration obtained at 10 cm away from the tool tip regardless of cutting conditions used, see Figure 3. Principal Component Analysis (PCA) was used to determine the relationships between concentrations and the process variables as shown in Figure 4. The size of circle is proportional to PM$_{10}$ concentration while the colours indicate distance categories. Closely aligned arrows indicate positive correlations (e.g. PM$_{10}$ with depth of cut). Oppositely aligned arrows indicate negative correlation (e.g. PM$_{10}$ and distance). PM$_1$ and PM$_{2.5}$ are more closely aligned with each other than they are with PM$_{10}$. Orange and red circles (closer distances), clearly associated with highest concentrations. In general, graphene/epoxy material had higher concentrations compared with clay/polyester regardless of cutting conditions and distance from tool tip, see Figure 5. Also, the PM$_{10}$ fraction is found to be closely associated with changes in cutting parameters (i.e. compared to PM$_{2.5}$ and PM$_1$), suggesting that most particulates produced are within this category. There is limited information on health hazards of nanoparticles (<0.1µm) and so, even though our study suggests low concentrations of this size fraction are generated, these concentrations may still be associated with significant health effects which means adequate precautions need to be taken.

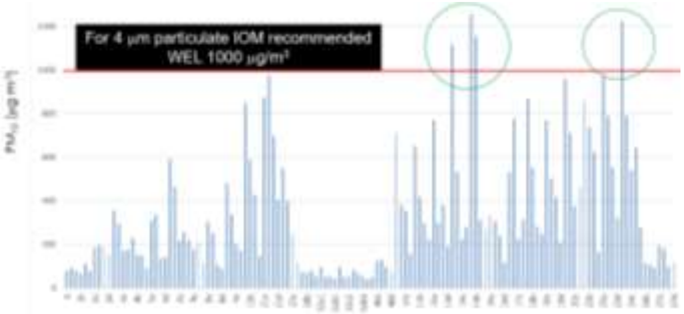

Figure 2. RHC for PM$_{10}$ (µg/m^3)

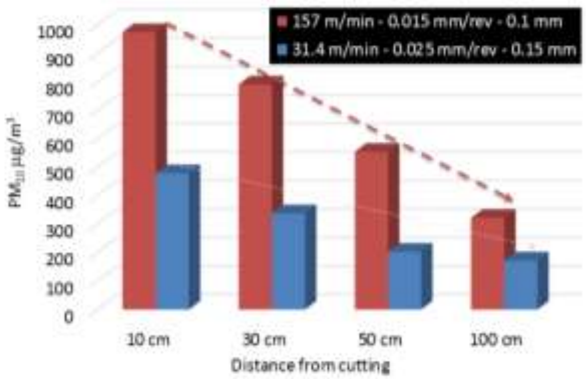

Figure 3. Effect of milling conditions on PM$_{10}$ concentration at different locations

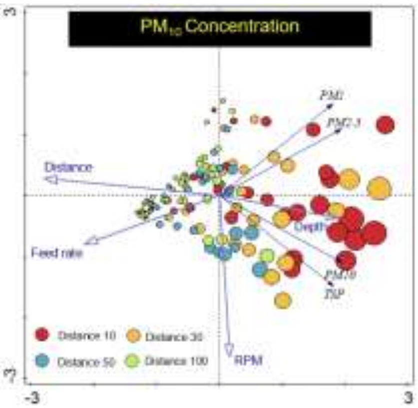

Figure 4. PCA for PM10 concentration

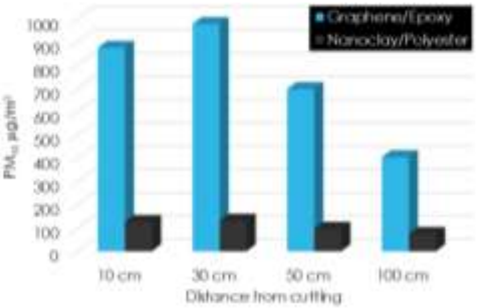

Figure 5. Effect of work material on PM$_{10}$ at different locations

CONCLUSIONS

Within the evaluated operating conditions, released particulate concentrations for most of the experiments were below the recommendation WEL for respirable dust (i.e. 1000 µg/m^3 recommended by IOM). It does not mean coming in under the available WELs, it is ok to machine nanocomposites with no extraction. Therefore, this work draws attention to the need for new WELs for nanomaterials and output from nanocomposites machining because current legal limits applied could really lull people into a false sense of security.

SUGGESTIONS FOR FURTHER WORK

The future work will need to focus on characterising morphology and toxicity of the particulates generated from micromachining nano-structured composites.

ACKNOWLEDGEMENTS/SOURCES

The authors would like to thank Mr. Guoyu Fu and Mr. Xiangyu Teng from Newcastle University for helping in conducting some of the experiments.

REFERECES

Froggett et al., 2014, "A review and perspective of existing research on the release of nanomaterials from solid nanocomposites", Particle and Fibre Toxicology, volume 11.

Shyha, I. et al., 2018, "Micro-machining of nano-polymer composites reinforced with graphene and nano-clay fillers", Int. Con. on Materials Sci. & Eng.: Recent Advances and Challenges, March 11 – 13, Alexandria, Egypt

SEMPOZYUM SPONSORLARI

SYMPOSIUM SPONSORS

POLYTEKS®

Tepar

maiTEKS
tekstil

AREKA
Advanced
Technologies

inovenso

Kutlucan®
TEKSTİL

RB KARESİ

TEZYAPARLAR
Textile

Sülekler®
TEKSTİL SANAYİ ve TİCARET A.Ş.

anipek®